



UCL

**Method development approaches towards the
identification and validation of disease-related
protein targets**

Isa Nobre da Cruz

**Thesis submitted in accordance with the requirements of UCL School of
Pharmacy for the degree of Doctor of Philosophy**

January 2014

UCL SCHOOL OF PHARMACY

29-39 Brunswick Square

London WC1N 1AX

Plagiarism Statement

This thesis describes research conducted in the University College London School of Pharmacy between February 2010 and January 2014 under the supervision of Dr. Min Yang. I, Isa Nobre da Cruz, confirm that the work presented in this thesis is my own. Where information has been derived from other sources, I confirm that this has been indicated in the thesis. I also certify that I have written all the text herein and have clearly indicated by suitable citation any part of this dissertation that has already appeared in publication.

Signature: _____**Date:** _____

Abstract

The search for novel biomarkers and therapeutic targets is a continuous process in the fight against disease. In this project, target identification and validation approaches were used towards the discovery of protein targets related to distinct, but equally relevant diseases.

The first approach involved the use of proteomics to identify protein targets in infertility. An affinity-enrichment proteomic method was developed and successfully applied to the identification of protein targets of a clinically utilised compound, which is known to cause reversible, dose-dependent male infertility in certain mouse strains.

The second approach demonstrated the versatility of proteomics in an attempt to answer a completely different question. In this study, it was applied to the discovery of protein targets of chemoresistance in ovarian cancer, using human ovarian cancer cell lines and tissue biopsies. Once again, this method was successful in identifying some very promising un-regulated protein targets and pathways involved in cancer resistance.

Finally, a more assay development orientated approach aimed for the functional characterisation of Hsp90 targeted compounds. The combined use of a native gel binding assay and an Hsp90 ATPase assay proved to be a convenient and robust method to characterise Hsp90 inhibitors and will aid the development of Hsp90 targeted anti-cancer drugs.

In summary, the work undertaken confirmed the recognised advantages of proteomics in the comparative study of un-regulated proteins connected to disease. It equally showed how two distinct techniques could be used in synergy to accomplish more valuable answers, in the screening of inhibitors of a known protein target.

Acknowledgements

This PhD has proven to be one of the most extraordinary experiences I have had at different levels. The dedication, commitment and, above all, the enthusiasm that most of those I have worked with share for research were decisive for my success.

First of all, I would like to express my acknowledgement to the UCL School of Pharmacy for giving me the opportunity to integrate an institution with such potential and to Fundação para a Ciência e a Tecnologia (FCT) Portugal for funding my doctoral studies.

I would like to acknowledge my supervisor, Dr. Min Yang, for accepting me to work in the laboratory under his supervision, for his commitment in providing me with all the tools I needed to develop this project and for the guidance. I would also like to thank Dr. Andreas Schätzlein for his wise ideas and helpful suggestions throughout the four years of my PhD, and Dr. Stephen Baines for providing me the animal tissue samples for the first stages of my work through the Royal Veterinary College (RVC) University of London.

I am very grateful to all the collaborators from different universities with whom I had the privilege of working and learning. They made me believe that collaborations make better science.

A special thank you to Sibylle Heidelberger for the invaluable help, advice and training without which I could not have been successful. To Andreia Guimaraes, Edwin Nkansah and Marjolein Schaap, thank you for sharing the day-to-day laboratory life with me and for offering your precious insights into my experiments.

I would also like to thank my colleagues and friends for helping me overcome all the obstacles in my work and for their contribution to make my stay in London more enjoyable, in special the 'Portuguese community' of the UCL School of Pharmacy for making me feel less homesick. A big thank you to Bruno Sil, Ines Pereira and Rita

Mateus for the friendship and support, greatly appreciated during the dreadful writing-up period.

Finally, I would like to express my sincere gratitude to my family for the unconditional support, belief and love. And the biggest thank you goes to my fiancé for listening to my endless complaints, for coping with my bad mood after many failed experiments, for the invaluable help towards the end of my PhD studies, for giving me the strength to take things forward and to never give up and, above all, for always standing by my side.

London, 31st January 2014

Table of Contents

Plagiarism Statement.....	2
Abstract.....	3
Acknowledgements	4
Table of Contents	6
Table of Figures	13
Table of Tables	16
List of the Most Common Abbreviations	18
Amino Acid Abbreviations	21
Chapter 1 – Introduction	22
1.1 Drug discovery	23
1.2 Target discovery.....	25
1.2.1 Target identification – Proteomics.....	25
1.2.1.1 Importance and advantages of proteomics.....	26
1.2.1.2 Top-down and bottom-up proteomics	27
1.2.1.3 Applications of proteomics.....	27
1.2.1.4 Complete workflow of a proteomics experiment.....	29
1.2.1.4.1 Electrophoresis analysis	30
1.2.1.4.2 Mass spectrometry analysis	41
1.2.1.4.3 Global bioinformatics	44
1.2.2 Target validation	48
1.2.2.1 Methods of target validation	48
1.2.3 Assay development.....	49
1.2.3.1 Methods for assay/screen development	49
1.3 General Aims & Objectives	50
Chapter 2 – Materials & methods.....	51
2.1 Chemicals and reagents.....	52
2.2 Biological samples.....	53

2.3 Sample preparation.....	54
2.3.1 Protein extraction from mammalian cells	54
2.3.1.1 Cell harvesting	54
2.3.1.2 Protein extraction from mammalian cells – Method 1.....	55
2.3.1.3 Protein extraction from mammalian cells – Method 2.....	55
2.3.2 Protein extraction from mammalian tissues.....	55
2.3.2.1 Protein extraction from canine lung and liver tissues	56
2.3.2.2 Protein extraction from mouse testis tissues	56
2.3.2.3 Protein extraction from human ovarian tissues	57
2.3.3 Determination of protein concentration	57
2.3.4 Protein precipitation	58
2.3.4.1 Trichloroacetic acid and acetone precipitation of proteins.....	58
2.3.4.2 2D clean-up kit.....	58
2.4 Methods of protein separation.....	60
2.4.1 SDS-PAGE	60
2.4.2 Native-PAGE.....	61
2.4.3 2D-PAGE	62
2.4.3.1 First dimension: isoelectric focussing (IEF)	63
2.4.3.2 Equilibration, reduction and alkylation	64
2.4.3.3 Second dimension: SDS-PAGE.....	65
2.5 Methods of protein visualisation	66
2.5.1 Coomassie blue staining.....	66
2.5.2 Silver staining	66
2.5.3 Gel image analysis.....	67
2.6 Methods of protein identification.....	68
2.6.1 LC-MS/MS.....	68
2.6.1.1 Spot excision, washing and in-gel trypsin digestion	68
2.6.1.2 Peptide extraction from gel pieces.....	69
2.6.1.3 MS analysis	69
2.6.1.4 Data processing and database searching.....	74
2.6.2 Western blotting	78
2.6.2.1 Electrophoretic separation	78
2.6.2.2 Protein transfer to nitrocellulose membranes	78
2.6.2.3 Blocking and antibody probing	79
2.6.2.4 Protein band detection and visualisation	79
Chapter 3 – Proteomics approach to identify protein targets in infertility	81

3.1 Introduction	82
3.1.1 Carbohydrate-active proteins (CAP)	82
3.1.2 The iminosugar glycomimetic NB-DNJ	83
3.1.3 NB-DNJ induces infertility in male mice.....	86
3.1.4 Affinity chromatography principle	87
3.1.5 Affinity-enrichment proteomics.....	89
3.2 Aims & Objectives	91
3.3 Materials & Methods	92
3.3.1 Affinity resin synthesis	92
3.3.1.1 Synthesis of methyl 6-oxohexanoate.....	93
3.3.1.2 Synthesis of methyl 6-((2 <i>R</i> ,3 <i>R</i> ,4 <i>R</i> ,5 <i>S</i>)-3,4,5-trihydroxy-2-(hydroxymethyl)piperidin-1-yl)hexanoate	93
3.3.1.3 Preparation of DNJ-affinity gel	93
3.3.2 Affinity resin validation	94
3.3.2.1 Ceredase activity assay	94
3.3.2.2 DNJ-affinity chromatography with Ceredase.....	95
3.3.2.3 Wessel-Flugge protein precipitation.....	95
3.3.2.4 SDS-PAGE	95
3.3.2.5 Silver staining	95
3.3.3 Affinity resin assay	95
3.3.3.1 Mouse testis tissue collection and homogenisation.....	96
3.3.3.2 DNJ-affinity chromatography with mouse testis tissue homogenate	96
3.3.4 Proteomics analysis.....	97
3.3.4.1 Protein precipitation.....	97
3.3.4.2 2D-PAGE.....	97
3.3.4.2.1 First dimension: isoelectric focussing (IEF).....	97
3.3.4.2.2 Equilibration, reduction and alkylation	98
3.3.4.2.3 Second dimension: SDS-PAGE	98
3.3.4.2.4 Gel staining: silver staining.....	98
3.3.4.3 Gel image analysis	98
3.3.4.4 Protein identification	98
3.3.4.4.1 Spot excision, washing and in-gel trypsin digestion	98
3.3.4.4.2 Peptide extraction from gel pieces	99
3.3.4.4.3 LC-MS/MS analysis	99
3.3.4.4.4 Data processing and database searching	99
3.3.5 Pathways analysis	100
3.3.6 Single-nucleotide polymorphism (SNP) analysis.....	100

3.4 Results & Discussion	101
3.4.1 Affinity resin synthesis	102
3.4.2 Affinity resin validation	103
3.4.3 2D-PAGE gels.....	106
3.4.4 Selection of proteins identified.....	107
3.4.5 Most interesting protein identifications	114
3.4.6 Single-nucleotide polymorphism (SNP) analysis results	117
3.5 Conclusions & Future Work	121
3.5.1 Conclusions	121
3.5.2 Future work.....	122
Chapter 4 – Proteomics approach to identify protein targets of chemoresistance in ovarian cancer	125
4.1 Introduction	126
4.1.1 Ovarian cancer	126
4.1.1.1 Types of ovarian cancer	127
4.1.1.2 Stages of ovarian cancer	129
4.1.1.3 Grades of ovarian cancer	131
4.1.1.4 Epidemiology	132
4.1.1.5 Causes and risk factors	134
4.1.1.6 Symptoms	136
4.1.1.7 Importance of early diagnosis, prognosis and screening.....	137
4.1.1.8 Treatment strategies	138
4.1.1.8.1 Platinum drugs	139
4.1.1.8.2 Taxanes.....	140
4.1.2 Chemoresistance.....	141
4.1.2.1 Mechanisms of resistance to platinum drugs.....	143
4.1.2.1.1 Resistance through insufficient DNA binding.....	143
4.1.2.1.2 Resistance mediated after DNA binding	145
4.1.2.2 Mechanisms of resistance to taxanes.....	146
4.1.2.2.1 Multidrug resistance (MDR)	147
4.1.2.2.2 Resistance through altered microtubule dynamics.....	147
4.1.2.2.3 Drug resistance through altered signalling pathways	149
4.1.2.3 Overcoming drug resistance	150
4.2 Aims & Objectives	154
4.3 Materials & Methods	155
4.3.1 Biological samples	156

4.3.2 Sample preparation.....	157
4.3.2.1 Cell culture.....	157
4.3.2.2 Cell harvesting	158
4.3.2.3 Protein extraction from PEO1 ovarian cancer cells	158
4.3.2.4 Protein extraction from ovarian tissue samples	158
4.3.2.5 Protein concentration assay	158
4.3.3 Proteomics analysis.....	158
4.3.3.1 SDS-PAGE	159
4.3.3.2 Protein precipitation.....	159
4.3.3.3 2D-PAGE.....	159
4.3.3.3.1 First dimension: isoelectric focussing (IEF).....	160
4.3.3.3.2 Equilibration, reduction & alkylation	160
4.3.3.3.3 Second dimension: SDS-PAGE	160
4.3.3.3.4 Gel staining: silver staining.....	160
4.3.3.4 Gel image analysis	160
4.3.3.5 Protein identification	161
4.3.3.5.1 Spot excision, washing and in-gel trypsin digestion	161
4.3.3.5.2 Peptide extraction from gel pieces	161
4.3.3.5.3 MS analysis	161
4.3.3.5.4 Data processing and database searching	161
4.3.4 Pathway analysis	162
4.3.5 Target validation – Western blotting.....	162
4.4 Results & Discussion.....	164
4.4.1 Preliminary observations and assays	165
4.4.1.1 Ovarian tissue biopsies	165
4.4.1.2 Protein concentration assay	167
4.4.1.2.1 Protein concentration assay of PEO1 cell lines	167
4.4.1.2.2 Protein concentration assay of tissue biopsies	168
4.4.2 Proteomics analysis.....	171
4.4.2.1 SDS-PAGE gels.....	171
4.4.2.1.1 SDS-PAGE gels of the PEO1 cell lines.....	171
4.4.2.1.2 SDS-PAGE gels of the tissue biopsies.....	172
4.4.2.2 2D-PAGE gels	174
4.4.2.2.1 2D-PAGE gels of the PEO1 cell lines	174
4.4.2.2.2 2D-PAGE gels of the tissue biopsies	178
4.4.2.3 Gel image analysis	182
4.4.2.3.1 Gel image analysis of the PEO1 cell lines	184

4.4.2.3.2 Gel image analysis of the tissue biopsies	185
4.4.2.4 Selection of protein hits.....	186
4.4.3 Pathway analysis	207
4.4.4 Target validation	212
4.4.4.1 Western blotting assay	212
4.4.5 Protein targets of chemoresistance in ovarian cancer	218
4.4.5.1 Proteins identified in the ovarian cancer cell lines	218
4.4.5.1.1 Cytoskeleton and cell structure.....	220
4.4.5.1.2 Detoxification and stress response	223
4.4.5.1.3 Multifunctional proteins	224
4.4.5.2 Proteins confirmed in the tissue biopsies.....	228
4.4.6 Other protein targets in ovarian cancer	231
4.4.6.1 Protein targets of ovarian cancer diagnosis	231
4.4.6.2 Protein targets of ovarian cancer histologic subtype	232
4.5 Conclusions & Future Work	234
4.5.1 Conclusions	234
4.5.2 Future work.....	237
Chapter 5 – Functional characterisation of heat shock protein 90 targeted compounds.....	239
5.1 Introduction.....	240
5.1.1 Heat shock proteins (Hsps)	240
5.1.2 Hsp90 characteristics and functions	241
5.1.3 Hsp90's role in cancer	242
5.1.4 Hsp90 inhibitors	244
5.1.4.1 Hsp90 N-terminal inhibitors	244
5.1.4.2 Hsp90 C-terminal inhibitors.....	246
5.1.5 Methods to study Hsp90 inhibition	248
5.2 Aims & Objectives	250
5.3 Materials & Methods	251
5.3.1 Western blot study of MCF-7 breast cancer cells treated with novobiocin analogues	251
5.3.1.1 Cell culture, treatment with novobiocin analogues and harvesting.....	251
5.3.1.2 Protein extraction from cells	252
5.3.1.3 Western blot assay	252
5.3.2 Hsp90 binding assay – native-PAGE.....	253
5.3.2.1 Qualitative assay.....	253

5.3.2.2 Quantitative assay	254
5.3.2.3 Native-PAGE.....	254
5.3.3 Hsp90 ATPase assay	254
5.3.3.1 Protein expression and purification.....	254
5.3.3.2 ATPase activity assay	255
5.4 Results & Discussion.....	256
5.4.1 Western blot study of MCF-7 breast cancer cells treated with novobiocin analogues	257
5.4.1.1 Protein concentration assay	257
5.4.1.2 Western blot assay	259
5.4.2 Hsp90 binding assay – native-PAGE	262
5.4.2.1 Commercial Hsp90 purity test	263
5.4.2.2 Qualitative assay	264
5.4.2.3 Quantitative assay	265
5.4.3 Hsp90 ATPase assay	272
5.4.3.1 Expressed Hsp90 purity test	272
5.4.3.2 ATPase activity assay	273
5.5 Conclusions & Future Work	278
5.5.1 Conclusions	278
5.5.2 Future work.....	279
Chapter 6 – Summary and general discussion & conclusions	281
References	286
Appendix: Accompanying DVD.....	310

Table of Figures

Figure 1.1 Possible stages in the drug discovery process	24
Figure 1.2 Complete workflow of a typical proteomics experiment	30
Figure 1.3 Isoelectric focussing of proteins	36
Figure 1.4 SDS-PAGE separation of proteins	38
Figure 1.5 Protein identification by MS/MS	47
Figure 2.1 Representation of the 63 min gradient LC method used in MS analysis	70
Figure 2.2 Parameters used in MASCOT searches	76
Figure 2.3 Parameters used in X!Tandem searches.....	77
Figure 3.1 Structure of NB-DNJ/Miglustat/Zavesca®	83
Figure 3.2 Structure relationships between NB-DNJ and the substrates of ceramide glycosyltransferase and acid α -glucosidase.....	84
Figure 3.3 Affinity chromatography procedure	89
Figure 3.4 Structure of the glyco-affinity resin matrix.....	90
Figure 3.5 Schematic diagram summarising the experiments done in this study	92
Figure 3.6 Synthesis of methyl 6-oxohexanoate.....	93
Figure 3.7 Synthesis of methyl 6-((2 <i>R</i> ,3 <i>R</i> ,4 <i>R</i> ,5 <i>S</i>)-3,4,5-trihydroxy-2-(hydroxymethyl)piperidin-1-yl)hexanoate.....	93
Figure 3.8 Preparation of DNJ-affinity gel.....	94
Figure 3.9 General scheme of the study	101
Figure 3.10 Glyco-affinity probe synthesis and preparation of the glyco-affinity resin	102
Figure 3.11 SDS-PAGE of Ceredase® and fractions eluted from DNJ-affinity gel loaded with Ceredase®	104
Figure 3.12 Comparative 2D-PAGE analysis of C57BL/6 mouse testis passed through unmodified control (A) and DNJ-modified affinity (B) matrices	106

Figure 3.13 Venn diagram of glyco-A ^e P proteins identified with a MASCOT score > 20	107
Figure 3.14 Six most significant proteins highlighted in comparative 2D-PAGE analysis of C57BL/6 mouse testis passed through unmodified control (A) and DNJ-modified affinity (B) matrices	108
Figure 3.15 Overlapped gel image of DNJ-modified and unmodified control gel images ..	110
Figure 3.16 Venn diagrams of the outcomes at different levels of protein score thresholds and different use of either (A) 'combined exclusion' or (B) 'overlap exclusion'	113
Figure 3.17 Pathways focussed on HYOU1 protein	115
Figure 4.1 Chemical structures of the two most used platinum compounds in ovarian cancer treatment.....	139
Figure 4.2 Chemical structures of the two most used taxanes in ovarian cancer treatment	141
Figure 4.3 Schematic diagram summarising the experiments done in this study	155
Figure 4.4 Protein concentration assay calibration curve	167
Figure 4.5 Protein concentration assay calibration curve	169
Figure 4.6 SDS-PAGE gel images of PEO1 sensitive, PEO1 TaxR and PEO1 CarbR resistant cell lines.....	171
Figure 4.7 SDS-PAGE gel images of SOV-1, SOV-2, SOV-3, SOV-4 and SOV-5 ovarian tissues	172
Figure 4.8 Representative 2D-PAGE silver stained gels of the PEO1 sensitive ovarian cancer cell line.....	174
Figure 4.9 Representative 2D-PAGE silver stained gels of the PEO1 TaxR ovarian cancer cell line.....	175
Figure 4.10 Representative 2D-PAGE silver stained gels of the PEO1 CarbR ovarian cancer cell line.....	175
Figure 4.11 Representative 2D-PAGE silver stained gels of the five ovarian tissue biopsies	179
Figure 4.12 Examples of spot selection using PDQuest Advanced 8.0.1	183
Figure 4.13 Spots in the ovarian cancer cell line gels that were selected for excision and further analysis by LC-MS/MS	184

Figure 4.14 Spots in the ovarian tissue gels that were selected for excision and further analysis by LC-MS/MS	185
Figure 4.15 Venn diagram of the protein lists generated using the two protein database search approaches: manual search and Scaffold 3 software search	187
Figure 4.16 Examples of proteins that were identified in more than one spot on the same gel and the respective spots where they were identified	199
Figure 4.17 Stacked bar charts illustrating the pathways most associated with the genes that codify for the proteins in the analysed datasets.....	208
Figure 5.1 Hsp90 chaperone cycle. ATP binding triggers the Hsp90 chaperone cycle	242
Figure 5.2 Hsp90 N-terminal inhibitors.....	245
Figure 5.3 Hsp90 C-terminal inhibitors	246
Figure 5.4 Schematic diagram summarising the experiments conducted in this study	251
Figure 5.5 Protein concentration assay calibration curve	258
Figure 5.6 Western blot study of MCF-7 breast cancer cells treated with novobiocin analogues	260
Figure 5.7 Structure of glucosyl-novobiocin (Glc-Nov)	263
Figure 5.8 Commercial Hsp90 gel analysis.....	264
Figure 5.9 Native polyacrylamide gel analysis to probe Hsp90 C- and N-terminal binding targets	265
Figure 5.10 Native polyacrylamide gel analysis to probe novobiocin IC ₅₀	266
Figure 5.11 Native polyacrylamide gel analysis to probe glucosyl-novobiocin IC ₅₀	268
Figure 5.12 Native polyacrylamide gel analysis to probe geldanamycin IC ₅₀	270
Figure 5.13 Expressed Hsp90 SDS-PAGE analysis	273
Figure 5.14 Inhibition of novobiocin (Nov) to Hsp90.....	275
Figure 5.15 Inhibition of glucosyl-novobiocin (Glc-Nov) to Hsp90	275
Figure 5.16 Inhibition of geldanamycin (Geld) to Hsp90	276

Table of Tables

Table 2.1 Example of the composition of an SDS-polyacrylamide gel.....	60
Table 2.2 Example of the composition of a native-polyacrylamide gel	62
Table 2.3 Rehydration and focussing conditions used in the first dimension of 2D-PAGE ...	64
Table 2.4 Parameters for the analysis of samples on the Waters Micromass Q-ToF Premier	72
Table 2.5 System checks and instrument calibration parameters for the Waters Micromass Q-ToF Premier	74
Table 3.1 Parameters used in the SNP analysis	100
Table 3.2 Significant proteins identified from mouse testis with putative NB-DNJ affinities using glyco-A ^e P	109
Table 3.3 Single-nucleotide polymorphism (SNP) analysis results	119
Table 4.1 Clinical information from 5 different patients and their respective ovarian tissue biopsies	157
Table 4.2 List of the primary antibodies used for target validation in the ovarian cancer study	163
Table 4.3 Visual observations and weights of ovarian tissue biopsies analysed	165
Table 4.4 Protein concentration of the three ovarian cancer cell line samples	168
Table 4.5 Protein concentration of the five ovarian tissue samples	169
Table 4.6 Proteins identified in the ovarian cancer cell lines (sensitive – PEO1 and resistant – PEO1 TaxR, PEO1 CarbR) and/or in the ovarian tissue biopsies (control – SOV-1 and cancer – SOV-2/3/4/5)	188
Table 4.7 Protein fold regulation using two methods of spot intensity analysis.....	201
Table 4.8 Results of a literature review on proteins reported with an association with ovarian cancer or ovarian cancer resistance	203

Table 4.9 Top 5 canonical pathways most related to the genes that codify for the proteins in the analysed datasets	210
Table 4.10 Results of target validation through Western blotting assay	215
Table 4.11 Possible protein targets of chemoresistance in ovarian cancer	229
Table 5.1 Protein concentration of the various MCF-7 breast cancer cell line samples treated with the three inhibitors in different concentrations.....	258

List of the Most Common Abbreviations

Abbreviations	
2D-PAGE	2-dimensional polyacrylamide gel electrophoresis
A ^e P	affinity-enrichment proteomics
ATP	adenosine triphosphate
BSA	bovine serum albumin
CID	collision induced dissociation
Da	daltons
DMSO	dimethylsulfoxide
DTT	dithiothreitol
<i>E. Coli</i>	<i>Escherichia coli</i>
ECL	enhanced chemiluminescence
EDTA	ethylenediaminetetraacetic acid
ESI	electrospray ionisation
FA	formic acid
fmol	femtomoles
g	grams
<i>g</i>	acceleration due to gravity
Gal_Nov	galactosyl-novobiocin
Geld	geldanamycin
Glc-Nov	glucosyl-novobiocin
glyco-A ^e P	glycomimetic affinity-enrichment proteomics
h	hour
HCl	hydrochloric acid
HPLC	high performance liquid chromatography
Hsp90	heat shock protein 90
i.d.	inner diameter
IC ₅₀	half maximal inhibitory concentration
IEF	isoelectric focussing

Igepal	non-idet P40 nonylphenoxypholyethoxyethanol
IgG	immunoglobulin G
IPG	immobilised pH gradient
IPTG	isopropyl- β -D-1-thiogalactopyranoside
ITRAQ	isotope tags for relative/absolute quantification
KCl	potassium chloride
LB	lysogeny broth
LC	liquid chromatography
M	molar concentration (moles/litre)
m/z	mass to charge
mA	milliamps
MALDI	matrix-assisted laser desorption/ionisation
mg	milligram
min	minute
mL	millilitre
mm	millimetre
mM	millimolar
mRNA	messenger ribonucleic acid
ms	millisecond
MS	mass spectrometry
MS/MS	tandem MS
MW	molecular weight
NaCl	sodium chloride
NAD	nicotinamide adenine dinucleotide
Nano-ESI-LC-MS/MS	nano electrospray liquid chromatography tandem mass spectrometry
NB-DNJ	n-butyldeoxynojirimycin
ng	nanogram
nGBA	native gel binding assay
nl	nanolitre
nM	nanomolar
nm	nanometers
$^{\circ}$ C	degrees Celsius

PAGE	polyacrylamide gel electrophoresis
PBS	phosphate-buffered saline
pI	isoelectric point
PMF	peptide mass fingerprint
ppm	parts per million
PTM	post-translational modification
QTOF	quadrupole time-of-flight
rpm	rotations per minute
SDS	sodium dodecyl sulphate
sec	seconds
SILAC	stable isotope labelling by amino acid in cell culture
SNP	single-nucleotide polymorphism
TEMED	N,N,N',N'-tetramethylethylenediamine
TOF	time-of-flight
Tris	Tris(hydroxymethyl)aminomethane / 2-amino-2-hydroxymethyl-1,3-propanediol
TS	Tris saline
V	volts
WB	western blotting
µg	microgram
µL	microlitre
µM	micromolar

Amino Acid Abbreviations

Amino Acid	One-letter code	Three-letter code
Alanine	A	Ala
Arginine	R	Arg
Asparagine	N	Asn
Aspartic Acid	D	Asp
Cysteine	C	Cys
Glutamic Acid	E	Glu
Glutamine	Q	Gln
Glycine	G	Gly
Histidine	H	His
Isoleucine	I	Ile
Leucine	L	Leu
Lysine	K	Lys
Methionine	M	Met
Phenylalanine	F	Phe
Proline	P	Pro
Serine	S	Ser
Threonine	T	Thr
Tryptophan	W	Trp
Tyrosine	Y	Tyr
Valine	V	Val

Chapter 1 – INTRODUCTION

1.1 Drug discovery

Drug discovery is defined as the process by which new candidate medicines are discovered. Historically, drugs were discovered through the identification of the active ingredients in traditional remedies. Later, screening of chemical libraries of synthetic small molecules and natural products, using intact cells or whole organisms, was how new medicines were identified. This phase was followed by the use of high throughput screening (HTS) of large compound libraries against biological targets, before efficacy was tested in cells and animals. Modern drug discovery involves the identification of screening hits, followed by medicinal chemistry and, finally, the optimisation of those hits to improve potency, affinity, selectivity, stability and bioavailability. When a compound fulfils all the previous requirements, it may enter the drug development process that anticipates clinical trials (Drews, 2000).

The drug discovery process used to be driven mainly by chemistry, but is nowadays increasingly guided by pharmacology and the clinical sciences. It has hugely contributed to the progress of medicine, aided by the profound impact that the advent of molecular biology, in particular, of genomic sciences, has had on drug research. In the past, taking medicines constituted by recombinant proteins or monoclonal antibodies would be unthinkable; yet, today, there is an increasing number of treatment options available for the majority of the diseases. Genomic sciences, combined with bioinformatic tools, allow the study of the genetic basis of multifactorial diseases, so that the most suitable targets for future medicines can be determined (Rask-Andersen et al., 2011).

The biotech industry has established itself as the discovery arm of the pharmaceutical industry, bridging the gap between academia and large pharmaceutical companies, with the aim of facilitating knowledge transfer. Nevertheless, drug discovery is still a lengthy, difficult and expensive process with a low rate of new therapeutic discovery. It has been reported that in 2010 the

research and development cost of each new molecular entity was approximately US \$1.8 billion (Paul et al., 2010).

The drug discovery process includes several stages, from target discovery to clinical trials and therapeutic use, through which a drug candidate has to pass before it becomes a commercially available drug. These stages are summarised in Figure 1.1.

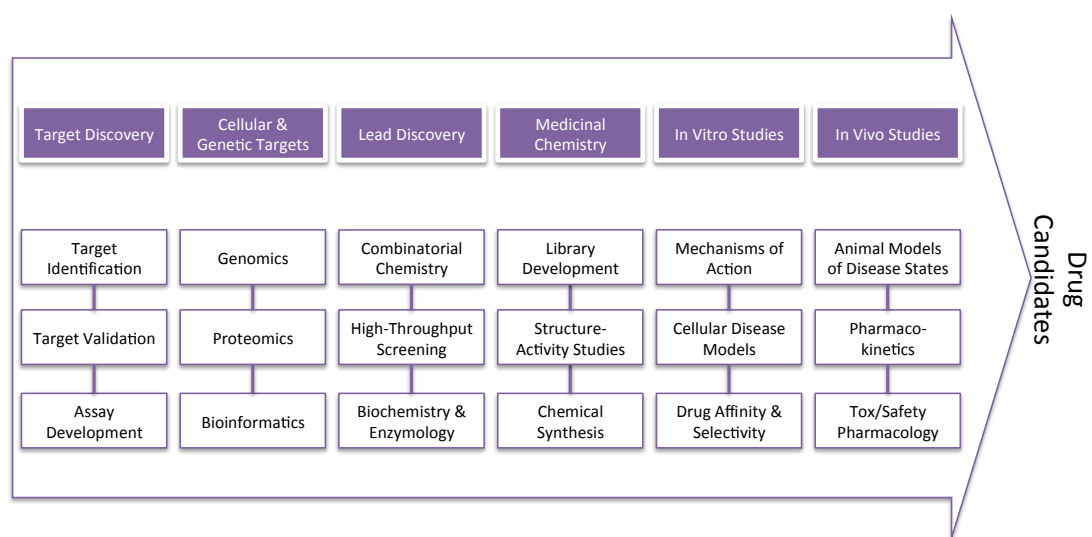


Figure 1.1 Possible stages in the drug discovery process.

The studies conducted in this project are part of the first stage of drug development, target discovery, which includes target identification through proteomics, target validation and assay development.

1.2 Target discovery

1.2.1 Target identification – Proteomics

The term proteomics results from the abbreviation of the words protein and genomics. The first protein studies that can be called proteomics began in 1975 with the introduction of the two dimensions (2D) gel by O’Farrell (1975), Klose (1975) and Scheele (1975), who started mapping proteins from *E. coli*, mouse, and guinea pig, respectively.

The word proteomics appeared for the first time in 1997 to describe the changes in all proteins expressed by a genome (James, 1997). Basic proteomic research is designed to further understand the molecular mechanisms underlying dysfunction in human disease. Clinical proteomics is the application of proteomic techniques to the medical field. The main aim of this methodology is to identify proteins involved in pathological processes and to understand how illness can lead to altered protein expression. Clinical proteomics offers the opportunity and the potential to develop new diagnostic and prognostic tests, to identify novel therapeutic targets, and eventually to allow the design of individualised patient treatment, through the application of proteomics in the drug development pipeline. More recently, proteomics has been used as a component of clinical trials (Azad et al., 2006). The results of proteomic studies are dedicated to the discovery and validation of diagnostic and prognostic disease biomarkers (Dominguez et al., 2007, Dunn, 2011).

Proteomics may also be classified as expression proteomics and functional proteomics. Expression proteomics seeks to recognise proteins that are differentially exhibited in tissues, and can be used as markers for disease detection, diagnosis and in the development of novel treatments; whereas functional proteomics involves the study of interactions of proteins with each other, with DNA and RNA, or as apparatus of bigger complexes. The ability to identify these

interactions is crucial for the characterisation of cellular processes (Joshi et al., 2011).

1.2.1.1 Importance and advantages of proteomics

Proteomics is one of a variety of approaches currently in use for the identification of molecular changes related to the progression of neoplastic disease. It has been widely used and strongly complements gene expression approaches (Righetti et al., 2005).

Proteome analysis is a direct measurement of proteins in terms of their presence and relative abundance (Wilkins et al., 1996). The overall aim of a proteomic study is the characterisation of the complex network of cell regulation. Neither the genomic DNA code of an organism nor the amount of mRNA that is expressed for each gene product (protein) yields an accurate picture of the state of a living cell (Lubec et al., 1999), which can be altered by many conditions, such as chemicals or drugs and radiation. Proteome analysis is required to determine which proteins have been conditionally expressed, how strongly, and whether any post-translational modifications (PTM) are affected. Two or more different states of a cell or an organism, for example healthy and diseased tissue, can be compared and an attempt made to identify specific qualitative and quantitative protein changes (Westermeier et al., 2008).

A fundamental scientific rationale for proteomics is that expression of a gene transcript is often a good indicator, but not equivalent to functional protein expression or activity. There are growing examples, which collectively show that the mRNA transcript level may not accurately reflect the true expression level of a functional protein, which is subjected to further translational and post-translational regulation (Westermeier et al., 2008). Proteomic approaches have the advantage of identifying changes in protein isoforms and PTM that are common in cancer and go undetected by microarray analyses of RNA expression (McCaw et al., 2007).

1.2.1.2 Top-down and bottom-up proteomics

Several sophisticated techniques including two-dimensional electrophoresis, imaging, mass spectrometry, and bioinformatics are used in proteomics to identify, quantify, and characterise proteins (Dominguez et al., 2007). In a proteomics study, two different approaches can be used: top-down proteomics and bottom-up proteomics.

Top-down proteomics is a method of protein identification that uses an ion trapping mass spectrometer to store an isolated protein ion for mass measurement and tandem mass spectrometry analysis (Sze et al., 2002, Kelleher, 2004). Proteins are typically ionised by electrospray ionisation and trapped in a Fourier transform ion cyclotron resonance (Bogdanov and Smith, 2005) or quadrupole ion trap mass spectrometer.

Bottom-up proteomics is a common method to identify proteins and characterise their amino acid sequences and PTM by proteolytic digestion of proteins, prior to analysis by mass spectrometry (Aebersold and Mann, 2003, Chait, 2006). The proteins may first be purified by a method such as gel electrophoresis, resulting in one or a few proteins in each proteolytic digest. Alternatively, the crude protein extract is digested directly, followed by one or more dimensions of separation of the peptides by liquid chromatography coupled to mass spectrometry, a technique known as shotgun proteomics (Washburn et al., 2001, Wolters et al., 2001). By comparing the masses of the proteolytic peptides, or their tandem mass spectra, with those predicted from a sequence database, peptides can be identified and multiple peptide identifications assembled into a protein identification.

1.2.1.3 Applications of proteomics

Researchers have long acknowledged that changes in genes or gene activity lead to cancer. However, it was difficult to understand the function of such specific genes and their interaction in communication networks. Their protein products have direct influence on the development of cancer, as it fundamentally arises due to aberrant signalling pathways. Identifying and understanding these changes is the

primary aim of cancer proteomics, also termed oncoproteomics. Its ultimate objective is to adapt proteomic technologies for regular use in clinical laboratories, for the purpose of diagnostic and prognostic categorisation of disease, as well as in assessing drug toxicity and effectiveness (Joshi et al., 2011).

The alterations in protein profiling, if specific for a certain cancer type, may serve as biomarkers for screening the disease in individuals. Alternatively, they may be used to design specific antibodies or fragments for disease treatment, or applied in diagnostic screenings. In combination with diagnosis chips, the direct proteome approach can save valuable time and resources in medical research and drug design (Wittmann-Liebold et al., 2006).

An important area in current cancer research is directed towards improving the molecular classification of cancer. Various subtypes exist for cancers arising in many organs, each with different histopathology and ultimately very different clinical outcomes. Here the task is to find markers, which can be used to differentiate cancers, with respect to organ of origin and benign *versus* aggressive behaviour, on the basis of its protein expression profile (Jones et al., 2002, Zhu et al., 2006).

Conventional diagnosis of cancer has been based on examination of the morphological appearance of stained tissue specimens in the light microscope. This method is subjective and depends on highly trained pathologists. Protein arrays and other proteomic approaches offer hope that cancer diagnosis could be objective and highly accurate, which can provide important information to clinicians regarding the most suitable treatment.

Proteomic analysis of cancers by using biomarker discovery techniques have provided new insights into the changes that occur in the early phases of tumourigenesis and represent a new resource for early-stage disease detection (Ornstein and Tyson, 2006). Identification of a sensitive and specific biomarker or a panel of biomarkers for the early detection of ovarian cancer could greatly increase the survival rate. In addition, these markers may present themselves as prognostic indicators or novel targets for cancer treatment (Asadollahi et al., 2010).

Evaluation of drug targets not only provides insights into the primary mechanism of action of a drug, but also the understanding of the side effects or toxicity, as a result of off-target interactions. It will further provide the rationale for optimisation of drug design to minimise toxicity. A better understanding of the long-term actions of anticancer drugs at the molecular level will definitely provide a broadened, informative and effectual approach (Joshi et al., 2011).

The identification of novel biomarkers that correlate with treatment response would allow therapy to be tailored on an individual patient basis. Ultimately, those patients, unlikely to respond to a particular treatment strategy, would be spared from serious life-threatening side effects for no therapeutic gain. Biomarkers may also provide information on new drug targets for future therapeutic intervention. Overcoming resistance to chemotherapy and radiotherapy would represent a major advance in the effective management of cancer (Smith et al., 2006).

1.2.1.4 Complete workflow of a proteomics experiment

A typical proteomic experiment, such as protein expression profiling, can be broken down into a series of steps (Figure 1.2). First, the experiment is designed so that the key parameters of the study have been vetted, transcribed and reviewed. Second, extraction, fractionation and solubilisation of proteins from a cell line, tissue or organism are carried out. Third, the levels of high-abundance proteins are reduced and weakly expressed proteins are enriched, to reduce the dynamic range in protein homogenates and increase the number of identified proteins. In the fourth step, gel-based separation of proteins in mixtures is followed by imaging and analysis to allow isolation and relative quantification of proteins. The gel extraction of protein spots is followed by identification by mass spectrometry (MS) and, finally, functional characterisation of the identified proteins is conducted (Taylor et al., 2008).

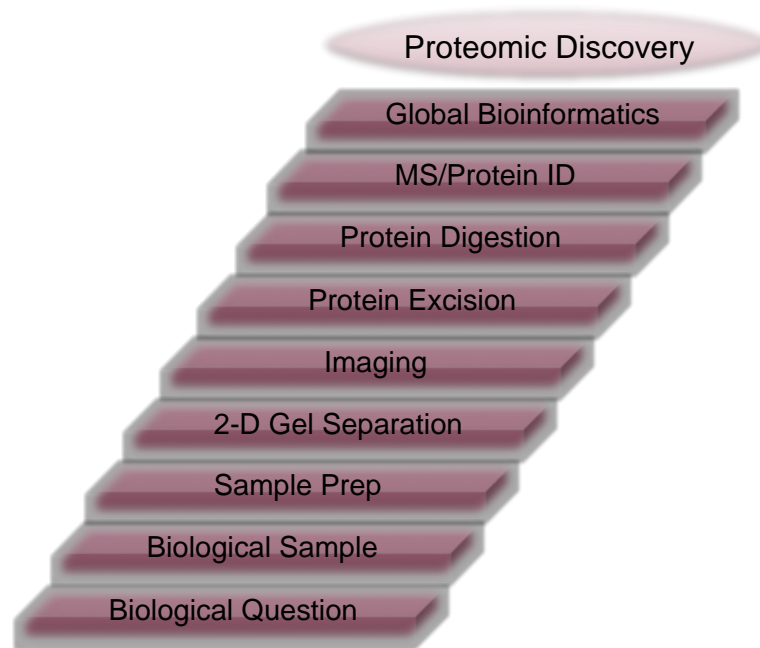


Figure 1.2 Complete workflow of a typical proteomics experiment.

The standard method for quantitative proteome analysis combines protein separation by high resolution two-dimensional electrophoresis (2-DE) with MS or tandem MS (MS/MS) identification of selected protein spots. Important technical advances related to 2-DE and protein MS have increased sensitivity, reproducibility and throughput of proteome analysis, while creating an integrated technology. It has facilitated the rapid characterisation of hundreds of proteins in a single gel (Chevalier, 2010).

There are many other proteomic-based techniques that have been developed in the latest years, such as difference gel electrophoresis (DIGE), gel-free liquid chromatography (LC)-MS and protein microarrays (Tonge et al., 2001, Wang and Hanash, 2003, Ardekani et al., 2008, Rabilloud, 2002).

1.2.1.4.1 Electrophoresis analysis

Electrophoresis is the process of moving charged molecules in solution by applying an electrical field across the mixture. Because molecules in an electrical field move with a speed dependent on their charge, shape, and size, electrophoresis has been

extensively developed for molecular separations. As an analytical tool, electrophoresis is simple and relatively rapid. It is used predominantly for analysis and purification of very large molecules such as proteins and nucleic acids, but can also be applied to simpler charged molecules, including charged sugars, amino acids, peptides, nucleotides, and simple ions. Highly sensitive detection methods have been developed to monitor and analyse electrophoretic separations (Hames and Rickwood, 1990).

Electrophoresis of macromolecules is normally carried out by applying a sample to a solution stabilised by a porous matrix. Under the influence of an applied voltage, different species of molecules in the sample move through the matrix at different speeds. At the end of the separation, the different species are detected as bands at different positions in the matrix. A matrix is required because electric current passing through the electrophoresis solution generates heat, which causes diffusion and convective mixing of the bands in the absence of a stabilising medium (Instruments, 1994).

The matrix can be composed of a number of different materials, including paper, cellulose acetate, or gels made of polyacrylamide, agarose, or starch. Polyacrylamide and agarose gels are the most common stabilising media used in research laboratories, and polyacrylamide is the most common matrix for separating proteins. In acrylamide and agarose gels, the matrix also acts as a size-selective sieve in the separation. At the end of the run the separated molecules can be detected in position on the gel by staining or autoradiography (Instruments, 1994).

Agarose and polyacrylamide gels are cross-linked, sponge-like structures in which the size of the pores is similar to the sizes of many proteins and nucleic acids. As molecules are forced through the gel by the applied voltage, larger molecules are retarded by the gel more than are smaller molecules. Gels can be tailored to sieve molecules of a wide range of sizes by appropriate choice of matrix concentration. The average pore size of a gel is determined by the percentage of solids in the gel

and, for polyacrylamide, the amount of cross-linker and total amount of polyacrylamide used (Hames and Rickwood, 1990).

Polyacrylamide, which makes a small-pore gel, is used to separate most proteins, ranging from <5,000 Da to >200,000 Da, and polynucleotides from <5 bases up to ~2,000 base pairs in size. Because the pores of an agarose gel are large, agarose is used to separate macromolecules such as nucleic acids, large proteins, and protein complexes (Instruments, 1994).

Polyacrylamide gel forms when a dissolved mixture of acrylamide and cross-linker monomers polymerise into long chains which are covalently cross-linked. The gel structure is held together by the cross-linker. The most common cross-linker is N-N'-methylenebisacrylamide (Instruments, 1994).

Atmospheric oxygen is a free-radical scavenger that can inhibit polymerisation. To avoid contact between oxygen and the gel, the acrylamide monomer solution is deaerated by purging it with an inert gas or by exposing it to a vacuum for a few minutes. Preparing solutions with a minimum of stirring, which introduces air, will reduce oxygen inhibition problems as well (Hames and Rickwood, 1990).

When the gel solution is poured into a mould, the top of the solution forms a meniscus. If the meniscus is ignored, the gel will polymerise with a curved top, which will cause the separated sample bands to have a similar curved pattern. To eliminate the meniscus and leave the upper surface of the gel flat, a thin layer of water or water-saturated n-butanol is carefully floated on the surface of the gel mixture before it polymerises. The layer of water or water-saturated n-butanol also excludes oxygen, which would otherwise inhibit polymerisation on the gel surface (Alberts et al., 2002). Alternatively, a flat-edged form, such as a comb, can be inserted into the top of the solution to give a mechanically flat surface (Hames and Rickwood, 1990).

Polymerisation of acrylamide gel can be initiated either by a chemical peroxide or by a photochemical method. The most common method uses ammonium

persulphate as the initiator peroxide and the quaternary amine, N,N,N',N'-tetramethylethylenediamine (TEMED) as the catalyst (Instruments, 1994).

Rapid polymerisation of acrylamide can generate too much heat, causing convection inconsistencies in the gel structure and occasionally breaking glass plates. This is a particular problem for high concentration gels. To prevent excessive heating, the concentration of initiator-catalyst reagents should be adjusted so that complete polymerisation requires 20 to 60 minutes (Hames and Rickwood, 1990).

SDS-PAGE

In SDS polyacrylamide gel electrophoresis (SDS-PAGE) separations, migration is determined by molecular weight. Sodium dodecylsulfate (SDS) is an anionic detergent that denatures proteins by wrapping around the polypeptide backbone. In so doing, SDS confers a net negative charge to the polypeptide in proportion to its length. When treated with SDS and a reducing agent, such as dithiothreitol (DTT), the polypeptides become rods of negative charges with equal 'charge densities' or charge per unit length (Alberts et al., 2002).

SDS-PAGE can resolve complex mixtures into hundreds of bands on a gel. The position of a protein along the lane gives a good approximation of its size, and, after staining, the band intensity is a rough indicator of the amount present in the sample. The ability to estimate size and amount of a protein leads to the various applications of SDS-PAGE: estimating purity and level of expression, immunoblotting, preparing for protein sequencing, and generating antibodies (Instruments, 1994).

Native-PAGE

Native-PAGE is an electrophoretic technique that is performed under non-denaturing conditions, i.e. in the absence of denaturing agents such as SDS, DTT and heat, unlike what happens in SDS-PAGE. Proteins in their denatured state assume a primary, linear structure, making it impossible to study conformational changes.

In native-PAGE, proteins keep their original structure and are separated on the basis of their size, shape and charge. While native-PAGE does not provide direct measurement of molecular weight, the technique can provide useful information about protein charge, conformation, self-association or aggregation, and the binding of other proteins or compounds. Since the protein retains its folded conformation, its size and mobility on a native gel will also vary with the nature of this conformation; more compact conformations will show higher mobility and larger structures will move slower (Robyt and White, 1987).

2D-PAGE

For many years there has been an increasing awareness of the limitations of one-dimensional electrophoretic separations for the analysis of complex protein mixtures. Proteins that have been resolved into perhaps 35 bands in a one-dimensional gel run may be further resolved into hundreds of components when separated in the second-dimension run (Gorg et al., 2000).

Since the recognition of the importance of 2D gel electrophoretic methods a great deal of work has been carried out to refine both the methodology of the separation technique itself and, equally important, to improve the analysis of two-dimensional gels. There has been increasing emphasis on the separation and characterisation of polypeptides on the basis of their isoelectric point and molecular mass. Gels have tended to become smaller and staining methods more sensitive thus allowing the analysis of much smaller samples (Hames and Rickwood, 1990).

All two-dimensional methods should be designed so that the polypeptides are separated on the basis of a different molecular property in each dimension. The commonest two-dimensional electrophoresis method for analysing mixtures of polypeptides is to separate the proteins in the first dimension on the basis of charge (isoelectric point) by isoelectric focusing and then to separate the polypeptides in the second dimension in the presence of SDS (SDS-PAGE) which, in most cases, gives a separation primarily on the basis of molecular weight of the polypeptides (O'Farrell, 1975).

One of the key problems of working with two-dimensional gels is the analysis and comparison of what can be very complex patterns that vary in only a relatively small area of the gel. Analysis of two-dimensional gels in its simplest form can be carried out by superimposing one photographic image over another. However, better results can usually be obtained by computer analysis of the gels. Although two-dimensional gel electrophoresis is a very powerful technique it is by no means infallible. Even after two-dimensional gel electrophoresis, some proteins may comigrate because either they are very similar proteins or because they are bound together very tightly. In addition, it is possible for protein mixtures to appear more heterogeneous than they really are as a result of artefactual changes during the preparation of the sample (Hames and Rickwood, 1990). Still, it is a remarkably sensitive and reproducible method and a valuable research tool (Westermeier et al., 2008).

The method of sample preparation depends on the aim of the research and is fundamental to the success of the experiment. Factors such as the solubility, size, charge, and isoelectric point (pI) of the proteins of interest enter into sample preparation. Sample preparation is also important in reducing the complexity of a protein mixture. The protein fraction to be loaded on a 2D-PAGE gel must be in a low ionic strength denaturing buffer that maintains the native charges of proteins and keeps them soluble (Bjellqvist et al., 1993).

Isoelectric Focussing

Proteins are charged molecules made up of amphoteric amino acids, which make them act as both acids and bases, depending on the pH of the local environment. Proteins often contain charged prosthetic groups such as phosphate or modified sugars. The net charge of a protein is the sum of the negative and positive charges on the molecule. For every protein, there is a pH at which its net charge is zero. This represents the isoelectric point (pI) of the protein (Instruments, 1994).

Proteins show considerable variation in pI, although pI values usually fall in the range of pH 3-12, with the majority falling between pH 4 and pH 7. A protein is positively charged in solution and is forced toward the cathode at pH values below

its pI. On the other hand, a protein is negatively charged and is driven toward the anode at pH values above its pI (Garfin and Heerdt, 2001).

When a protein is placed in a medium with a pH gradient and subjected to an electric field, it will initially move toward the electrode with the opposite charge. During migration through the pH gradient, the protein will either pick up or lose protons and its net charge and mobility will decrease and the protein will slow down until it reaches the pH equal to its pI. There, being uncharged, it will stop migrating. Factors that affect the pI of a protein include ionic strength, cofactors, temperature, and native or denaturing conditions. The sum of these factors results in a unique migration termination point (i.e., pI) that is visualised in a gel as a sharply focused band. Isoelectric focusing is the method used to accomplish this separation (Figure 1.3) (Garfin and Heerdt, 2001, Instruments, 1994).

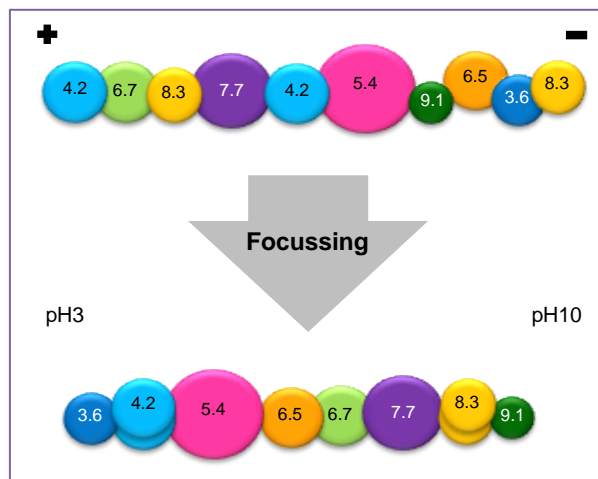


Figure 1.3 Isoelectric focussing of proteins.

Focusing is a steady-state mechanism with regard to pH. Proteins approach their respective pI values at differing rates but remain relatively fixed at those pH values for extended periods. By contrast, proteins in conventional electrophoresis continue to move through the medium until the electric field is removed. Moreover, in IEF, proteins migrate to their steady-state positions from anywhere in the system (Hames and Rickwood, 1990).

Thin gels made of either agarose or polyacrylamide are used as the support matrix for the migration and focusing (Instruments, 1994). Proteins are separated in the first dimension using slab gels, which have the advantage of all the samples being separated in the same gel and thus under identical conditions giving more reproducible separations. Irrespective of the format of the gel chosen for the first dimension, it is essential that the gel is sufficiently strong to withstand the manipulations required in preparing it for the second dimension (Hames and Rickwood, 1990). Charge-carrying molecules, either carrier ampholytes or acrylamido buffers, are mixed with the gel before pouring the gel and, in response to an electric field, establish the pH gradient in the gel (Instruments, 1994).

More recently, many proteomics laboratories are using immobilized pH gradient (IPG) strips to performed 2D-PAGE. The IPG method has numerous advantages over the older method (Gorg et al., 2004). A stable, linear, and reproducible pH gradient is crucial to successful IEF. IPG strips offer the advantage of gradient stability over extended focusing runs (Bjellqvist et al., 1982). IPG strips are much more difficult to cast than carrier ampholyte gels (Righetti, 1990); however, they are commercially available in a wide variety of pH ranges. Use of broad-range strips (for example, pH 3–10) allows the display of most proteins in a single gel, but with narrow-range and micro-range overlapping gradient strips, resolution is increased by expanding a small pH range across the entire width of a gel. Because proteins outside the pH range of the strip are excluded, more total protein amount can be loaded per strip, allowing more proteins to be detectable (Garfin and Heerdt, 2001).

The transition from first-dimension to second-dimension gel electrophoresis involves two steps. The first step is the equilibration of the resolved IPG strips in SDS reducing buffer. This process reduces disulfide bonds and alkylates the resultant sulfhydryl groups of the cysteine residues. Simultaneously, proteins are coated with SDS for separation on the basis of molecular weight. On the second step the equilibrated IPG strips are placed on top of the second-dimension gel and fixed with molten agarose solution to ensure good contact between the gel and the strip (Westermeier et al., 2008).

Second dimension – SDS-PAGE

Second-dimension separation is based on protein molecular weight, using SDS-PAGE (Figure 1.4). The proteins resolved in IPG strips in the first dimension are applied to second-dimension gels and separated by molecular weight perpendicularly to the first dimension (Garfin and Heerdt, 2001).

The pores of the second-dimension gel sieve proteins according to size because SDS coats all proteins essentially in proportion to their mass. The net effect is that proteins migrate as ellipsoids with a uniform negative charge-to-mass ratio, with mobility related logarithmically to mass (Westermeier et al., 2008).

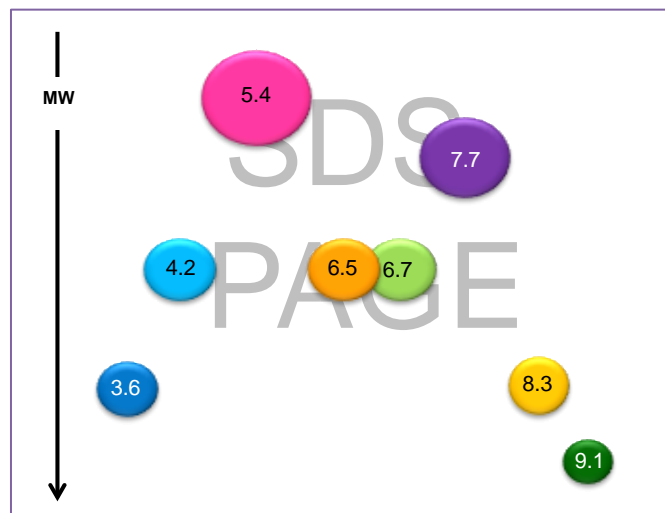


Figure 1.4 SDS-PAGE separation of proteins.

The choice for the SDS-PAGE second-dimension gel depends on the protein molecular weight range to be separated, as for SDS-PAGE. Single-percentage acrylamide gels generally give excellent resolution of sample proteins that fall within a narrow molecular weight range. On the other hand, gradient gels have some advantages: they allow proteins with a wide range of molecular weight to be analysed at the same time and the decreasing pore size along the gradient functions to sharpen the spots (Garfin and Heerdt, 2001).

Second-dimensional separations are always carried out in slab gels. Gels between 0.5-1.5 mm thick are not only easier to dry down after electrophoresis but they are

also easier to keep cool during electrophoresis. It is extremely important to ensure efficient cooling of the gel in order to obtain distortion-free and reproducible gel patterns (Hames and Rickwood, 1990).

The ability to run many gels at the same time and under the same conditions is important for the purpose of gel-to-gel comparison.

Staining

After the electrophoresis run is complete, the gel must be analysed qualitatively or quantitatively to answer analytical or experimental questions. Since most proteins and all nucleic acids are not directly visible, the gel must be processed to determine the location and quantity of the separated molecules (Instruments, 1994).

The most common analytical procedure is staining. The choice of staining method is determined by several factors, including desired sensitivity, linear range, ease of use, expense, and the type of imaging equipment available. The sensitivity that is achievable in staining is also determined by a number of factors, such as the amount of stain that binds to the proteins; the intensity of the coloration; the difference in coloration between stained proteins and the residual background in the body of the gel. Unbound stain molecules can be washed out of the gels without removing much stain from the proteins (Garfin and Heerdt, 2001).

All stains interact differently with different proteins. At present there is no ideal universal stain; no stain will stain all proteins in a gel in proportion to their mass. The only observation that seems to hold for most stains is that they interact best with basic amino acids. Sometimes proteins are detected after transfer to a membrane support by western blotting. For critical analysis, replicate gels should be stained with two or more different stains (Garfin and Heerdt, 2001).

Proteins are usually stained with Coomassie Brilliant Blue in a fixative solution, or, after fixation, with silver by a photographic-type development. Once the gel is stained, it can be photographed or dried on a transparent backing for a record of the position and intensity of each band (Instruments, 1994).

Coomassie blue staining

Coomassie Brilliant Blue R-250 appears to stain the broadest spectrum of proteins and is the most common stain for protein detection in polyacrylamide gels. Coomassie Brilliant Blue R-250 and G-250 are wool dyes that have been adapted to stain proteins in gels (Garfin and Heerdt, 2001). Coomassie Blue staining is able to detect about 1 µg of protein in a normal band. This staining method is based on non-specific binding of Coomassie Blue dye to proteins. Separated proteins are simultaneously fixed and stained in the gel, and then destained to remove the background prior to drying and photographing. The proteins are detected as blue bands on clear background. Absolute sensitivity and staining linearity depend on the proteins being stained (Instruments, 1994).

Silver staining

The silver stain systems are about 100 times more sensitive than Coomassie Blue staining, detecting about 10 ng of protein. Silver staining is based on binding of silver ions to sulfhydryl and carboxyl groups of the separated proteins. After electrophoresis, the proteins are fixed, exposed to silver nitrate, and developed to form a black precipitate of silver. The degree of development of the protein bands can be controlled with the amount of time the gel is exposed to the developer (Blum et al., 1987).

There are also some fluorescent stains for proteins, such as the SYPRO Ruby fluorescent staining, which is an endpoint stain with little background staining, it is sensitive and easy to use. This protein stain is sensitive to 1-10 ng, it is compatible with mass spectrometry and allows detection of proteins that are not stained well by other stains. Though, in order to visualise the proteins, specific equipment is required: UV or blue-light transilluminators (Garfin and Heerdt, 2001).

1.2.1.4.2 Mass spectrometry analysis

Once interesting proteins are selected by differential analysis or other criteria, they can be excised from gels and digested to release peptides for detailed sequence analysis by MS, leading to protein identification. The ability to precisely determine molecular weight by MS and to search databases for peptide mass matches has made high-throughput protein identification possible (Wilkins et al., 1996).

2D electrophoresis has the virtually unique capability of simultaneously displaying several hundred gene products. 2D gels are an ideal starting point for protein chemical identification and characterisation. Peptide mass fingerprint or sequence data can be derived following 2D electrophoresis with MS or amino acid sequence analysis (Ducret et al., 1996). The sensitivity of currently available instruments makes 2D electrophoresis an efficient ‘preparative’ analytical method. Most current protein identification depends on MS of proteins excised from gels or blots (Wilkins et al., 1996).

One of the most used methods to characterise biopolymers is the determination of molecular weight. Before the 1980s, the techniques that used to provide this information were electrophoresis, chromatography or ultracentrifugation and the results obtained were not very precise, because these methodologies depended also on characteristics other than the molecular weight, such as conformation and hydrophobicity. Therefore, the only chance of knowing the exact molecular weight of a macromolecule was its calculation based on the chemical structure (Hoffmann and Stroobant, 2007).

Ionisation methods

The development of MS, particularly the desorption ionization methods, allowed a first breakthrough for MS in the field of biomolecular analysis. In the 1990s, two new ionization methods, which were capable of analysing high-mass singly charged ions with good sensitivity and resolution, were developed and continue to revolutionise the role of MS in biological research. These methods are the electrospray ionization (ESI) (Fenn et al., 1989) and the matrix-assisted laser

desorption/ionization (MALDI) coupled to time-of-flight (TOF) analysers (Karas and Hillenkamp, 1988) and they allow the high-precision analysis of biomolecules of very high molecular weight (Hoffmann and Stroobant, 2007).

Mass analysers

There are four basic types of mass analyser currently used in proteomic research. These are ion trap, TOF, Q and Fourier Transform ion cyclotron analyser.

MS/MS combines two mass analysers and a collision cell to collect structural information for individual peptides. In this method, the first mass analyser acts to scan all the precursor ions from the ionisation source. The spectrum is used to select those ions of a particular m/z value. Such ions can be isolated and are dissociated by a process known as collision-induced dissociation (CID). CID energetically activates ions to dissociate. The selected ions enter a collision cell and are subjected to low energy collisions with neutral gas atoms, such as argon or nitrogen. As the ions become excited, covalent bonds fragment in a predictable manner. The fragmentation process predominates primarily along the mass spectrometer (Smith et al., 2006).

A TOF instrument is one of the simplest mass analysers. The m/z value is measured by determining the time required for the ions to traverse the length of the flight tube and strike a detector. Some TOF mass analysers include an ion mirror at the end of the flight tube, which reflects ions back through the flight tube to a detector. In this way, the ion mirror serves to increase the length of the flight tube. The ion mirror also corrects for small energy differences among ions. Both of these factors contribute to an increase in mass resolution (Graves and Haystead, 2002).

In recent years, several hybrid mass spectrometers have emerged from the combination of different ionisation sources with mass analysers. One example is the Q-TOF mass spectrometer. In this machine, the first Q and the Q collision cell of a triple-Q instrument have been combined with a reflector TOF section for measuring the mass of ions (Aebersold and Mann, 2003).

Ions pass through the mass analyser and are detected by an instrument, such as an electron multiplier, and the magnitude of current produced at the detector is used to determine the m/z value of the ion. MS data are recorded as spectra, which display ion intensity *versus* their m/z value.

This feature allows large analytes, such as proteins, to be measured in a mass analyser within a limited mass range. Current ESI-TOF instruments are able to measure proteins up to 80 kDa with 100-400 ppm mass accuracy by surveying only a mass range from 0-5000 m/z (Smith et al., 2006).

Applications of MS

MS has become one of the most extensively used analytical techniques in the life sciences, able to analyse different classes of biomolecules, such as peptides, proteins, nucleic acids, oligosaccharides and lipids (Siuzdak, 2003, Burlingame, 2005). It not only allows the precise determination of the molecular mass of peptides and proteins but also the determination of their sequence, especially if used with tandem mass techniques. Sequence information resultant from peptides and proteins fragmentation can be used for protein identification, *de novo* sequencing, and identification and localisation of post-translational or other covalent modifications (Aebersold and Mann, 2003).

In the study of peptides and proteins the most commonly used ionization methods are ESI and MALDI, both capable of forming stable ions and no fragments. ESI produces multiply charged ions, which allow the detection of large molecules with conventional mass spectrometers such as quadrupole, ion trap and magnetic instruments. Its detection limit depends on several factors, for example the nature of the sample, its preparation and purity, the instrument used and the skill of the operator. The detection limit for peptides and proteins is situated between femtomoles and picomoles (Hoffmann and Stroobant, 2007).

Limitations of MS

Concentration of the sample and complexity of the contaminants are two factors that play an important role in both sensitivity and the mass accuracy. Biological samples are often diluted solutions of peptides or proteins containing a great number of contaminants. These two problems, dilution and contaminants, are not easy to handle, particularly when the total amount of sample is low, such as picomoles. These contaminants can reduce the abundance of the ions from the compound of interest or even totally suppress them. They can also result in the formation of adduct ions, further reducing the sensitivity by distribution of the ion current over various species and they may complicate or reduce the accuracy of the molecular mass determination (Hoffmann and Stroobant, 2007). The low concentration of the compound of interest is also an important problem in biological samples, because it has a marked influence on the observed spectra. The volumes needed for the analysis are very low, in the microliter range, and only part of it is actually consumed during the analysis (Siuzdak, 2003).

In order to minimise these problems, a separation method should be used for both purification and separation of the sample. The classical method for peptides and proteins is a reverse-phase liquid chromatography preparation of the sample before the MS analysis. The use of separation methods on-line with the mass spectrometer are often preferred. The most frequent separation methods coupled to electrospray ionization/mass spectrometry (ESI-MS) are micro- or nano-HPLC systems (Siuzdak, 2003).

1.2.1.4.3 Global bioinformatics

Mass spectrometry data

MS can generate two types of data, which can be used for protein identification. A characteristic mass spectrum is known as a peptide mass fingerprint, which is a list of masses for the peptides in a sample. The peptide fingerprint obtained is compared with the predicted masses of peptides from the theoretical digestion of all proteins in a database. If enough peptides from the real mass spectrum and the

theoretical spectrum match in mass, the protein can be identified. Unfortunately, a single peptide is rarely unique to one protein, thus several peptides (more than three) that are derived from the same protein are typically required for identification. PMF is currently a method of choice for identification, because it combines a conceptually simplistic approach with robust high-throughput instrumentation (usually MALDI-TOF MS).

Unfortunately, there are several limitations in technique application. Peptide mass redundancy results in ambiguity of protein identification. Post-translationally modified proteins also reduce the success of PMF, since peptides from a modified protein will not match the masses of the peptides from the unmodified protein in the database. The presence of contaminants, such as keratin and peptides from the autolysis of trypsin, may also be problematic. Moreover, not all proteins are able to be identified by PMF alone. The full lengths of a large percentage of human proteins are not represented in databases. In addition, small proteins may not yield a sufficient number of peptides from the tryptic digest, which leads to an ambiguous identification. In such cases, it is preferable to subject selected ions to further fragmentation, which can provide the amino acid sequence of the peptide.

The amino acid sequence for a specific peptide can be deduced by MS/MS. A higher level of confidence can be assigned to protein identification when searching databases with MS/MS data (Smith et al., 2006).

Database searching

The goal of database searching is to be able to quickly and accurately identify large numbers of proteins. The success of database searching depends on the quality of the data obtained in the mass spectrometer, the quality of the database searched and the method used to search the database.

The most specific type of database searching for protein identification uses peptide amino acid sequence. If the amino acid sequence of a peptide can be identified, it can be used to search databases to find the protein from which it was derived. One method which uses this information is peptide mass tag searching. In this method, a

partial amino acid sequence is obtained by interpretation of the MS/MS spectrum (the sequence tag). That information is combined with the mass of the peptide or the masses of the peptides on either side of the sequence tag, when the sequence is not known. Also included in the search is the type of protease used to produce the peptides.

In addition, one of the biggest advantages of using MS/MS to obtain peptide amino acid sequence is that, unlike PMF, it is compatible with protein mixtures (Graves and Haystead, 2002). The major disadvantage of performing MS/MS is that the process is not easily automated.

MS is the most efficient way to identify proteins. This is achieved by comparison of the data obtained from the MS with those predicted for all the proteins contained in a database. The efficiency of the method results from the development of MS into a rapid and sensitive method to analyse peptides and proteins and also from the availability of larger and larger databases (Lin et al., 2003, Kolker et al., 2006).

The widely used strategy for protein identification is depicted in Figure 1.5. In this strategy, the protein is cleaved using an enzyme such as trypsin and the mixture then is analysed by MS to obtain the molecular masses of the largest possible number of peptide sequences resulting from MS/MS. In this approach, based on MS/MS, the observed masses of fragment ions are compared with those expected for the various proteolytic peptides deduced from each protein contained in the database. This method uses the SEQUEST or MASCOT algorithms for this comparison and is called peptide fragmentation fingerprinting (PFF). The partial sequence information that is contained in a tandem mass spectrum of a peptide is more specific than the information based on the precise molecular mass of this peptide. In fact, two peptides with the same amino acid contents but different sequences have the same molecular mass but different fragmentation patterns (Hoffmann and Stroobant, 2007).

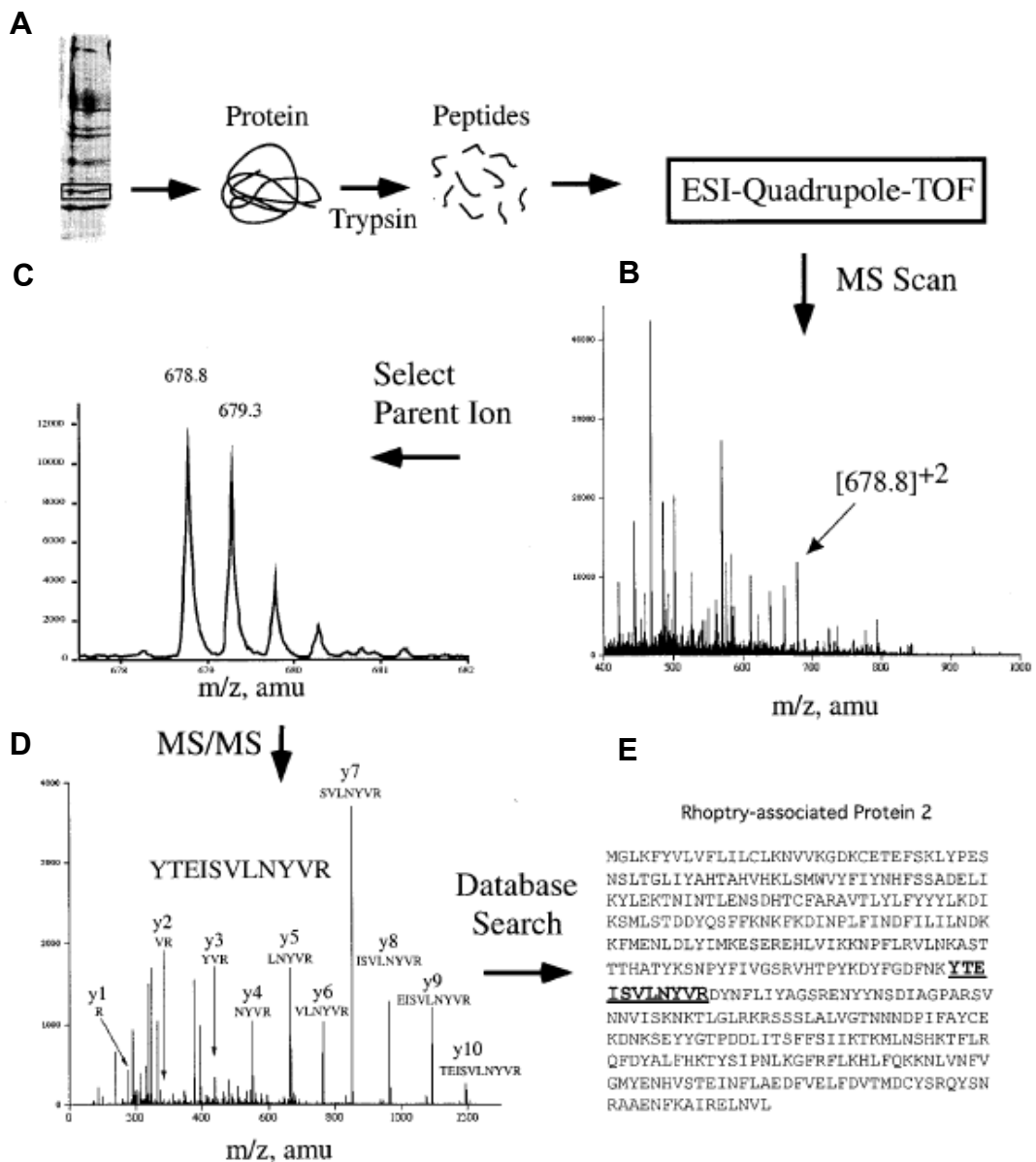


Figure 1.5 Protein identification by MS/MS. [A] Proteins from *Plasmodium falciparum* were resolved on a one-dimensional gel electrophoresis (1-DE), excised and in-gel digested with trypsin. The resulting peptides were ionised by ESI and analysed by a Q-TOF mass spectrometer. [B] The MS spectrum produced was scanned and a parent ion of 678.8 was selected for fragmentation. [C] An enlargement of the parent ion peak at 678 is shown. A mass difference between the peaks of 0.5 Da indicates that the peptide is doubly charged. [D] MS/MS scan of the 678 parent ion and analysis of the daughter ions produced. All y-ions (except for y-11) produced from fragmentation of the peptide are shown. [E] Identification of rhopty-associated protein-2 using BioAnalyst software. (Graves and Haystead, 2002)

1.2.2 Target validation

Target validation is a crucial step in the drug discovery process and has been proposed as the major reason for the later failure of drug candidates. Most drugs are inhibitors that block the action of a particular protein target. However, the only way to be completely certain that a protein is instrumental in a given disease is to test the hypothesis in humans. Though, for obvious reasons such clinical trials cannot be used for initial drug discovery, which means that a potential target must undergo a validation process (Metcalf and Dillon, 2006).

1.2.2.1 Methods of target validation

Computer models are a fast, relatively cheap choice for initial screening of both targets and potential drugs. These models usually focus on how the two types of candidate structures interact with each other. Another route to target validation hinges on disrupting gene expression to reduce the amount of the corresponding protein, and so identify the physiological role of the target. However, one disadvantage of doing target validation at the genetic level is that many genes produce several different proteins with different functions. Proteomics overcomes this drawback, making it easier to distinguish and target just one specific form of a protein (Metcalf and Dillon, 2006).

Western blotting is a widely used technique for the detection and analysis of proteins based on their ability to bind to specific antibodies. It was first described by Towbin et al. in 1979 and has since become one of the most commonly used methods in life science research. This technique is accomplished rapidly, using simple equipment and inexpensive reagents, which makes it a good option for target validation. The specificity of the antibody-antigen interaction enables for a target protein to be identified in the midst of a complex protein mixture (Mahmood and Yang, 2012).

1.2.3 Assay development

Once a biological target for drug discovery has been validated, an assay format needs to be developed. The aim of the assay is to enable characterisation of novel compounds and obtain potency of these compounds against the target in question. With the information gained from the potency assays and using similar clusters of compounds, structure activity relationships (SAR) can be determined. This will drive the production of future lead compounds for the target and further optimisation.

1.2.3.1 Methods for assay/screen development

The type of assay format to use has to be carefully determined depending on a variety of factors. The primary factor is the choice of target itself and the type of activity that is required to be measured. Another factor in assay choice depends on the number of compounds that will be screened. Libraries of compounds can vary from tens to millions of compounds, particularly within big pharmaceutical companies (Sittampalam et al., 2004, Vogel, 2002).

Before an assay can be used in a screening method, it has to be proven to be sensitive with respect to the target, for example known inhibitors have to show reproducibility to literature values. Kinetic parameters have to be determined to ensure that the assay is functioning correctly. The assay should have a robust signal change to enable detection of activity, when compared to background noise. It has to be stable to allow practicable numbers of compounds to be tested within a set timeframe. The cost of the reagents required is also an important factor, combined with the consumption of the target protein, which can be very time consuming and costly to produce and purify. All these factors have to be balanced when determining the most suitable assay format to use (Sittampalam et al., 2004).

There are many different types of assay format available, such as biophysical, biochemical and cell based assays. Typically multiple assay formats are combined together to build a screening sequence or cascade. The types of technology and techniques used for assay development vary considerably, with examples including fluorescent, luminescent, radioactive and absorbance methods (Vogel, 2002).

1.3 General Aims & Objectives

The general aims of this project were to develop, optimise and apply method approaches capable of aiding target identification, validation and assay development, in order to discover novel protein targets directly related to disease and screen inhibitors of known protein targets.

With these aims in mind, the first objectives were to understand the importance of proteomics in research, recognise its different applications in biomarker and target discovery and know various techniques frequently used in proteomic studies. These were followed by the development and optimisation of the proteomic method of choice: a 2D-PAGE protein separation proceeded by identification by LC-MS/MS and database searching. Another objective of this project was to acknowledge the use of Western blotting as a validation method for protein targets and biomarkers. Furthermore, this project also aimed to appreciate the need for a continuous assay development as a powerful tool in the drug discovery process. As a result, the development and optimisation of a robust and reliable screening assay for inhibitors of a widely recognised protein target in cancer research was another objective of this project. The optimised method approaches would, therefore, be applied to the following research purposes:

- Elucidation of a focused subsection of the proteome hypothetically relevant to mammalian reproduction, using a glycomimetic affinity-enrichment proteomic strategy applied to the study of mouse testis tissue;
- Identification of protein targets of chemoresistance in ovarian cancer by comparison of the protein expression profile of sensitive and resistant human ovarian cancer cell lines and tissues;
- Development of a screening assay for the functional characterisation of Heat Shock Protein 90 targeted compound.

Chapter 2 – MATERIALS & METHODS

This chapter includes a detailed description of all the major techniques utilised in the different studies presented. Optimisation and troubleshooting strategies for sample preparation and methods of protein separation, visualisation and identification can be found in Appendix.

2.1 Chemicals and reagents

Chemicals and reagents were purchased as mentioned below, unless stated otherwise in the methods description. The source of all the equipment used in the following experiments is specified after each one of them in the descriptions ahead.

Tris, urea, DTT, Triton X-100, glycerol, bromophenol blue, iodoacetamide, acrylamide/bisacrylamide, SDS, ammonium persulphate, TEMED, agarose, trichloroacetic acid, acetic acid, sodium thiosulphate, silver nitrate, formaldehyde, EDTA disodium salt, glycine, sodium chloride (NaCl), Tergitol-type NP-40 (NP-40), phenylmethanesulfonyl fluoride (PMSF), aprotinin, leupeptin, sodium orthovanadate (Na_3VO_4) and sodium cholate were purchased from Sigma-Aldrich (UK). CHAPS, methanol, ethanol, acetone, sodium carbonate, formic acid, water, hydrochloric acid and acetonitrile were from Fisher Scientific (UK). Thiourea, ampholytes solution and ammonium bicarbonate were obtained from Fluka (UK). All solvents used for mass spectrometry analysis were HPLC grade. The water used in all the experiments was ultrapure water.

2.2 Biological samples

Several different types of biological samples were used in the various experiments performed.

On a first stage, canine liver and lung tissues were used to develop and optimise the 2D-PAGE method. Normal and tumour tissue pairs from the same animal were collected during biopsy by Dr. Stephen Baines' group at The Royal Veterinary College, University of London. Tissue samples were snap frozen in liquid nitrogen. Upon arrival, samples were weighted and randomly cut into 100 mg portions, which were stored at -80 °C until used.

For the proteomics study of infertility, mouse testes from C57BL/6 male mice aged 8-10 weeks were obtained with the help of Dr. Schatzlein's group. Mice were sacrificed by elevating CO₂ concentration. All animal studies were performed in accordance with the UK Home Office Animals (Scientific Procedures) Act 1986. Mouse testes were dissected and immediately frozen in liquid nitrogen until further use.

Ovarian cancer cells and tissue protein samples were kindly supplied by Dr. Helen Coley from the Faculty of Health and Medical Sciences, University of Surrey, for the proteomics study of ovarian cancer. The parental ovarian cancer cell line model PEO1 was used as drug sensitive reference cell line. Novel drug resistant models, derived from the parental line, with *in vitro* acquired resistance to paclitaxel (taxol) – PEO1 TaxR – and carboplatin – PEO1 CarbR – were used alongside their respective drug sensitive parental counterparts. The ovarian tissues – SOV-1, SOV-2, SOV-3, SOV-4, SOV-5 – represented 5 different patients, 4 of which were diagnosed with ovarian cancer and 1 suffered from endometriosis, a benign gynaecologic condition.

For the functional characterisation of Hsp90 targeted compounds, human Caucasian breast adenocarcinoma (MCF-7) cells were obtained from the European Collection of Cell Cultures (ECACC), cultured and treated with Hsp90 inhibitors by Dr. Schatzlein's group from the Department of Pharmaceutical and Biological Chemistry of the UCL School of Pharmacy.

2.3 Sample preparation

Sample preparation is one of the most important steps of every method. It refers to the ways in which a sample is treated prior to its analysis, in order to isolate the analyte from other interfering species and to prepare it for the technique being used. In biochemistry, sample preparation involves extraction and purification or concentration of proteins prior to their separation and further analysis. The method of protein extraction depends on the type of biological sample used and is different whether the proteins are extracted from mammalian cells or mammalian tissues. In turn, the method of purification or concentration depends upon the level of protein purity required, the complexity of the sample and the type of contaminants present, as well as on the compatibility of the solvent or buffer system with the subsequent techniques (Westermeier et al., 2008). The following sections include a few techniques frequently used in sample preparation for protein analysis.

2.3.1 Protein extraction from mammalian cells

Prior to the extraction of proteins from mammalian cell lines, cells were harvested from the cell culture flasks. Cell harvesting and protein extraction procedures are described below.

2.3.1.1 Cell harvesting

Cell confluence was checked using a light microscope before harvesting. The growth medium was aspirated and the cell monolayer was rinsed twice with phosphate-buffered saline (PBS, Oxoid, UK). Cells were harvested by trypsinization with 0.05 % Trypsin-EDTA solution (Gibco, Invitrogen, UK) by adding the trypsin solution and incubating at 37 °C for a few minutes. Alternatively, cells can be scraped using a sterile plastic scraper with washing of the slurry using PBS. The trypsin solution was neutralised with complete tissue culture medium and cells were collected into 1.5 mL sterile microfuge tubes. Cells were pelleted by centrifugation at 13,000 rpm for 10 min at room temperature in a Technico Maxi centrifuge (Fisher Scientific, UK).

Supernatants were discarded and pellets were washed 3 times with ice cold PBS, before being stored dried at -80 °C until further use.

2.3.1.2 Protein extraction from mammalian cells – Method 1

Stored dried pellets were thawed and resuspended in 200 µL lysis buffer (50 mM Tris-HCl pH 8.3; 0.5 % SDS) containing protease inhibitor cocktail (Amersham Biosciences, UK). The cellular mixtures were boiled for 10 min at 100 °C and spun at 13,000 *g* for 30 min at 4 °C in a Biofuge Fresco centrifuge (Heraeus, UK). The supernatants with dissolved proteins were transferred to clean microfuge tubes and protein concentrations of cell lysate samples were determined.

2.3.1.3 Protein extraction from mammalian cells – Method 2

Stored dried pellets were defrosted and homogenised in 200 µL lysis buffer (50 mM Tris-HCl pH 7.5, 150 mM NaCl, 1 % NP-40, 0.2 % SDS, 1 mM PMSF, 10 µg/mL aprotinin, 10 µg/mL leupeptin, 1 mM sodium orthovanadate (Na₃VO₄); lysis buffer should be freshly prepared each time and used within approximately 30 min), disaggregating the pellets using the pipette tip and leaving on ice for 10 min. Cells were further lysed using a 23 gauge needle or using a tip sonicator, holding the tube in ice and avoiding excessive frothing. Cell lysates were left on ice for a further 20-30 min. Tubes were spun down at 500 *g* for 10 min at 4 °C to remove nuclei and unbroken cells and the supernatants were transferred to fresh tubes and labelled appropriately. Protein concentrations of the whole cell lysate samples were determined lysates were stored at -80 °C until further use.

2.3.2 Protein extraction from mammalian tissues

Proteins were extracted from mammalian tissues using distinct extraction methods, depending on the animal and tissue type under study.

2.3.2.1 Protein extraction from canine lung and liver tissues

Approximately 100 mg of normal lung/liver and tumour lung/liver tissues were homogenised separately using an Ettan sample grinding kit (Amersham Biosciences, UK). Samples were firstly washed with extraction solution (40 mM Tris-HCl, pH 8.0) to remove blood. After removing as much of the liquid as possible from the grinding resin pellet by centrifugation at 14,000 rpm, samples were put into contact with the grinding resin and homogenised in 200 µL of extraction solution (40 mM Tris-HCl, pH 8.0) containing Ettan protease inhibitor mixture (EDTA-free, Amersham Biosciences, UK), using a pestle to thoroughly grind the samples for about 20 min. Samples were vortex mixed and incubated for 30 min on ice. Lysis buffer (100 µL; 9.5 M urea, 4 % CHAPS, 5 mM DTT, 0.1 % Triton X-100) was added thereafter and samples were homogenised and incubated for 1 h on ice, followed by centrifugation to remove resin and cellular debris at 13,000 *g* for 30 min at 4 °C in a Biofuge Fresco centrifuge (Heraeus, UK). Supernatants were carefully transferred to clean tubes and stored at -80 °C until further use.

2.3.2.2 Protein extraction from mouse testis tissues

Mouse testis tissue (161.6 mg) was homogenised with a sample grinding kit (Amersham Biosciences, UK), using one grinding tube per 100 mg of tissue sample. The grinding tubes were briefly centrifuged at maximum speed to pellet the grinding resin and the liquid was removed from the grinding resin pellet. Each piece of solid tissue of up to 100 mg was placed into a 1.5 mL tube and washed with cold PBS, after which it was transferred to a grinding tube. Testis tissue was homogenised in 1 mL PBS containing 0.5 % sodium cholate and 1 % protease inhibitor (Amersham Biosciences, UK), using a pestle to thoroughly grind the sample for 15 to 60 min on ice. Tissue homogenates were lysed by 3 cycles of freeze/thawing (dry ice/37 °C). In order to remove insoluble materials, homogenates were spun at 13,000 *g* for 20 min at 4 °C in a Biofuge Fresco centrifuge (Heraeus, UK). Supernatants were collected and transferred to clean tubes. Solubilised proteins were loaded on to the affinity columns immediately.

2.3.2.3 Protein extraction from human ovarian tissues

Ovarian tissues were individually weighed and washed with 40 mM Tris-HCl, pH 8.0 to remove excess blood. Tissue samples were cut into 2-5 mm pieces, which were placed into microfuge tubes on ice and a suitable volume of modified lysis buffer (9.5 M urea, 4 % CHAPS, 0.1 % Triton X-100, 5 mM DTT) containing protease inhibitor cocktail (Amersham Biosciences, UK) was added to each tube. Tissues were homogenised using steel beads in a TissueLyser (Qiagen, UK) for 2 x 2 min at a frequency of 30.0 cycles 1/s. After homogenisation, tissue lysates were transferred to clean tubes, followed by centrifugation to remove cellular debris at 13,000 *g* for 30 min at 4 °C in a Biofuge Fresco centrifuge (Heraeus, UK). The supernatants were carefully transferred to other tubes and stored at -80 °C until further use.

2.3.3 Determination of protein concentration

Protein concentrations of all cell and tissue lysate samples were determined using the RCDC Protein Assay Kit (Bio-Rad, UK). Bovine plasma γ -globulin (Bio-Rad, UK) was used as standard and serial dilutions were prepared from the initial stock concentration of 1.5 mg/mL, using the same buffer as for the samples, in order to build a standard curve. A blank without protein was prepared in parallel with the samples for instrument calibration. The assay was performed in triplicate and in accordance to the manufacturer's instructions.

Briefly, an aliquot of 25 μ L of each standard and sample was added to 125 μ L of RC reagent I and the mixture was homogenised. After 1 min incubation at room temperature, 125 μ L of RC reagent II were added to each tube and the mixture was homogenised again. Mixtures were centrifuged at 14,000 rpm for 5 min and the supernatants were discarded. Reagent A', prepared by adding 5 μ L of DC reagent S to each 250 μ L of DC reagent A that would be needed for the run, was used to resuspend the pellets. A volume of 127 μ L of that reagent was added to standards and samples, and the mixtures were vortex mixed and incubated at room temperature for 5 min, or until precipitate was completely dissolved.

Finally, and after homogenising the mixtures once again, 1 mL of DC reagent B was added to each tube and vortex mixed immediately, followed by incubation at room temperature for 15 min. Absorbance values were measured at 750 nm in a spectrophotometer (Biochrom Libra S22), and the linear regression and protein concentrations calculated using Excel 2007.

2.3.4 Protein precipitation

For protein precipitation, two different approaches were followed, although they share some common points. The detailed procedures are presented below.

2.3.4.1 Trichloroacetic acid and acetone precipitation of proteins

Prior to 2D-PAGE, samples were subjected to treatment with trichloroacetic acid (TCA) in order to remove contaminants and concentrate proteins of interest. Samples were thawed and mixed with 4 volumes of 20 % TCA. The mixtures were incubated on ice for 1 h and then centrifuged at 13,000 rpm for 10 min, at room temperature, to pellet the precipitate. TCA was removed and pellets were washed with 300 μ L of 90 % ice cold acetone and centrifuged at 13,000 rpm for a further 10 min, at room temperature. Acetone was then removed. This washing/centrifugation step was repeated to completely remove TCA and, finally, pellets were allowed to air-dry.

2.3.4.2 2D clean-up kit

In alternative to trichloroacetic acid and acetone precipitation of proteins, before 2D-PAGE, cell and tissue lysates were pre-treated with the ReadyPrep 2-D Clean Up Kit (Bio-Rad, UK) to remove contaminants, such as salts, lipids, carbohydrates and nucleic acids, and concentrate proteins. Protein samples (50 μ g) were transferred to 1.5 mL microfuge tubes and distilled water was added to obtain a final volume of 100 μ L per sample.

Precipitation was started by adding 300 μ L of precipitating agent 1, mixing well and incubating the protein samples on ice for 15 min. Then, 300 μ L of precipitating

agent 2 were added to the mixtures and mixed well. Tubes were centrifuged at 13,000 *g* for 5 min to form a tight pellet and, without disturbing the pellets, supernatants were removed and discarded. Tubes were centrifuged once again for a few seconds to collect any residual liquid at the bottom of the tubes, which was carefully discarded. Pellets were washed with 40 μ L of wash reagent 1 and tubes were centrifuged for 5 min at 13,000 *g*. After removing and discarding the supernatants, 25 μ L of distilled water were added on top of the pellets, which were quickly washed by vortex mixing. A volume of 1 mL of wash reagent 2, pre-chilled at -20 °C for at least 1 h, was added to the mixtures, followed by 5 μ L of wash 2 additive. Tubes were homogenised for 1 min and incubated at -20 °C for 30 min, during which mixtures were homogenised for 30 sec every 10 min.

After the incubation period, tubes were centrifuged as before at 13,000 *g* for 5 min, the supernatants were discarded, and the centrifugation was repeated for a few seconds and any remaining wash was removed. Pellets were allowed to air-dry at room temperature for no more than 5 min and were resuspended in an appropriate volume of 2D rehydration buffer.

2.4 Methods of protein separation

Depending on the aim of each study, proteins were separated according to one of the following electrophoretic methods: SDS-PAGE, native-PAGE and 2D-PAGE. Their procedures are described in the sections ahead.

2.4.1 SDS-PAGE

Samples were prepared by adding 1x SDS sample buffer (60 mM Tris-HCl pH 6.8, 2 % SDS, 10 % glycerol, 0.01 % bromophenol blue) (Laemmli, 1970) and 10 mM DTT to the protein samples previously diluted in distilled water. The concentration of sample in the solution should be such as to give a sufficient amount of protein in a volume not greater than the size of the sample well. Blanks were prepared in the same manner, but containing only 1x SDS sample buffer, 10 mM DTT and distilled water. All sample and blank mixtures were homogenised and incubated at 95 °C for 10 min. Samples and blanks, as well as a molecular weight marker (Precision Plus Protein Standards, Bio-Rad, UK), were loaded into the wells of an SDS-polyacrylamide gel prepared in advance. An example of the composition of a 10 % SDS-polyacrylamide gel is illustrated in Table 2.1.

Table 2.1 Example of the composition of an SDS-polyacrylamide gel. Gel formed by a 10 % resolving gel and a 6 % stacking gel. Volumes used for the preparation of one gel.

Components of the gel	10 % Resolving gel	6 % Stacking gel
Distilled water	3.8 mL	2.9 mL
40 % Acrylamides solution	2 mL	0.75 mL
Resolving buffer 1.5 M Tris-HCl pH 8.8	2 mL	—
Stacking buffer 0.5 M Tris-HCl pH 6.8	—	1.25 mL
10 % SDS	80 µL	50 µL
10 % Ammonium persulphate	80 µL	50 µL
TEMED	8 µL	5 µL
	8 mL	5 mL

The resolving gel was prepared by pouring 4.5 mL of the resolving gel solution between two glass plates (spacer plate and short plate) fixed in a casting frame and,

immediately after, by adding distilled water on top of the gel to the top of the glass, and leaving it to set for 1 h. After this period of time, the overlaying water was drained off and the stacking gel solution was poured onto the top of the set gel. The comb was placed taking care not to form air bubbles, and the gel was left to set for 30 min, after which it was ready to load. Precast gels, Mini-Protean TGX Precast Gel, any kD, 10-well comb, 30 μ L/well (Bio-Rad, UK) were sometimes used as an alternative to handcast gels.

After standing the gel vertically in the electrophoresis cell and filling the reservoirs with 1x Tris-Glycine-SDS running buffer (0.025 M Tris-HCl, 0.192 M glycine, 0.1 % SDS at pH 8.3; Bio-Rad, UK), 10 μ L of each sample, blank and the molecular weight marker were loaded into the wells of the gel. Electrophoresis was then started and carried out using a Mini-Protean II Tetra Cell System (Bio-Rad, UK) at 40 V until the blue dye had reached the main gel, and then increased to 100-150 V until the dye front had reached the bottom of the gel. The migration of bromophenol blue, present in the sample buffer, was used to monitor the electrophoresis progress.

2.4.2 Native-PAGE

Two glass plates (spacer plate and short plate) per gel were thoroughly cleaned and dried, fixed in a casting frame and clamped in an upright, level position. The separating gel mixture was prepared as shown in Table 2.2, mixed gently and immediately poured into the glass chamber without generating air bubbles. As no stacking gel was used, the separating gel solution was poured until the top of the chamber and the well-forming comb was inserted. Gel was left to polymerise for 1 h.

Table 2.2 Example of the composition of a native-polyacrylamide gel. Gel formed by an 8 % separating gel and no stacking gel. Volumes used for the preparation of one gel.

Components of the gel	8 % Separating gel
Distilled water	5.5 mL
40 % Acrylamides solution	2 mL
Resolving buffer 1.5 M Tris-HCl pH 8.8	2.5 mL
Stacking buffer 2.5 M Tris-HCl pH 6.8	—
10 % Ammonium persulphate	50 μ L
TEMED	10 μ L
	10 mL

While the gel was polymerising, samples were prepared. Diluted protein samples were mixed with the same volume of 2x sample buffer (2.5 M Tris-HCl pH 6.8, 20 % glycerol, 0.02 % bromophenol blue), or dry samples were dissolved in 1x sample buffer. Blanks were prepared just with 1x sample buffer. When the separating gel had polymerised, the comb was removed without distorting the shapes of the wells and the gel was released from the casting frame and installed in the electrophoresis apparatus. The reservoirs were filled with reservoir buffer (0.192 M glycine, 0.025 M Tris-HCl pH 8.3) and 10 μ L of each sample, blank and the molecular weight marker (Precision Plus Protein Standards, Bio-Rad, UK) were loaded into the wells of the gel. Electrophoresis was then started and carried out using a Mini-Protean II Tetra Cell System (Bio-Rad, UK) at 4 °C and 150 V, until the dye front had reached the bottom of the gel. The migration of bromophenol blue, present in the sample buffer, was used to monitor the electrophoresis progress.

2.4.3 2D-PAGE

Proteins were separated by 2D-PAGE on immobilised pH gradient (IPG) strips and according to their isoelectric point in the first dimension, followed by separation based on the molecular weight using SDS-PAGE in the second dimension. The detailed procedures are given below.

2.4.3.1 First dimension: isoelectric focussing (IEF)

Isoelectric focussing was performed using Protean IEF Cell (Bio-Rad, UK) with 7 and 11 cm ReadyStrips, pH 4-7, pH 5-8, pH 3-10 and pH 3-10 non-linear (Bio-Rad, UK). Pellets resulting from the pre-treatment were resuspended in rehydration buffer I (7 M urea, 2 M thiourea, 4 % CHAPS, 0.5 % ampholytes solution, pH 3-10) or in rehydration buffer II (7 M urea, 2 M thiourea, 4 % CHAPS, 20 mM DTT, 0.5 % ampholytes solution, pH 3-10) to a total volume of 125 or 200 μ L, depending on the size of the strip (7 or 11 cm, respectively). Mixtures were centrifuged at 14,000 rpm for 5 min at room temperature and the supernatants were loaded into a rehydration tray or a focussing tray, depending on the type of rehydration performed (passive or active, respectively). The IPG strips were placed above the mixtures with the gel side facing down, making sure the entire strips were wetted and without air bubbles, which could interfere with the even distribution of the sample in the strip. The liquid was allowed to distribute for about 1 h before covering the strips with mineral oil (Bio-Rad, UK), to prevent evaporation of the samples, and rehydration was started.

The rehydration procedure was performed with no voltage applied (passive rehydration) or at 50 V (active rehydration) for 12-16 h (overnight). After rehydration was complete, two electrode wicks per strip were wetted with 5-8 μ L of ultrapure water and placed below the IPG strips, covering each electrode of the focussing tray. In case of passive rehydration, before starting the focussing steps, the IPG strips were removed from the rehydration tray with a pair of forceps, placed on a dry tissue paper with the gel side facing up and covered with wet tissue paper, in order to remove any excess mineral oil from the surface. The IPG strips were then positioned on the focussing tray with the gel side facing down, on top of the electrode wicks, and completely covered with mineral oil. Focussing was then started. Both rehydration and focussing took place at 20 °C and were carried out in the Protean IEF Cell equipment, according to Table 2.3.

Table 2.3 Rehydration and focussing conditions used in the first dimension of 2D-PAGE.

Conditions	Isoelectric Focussing Step								
	Rehydration		Focussing						
	Passive	Active	Linear ramp			Rapid ramp			
			Step 1	Step 2	Step 3	Step 1	Step 2	Step 3	
A	Voltage	0 V	—	4000 V	—	—	—	—	—
	Duration	16 h	—	20,000 V/h	—	—	—	—	—
B	Voltage	0 V	—	250 V	4000 V	4000 V	—	—	—
	Duration	16 h	—	15 min	2 h	20,000 V/h	—	—	—
C	Voltage	—	50 V	250 V	4000 V	4000 V	—	—	—
	Duration	—	12 h	15 min	2 h	20,000 V/h	—	—	—
D	Voltage	—	50 V	—	—	—	250 V	8000 V	8000 V
	Duration	—	12 h	—	—	—	15 min	2 h	40,000 V/h

After IEF, IPG strips were promptly removed from the tray, placed on dry tissue paper with the gel side facing up and covered with wet tissue paper to remove any excess mineral oil from the surface. The IPG strips were then transferred to a clean rehydration tray with the gel side facing up and either immediately prepared for the second dimension or stored at -80 °C.

2.4.3.2 Equilibration, reduction and alkylation

The reduction and alkylation step was performed after isoelectric focussing and before SDS-PAGE. IPG strips were washed 3 times with equilibration buffer (0.375 M Tris-HCl pH 8.8, 6 M urea, 20 % glycerol, 2 % SDS) and then incubated in 55 mM DTT solution in equilibration buffer for 1 h at room temperature with constant shaking. After incubation, the DTT solution was discarded and 100 mM iodoacetamide solution in equilibration buffer was added to the strips to alkylate the free thiol groups. The strips were then incubated in the dark for 1.5 h at room temperature with constant shaking, after which the iodoacetamide solution was discarded. The alkylation process was stopped by washing the strips with an equal

volume of rehydration buffer without DTT (7 M urea, 2 M thiourea, 4 % CHAPS) for 10 min at room temperature.

2.4.3.3 Second dimension: SDS-PAGE

After the reduction and alkylation process was complete, the equilibrated IPG strips were removed from the rehydration/equilibration tray using forceps and dipped briefly into a graduated cylinder containing 1x Tris-Glycine-SDS running buffer (Bio-Rad, UK). Each strip was transferred to the top of a 12.5 % SDS-polyacrylamide gel, previously prepared. No stacking gel was used. Gel preparation is described in section 2.4.1. Alternatively, strips were transferred to the top of precast gels, Mini-Protean TGX Precast Gels, any kD, IPG well comb, 7 cm IPG strip (Bio-Rad, UK), or Criterion TGX Precast Gels, any kD, IPG + 1 well comb, 11 cm IPG strip (Bio-Rad, UK), used instead of handmade gels. A molecular weight marker was loaded into the single well of the 11 cm precast gels.

The strips were laid, with the gel side facing out, onto the back plate of the SDS-PAGE gels above the IPG well, pushing each strip against the gel to remove air bubbles. The IPG strips were fixed to the second dimension gels with 1 % low melting agarose in stacking buffer (0.5 M Tris-HCl pH 6.8) with a trace of bromophenol blue. The agarose solution was melted in a microwave oven and layered into the IPG well on the gel, filling the well to the top of the inner gel plate, and left to set. After allowing the agarose to solidify for 5 min, gels were placed in the electrophoresis cassette, the reservoirs were filled with 1x Tris-Glycine-SDS running buffer, and electrophoresis was started. This process was carried out using a Mini-Protean Tetra Cell System or Criterion Cell System (Bio-Rad, UK) at 40 V until the blue dye had reached the main gel, and then increased to 100-150 V until the dye front had reached the bottom of the gel. The migration of bromophenol blue, present in the overlaying agarose, was used to monitor the electrophoresis progress. Gels were stained immediately after the second dimension.

2.5 Methods of protein visualisation

At the end of the electrophoresis run, gels were carefully removed from the cassette and placed in clear plastic staining trays. Two distinct methods of protein staining were used.

2.5.1 Coomassie blue staining

Coomassie blue staining was used preferably to stain 1D gels. After a few washes in ultrapure water, gels were stained with Instant Blue Solution (Expedeon, UK) or Bio-Safe Coomassie Stain (Bio-Rad, UK) for 1 h with constant shaking. The background was destained overnight in ultrapure water with constant shaking. After staining, gels were stored in water at 4 °C.

2.5.2 Silver staining

This staining method was used preferably to stain 2D gels. Silver staining was performed according to the modified silver staining method of Blum et al. (Blum et al., 1987). Gels were fixed in a fixation solution (50 % water, 40 % methanol, 10 % acetic acid) for at least 1 h, or overnight, and then washed 3 times with 50 % ethanol for 20 min. Gels were sensitised in 0.8 mM sodium thiosulphate for 1 min, rinsed with ultrapure water 3 x 20 sec and incubated for 20 min in 0.2 % silver nitrate with 0.02 % (v/v) formaldehyde. Gels were then rinsed with ultrapure water 2 x 20 sec and soaked in developing buffer (3 % sodium carbonate with 0.05 % (v/v) formaldehyde and 0.01 mM sodium thiosulphate) for 3 to 5 min. The development was stopped in 1.4 % EDTA disodium salt solution for 10 min, after rinsing the gels once again with water for 2 x 2 min. Finally, gels were washed with 50 % methanol for at least 20 min and stored in the same solution at 4 °C.

Alternatively, gels were silver stained using the Pierce Silver Stain Kit (Thermo Scientific, UK) according to the manufacturer's instructions. Briefly, gels were washed in ultrapure water twice for 5 min and fixed in fixation solution (60 % water, 30 % ethanol, 10 % acetic acid) for 2 x 15 min or overnight. Gels were then washed in 10 % ethanol solution twice for 5 min and ultrapure water 2 x 5 min, followed by

incubation in sensitizer working solution (1 part silver stain sensitizer with 500 parts ultrapure water) for exactly 1 min, and then washed with two changes of ultrapure water for 1 min each. Gels were incubated in stain working solution (1 part silver stain enhancer with 50 parts silver stain) for 30 min, after which they were quickly washed with two changes of ultrapure water for 20 sec each. Immediately after, developer working solution (1 part silver stain enhancer with 50 parts silver stain developer) was added and gels were incubated in this solution for 2-3 min, until protein bands appeared. When the desired band intensity was achieved, developer working solution was replaced with stop solution (5 % acetic acid in ultrapure water), and gels were first washed briefly and then incubated for 10 min in the same solution. Gels were stored in stop solution at 4 °C.

2.5.3 Gel image analysis

Gel images were obtained with a digital photographic camera and/or using the camera device of EXQuest Spot Cutter (Bio-Rad, UK), and analysed using PDQuest Advanced software version 8.0.1 (Bio-Rad, UK). Spots of interest were selected either visually or using PDQuest Advanced software.

2.6 Methods of protein identification

Protein identification was attained by two different methods: liquid chromatography coupled to tandem mass spectrometry (LC-MS/MS) and Western blotting. Both methods comprise a first stage of protein/peptide separation (liquid chromatography in LC-MS/MS and electrophoresis in Western blotting) in order to make protein identification more effective and accurate.

2.6.1 LC-MS/MS

In this method, proteins were firstly subjected to in-gel trypsin digestion, and then peptides were extracted from the gel pieces and analysed by LC-MS/MS, followed by data processing and database searching for protein identification. The respective procedures are described in the following sections.

2.6.1.1 Spot excision, washing and in-gel trypsin digestion

Spots of interest were excised from the gels and cut into 1-2 mm³ gel pieces, either manually or using an EXQuest Spot Cutter (Bio-Rad, UK) with a picker head of 1.5 mm, and placed into 0.6 mL siliconised tubes or 96-well microplates, for the manual and automated excisions respectively. Gels pieces were stored without any liquid at -80 °C until further use.

Gel pieces were thawed, transferred to 0.6 mL siliconised tubes in case they had been stored in 96-well microplates, and rinsed twice with 190 µL of wash solution (50 % methanol, 45 % water, 5 % acetic acid) at room temperature for 3 h and overnight, respectively. Gel pieces were then dehydrated in 190 µL of acetonitrile at room temperature for 5 min, after which the samples were dried in a vacuum centrifuge (SpeedVac RC 1022, Jouan, UK) for 3 min at 40 °C. Sample reduction was performed with 30 µL of 10 mM DTT in 100 mM ammonium bicarbonate solution at room temperature for 30 min, followed by alkylation with the same volume of 100 mM iodoacetamide in 100 mM ammonium bicarbonate solution at room temperature for another 30 min. Samples were dehydrated again in 190 µL of acetonitrile at room temperature for 5 min, and dried in a vacuum centrifuge for 3

min at 40 °C. Gel pieces were rehydrated in 190 µL of 100 mM ammonium bicarbonate at room temperature for 10 min, and then dehydrated in acetonitrile and dried in a vacuum centrifuge another time.

Finally, samples were rehydrated on ice, for 10 min, with 20 µL of trypsin solution (20 ng/µL sequencing grade modified porcine trypsin (Promega, UK) in ice cold 50 mM ammonium bicarbonate pH 8.0) with occasional vortex mixing. Samples were spun down for 30 sec and excess trypsin solution was removed. An aliquot of 10 µL of 50 mM ammonium bicarbonate solution was added to the gel pieces to prevent dehydration and proteins were digested overnight at 37 °C.

2.6.1.2 Peptide extraction from gel pieces

After digestion, 30 µL of 50 mM ammonium bicarbonate solution were added to each tube containing the gel pieces and the mixtures were vortex mixed for 10 min, after which supernatants were collected and transferred to new tubes. Peptides were firstly extracted from the gel pieces with 30 µL of extraction buffer I (50 % acetonitrile, 45 % water, 5 % formic acid) for 10 min. A second extraction was performed with 30 µL of extraction buffer II (85 % acetonitrile, 10 % water, 5 % formic acid) for another 10 min. Supernatants were collected after each extraction and combined with the previous fraction. The volume of the extracts was reduced to <10 µL by evaporation in a vacuum centrifuge at 40 °C. The final dried extracts were re-dissolved in 7 µL of 99.9 % water + 0.1 % formic acid, sonicated in ice cold water for 10 min, centrifuged for 5 min and transferred to MS compatible vials.

2.6.1.3 MS analysis

LC-MS/MS analysis of the extracted peptide mixtures was performed on a Waters CapLC system coupled to the front end of a Waters Micromass Q-ToF Premier. The Waters CapLC comprised an autosampler and an LC-pump system that was connected directly to the mass spectrometer through a switching valve. Depending on the intensity of the spot on the 2D gel, 1-5 µL were injected per sample. The total run time for each injection was 63 min.

As the sample was injected through the sample loop, it was subjected to a pre-wash in the pre-column (5 mm x 0.3 mm, 5 μ m, PepMap C18 Guard Column, Dionex, UK) by pump C (0.1 % formic acid), where salt and other small molecules were removed and led to the waste. Desalting took approximately 3 min at a flow rate of 15 μ L/min and in stream select position 1. After desalting, the stream select valve switched to position 2 to allow pumps A (95 % water, 5 % acetonitrile, 0.1 % formic acid) and B (95 % acetonitrile, 5 % water, 0.1 % formic acid) to flow through the pre-column at a flow rate of 1 μ L/min. Once 53 min of run were completed, stream select valve switched back to position 1 to re-equilibrate the pre-column before loading the following sample.

Upon switching of the stream select valve, the flow from the pre-column moved through to the analytical nano-column (150 mm x 0.075 mm i.d., 3 μ m, C18, Dionex) and into the mass spectrometer. Peptides were eluted from the columns with a mixture of mobile phases A and B, according to the 63 min gradient LC method shown in Figure 2.1.

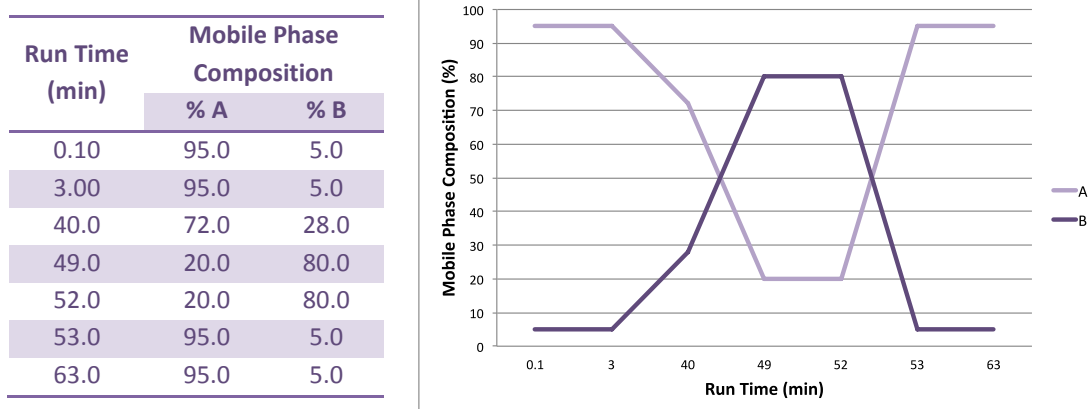


Figure 2.1 Representation of the 63 min gradient LC method used in MS analysis. Mobile phase A = 95 % water, 5 % acetonitrile, 0.1 % formic acid; mobile phase B = 95 % acetonitrile, 5 % water, 0.1 % formic acid.

The gradient formed by the mixture of A and B contained less than 50 % organic solvent for the most part of the run, as these are the optimal conditions for the elution of most of the peptides from the column. Initial flow from the CapLC was at

6 $\mu\text{L}/\text{min}$, which was split before the column by the LC system incorporated flow splitting device, so the flow through the analytical column to the mass spectrometer was only 200 nL/min . Two blank runs were incorporated after each group of five samples to establish that there was no significant carry-over of the previous samples. Peptides eluted from the column were directly sprayed into the mass spectrometer for analysis.

MS and MS/MS data were acquired using a Waters Micromass Q-ToF Premier equipped with a nanospray source attached to the LC outflow for increased sensitivity, as it allows lower injection volumes, operating at 1.8 kV. The acquisition and processing software used was Waters MassLynx Version 4.1. Table 2.4 displays the general experiment setup for the MS/MS method.

Table 2.4 Parameters for the analysis of samples on the Waters Micromass Q-ToF Premier.

Waters Micromass Q-ToF Premier	Parameters	
ACQUISITION	Survey start time	3.0 min
	Survey end time	60.0 min
	Survey ion mode	ES V mode
	Survey polarity	Positive
MS SURVEY	Survey start mass	400 Da
	Survey end mass	1700 Da
	Intensity threshold	10 counts/sec
	Survey scan time	0.5 sec
	Survey inter-scan time	0.1 sec
	Survey data format	Continuum
	Survey use tune page cone voltage	Yes
	Survey cone voltage	35 V
MS/MS	MSMS start mass	50 Da
	MSMS end mass	1700 Da
	Number of components	4
	MSMS to MS switch criteria	Intensity falling below threshold
	MSMS switchback threshold	3 counts/sec
	Use MSMS to MS switch after time	Yes
	MSMS switch after time	5 sec
	MSMS scan time	1 sec
	MSMS inter-scan time	0.1 sec
	MSMS data format	Continuum
	MSMS use tune page cone voltage	Yes
	MSMS cone voltage	35 V
PEAK DETECTION	Peak detection window	3 Da
	Use include by charge state	Yes
	Charge states	2, 3, 4
	Number of include components	60
	Charge state tolerance window	3 Da
	Charge state extraction window	2 Da
	Discard survey data	No
COLLISION ENERGY	Use charge state recognition	Yes
	Maximum charge state	4
	Charge state 1 filename	Default_CS_1
	Charge state 2 filename	Default_CS_2
	Charge state 3 filename	Default_CS_3
Charge state 4 filename	Default_CS_4	
EXCLUDE	Detected precursor inclusion	Using real time exclusion
	Detected precursor inclusion	Include after time
	Include after time	60 sec
	Use exclude mass list	No
	Exclude window	+/- 1.5 Da
	Exclude retention time window	10 sec

MS was monitored over a m/z range of 400-1700 Da and MS/MS was monitored over a m/z range of 50-1700 Da. Spectra were acquired in MS mode and the software was configured to enable scanning of multiple channels, in order to simultaneously fragment up to 4 individual co-eluting peptides per MS scan, and collect fragmentation data from each.

The mass spectrometer was programmed to automatically switch to MS/MS mode and to generate fragmentation data, whenever a peptide with an associated charge of 2+, 3+ or 4+ was detected above a pre-set threshold signal. Multiply charged masses were fragmented by the mass spectrometer once their intensity reached 10 counts/sec or above, and fragmentation occurred for a total of 5 seconds or until the intensity fell below 3 counts/sec. That particular mass and a window of 1.5 Da around it were excluded for 60 seconds, allowing the mass spectrometer to fragment as many different components as possible during the run time. A pre-set range of collision voltages was applied, so that each peptide was fragmented as efficiently as possible.

Calibration of the instruments was performed prior to analysis. In order to ensure optimal sensitivity of the mass spectrometer and for calibration purposes, a reference solution containing a peptide of known mass was used. Glu-Fibrinopeptide (Glu-Fib, peptide sequence EGVNDNEEGFFSAR, Sigma-Aldrich, UK) was sprayed into the mass spectrometer at a concentration of 100 fmol/ μ L and a flow rate of 0.3 μ L/min. A calibration file was prepared by fragmenting the $[M+2H]^{2+}$ ion of Glu-Fib, and the resulting fragment ions were processed and compared to a theoretical fragment ion peak list for calibration. In addition, other parameters of the instrument, listed on Table 2.5, were also checked.

Table 2.5 System checks and instrument calibration parameters for the Waters Micromass Q-ToF Premier.

Parameters	
Backing pirani	1.94 x 10 ⁰ mbar
Collision cell	4.07 x 10 ⁻³ mbar
Quadrupole	2.75 x 10 ⁻⁸ mbar
TOF	9.64 x 10 ⁻⁷ mbar
Collision gas	Approx. 0.36 (to give pressure reading above)
Source temperature	80 °C
Test sample MS	0.1 pmol GluFib 0.3 µL/min
LM/HM/CE	4.9/15/5
400-1700, 1sec/scan	200 counts on 785/scan
MS signal/scan	
50-1700, 1sec/scan	100 counts on 785 (5 eV)
MS/MS signal/scan	20 counts on 684 (30 eV)
	400 10 10
MS profile	500 10 70
	600
Detector voltage MCP	1700-2100
Calibration file	131225GFPQT1165
<i>m/z</i> measured	785.8426
Resolution	> 10,000 on 785.8
Capillary/S Cone/E Cone	2.8-3.3(1.8)/35/3.0
Trigger/Signal/Veff	700/60/5535.2

Subsequently, to guarantee the LC-MS system was correctly optimised, pre-digested bovine serum albumin (BSA, Waters, UK) at a concentration of 100 fmol was injected into the LC-MS, and the base peak chromatogram generated to ensure satisfactory performance (resolution and sensitivity). To accept the system is running normally, peak width at half height must be less than 0.3 min and retention times must not differ by more than 0.5 min from the last BSA run. Additionally, a BSA search using the data resulting from this analysis on an online search engine must result in over 35 % coverage of BSA.

2.6.1.4 Data processing and database searching

Raw LC-MS/MS data were processed using MassLynx ProteinLynx version 4.1 (Waters, UK). The system was set up using Peptide Auto and the parameters used were from the file Process.mlp. Processing parameters comprised combining all

sequential scans with the same precursor and processing all combined scans. Mass measurement of the combined scans involved spectral smoothing, which was performed twice, using the Savitzky Golay method with a 3.00 channel window. A centroid peak list was then created using the top 80 % of the peak with a minimum peak width at half height of 4. After the data had been processed, it was combined into a single pkl file that could then be used for searching against databases. PKL is an extension for a text file created by MassLynx, which lists all the MS data (m/z and charge) and MS/MS data associated with that m/z and charge.

These files were used to perform database searches using two online search engines. Primary searches were done using the online version of MASCOT (Matrix Science, version 2.4) (Perkins et al., 1999). This is a probability based search engine that can utilise any available database in FASTA format. The principle of MASCOT is based on calculation of the probabilities that an observed match between an experimental spectrum and a theoretical spectrum from a sequence entry is a random event. These probabilities are calculated based on $P < 0.05$, however they are listed as a score that is calculated by $-10\log P$. Accordingly, the lower the probability of a random match, the higher the score would be. The match with the lowest probability of being a chance event is in fact the best match, although the significance of that match depends on the size of the used database of theoretical spectra (Simpson, 2003).

When performing a search, entering the appropriate searching parameters is fundamental. The parameters used for MASCOT searches are depicted in Figure 2.2.

MASCOT MS/MS Ions Search

The screenshot displays the MASCOT MS/MS Ions Search web interface with the following parameters:

- Your name:** isa cruz
- Email:** isa.cruz.11@ucl.ac.uk
- Search title:** Sample X
- Database(s):** Invertebrates_EST, Human_EST, Fungi_EST, Environmental_EST, SwissProt
- Enzyme:** Trypsin
- Allow up to:** 1 missed cleavages
- Quantitation:** None
- Taxonomy:** Homo sapiens (human)
- Fixed modifications:** --- none selected ---
- Variable modifications:** Carbamidomethyl (C), Oxidation (M)
- Peptide tol.:** 100 ppm
- # ¹³C:** 0
- MS/MS tol.:** 0.1 Da
- Peptide charge:** 2+, 3+ and 4+
- Monoisotopic:** Average
- Data file:** Choose File 1212051C1QTP2010.pkl
- Data format:** Micromass (.PKL)
- Instrument:** ESI-QUAD-TOF
- Precursor:** m/z
- Error tolerant:**
- Decoy:**
- Report top:** AUTO hits

Buttons: Start Search ..., Reset Form

Figure 2.2 Parameters used in MASCOT searches.

MASCOT takes into account post-translational modifications and missed cleavage sites, as well as the peptide and MS/MS error windows. These values must be carefully judged, as too small windows might miss valid matches and too large windows increase randomness (Simpson, 2003).

Depending on the origin of the sample analysed, SwissProt databases were chosen to look for canine proteins (taxonomy — *Mammalia* or *Canis familiaris*), mouse proteins (taxonomy — *Mus musculus*), or human proteins (taxonomy — *Homo sapiens*). Searches were performed without restriction of protein molecular mass or pI, but with variable modifications such as carbamidomethylation of cysteines and oxidation of methionine residues. One trypsin missed cleavage was allowed. Peptide and fragment mass tolerances were set to 100 ppm and ± 0.1 Da, respectively, and peptide charge to 2+, 3+ and 4+. The instrument type chosen was ESI-QUAD-TOF.

A second online search engine, X!Tandem (The GPM, version 2012/10/19) (Craig and Beavis, 2004) was used to search the data, using the pkl files generated by MassLynx 4.1. The parameters used for X!Tandem searches were similar to the ones used for MASCOT searches and are shown in Figure 2.3. Data resulting from both searches were manually inspected and compared to each other.

The image shows a screenshot of the 'GPM Cyclone, simple search form' interface. The form is divided into several numbered sections:

- 1. spectra:** Includes a dropdown for 'common, mzXML, mzData, DTA, PKL or MGF only' and a 'Choose File' button with the filename '121205IC1.GTP1994.pkl'.
- 2. taxon:** Features a 'Select one or more' section with radio buttons for 'Eukaryotes', 'Prokaryotes', and 'Viruses'. A list of organisms is shown, with 'H. sapiens (human)' selected. Below this are options for 'Include reversed sequences' (none, mixed, only) and 'all ¹⁵N amino acids'.
- 3. measurement errors:** Contains a 'Find proteins' section with a 'with peptide log(e) < -1' and 'and protein log(e) < -1' filter.
- 4. residue modifications:** Includes 'Complete modifications 1' and '2' (both set to 'Unmodified'), 'Potential modifications' (listing Carboxyethyl [K], Carbamidomethyl [nt], Carbamidomethyl [K], and Carbamidomethyl [C]), and a 'Check for known PTMs' section.
- 5. refinement specification:** A section for 'protein cleavage specification'.
- 6. protein cleavage specification:** Includes 'Cleavage site' (set to 'trypsin, [RK][P]') and 'Semi-style cleavage' (yes/no).
- 7. spectrum conditioning:** Includes 'Remove redundant' (yes/no, angle: 40) and 'Spectrum synthesis' (yes/no).
- 8. predefined methods:** A list of methods including 'Orbitrap (20 ppm)', 'Quad-TOF (100 ppm)', 'Quad-TOF (0.5 Da)', and 'Ion Trap (4 Da)'. A 'view method' button is present.
- 9. gpmdb:** A final section at the bottom.

Figure 2.3 Parameters used in X!Tandem searches.

Decoy databases were used to determine the false-positive rates of identification. Decoy databases contain the forward-normal sequences with the amino acid sequences reversed. The parameters used for this search were the same as for the original search. For each analysis it was required a less than 5 % false-positive rate. In addition, some fragmentation data were analysed manually.

Scaffold 3 software (Proteome Software, USA, version 3.6.4) was used to validate MS/MS based peptide and protein identification. This software also allowed combining and comparing proteins identified among different biological samples and grouping proteins by biological relevance and molecular function. Peptide

identifications were accepted if established at greater than 95 % probability, as specified by the Peptide Prophet algorithm (Keller et al., 2002). In turn, protein identifications were accepted if established at greater than 99 % probability and contained at least 2 assigned peptides, as specified by the Protein Prophet algorithm (Nesvizhskii et al., 2003). Proteins that contained similar peptides and could not be differentiated based on MS/MS analysis alone were grouped together to satisfy the principles of parsimony (minimal set of protein sequences which explain the maximum number of identified peptides).

2.6.2 Western blotting

In this method, proteins were initially separated by electrophoresis, and then transferred to nitrocellulose membranes, which were probed with antibodies, followed by protein band detection and visualisation for protein identification. The respective procedures are described in the following sections.

2.6.2.1 Electrophoretic separation

A minimum of 10 µg of protein per well was loaded onto precast gels, Mini-Protean TGX precast gels, any kD, 10-well comb, 30 µL/well (Bio-Rad, UK) and proteins were separated by SDS-PAGE as described in section 2.4.1. Gels were run in duplicate, so that one of the replicates could be stained and the presence of protein bands could be confirmed, and the other was kept in Tris-glycine buffer (25 mM Tris, 192 mM glycine, 20 % methanol, 80 % water) to be used for blotting. A pre-stained molecular weight marker (ColorPlus prestained protein marker, broad range, New England BioLabs, UK) was used in order to verify the transfer of proteins from the gel to the membrane after the blotting procedure.

2.6.2.2 Protein transfer to nitrocellulose membranes

For each blot, one nitrocellulose membrane (9.5 cm x 6.5 cm, Hybond-C Extra, Amersham Biosciences, UK), two pieces of 3 mm paper (10 cm x 7 cm), and two fibre pads were pre-wetted in Tris-glycine buffer. When making the sandwich, the various components were mounted in the cassette on the black (negative) side in

the following order: one fibre pad, one 3 mm paper, SDS-PAGE gel, nitrocellulose membrane, one 3 mm paper, one fibre pad. All the components were kept moist while assembling and all air bubbles were removed from between the gel and the membrane. The sandwich was closed and placed inside the Mini Trans-Blot Transfer Cell (Bio-Rad, UK) according to the manufacturer's instructions (black to black and clear to red). The ice block was placed at the front of the electroblotting apparatus and the reservoirs were filled with Tris-glycine buffer. Proteins were transferred onto the nitrocellulose membrane for 1 h at 100 V.

2.6.2.3 Blocking and antibody probing

When the electroblotting was finished, the membrane was placed in a small staining tray and blocked in 1 % bovine serum albumin (BSA, Sigma-Aldrich, UK) or 1 % milk (dried skimmed milk, Marvel) in Tris-buffered saline (TBS; 1 % of 1 M Tris-HCl pH 7.0, 3 % of 5 M NaCl, 96 % of water) buffer for 1 h at room temperature or overnight at 4 °C on a rocker. The choice of blocking agent depended on the manufacturer's recommendations for each particular antibody. After blocking, the blocking solution was discarded and the membrane was probed with primary antibody, diluted in blocking solution, overnight at 4 °C on a rocker. The primary antibody was then removed and the membrane was washed a few times for 10 min with TBS buffer containing 0.05 % Igepal (Sigma-Aldrich, UK) or 0.05 % Tween 20 (Sigma-Aldrich, UK). The membrane was subsequently incubated for 1.5 h at room temperature on a rocker with secondary antibody diluted in blocking solution. After incubation, the membrane was washed again with TBS buffer containing 0.05 % Igepal or Tween 20 for 10 min a few times.

2.6.2.4 Protein band detection and visualisation

Protein bands were developed using a Pierce Enhanced Chemiluminescence (ECL) Western Blotting Substrate or a SuperSignal West Pico Chemiluminescent Substrate (Thermo Scientific, UK) according to the manufacturer's instructions. Briefly, substrate working solution was prepared by mixing equal parts of detection reagents 1 and 2 immediately before use. A volume of 0.125 mL working solution

per cm² of membrane was used. The membrane was incubated with working solution for 1 min, or 5 min for the SuperSignal substrate, at room temperature, after which it was removed from the working solution and placed in a plastic sheet protector or clear plastic wrap, removing excess liquid and pressing out any bubbles.

Protein bands were visualised with the GeneGnome chemiluminescence imaging system, using the GeneSnap software (SynGene Bio Imaging, UK). Band quantification was performed by densitometry using the GeneTools software (SynGene, UK). Alternatively, protein bands were visualised with a Bio-Rad gel imager, using Image Lab software (Bio-Rad, UK). The western blot assay was performed at least two times for each antibody.

**Chapter 3 – PROTEOMICS APPROACH TO IDENTIFY PROTEIN
TARGETS IN INFERTILITY**

3.1 Introduction

3.1.1 Carbohydrate-active proteins (CAP)

Approximately 2-3% of most genomes are devoted to carbohydrate-active proteins (CAP) (Coutinho et al., 2003). These include lectins that bind carbohydrates, glycosidases (glycosylhydrolases) that degrade them, and glycosyltransferases that construct them (<http://www.cazy.org>) (Cantarel et al., 2009). The biosynthesis of carbohydrates and polysaccharides is of extreme biological importance, as these molecules control a diverse range of cellular functions, including energy storage, cell-wall structure, cell-cell interactions and signalling, host-pathogen interactions, and protein glycosylation (Rudd et al., 2001, Wells et al., 2001).

Deficiencies of CAP can lead to pathological states, such as congenital muscular dystrophies (Blake et al., 2002), virus infection of HIV, influenza, tumour metastasis and lysosomal storage disorders (Kajimoto and Node, 2009) among others. CAP are implicated in a range of host-pathogen interactions that lead to disease (Gattegno et al., 1992, Kannagi et al., 2004).

Therefore, agents that control the activities of glycosidases and glycosyltransferases could have therapeutic effects against some of the above mentioned diseases. In fact, many efforts have been made to synthesise inhibitors of carbohydrate-related enzymes, either using natural products or synthetic compounds designed on the basis of information obtained from studies on mechanisms of the enzymes (Asano et al., 2000, Lillelund et al., 2002).

Despite these vital roles, most current strategies for determining CAP interactions (e.g. arrays or assays), whilst powerfully allowing the determination of *in vitro* specificities, do not permit widescale probing of cellular or organismal samples.

Affinity strategies have rarely been used to identify novel binding partners or profile the carbohydrate-active proteome (Lin et al., 2008). One such conceivable strategy

is to use clinically utilised compounds to identify novel binding partners. This would advantageously allow the repurposing of pre-approved drugs and, hence, facilitate rapid translation and application.

One glycomimetic suitable for this purpose is the iminosugar *n*-butyldeoxynojirimycin (*NB*-DNJ) (Figure 3.1).

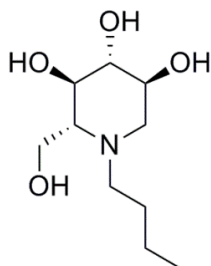


Figure 3.1 Structure of *NB*-DNJ/Miglustat/Zavesca®.

3.1.2 The iminosugar glycomimetic *NB*-DNJ

Iminosugars are naturally occurring polyhydroxylated alkaloids with a structure resembling that of monosaccharides, characterised by the presence of a nitrogen replacing the oxygen of the ring (Watson et al., 2001). Alkylated deoxynojirimycin (DNJ) compounds are a type of iminosugar with an alkyl chain branching from the nitrogen atom of the ring. It has been reported that the *N*-alkylated DNJ can inhibit the *N*-glycan processing glycolipid metabolic enzymes, including ceramide glucosyltransferase (CGT; glucosylceramide synthase, GCS/UGCG) (Platt et al., 1994a), glucosylceramidase (β -glucocerebrosidase; lysosomal acid β -glucosidase 1, GBA) (Platt et al., 1994b), glucosylceramidase 2 (non-lysosomal glucosylceramidase; β -glucocerebrosidase 2; β -glucosidase 2, GBA2) (Walden et al., 2007), lysosomal α -glucosidase (acid α -glucosidase, GAA) and neutral α -glucosidase (Saunier et al., 1982, Elbein, 1987).

Structural similarities between alkylated iminosugars and the substrates of *N*-glycan processing enzymes have been described (Butters et al., 2000). Figure 3.2 illustrates the structure of the *N*-butyl-DNJ (*NB*-DNJ), also known as miglustat, and its interaction with two substrates of *N*-glycan processing enzymes. *NB*-DNJ overlays

with the head and part of the *N*-acyl chain of ceramide, where a glucose is added by ceramide glucosyltransferase. NB-DNJ also overlaps with the terminal glucose residue of $\text{Glc}_3\text{Man}_9\text{GlcNAc}_2$, which is a substrate of acid α -glucosidase (Butters et al., 2000, Butters et al., 2003).

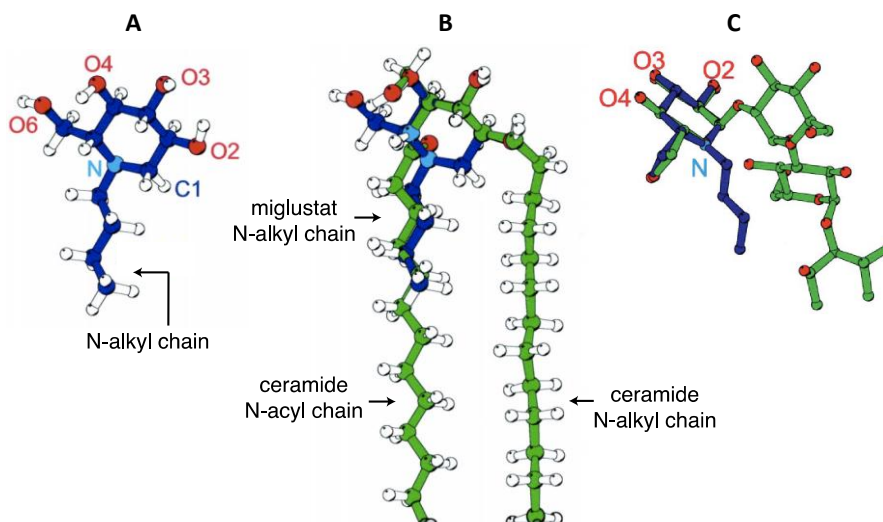


Figure 3.2 Structure relationships between NB-DNJ and the substrates of ceramide glycosyltransferase and acid α -glucosidase. (A) Miglustat (NB-DNJ) structure based on NMR studies and molecular modelling. (B) One possible overlay of miglustat and ceramide. Ceramide structure was taken from the crystal structure of galactosylceramide. (C) Superimposition of miglustat and the terminal glucose residue of $\text{Glc}_3\text{Man}_9\text{GlcNAc}_2$, which is removed by acid α -glucosidase. Adapted from (Butters et al., 2000).

NB-DNJ was approved by the FDA in 2002 as a therapeutic under the commercial name Zavesca[®]. This compound is prescribed for the treatment of inherited lysosomal storage disorders such as type 1 Gaucher disease and Niemann-Pick type C disease, to reduce the accumulation of glycosphingolipids in patients (Aerts et al., 1985, Aerts et al., 1986, van der Spoel et al., 2002).

Gaucher disease is the most common of the lysosomal storage disorders. It is a genetic condition characterised by dysfunctional metabolism of glycosphingolipids, which accumulate in cells and certain organs, causing the symptoms of the disease. Gaucher disease is caused by a hereditary partial deficiency of the enzyme glucocerebrosidase, whose main role is to eliminate the toxic fatty acid glucosylceramide. When glucocerebrosidase is defective, glucosylceramide

accumulates in vital organs such as the liver, kidneys, lungs and brain, and in the macrophage system (Pastores et al., 2004).

The chosen treatment for most Gaucher disease patients is enzyme replacement therapy (ERT), using mannose-terminated recombinant human glucocerebrosidase (aglucerase and imiglucerase). Despite the success of ERT, several drawbacks encouraged the search for other treatment approaches. The fact that some complications of Gaucher disease may remain refractory to ERT, that this treatment option does not appear to pass the blood-brain barrier and that ERT requires regular intravenous infusion and continued patient compliance, led to a new treatment alternative known as substrate reduction therapy (SRT) (Bruni et al., 2007, Cox et al., 2003).

SRT is a different method to decrease the accumulation of toxic storage material. In this approach, instead of replacing the defective enzyme, partial inhibition of the enzyme that produces the toxic products (CGT) is required to treat the accumulation of glycosphingolipids in Gaucher disease patients. The residual enzyme activity of the impaired glucocerebrosidase will then be enough to catabolise stored and incoming lysosomal substrate. *NB-DNJ* is the molecule of choice for SRT. Its main advantages are that it is orally bioavailable, it can pass through the blood-brain barrier and it is generally well tolerated in humans (Cox et al., 2003, Bruni et al., 2007).

Other treatment options include bone marrow transplantation, although this carries significant risk and is rarely performed in Gaucher patients, splenectomy and blood transfusion. Several lysosomal storage disorders have recently become a target of chaperone therapy, a technique used to stabilise the defective enzymes produced by the patients using orally administered drugs that operate at a molecular level. Gene therapy may offer a cure in the future (Bruni et al., 2007).

Alkylated iminosugars present different potency for inhibiting the glycolipid metabolic enzymes, as the drug effect can vary depending on the dose administered and the affinity, IC_{50} and inhibition constant (K_i) of the inhibitor (Platt et al., 1994b, Butters et al., 2003). Taking *NB-DNJ* as an example, its IC_{50} for the known enzyme

targets can be as low as 0.14 μM for GBA2, while the IC_{50} for CGT, the drug target for treating Gaucher disease, is approximately 20 μM (Platt et al., 1994b, Walden et al., 2007, Li et al., 2008a).

This powerful glycomimetic is therefore an archetype of modulation of glycobiology by small molecules.

3.1.3 NB-DNJ induces infertility in male mice

One of the most remarkable properties of NB-DNJ is that in certain mouse strains from the C57-lineage (Beck et al., 2000), e.g. C57BL/6, AKR/J and BALB/c, it induces reversible, dose-dependent male infertility at very low dosage (15 mg/kg/day; serum level 0.3-1.7 μM) (van der Spoel et al., 2002, Bone et al., 2007). In contrast, other mouse strains from the Swiss Castle lineage, such as FVB/N (Wang et al., 2012a), display a phenotype insensitive to NB-DNJ-induced infertility (Bone et al., 2007). In mouse studies, NB-DNJ is typically administered at 2400 mg/kg/day, with a serum concentration around 56.8 μM (Platt et al., 1997). It is likely that the drug target(s) related to the induced infertility have a higher affinity for NB-DNJ.

Studies with C57BL/6 x FVB/N interstrain hybrid mice have suggested multiple genes and, thus, multiple protein targets contribute to this striking function (infertility) induced by NB-DNJ (Bone et al., 2007). This raises the intriguing possibility that modulation of the carbohydrate-active proteome may be intimately linked to reproduction, as the induction of infertility after NB-DNJ treatment might be caused by a change in the glycosphingolipid metabolism. There are some early indications of the origins of this exciting effect. Mice treated with NB-DNJ displayed lower sperm counts and abnormal sperm morphologies, with deformed or no acrosomes and non-falciform nuclei (van der Spoel et al., 2002, Bone et al., 2007), rendering them incapable of binding the zona pellucida to initiate fertilisation (Suganuma et al., 2005). However, the exact protein targets that are responsible for the strain differences in drug susceptible strains remain unknown, providing a suitably challenging test for a glyco-affinity strategy.

As mentioned before, NB-DNJ is known to inhibit intracellular enzymes including β -glucosidase 2 (GBA2), lysosomal acid β -glucosidase 1 (GBA) and glucosylceramide synthase (GCS/UGCG) (Li et al., 2008a, Platt et al., 1994a, Walden et al., 2007, Platt et al., 1994b). Knockout of GBA2 impairs mouse fertility and results in sperm abnormalities (Yildiz et al., 2006). The epididymal spermatozoa of NB-DNJ-insensitive strains only display minor morphological imperfections and, consequently, these mice are normally fertile (Bone et al., 2007). Nonetheless, all mouse strains show similar elevated level of glucosylceramide when treated with NB-DNJ. This suggests no direct link to glycosphingolipid metabolising enzymes GBA/GBA2 and/or GCS/UGCG and implicates instead the differences in genetic background and other protein partners.

In fact, to date, no comprehensive study of the cellular targets of NB-DNJ has been conducted and the proteins involved in induced male infertility remain unknown. This study reports the investigation of possible as yet unknown NB-DNJ targets by an affinity-enrichment proteomics method.

3.1.4 Affinity chromatography principle

Biomolecules are separated using separation techniques that function according to differences in specific properties. Affinity chromatography separates or purifies proteins on the basis of a reversible interaction between a protein or group of proteins and a specific ligand coupled to a chromatography matrix. Biorecognition (ligand specificity) is the property used by affinity chromatography, which makes this technique unique in separation technology, since it enables the purification of a biomolecule on the basis of its biological function or individual chemical structure (Uhlen, 2008, Urh et al., 2009).

Affinity chromatography is a relatively simple, yet quite effective technique that offers high selectivity, hence high resolution, and usually high capacity for the protein(s) of interest. Purification can be achieved in the order of several thousand-fold and recoveries of active material are generally very high. Examples of

biomolecules that can be separated using this technique are antibodies/antigens, enzymes/substrates, or ligands/receptors (Hage, 1999).

The main materials required for an affinity chromatography procedure are 1) a gel matrix, 2) a ligand, 3) a solution containing the substrate to be isolated, 4) a wash solution to elute the non-bound impurities in the solution, and 5) a final elution solution to extract the bound substrate from its ligand (Urh et al., 2009).

The ligand must bind specifically and reversibly to the substrate and should be capable of covalently bonding to the matrix without disrupting its binding ability. This is usually facilitated by the placement of spacer arms between the ligand and the matrix, so that in case the active site is buried deep within the ligand, it is not physically hidden from its binding substrate (Cuatrecasas, 1970).

In summary, during an affinity chromatography procedure, the following steps take place (Urh et al., 2009):

- 1) Binding of the selected ligand to the matrix and the ligand-matrix gel is loaded into an elution column;
- 2) The mixture containing the substrate to isolate is poured into the elution column and the solution is pulled through the gel by gravity. The substrate of interest binds to the ligand-matrix complex and the impurities remain unbound in the gel column (Figure 3.3);
- 3) Unbound impurities are removed by a wash of extreme pH, salt concentration or temperature (Figure 3.3);
- 4) The substrate of interest is eluted from the ligand-matrix complex by a stronger second wash, which relies on the reversible binding properties of the ligand, allowing the bound proteins to dissociate from their ligand (Figure 3.3).

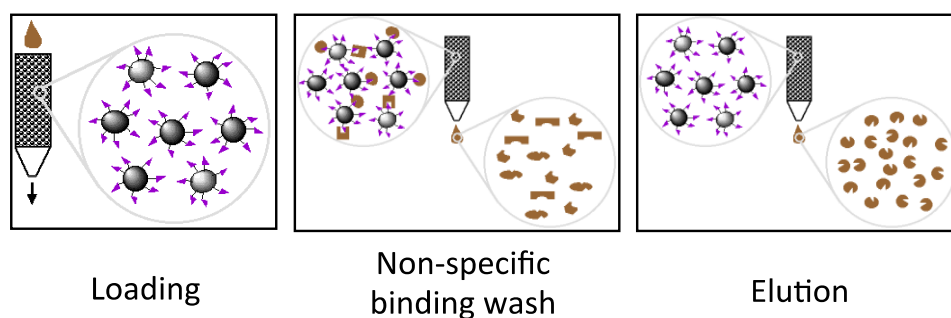


Figure 3.3 Affinity chromatography procedure.

3.1.5 Affinity-enrichment proteomics

In this chapter, a comprehensive affinity-enrichment proteomics (A^eP) study, utilising an immobilised glyco-affinity probe to identify proteins that interact with NB-DNJ and are potentially responsible for its contraceptive activity, is reported.

In order to achieve binding of NB-DNJ to enzyme targets using affinity chromatography, a resin matrix with maximal structural similarity to NB-DNJ was synthesised. Firstly, the DNJ ring was preserved in the resin matrix, as the protonated DNJ mimics the charge of sugar substrates during hydrolysis and is, therefore, of great importance for inhibiting glucosidases (Butters et al., 2000). Secondly, the alkyl chain length was synthesised to be butyl (CH₃-CH₂-CH₂-CH₂-) or longer, since only DNJ compounds with these characteristics are able to inhibit CGT (Mellor et al., 2002). Thus, the alkyl chain was designed to be longer than four carbons and the gel matrix was linked to the end of the alkyl chain. The structure and potential binding sites of the glyco-affinity resin matrix obtained, and shown in Figure 3.4, were as similar to NB-DNJ as possible.

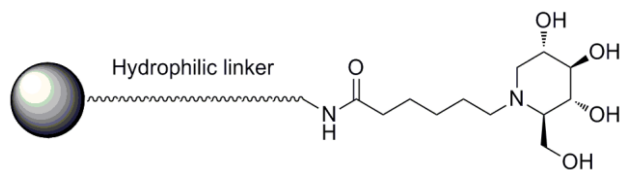


Figure 3.4 Structure of the glyco-affinity resin matrix.

Work conducted in collaboration with the University of Oxford provided protein samples from C57BL/6 mouse testis, which were enriched by DNJ-resin treatment. The mouse testis lysate was incubated with the DNJ-resin and washed to remove non-specifically bound proteins. A second wash with NB-DNJ-containing buffer eluted the proteins that had been retained by the resin. A control sample was obtained through the same procedure but using an unmodified agarose gel. Proteins in the enriched and control samples were then separated by two-dimensional polyacrylamide gel electrophoresis (2D-PAGE), followed by in-gel trypsin digestion and liquid chromatography coupled to tandem mass spectrometry (LC-MS/MS) analysis. Protein database searches performed with the resulting mass spectrometry data led to protein identification.

Immobilised iminosugars have previously been used for simple glycosidase affinity chromatography (Bernotas and Ganem, 1990, Faridmoayer and Scaman, 2004, Matern et al., 1997, Scudder et al., 1990). Though, in this study it is shown in a proof-of-concept method, how this model glycomimetic can allow proteomics directed towards its interactome.

Unlike designed purification methods, which intentionally exploit a known protein-ligand partnership for affinity, NB-DNJ was chosen in this study as a clinically approved probe molecule that is known to induce phenotypic changes, but in the absence of any such clear partnership(s). In this way, the glyco-A^eP method has the potential to identify unanticipated protein-ligand interactions that may be important in a therapeutically relevant phenotype and so, reveal a relevant focused subset of the carbohydrate-active proteome, previously not considered.

3.2 Aims & Objectives

The main aim of this study was to develop and apply an affinity-enrichment proteomic (A^eP) method to identify protein targets of NB-DNJ, with the future goal of potential drug development of a male contraceptive.

To this end, a glyco-affinity resin mimicking the structure of NB-DNJ was firstly synthesised and validated. Then, testis tissue was collected from NB-DNJ-sensitive mice (C57BL/6) and the protein fraction was analysed using the synthesised affinity resin, by a glyco-affinity chromatography followed by proteomics method, in order to find protein targets of NB-DNJ possibly responsible for the infertility phenotype.

3.3 Materials & Methods

All chemicals used in the following experiments were purchased from Sigma-Aldrich (UK) or Fisher Scientific (UK), unless stated otherwise in the descriptions below or mentioned previously. A schematic diagram summarising the experiments carried out in this study is represented in Figure 3.5.

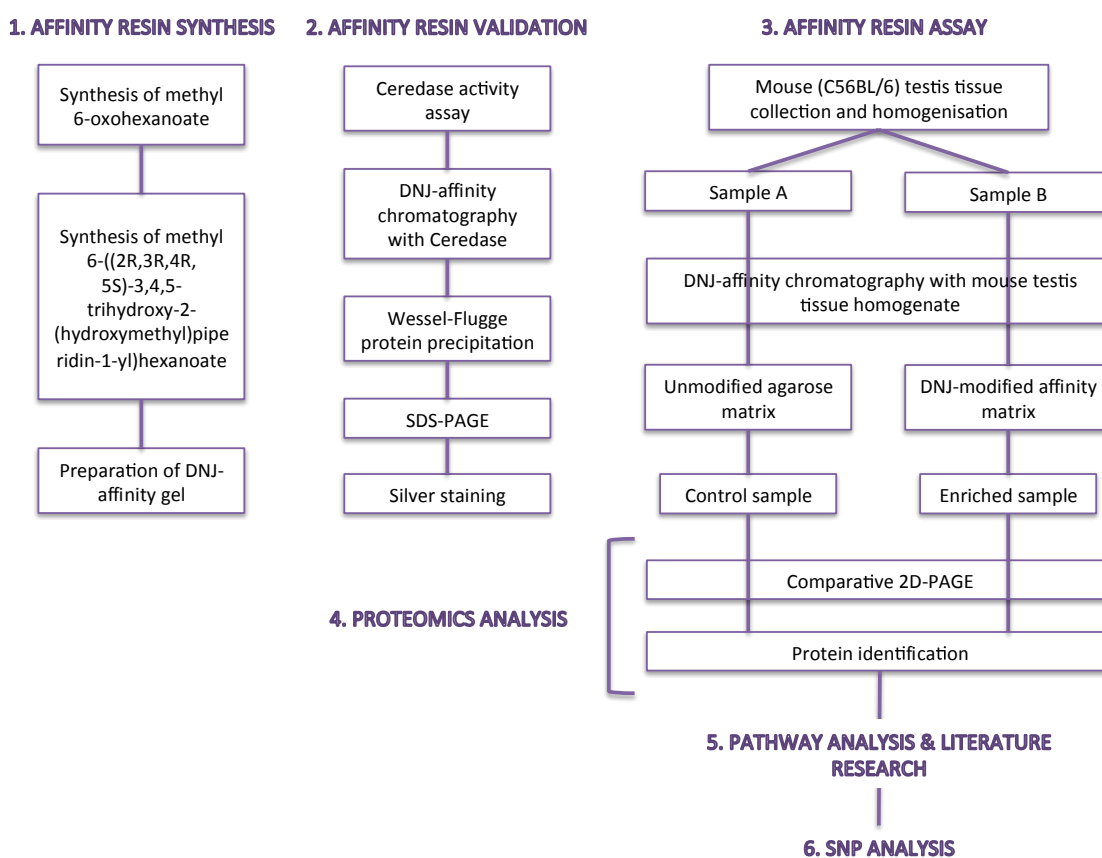


Figure 3.5 Schematic diagram summarising the experiments done in this study.

3.3.1 Affinity resin synthesis

The iminosugar affinity resin was synthesised in a few consecutive steps as detailed in the following sections. These works were done by Dr. Conor Barry and Prof. Benjamin Davis from the Department of Chemistry of the University of Oxford.

3.3.1.1 Synthesis of methyl 6-oxohexanoate

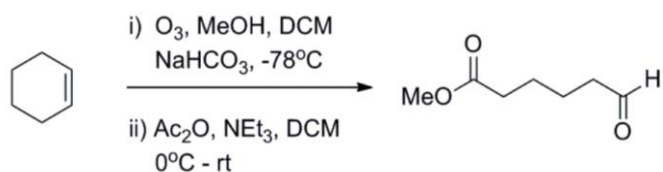
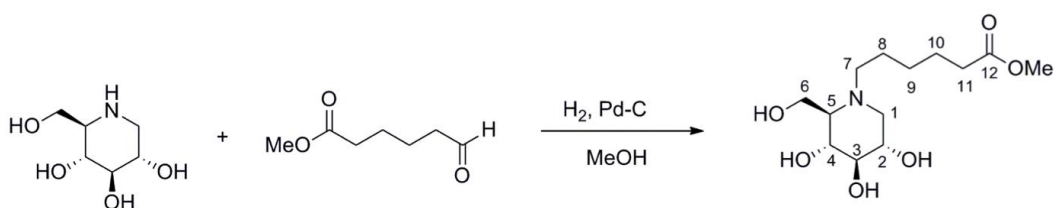


Figure 3.6 Synthesis of methyl 6-oxohexanoate.

Synthesis of methyl 6-oxohexanoate (Figure 3.6) was achieved according to the literature (Schreiber et al., 1982). A detailed description of the procedure followed by Dr. Conor Barry can be found in the electronic supplementary information of the paper in Appendix (Cruz et al., 2013a).

3.3.1.2 Synthesis of methyl 6-((2*R*,3*R*,4*R*,5*S*)-3,4,5-trihydroxy-2-(hydroxymethyl)piperidin-1-yl)hexanoateFigure 3.7 Synthesis of methyl 6-((2*R*,3*R*,4*R*,5*S*)-3,4,5-trihydroxy-2-(hydroxymethyl)piperidin-1-yl)hexanoate.

Synthesis of methyl 6-((2*R*,3*R*,4*R*,5*S*)-3,4,5-trihydroxy-2-(hydroxymethyl)piperidin-1-yl)hexanoate (Figure 3.7) was attained according to the literature (Bernotas and Ganem, 1990). Step-by-step guidance of the procedure followed by Dr. Conor Barry can be found in the electronic supplementary information of the paper in Appendix (Cruz et al., 2013a).

3.3.1.3 Preparation of DNJ-affinity gel

A scheme of the preparation of DNJ-affinity gel is represented in Figure 3.8. The detailed description of the procedure followed by Dr. Conor Barry for this step can

also be found in the electronic supplementary information of the paper in Appendix (Cruz et al., 2013a).

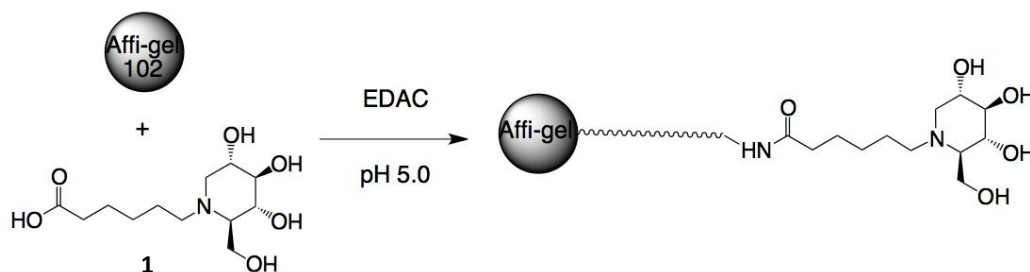


Figure 3.8 Preparation of DNJ-affinity gel.

Affi-Gel 102 was chosen as the solid matrix upon which to support the DNJ-tag. This is an agarose gel modified with an amino group at the end of a short hydrophilic chain. The modified gel was collected by gravity filtration and washed with distilled water to give the final immobilised glyco-affinity probe. The initial flow through was concentrated and analysed by proton nuclear magnetic resonance (^1H NMR) spectroscopy to allow the loading of the gel to be determined.

3.3.2 Affinity resin validation

The synthesised glyco-affinity resin was validated using a commercial preparation of acid β -glucosidase 1 (GBA)/alglucerase/Ceredase[®], a known target of NB-DNJ. The affinity resin validation was done by Dr. Celeste Chuang, Prof. Aarnoud van der Spoel and Prof. Frances Platt from the Department of Pharmacology of the University of Oxford.

3.3.2.1 Ceredase activity assay

Ceredase activity assay was one of the methods used to validate the affinity resin. A complete description of the procedure followed by Dr. Celeste Chuang can be found in Dr. Chuang's PhD thesis (Chuang, 2010) or in the electronic supplementary information of the paper in Appendix (Cruz et al., 2013a).

3.3.2.2 DNJ-affinity chromatography with Ceredase

The other method used to validate the affinity resin was DNJ-affinity chromatography with Ceredase. A comprehensive description of the procedure followed by Dr. Celeste Chuang can be found in Dr. Chuang's PhD thesis (Chuang, 2010) or in the electronic supplementary information of the paper in Appendix (Cruz et al., 2013a).

3.3.2.3 Wessel-Flugge protein precipitation

Proteins from column fractions were precipitated as described previously (Wessel and Flugge, 1984). The full Wessel-Flugge protein precipitation procedure followed by Dr. Celeste Chuang can be found in Dr. Chuang's PhD thesis (Chuang, 2010) or in the electronic supplementary information of the paper in Appendix (Cruz et al., 2013a).

3.3.2.4 SDS-PAGE

Precipitated proteins were analysed by SDS-PAGE. The SDS-PAGE procedure followed by Dr. Celeste Chuang can be found in Dr. Chuang's PhD thesis (Chuang, 2010).

3.3.2.5 Silver staining

Proteins separated by SDS-PAGE were visualised on the gels using silver staining. The detailed silver staining procedure followed by Dr. Celeste Chuang can be found in Dr. Chuang's PhD thesis (Chuang, 2010).

3.3.3 Affinity resin assay

Once validated, the glyco-affinity resin was used to carry out affinity chromatography with mouse testis tissue homogenate and test the hypothesis of this study.

3.3.3.1 Mouse testis tissue collection and homogenisation

Mouse testes from C57BL/6 male mice aged 8-10 weeks were obtained with the help of Dr. Schatzlein's group. Mice were sacrificed by elevating CO₂ concentration. All animal studies were performed in accordance with the UK Home Office Animals (Scientific Procedures) Act 1986. Mouse testes were dissected and immediately frozen in liquid nitrogen until further use.

Mouse testis tissue was homogenised with a sample grinding kit (Amersham Biosciences, UK) and proteins were extracted according to the procedure described in section 2.3.2.2.

3.3.3.2 DNJ-affinity chromatography with mouse testis tissue homogenate

The DNJ-affinity column matrix (1 mL) was loaded on to a 5 mL solid phase extraction cartridge. The column was equilibrated with 4 x 4 mL water and 2 x 4 mL washing buffer (PBS containing 0.5 % sodium cholate). Solubilised proteins were added on to the column and the column was sealed. Proteins and column matrix were incubated on a roller bank at 4 °C overnight to allow maximum binding.

Washing buffer (12 x 4 mL) was applied to remove non-column-binding proteins. The flow-through was collected along with the washing fraction. Bound proteins were incubated with 4 mL miglustat buffer (PBS containing 10 mM miglustat and 0.5 % sodium cholate) for 4 h at 4 °C, and competitively eluted with 11 x 4 mL miglustat buffer and collected as the eluate fraction.

The column was cleaned with 5 x 4 mL 1 M acetic acid (pH 2.4), 2 x 4 mL water and 5 x 4 mL 3.5 M magnesium chloride. The flow-through was collected in the cleaning fraction. The column was stored in water supplemented with 1 µM sodium azide at 4 °C.

The flow-through of the washing, eluting and cleaning steps was collected in separate fractions and concentrated by 15 mL centrifugal filter units (3 kDa molecular weight cut-off, Amicon-Ultra, Millipore, MA, USA) at 3,700 *g* for approximately 60 min, and further reduced to 50-100 µL by 500 µL centrifugal units

(3 kDa molecular weight cut-off, Millipore) at 14,000 *g* for 20-30 min. Each fraction was added with 1 % protease inhibitor (Amersham Biosciences, UK) and stored at -80 °C.

A control sample was obtained through the same procedure but using an unmodified agarose gel instead of the DNJ-affinity gel.

3.3.4 Proteomics analysis

The eluting fractions, resulting from affinity chromatography carried out in parallel with the DNJ-resin and the agarose gel (control), were then subjected to proteomics analysis in order to separate and identify the proteins.

3.3.4.1 Protein precipitation

TCA and acetone precipitation of proteins was used to remove contaminants and concentrate proteins in the samples, prior to separation by 2D-PAGE. This precipitation method was performed as described in section 2.3.4.1.

3.3.4.2 2D-PAGE

Protein separation was achieved through 2D-PAGE, which was performed according to the following steps.

3.3.4.2.1 First dimension: isoelectric focussing (IEF)

Isoelectric focussing was performed using Protean IEF Cell (Bio-Rad, UK) with 7 cm ReadyStrips, pH 3-10 (Bio-Rad, UK), according to the description in section 2.4.3.1. Pellets resulting from TCA and acetone precipitation were resuspended in rehydration buffer II to a total volume of 125 µL. Mixtures were centrifuged and the supernatants were loaded into a focussing tray. The rehydration procedure took place at 50 V (active rehydration) for 12 h (overnight). Focussing was then started and carried out on a linear ramp according to the following steps: 250 V for 15 min, 4000 V for 2 h, 4000 V until 20 000 V/h (Table 2.3, focussing conditions C).

3.3.4.2.2 Equilibration, reduction and alkylation

The equilibration, reduction and alkylation step was performed in accordance to section 2.4.3.2.

3.3.4.2.3 Second dimension: SDS-PAGE

Each strip was transferred to the top of a precast gel, Mini-Protean TGX Precast Gels, any kD, IPG well comb, 7 cm IPG strip (Bio-Rad, UK), as described in section 2.4.3.3. Electrophoresis was carried out using a Mini-Protean Tetra Cell System (Bio-Rad, UK) at 40 V until the blue dye had reached the main gel, and then increased to 150 V until the dye front had reached the bottom of the gel.

3.3.4.2.4 Gel staining: silver staining

The Pierce Silver Stain Kit (Thermo Scientific, UK) was used to visualise the proteins on the 2D gels, according to the details given in section 2.5.2.

3.3.4.3 Gel image analysis

Gel images of the DNJ-resin gel and the control gel were obtained with a digital photographic camera and using the camera device of EXQuest Spot Cutter (Bio-Rad, UK), and analysed using PDQuest Advanced software version 8.0.1 (Bio-Rad, UK). The Multi-Channel Viewer tool was used to overlap the two gel images.

3.3.4.4 Protein identification

Protein identification was attained by in-gel trypsin digestion, followed by LC-MS/MS analysis. The respective procedures are depicted in the subsequent sections.

3.3.4.4.1 Spot excision, washing and in-gel trypsin digestion

Spots of interest were manually excised from the gels, cut into 1-2 mm³ gel pieces and placed into 0.6 mL siliconised tubes. The subsequent washing steps and in-gel trypsin digestion were performed as described in section 2.6.1.1.

3.3.4.4.2 Peptide extraction from gel pieces

Peptides were extracted from the gel pieces in accordance to the procedure described in section 2.6.1.2. The final dried extracts were re-dissolved in 95 % water + 5 % acetonitrile + 0.1 % formic acid, sonicated in ice cold water for 10 min, centrifuged for 5 min and transferred to MS compatible vials.

3.3.4.4.3 LC-MS/MS analysis

Peptide samples were analysed in two distinct instruments. The analytical conditions and equipment details can be found according to the information below.

The initial analysis was conducted with the collaboration of Dr. Holger Kramer from the Department of Physiology, Anatomy and Genetics of the University of Oxford. A detailed description of the procedure for the initial analysis of in-gel digested protein material followed by Dr. Holger Kramer can be found in the electronic supplementary information of the paper in Appendix (Cruz et al., 2013a).

LC-MS/MS confirmation analysis was performed on a Waters CapLC system coupled to the front end of a Waters Micromass Q-ToF Premier, as described in section 2.6.1.3.

3.3.4.4.4 Data processing and database searching

For the initial analysis dataset, raw LC-MS/MS data were processed and MASCOT compatible files created using DataAnalysis 4.0 software (Bruker Daltonics) with the help of Dr. Holger Kramer. Parameters used for database searching can be found in the electronic supplementary information of the paper in Appendix (Cruz et al., 2013a).

For the confirmation analysis dataset, raw LC-MS/MS data were processed using MassLynx ProteinLynx version 4.1 (Waters, UK) and searches were done using the online version of MASCOT, as described in section 2.6.1.4. SwissProt databases were chosen to look for mouse proteins (taxonomy — *Mus musculus*). The search

parameters used were the ones listed in the same section of Chapter 2, with the exception of the peptide and fragment mass tolerances, which were set to ± 0.3 Da.

3.3.5 Pathways analysis

All interactions of HYOU1 protein were analysed using Pathway Studio 9 software (Elsevier).

3.3.6 Single-nucleotide polymorphism (SNP) analysis

SNP analysis was applied to the genes encoding for the 6 most interesting proteins identified, examining differences between NB-DNJ-sensitive strain C57BL/6 and insensitive strain FVB/N. This analysis was performed by Dr. Sarah Lloyd from the MRC Prion Unit of the UCL Institute of Neurology.

The SNP differences between C57BL/6 and FVB/N were downloaded from the Sanger Centre ftp site (<ftp://ftp-mouse.sanger.ac.uk/REL-1206-FVBNJ/>, data file: 2012-0612- snps+indels_FVBNJ_annotated.vcf). The genes and chromosome positions that were used are listed in Table 3.1. Annotated gene sequences were searched 5 kb both upstream and downstream. All SNP data come from the Sanger Institute sequence data and all base position numbers refer to NCBI Build 37.

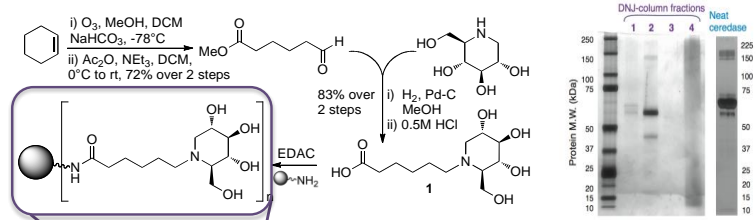
Table 3.1 Parameters used in the SNP analysis.

Gene Name	Chromosome	Start	Start-5000	End	End+5000
<i>Hyou1</i>	9	44187573	44182573	44200452	44205452
<i>Hspa2</i>	12	77505357	77500357	77507923	77512923
<i>Jup</i>	11	100239403	100234403	100259053	100264053
<i>Set</i>	2	29922246	29917246	29927314	29932314
<i>Cct6a</i>	5	130293261	130288261	130322231	130327231
<i>Anp32a</i>	9	62189150	62184150	62226609	62231609
<i>Anp32b</i>	4	46463989	46458989	46485395	46490395

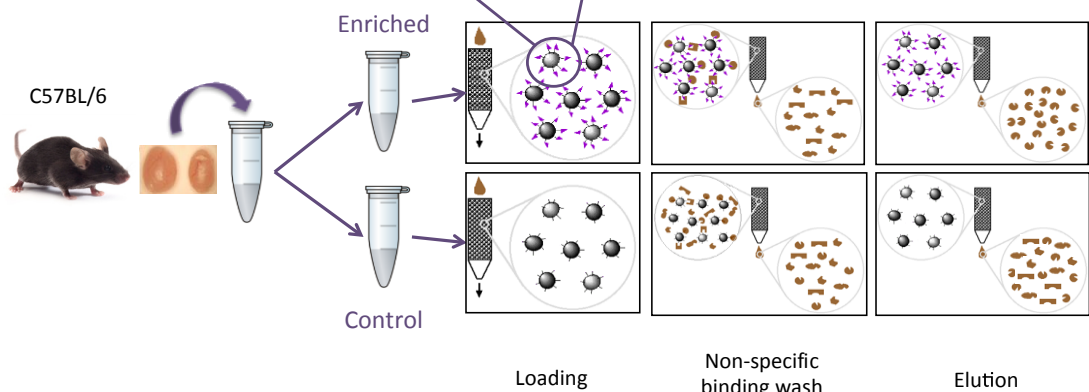
3.4 Results & Discussion

The following scheme illustrates the different steps in which this study was divided and summarises the experiments performed (Figure 3.9).

1) Affinity probe synthesis & validation



2) Affinity chromatography



3) Proteomics

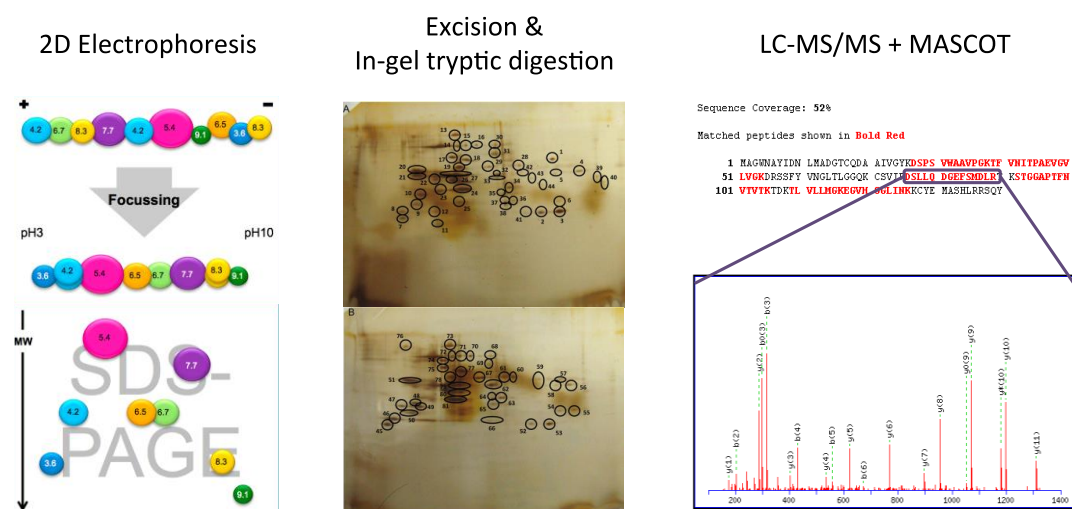


Figure 3.9 General scheme of the study.

3.4.1 Affinity resin synthesis

With the collaboration of Dr. Conor Barry from the Department of Chemistry of the University of Oxford, a carboxyl-bearing probe ligand **1** derived from DNJ (Paulsen et al., 1967) was prepared in a two-step protecting-group-free synthesis, employing methanolytic ozonolysis of cyclohexene (Schreiber et al., 1982) followed by reductive alkylation of DNJ. The glyco-affinity probe **1** was immobilised on amino-terminated agarose support through EDAC (1-ethyl-3-(3-dimethylaminopropyl)-carbodiimide)-mediated amide bond formation. A simplified scheme of the glyco-affinity probe synthesis and preparation of the glyco-affinity resin is shown in Figure 3.10.

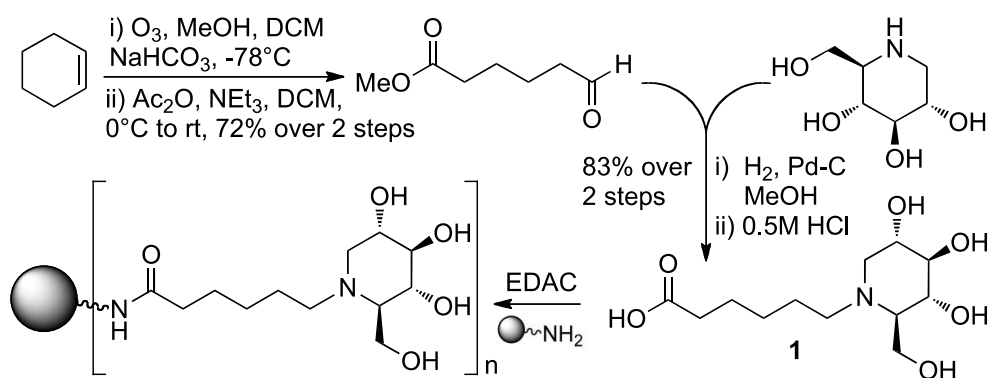


Figure 3.10 Glyco-affinity probe synthesis and preparation of the glyco-affinity resin.

During the coupling reaction of DNJ-probe and Affi-Gel, DMSO was added as an internal standard to allow the loading of the gel to be determined by ^1H NMR spectroscopy. When the coupling reaction was complete, the modified gel was collected by gravity filtration and washed through with water to elute any unbound DNJ-probe. The flow-through was collected, concentrated and analysed by ^1H NMR spectroscopy. Comparison of the integrals of the DMSO peak and one of the 6-*HH* signals of the DNJ-probe in the ^1H NMR spectrum indicated a loading of $40.6\ \mu\text{mol}$ DNJ-probe per mL of gel (Cruz et al., 2013a).

3.4.2 Affinity resin validation

The binding ability of the resulting glyco-A⁶P probe matrix was validated with a clinically utilised acid β -glucosidase 1 (GBA)/Ceredase[®] preparation (Platt et al., 1994a, Alfonso et al., 2005, Platt et al., 1994b). Ceredase[®] is used in enzyme replacement therapy to treat type 1 Gaucher patients. It is a modified form of glucosylceramidase (glucocerebrosidase), which is moderately inhibited by NB-DNJ. Therefore, Ceredase[®] is a known target of NB-DNJ.

In the Ceredase[®] activity assay, performed by Dr. Celeste Chuang from the Department of Pharmacology of the University of Oxford, the glucosylceramidase activity was compared between Ceredase[®] and fractions eluted from DNJ-affinity gel loaded with Ceredase[®]. The results of this assay showed that control Ceredase[®] released 2.7 and 0.5 pmol 4-MU per min for 0.16 and 0.016 U of Ceredase[®], respectively. The activity of the fractions eluted from DNJ-affinity gel loaded with Ceredase[®] was reduced to 38.9 % (0.16 U) and 11.4 % (0.016 U), suggesting a significant amount of Ceredase[®] was bound to the DNJ-affinity probe (Chuang, 2010).

In order to confirm the binding of Ceredase[®] to the glyco-affinity probe, 0.16 U of Ceredase[®] were incubated with the DNJ-affinity resin for 2 h at 4 °C. The DNJ-resin was then washed, eluted and cleaned as described earlier. The flow-through of the washing, eluting and cleaning steps was collected in separate fractions, concentrated and analysed by SDS-PAGE (Chuang, 2010). An image of the gel obtained is depicted in Figure 3.11.

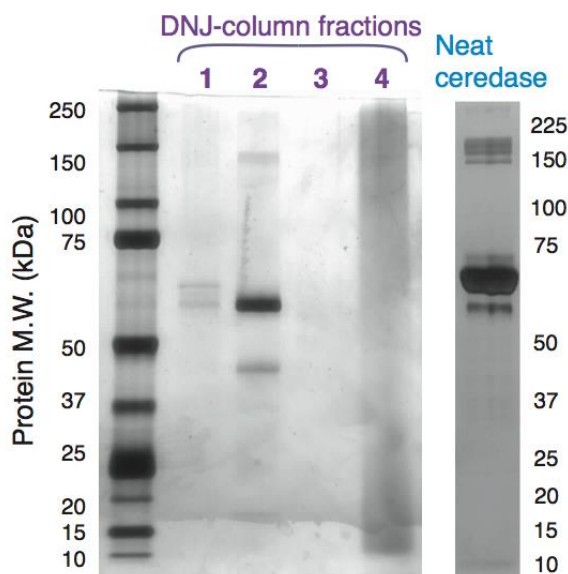


Figure 3.11 SDS-PAGE of Ceredase® and fractions eluted from DNJ-affinity gel loaded with Ceredase®. DNJ-affinity gel (1 mL) was equilibrated with water and washing buffer (PBS, 0.5 % sodium cholate), then incubated with 0.16 U Ceredase® for 2 h at 4 °C. The gel column was washed with 50 mM sodium acetate (1); eluted with 10 mM NB-DNJ in washing buffer (2); and cleaned with 1 M acetic acid (3), water, 3.5 M magnesium chloride (4). Gel was stained with silver staining. This assay was performed by Dr. Celeste Chuang (Chuang, 2010).

In Figure 3.11, protein bands of control Ceredase® are shown, the major band being the one between 50 and 75 kDa, which corresponds to the active ingredient alglucerase. From the observation of Figure 3.11, it is possible to conclude that the majority of Ceredase® was eluted with 10 mM miglustat buffer, as fraction 2 presented a protein band between 50 and 75 kDa, corresponding to alglucerase. A minor amount of Ceredase® was visualised in the washing buffer fraction (fraction 1) and no detectable protein bands were present in the acid (fraction 3) and high salt concentration (fraction 4) cleaning steps (Chuang, 2010).

These results confirmed the binding of Ceredase® to the DNJ-affinity resin and that Ceredase® can be completely eluted with a high concentration of miglustat buffer. The negligible amounts of Ceredase® in the washing fraction demonstrated that binding of Ceredase® to the DNJ-affinity probe could withstand stringent washes (Chuang, 2010).

These validation experiments importantly confirmed functional utility of the glyco-A^eP probe matrix through extraction of a known protein partner. The unknown

targets of NB-DNJ that are related to the infertility phenotype are likely to have high affinity to NB-DNJ. The interaction between Ceredase® and NB-DNJ is known to be weak at submillimolar levels. The fact that Ceredase® could be isolated by DNJ-affinity chromatography under Ceredase®-optimised buffer conditions suggested that decent bindings between the glyco-A^eP probe matrix and NB-DNJ target proteins can be expected.

After validation of the glyco-A^eP probe matrix, tissue was collected from a mammal with relevant phenotype (mouse testis from NB-DNJ-sensitive male C57BL/6 mice) to identify proteins contributing to inducible infertility. Protein fraction from homogenised tissue was split into two and interrogated with either glyco-A^eP probe matrix or unmodified agarose (control). Washing removed unbound and non-specifically bound fractions. The many selected or enriched binding proteins were eluted from the respective matrices with NB-DNJ-containing buffer and were concomitantly further fractionated and directly visualised by comparative 2D-polyacrylamide gel electrophoresis (2D-PAGE), detected by silver staining.

3.4.3 2D-PAGE gels

Approximately 70 μg of protein for the control sample and 60 μg of protein for the enriched sample were separated by 2D-PAGE, using pH 3-10 IPG strips for the first dimension and precast gels for the second dimension (SDS-PAGE). Gels were stained with silver staining, which allows the observation of lower concentration proteins, and then photographed. Images of the resulting 2D gels are shown in Figure 3.12.

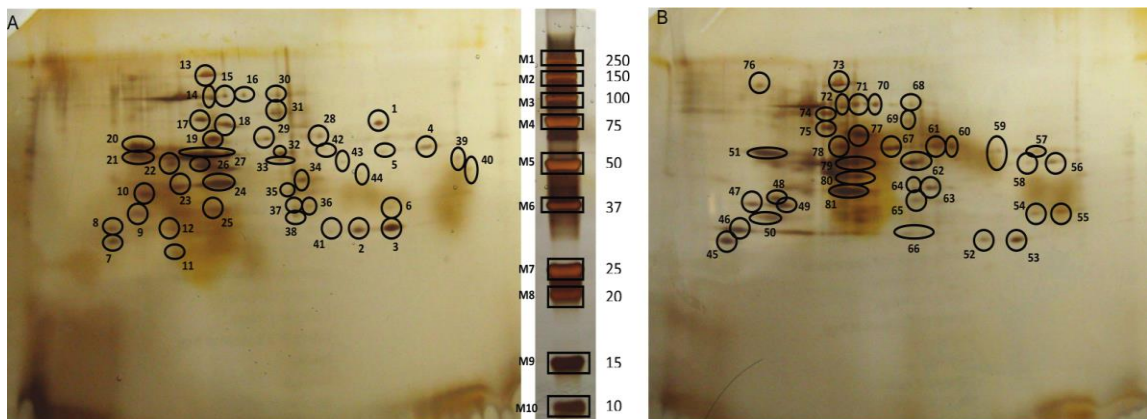


Figure 3.12 Comparative 2D-PAGE analysis of C57BL/6 mouse testis passed through unmodified control (A) and DNJ-modified affinity (B) matrices. pl scale 3-10. Middle: molecular weight marker. Gels were stained with silver staining. All 81 labelled spots were analysed by LC-MS/MS.

In Figure 3.12 individual protein spots are visible in both gels, indicating that pH 3-10 strips successfully separated proteins in this pH range. Some protein spots showed intensity differences between the control and the enriched sample, a number of which were even only present in one of the gels, suggesting the presence of proteins with different affinity for the modified resin. The most interesting proteins would be the ones that were present in the enriched sample and absent from the control sample, since these proteins may have a stronger affinity to the DNJ-resin and, consequently, interact more closely with NB-DNJ. One of these proteins which were unique to the enriched gel, might be a specific target of NB-DNJ and be responsible for the reduction of male fertility in particular mouse strains.

In order to identify these proteins, all 81 labelled spots were excised, subjected to in-gel trypsin digestion, and the peptides were extracted from the gel matrix and analysed by proteomic LC-MS/MS. A control for trypsin efficiency was analysed in parallel. MS/MS data were used to perform database searches, employing a licenced search engine – MASCOT (Perkins et al., 1999), with suitable search parameters and choice of SwissProt database to look for mouse proteins (taxonomy – *Mus musculus*).

3.4.4 Selection of proteins identified

Firstly, two very common contaminants abundantly seen in proteomics analysis were eliminated from the hits list of each spot. Those two contaminants were keratin, a constituent of skin, hair and nails from a family of fibrous structural proteins, and trypsin, an enzyme widely used in in-gel digestion (Keller et al., 2008). Keratin is usually inadvertently introduced by the operator and trypsin, which is used in excess to guarantee that all the proteins in a specific spot are digested, suffers autolysis and its peptides can be detected by MS.

From 351 proteins identified, 64 that were also identified in the control were discounted from the glyco-A^eP screen (Figure 3.13).

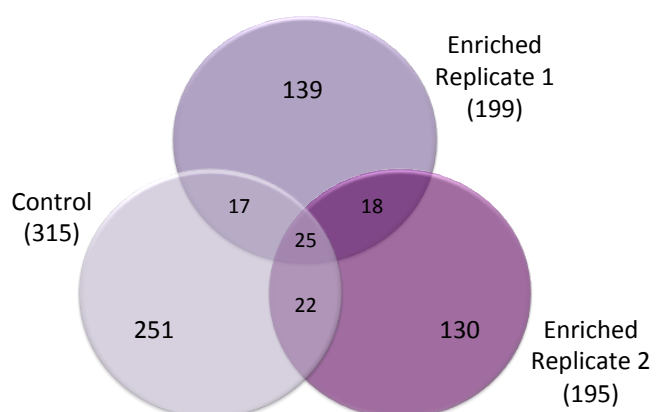


Figure 3.13 Venn diagram of glyco-A^eP proteins identified with a MASCOT score > 20.

The following strategy was applied to minimise the chances of false-positive identification of contaminant proteins:

Only significant (P-value cut-off < 0.05) protein identifications were accepted throughout all searches;

Protein hits in the enriched sample were only considered if identified twice (in replicates 1 and 2);

At the same time, all protein hits which were found in either replicate of the control sample (replicate 1 or 2) were discarded and not considered as potential interaction proteins.

This generated a focused list of 18 proteins reliably identified through glyco-A^eP probing (but not in controls) as strong carbohydrate-active candidates (Table 3.2).

Cross-validation of theoretical molecular weights and isoelectric points allowed further narrowing of this focus group and reduced the protein cohort to 6 proteins with plausible function roles. These 6 most significant proteins are highlighted in Figure 3.14 and Table 3.2.

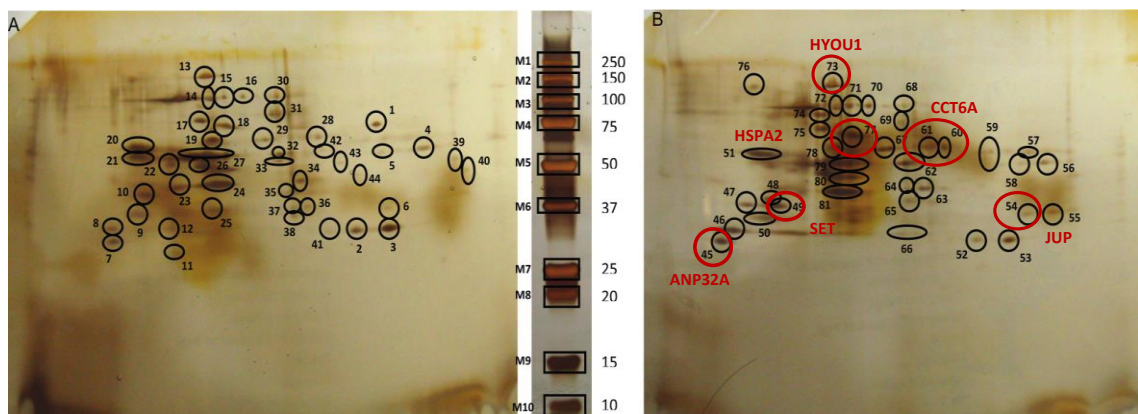


Figure 3.14 Six most significant proteins highlighted in comparative 2D-PAGE analysis of C57BL/6 mouse testis passed through unmodified control (A) and DNJ-modified affinity (B) matrices. pI scale 3-10. Middle: molecular weight marker.

Table 3.2 Significant proteins identified from mouse testis with putative NB-DNJ affinities using glyco-A⁶P.

Spot ^(a)	Accession Number	Protein Name	Protein Code	Score	Mr (Da)	pI	% Coverage
73	Q9JKR6	Hypoxia up-regulated protein 1	HYOU1	291	111 340	5.12	68
54	Q02257	Junction plakoglobin	JUP	65	82 490	5.75	37.3
77	P17156	Heat shock-related 70 kDa protein 2	HSPA2	92	69 884	5.51	51
45	O35381	Acidic leucine-rich nuclear phosphoprotein 32 family member A	ANP32A	86	28 691	3.99	23.9
49	Q9EQU5	Protein SET	SET	49	33 358	4.22	29.1
60/61	P80317	T-complex protein 1 subunit zeta	CCT6A	45	58 424	6.63	51.8
50	P70670	Nascent polypeptide-associated complex subunit alpha	NACA	104	221 277	9.39	49.1
62	P80314	T-complex protein 1 subunit beta	CCT2	60	57 783	5.96	13.8
56	Q059Y8	DC-STAMP domain-containing protein 1	DCST1	41	85 646	9.42	37.8
71	Q8BJQ2	Ubiquitin carboxyl-terminal hydrolase 1	USP1	38	88 314	5.33	41.6
77	P17879	Heat shock 70 kDa protein 1B	HSPA1B	60	70 418	5.53	44.1
46	Q63ZV0	Insulinoma-associated protein 1	INSM1	46	55 042	9.24	41.5
54	P01643	Ig kappa chain V-V region MOPC 21	-	40	15 063	6.26	38.2
54	Q52KB6	C2 domain-containing protein 3	C2CD3	38	257 281	6.52	37.8
77	Q6A068	Cell division cycle 5-related protein	CDC5L	37	92 361	7.98	37.3
52	A2ARV4	Low-density lipoprotein receptor-related protein	LRP2	27	537 628	4.94	18.6
54	Q8VHJ7	Peroxisome proliferator-activated receptor gamma coactivator 1	PPARGC1B	26	113 773	4.92	25
45	Q8C9J3	Sperm flagellar protein 2	SPEF2	23	199 477	5.65	35.6

(a) Spots in bold and italic indicate proteins unique to the enriched sample; spots in bold indicate enriched proteins.

Gel images were also obtained using the camera function of EXQuest Spot Cutter and analysed using PDQuest Advanced software. The Multi-Channel Viewer tool of the software allows overlapping of up to three gel images, assigning a different filter/colour to each individual image. This tool was used to overlap the two gel images (unmodified control gel – A and DNJ-modified gel – B), which are represented in blue and orange, respectively, in Figure 3.15. The 6 most relevant proteins identified are highlighted in the overlapped image.

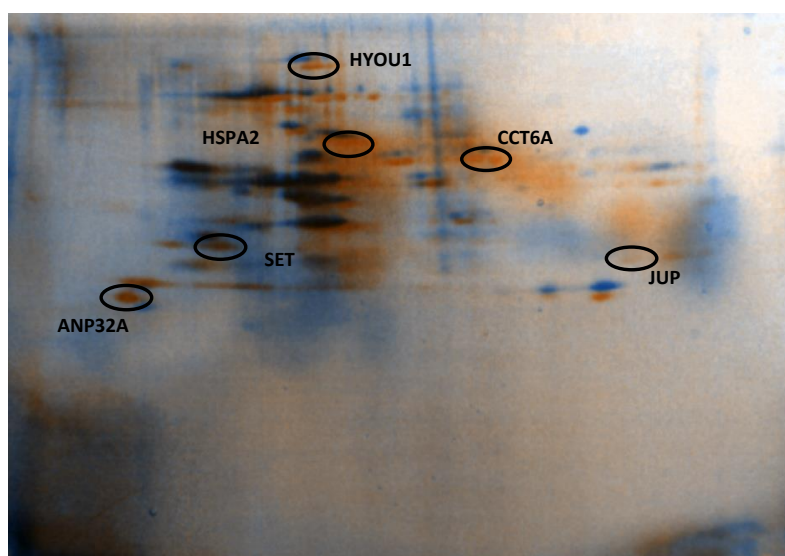


Figure 3.15 Overlapped gel image of DNJ-modified and unmodified control gel images. Spots in the control gel are represented in blue and spots in the DNJ-modified gel can be seen in orange. Overlapped spots are shown in a darker colour. The six most relevant proteins identified are highlighted in the image (HYOU1, HSPA2, JUP, SET, CCT6A, ANP32A).

The overlapped image in Figure 3.15 confirms the importance and uniqueness of the protein focus group, as it is possible to observe that the spots in which those 6 proteins were identified are only present in the DNJ-modified gel (orange).

Interestingly, for one of the 6 selected proteins – JUP, which was identified in spot 54, the theoretical molecular weight and isoelectric point do not correspond to the observed values. In fact, spot 54 on the DNJ-modified gel image has an observed molecular weight of 25-37 kDa and isoelectric point of 8-9, which are quite different from the theoretical values of 82.5 kDa and 5.75, respectively (Table 3.2). Despite these discrepancies, JUP has been selected to integrate the protein focus group, as literature search revealed interesting functions and a possible relationship of this

protein with infertility. The disparities in the observed values are consistent with the possible presence of a post-translational modified form of the same protein. Most proteins undergo some form of modification following translation. These modifications result in molecular weight and/or isoelectric point changes that are detected during MS analysis (Mann and Jensen, 2003). Further studies would be needed to confirm this hypothesis.

It should be noted that the identification of some membrane bound CAP glycosidases and glycosyltransferases has required bespoke separation methods, such as sucrose gradient for Golgi membranes (Lin et al., 2008), and this may lead to a potential under-representation of these proteins in the broad-ranging glyco-A^eP strategy that was employed in this study.

For a minority of spots, protein identification results were unsatisfactory, since there were only a few and not very intense peaks in the chromatograms, resulting in insufficient MS/MS fragmentation data, which did not permit the identification of possible proteins. This could most likely have been caused by experimental errors, such as incorrect handling of samples that could result in loss of pieces of the gel spot, or inappropriate instrument sensitivity to detect very low abundance proteins.

Intriguingly, some proteins were identified in more than one spot. Examples of those were serum albumin; Arf-GAP with SH3 domain, ANK repeat and PH domain-containing protein 2; glial fibrillary acidic protein; AT-rich interactive domain-containing protein 5A; tyrosine-protein phosphatase non-receptor type 1.

The proteins listed above were identified in more than one spot that had been excised from both the control and the enriched gel, which is in line with the possible presence of different post-translational modified forms of the same proteins. As mentioned before, the majority of proteins undergo some form of modification following translation, which may result in molecular weight and/or isoelectric point changes that are detected during MS analysis (Mann and Jensen, 2003). Further studies would be needed in order to corroborate this hypothesis.

On the other hand, proteins are identified on the basis of peptide sequence matching with a database. The smaller in number of amino acids the sequences identified are, the lower is the probability of identifying specific proteins with a high score. In addition, several small amino acid sequences are shared among many proteins, whereas unique peptide sequences are characteristic of a specific protein. Therefore, if those proteins were identified based on small non-unique peptide sequences, it is possible that these sequences were present in more than one spot, regardless of the gel from which they were cut (Hoffmann and Stroobant, 2007).

Furthermore, the proteins mentioned above were probably present in high abundance in both samples, masking lower concentration proteins. Serum albumin, for example, as a major constituent of plasma, is present in blood. The samples analysed were tissue homogenates, which were likely to be contaminated with blood, explaining the presence of serum albumin (You et al., 2005).

It should be noted that there might be inherent variability in tissue sample, phenotypic state and through handling variations. Still, it is noteworthy that the glyco-A^eP method showed apparent robustness in this regard, since an additional glyco-A^eP experimental round using testis tissue, successfully identified with high significance five out of the six proteins identified in the primary rounds. Preliminary experiments using brain tissue did not identify these proteins.

Moreover, the methods of data analysis performed in this study, using the MOWSE scoring system as implemented by MASCOT (Perkins et al., 1999), will have a profound effect upon initial agreements on identified proteins (Figure 3.16). At low thresholds (score > 20) there is a lower initial overlap between enriched sets, whereas at higher thresholds (score > 50) there is almost complete overlap (all non-excluded proteins in set 2 are also found in set 1). Notably, all of the proteins listed in Table 3.2 have a score significantly above the threshold of 33 (> 45, in fact) that has been recommended for mammalian tissue samples (Koenig et al., 2008).

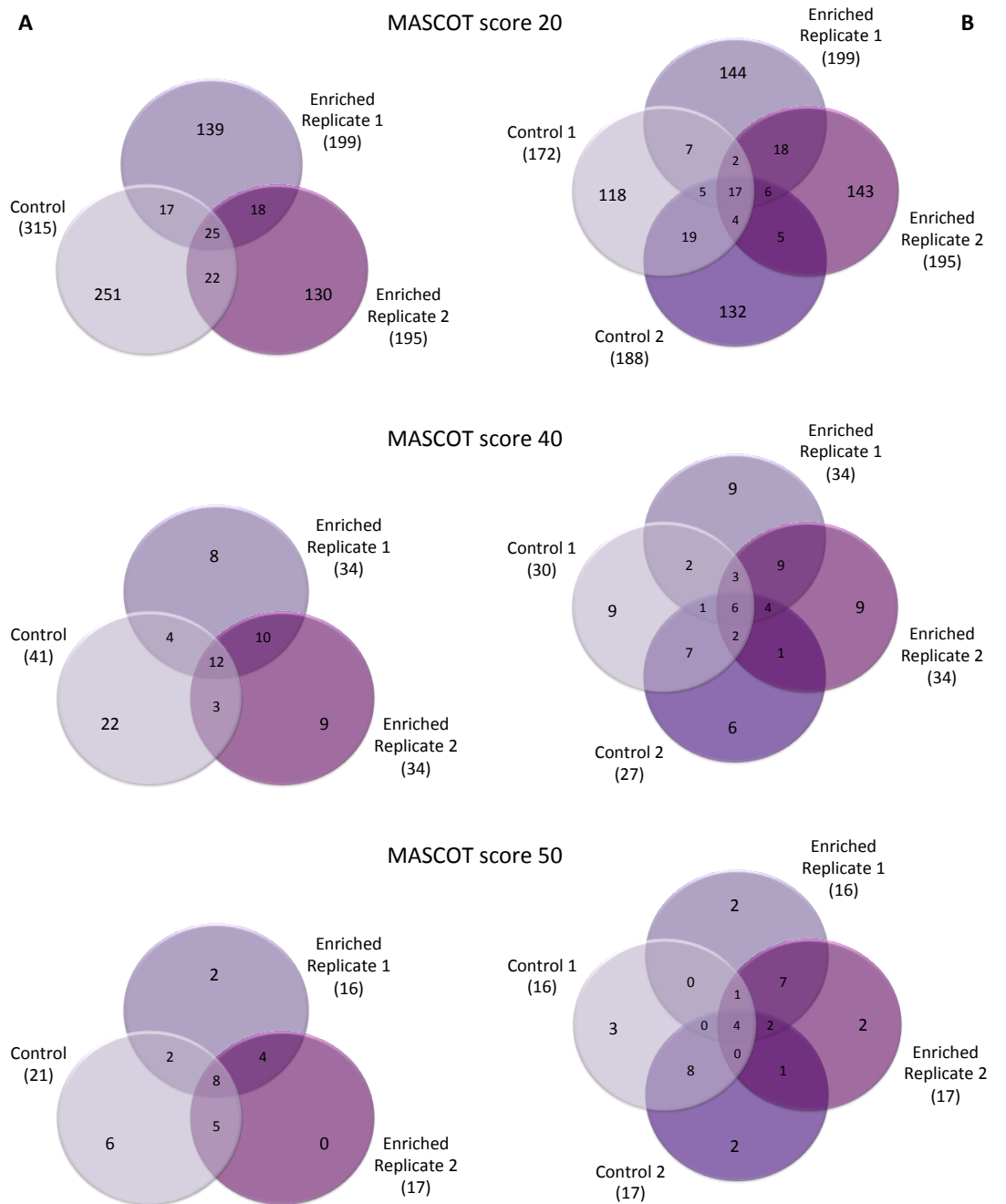


Figure 3.16 Venn diagrams of the outcomes at different levels of protein score thresholds and different use of either (A) ‘combined exclusion’ or (B) ‘overlap exclusion’. Different protein scores from the MASCOt software lead to different outcomes in the excluded and overlapped sets of identified proteins. As the score threshold increases, as would be expected, the agreement between sets also increases.

3.4.5 Most interesting protein identifications

Two Hsp70 proteins, Heat shock-related 70 kDa protein 2 (HSPA2) and Hypoxia up-regulated protein 1 (HYOU1), were identified. The 70 kDa heat shock proteins (Hsp70s) are a family of ubiquitously expressed proteins that stabilise pre-existent proteins against aggregation, and mediate the folding of newly translated polypeptides in the cytosol as well as within organelles, in cooperation with other chaperones (Tavaria et al., 1996, Morano, 2007, Zakeri et al., 1988). Members of the Hsp70 family are strongly up-regulated by heat stress and toxic chemicals, and participate in the disposal of damaged or defective proteins (Luders et al., 2000). In addition to improving overall protein integrity, Hsp70s directly inhibit apoptosis (Beere et al., 2000), hence having a recognised role in cancer (Ricanadis et al., 2001, Ramp et al., 2007).

The testis functions on the brink of hypoxia (Lysiak et al., 2000) and low oxygen levels in the testis are required for spermatogenesis (Gruber et al., 2010). Proteins that are up-regulated by low oxygen concentrations, such as HYOU1, also known as Grp170, may play key roles in spermatogenesis. Additionally, HYOU1 directly regulates insulin (INS) (Kobayashi and Ohta, 2005) and vascular endothelial growth factor (VEGF) (Semenza, 2001), as demonstrated in Figure 3.17. Abnormal VEGF levels in seminal plasma correlate with IVF (*in vitro* fertilisation) pregnancy success (Obermair et al., 1999). Insulin affects reproductive function in humans and animals at multiple levels by effecting endocrine control of spermatogenesis, as well as on mature ejaculated spermatozoa (Lampiao et al., 2009).

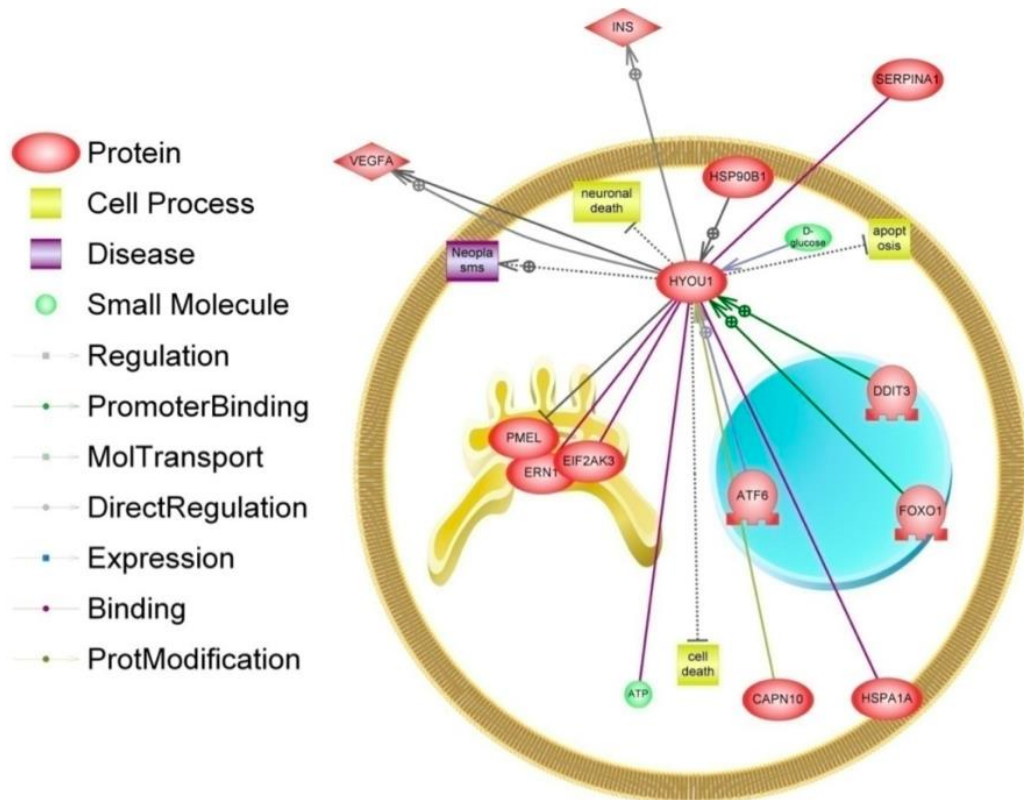


Figure 3.17 Pathways focused on HYOU1 protein. Pathway analysis performed using Pathway Studio 9 (Elsevier).

The second Hsp70 protein, HSPA2, is a testis-specific form in mice, where it is regulated developmentally and expressed in spermatogenic cells (Eddy, 1999). It has a unique role during germ cell differentiation (Vos et al., 2008) and is necessary for progression of meiosis in mouse germ cells (Eddy, 1999, Dix et al., 1996). Regarding the relationship between HSPA2 and human male infertility, a study performed in men undergoing testicular biopsy during an investigation of subfertility demonstrated that decreased expression of this protein is associated with the pathogenesis of male infertility (Feng et al., 2001).

Junction plakoglobin (JUP, desmoplakin 3) is a junctional plaque protein involved in the formation of desmosomes and tight junctions (Kowalczyk et al., 1998). Mice with impaired ability to form tight junctions (e.g. *Epas1^{-/-}*) display higher testicular oxygen levels, which interferes with spermatogenesis (Gruber et al., 2010). It is conceivable that desmosome disruption by NB-DNJ may affect spermatogenesis by such a mechanism. Indeed reversible male infertility has been demonstrated by

unrelated small molecules that disrupt adherens junctions in the testis (Mruk et al., 2006).

A somewhat intriguing discovery in this study was protein SET, also designated as template activating factor 1 β , a histone chaperone for nucleosome assembly (Kato et al., 2011) and as I2PP2A (Li et al., 1996). I2PP2A inhibits multifunctional protein phosphatase PP2A. Notably, I2PP2A binds sphingolipids, including ceramide and PTY720, a clinical sphingosine analogue (Saddoughi et al., 2013). Given that NB-DNJ, in its inhibition of GCS, competitively inhibits ceramide binding, it may be possible that NB-DNJ binds SET/I2PP2A in a similar manner (Butters et al., 2000).

Interestingly, several of the discovered proteins are chaperones. Not only HYOU1, HSPA2 and SET, but also T-complex protein 1 subunit zeta (CCT6A), which is a chaperone protein involved in the folding of tubulin and actin and other proteins (Gao et al., 1992). Curiously, NB-DNJ-sensitive strains (C57BL/6) showed decreased levels of acrosomal proteins after treatment with miglustat, when compared with non-sensitive strains (FVB/N) (Bone et al., 2007). It is possible that NB-DNJ impairment of chaperone protein function may be responsible for this phenotype.

Some of the selectively identified partners have no obvious potential role. The acidic leucine-rich nuclear phosphoprotein 32 family members (ANP32), identified in spot 45, have been implicated in a number of cellular processes including cell cycle progression, differentiation and apoptosis (Reilly et al., 2011). However, gene disruption studies of ANP32A produced mouse strains which were both viable and fertile (Opal et al., 2004), suggesting that these proteins are not directly implicated in NB-DNJ induced male infertility and potentially highlight a functionally unrelated interaction.

Together these data implicate a glycomimetic-interactome (Hsps, junctional proteins, chaperones and ceramide binders) that would not have been readily predicted, but that suggest functionally plausible pathways for investigation, such as the effects of chaperones and tight junction assembly on spermiogenesis. In a near future, these results could lead to validated drug targets for contraception.

3.4.6 Single-nucleotide polymorphism (SNP) analysis results

Single-nucleotide polymorphism (SNP) is a DNA sequence variation occurring when a single nucleotide — A (adenine), T (thymine), C (cytosine) or G (guanine) — differs between members of a biological species or between a pair of chromosomes in a human. For example, two sequenced DNA fragments from distinct individuals, AAGCCTA to AAGCTTA, contain a difference in a single nucleotide (Brookes, 1999).

SNPs are the most common type of genetic variation among humans. They occur with a frequency of 1 in every 300 nucleotides on average. The genomic distribution of SNPs is not homogeneous. Most commonly, these variations are found in the DNA between genes, in non-coding regions, and they can be used as biological markers to highlight the location of genes that are associated with diseases. However, when SNPs occur within a gene or in a regulatory region near a gene (coding region), they may play a more direct role in disease by affecting the gene's function. Gene's function is only affected if an SNP within a coding region changes the amino acid sequence of the protein that is produced, which does not necessarily happen due to the degeneracy of the genetic code (Varela and Amos, 2010, Nachman, 2001).

The vast majority of SNPs have no effect on health or development. Nevertheless, some of these genetic differences have proven to be very important in the study of diseases. Moreover, SNPs may help predict an individual's response to certain drugs, susceptibility to environmental factors such as toxins, and risk of developing particular diseases. They can also be helpful to track the inheritance of disease genes within families (Ginsburg and McCarthy, 2001, Sachidanandam et al., 2001).

Inspection of the genetic differences that code for the identified proteome between sensitive and insensitive mice allows identification of SNPs. In this study, SNP analysis was used in order to investigate the occurrence of genetic differences between NB-DNJ-sensitive and insensitive mice that would explain this phenotypic distinction.

With the help of Dr. Sarah Lloyd from the MRC Prion Unit of the UCL Institute of Neurology, SNP analysis was applied to genes encoding for the proteins identified using the glyco-A^eP strategy, examining differences between NB-DNJ-sensitive strain C57BL/6 and insensitive strain FVB/N (Wang et al., 2012a). Annotated gene sequences were searched 5 kb both upstream and downstream.

Among the focus group of the 6 most promising proteins, no SNPs were found in the respective genes for *Hyou1*, *Jup* or *Set*, but were found for *Cct6a* (180), *Hspa2* (57 in total) and *Anp32a* (367) (Table 3.3).

Table 3.3 Single-nucleotide polymorphism (SNP) analysis results. SNP analysis was applied to genes encoding for the 6 most relevant proteins identified using the glyco-AeP strategy, examining differences between NB-DNJ-sensitive strain C57BL/6 and insensitive strain FVB/N. Detailed SNP results for *Cct6a*.

Single-nucleotide Polymorphisms (SNPs)		VS		
				
Gene name	Non-coding regions (including 3'UTR)	Coding region		Total SNPs
		No change in amino acid	Change in amino acid	
<i>Hyou1</i>	—	—	—	—
<i>Hspa2</i>	54	3	—	57
<i>Jup</i>	—	—	—	—
<i>Set</i>	—	—	—	—
<i>Cct6a</i>	174	5	1	180
<i>Anp32a</i>	367	—	—	367

Chr	Location	Base pair	C57BL/6	FVB/N
...				
5	Ex4 coding gcg-gcc – A152A	130295812	G	C
...				
5	Ex6 coding act-acg – T232T	130297427	T	G
...				
5	Ex9 coding gag-ggg – E348G	130299586	A	G
...				
5	Ex11 coding tcg-tca – S471S	130320911	G	A
5	Ex11 coding tcc-tcg – S473S	130320917	C	G
...				
5	Ex12 coding gct-gcc – A489A	130321475	T	C
...				

In *Cct6a* (NM_009838) the majority of the SNPs were found in non-coding regions, including the 3' untranslated region (3'UTR). Nevertheless, six changes were found in the coding region, five of which do not change the corresponding amino acid. One, in exon 9, Chr5 position 130299586, has the SNP designation rs13470985 and changes amino acid 348 from E/glutamic acid in C57BL/6 to G/glycine in FVB/N.

In *Hspa2* (NM_001002012) again non-coding region SNPs were the majority, including the 3'UTR. Three SNPs were identified in the coding region, but these do not change the corresponding amino acids.

In *Anp32a* (NM_009672) only SNPs in non-coding regions, including the 3'UTR, were found. As well as the single CCT6A-E348G difference identified, it cannot be discounted that the identified non-coding changes may affect gene regulation. SNPs that are not located in protein-coding regions may still affect gene splicing, transcription factor binding, messenger RNA degradation, or the sequence of non-coding RNA. However, in the absence of microarray analysis of FVB/N testis tissue, it is not yet possible to compare expression levels.

3.5 Conclusions & Future Work

3.5.1 Conclusions

Synthetic oligosaccharides and glycoconjugates provide materials for correlating structure with function. Natural and synthetic mimics of the complex assemblies found on cell surfaces can modulate cellular interactions and small molecule inhibitors of carbohydrate biosynthetic and processing enzymes can block the assembly of specific oligosaccharide structures. These are currently under development as therapeutic agents, although it can be very long until they are approved as medicines.

The repurposing of an existing therapeutic is a potentially strong strategy for probes with wide-ranging utility, since it creates a more direct route to *in vivo* function. While strategies in some key areas of biology have followed this logic (Albrow et al., 2012, Aye et al., 2009, Dadvar et al., 2009, Ong et al., 2009), the detailed examination of the modulation of glyco-biological function has not, until now, scrutinised such valuable interactomes. In other words, widescale evaluation of interacting partners for carbohydrates is an underexploited area. Exploring the glyco-interactome has particular relevance given the lack of direct genetic control of glycoconjugate biosynthesis.

In this study the archetypal glycomimetic iminosugar and therapeutic NB-DNJ/miglustat/Zavesca was utilised in a glycomimetic affinity-enrichment proteomics (glyco-A[®]P) strategy to elucidate a focused subsection of the proteome hypothetically relevant to mammalian reproduction. Because miglustat passed the safety tests to be approved for the treatment of Gaucher disease in humans, it appears to hold promise as a male birth control pill. However, further studies in humans are needed.

The discovered binding partners (Hsps, junctional proteins, chaperones, ceramide binders) and the associated genomic analysis implicate a subset of proteins as

important in male fertility. These new interactions would not have been readily predicted and might define the mechanisms by which NB-DNJ causes male infertility.

The success of the strategy used suggests a general approach to discovering carbohydrate-active partners in biology.

The work reported in this chapter has been published (Cruz et al., 2013a) and the article can be found in Appendix.

Key Findings	
Comprehensive study utilising an immobilised glyco-affinity probe to identify proteins that interact with NB-DNJ and are potentially responsible for its contraceptive properties.	
Glyco-A ^e P	Proteins Identified
Powerful technique for identifying unforeseen protein-ligand interactions in a therapeutically relevant phenotype	Elucidated a focused subsection of the proteome hypothetically relevant to mammalian reproduction – HYOU1, HSP2A, SET, CCT6A, JUP, ANP32A/B
Repurposing of an existing therapeutic is a powerful strategy to develop a probe with wide-ranging utility since it creates a more direct link to <i>in vivo</i> function.	

3.5.2 Future work

While traditional hormonal contraceptive methods have focused on women, hormonal and non-hormonal male contraception is an attractive alternative. The biological basis for male contraception was established long ago and some promising breakthroughs have been achieved. Nevertheless, and despite the financial burden families increasingly bare due to better enforcement of child support policies, no viable alternative to the widely used barrier device, the condom, has been brought to the market. Up until now, men who wish to control

their fertility must rely on barrier methods, female compliance with contraceptives, vasectomy or abstinence.

Over the last decade, the pharmaceutical industry has abandoned most of its investment in the field, due to uncertain estimates of market demand allied to the need for critical funds to demonstrate the safety of existing candidate products. However, survey data indicate strong interest on both women and men in having more male options for fertility control (Heinemann et al., 2005). This strongly supports the development of studies like the one reported in this chapter.

The next logical step to further develop this particular study would be to validate the identified targets. Several methodologies can be used for target validation, including western blotting using antibodies against the proteins identified, to confirm their presence in the glyco-affinity enriched sample and absence from the control.

The following step would be to perform animal studies, which should include *NB-DNJ* sensitive and insensitive mouse strains to further investigate interstrain differences. Each mouse strain group should be split into two sub-groups: the study group, whose mice are treated with low doses of *NB-DNJ* to cause infertility, and the control group with non-treated mice. Following treatment, a 2D-PAGE followed by MS approach could be used to compare the protein profile of the testis tissue of both groups. The presently identified proteins should be found solely in the treated group.

Another useful approach for target validation would be the use of knockout studies in *NB-DNJ* sensitive and insensitive mouse strains to explore the effect of the identified protein targets on fertility. These studies could shed light not only on the individual role of each gene, but also of combined genes, on fertility by using multiple knockouts.

Ultimately, the contraceptive effect of *NB-DNJ* should be tested in humans. In a small-scale study involving five human subjects, miglustat has shown to cause no apparent effect on spermatogenesis (Amory et al., 2007). Yet, apart from the small

number of individuals participating in this study, a fixed oral dose of NB-DNJ was administered and all participants were followed over the same period of time (6 weeks). Further longitudinal studies with a greater number of participants and several dose regimens are needed to better conclude on the effect of NB-DNJ on human fertility.

Moreover, the application of the developed glyco-A^eP strategy to other glycomimetics would certainly result in the discovery of more interesting carbohydrate-active partners. Remarkably, the primary probe used in this study is a derivative of the natural product nojirimycin (Inouye et al., 1966). The increasing utility of both functionalised natural products (Hegde et al., 2011) and therapeutics as two classes of small molecules that have been selected in contrasting manners for protein interaction, suggests that future affinity strategies might also be usefully based on their exploitation. To this end, extension of the glyco-A^eP strategy to other small molecule, natural product glycomimetics is currently under exploration.

**Chapter 4 – PROTEOMICS APPROACH TO IDENTIFY PROTEIN
TARGETS OF CHEMORESISTANCE IN OVARIAN CANCER**

4.1 Introduction

4.1.1 Ovarian cancer

Cancer is a generic term for a large group of genetic diseases that can affect any part of the body. In this type of disease, the control mechanisms of cell growth are deficient or lost, leading to the formation of a solid mass of cells known as tumour or neoplasm. The initial tumour becomes life threatening when it invades surrounding tissues, obstructing vessels or organs, or spreads through the bloodstream to one or more sites in the body (metastasis). In the early stages of tumour growth, cancer cells usually resemble the original cells from which they derive; however, they can lose their appearance and function during the multi-step tumorigenesis process (Thurston, 2007).

Every cell in our body goes through a cell cycle to divide and produce new cells. In a healthy individual the cell division is carefully controlled by a combination of regulatory proteins, such as cyclin-dependent kinases, and checkpoint proteins, such as p53, which cause cell cycle arrest and possible apoptosis in response to DNA damage. Loss of this regulation due to mutations can therefore lead to uncontrolled cell proliferation, tumour formation and cancer. Mutations in two particular classes of genes are the most common. Firstly, mutations in oncogenes, which code for proteins promoting cell proliferation, result in tumour formation and growth. Secondly, mutations in tumour suppressor genes, which code for proteins normally involved in causing cell cycle arrest, prevent the inhibition of cell division (Vermeulen et al., 2003).

The defining characteristics of cancer include continuous signalling, which promotes cell growth and proliferation, and while normal cells have limited replication, cancer cells have not. They also have the ability to avoid apoptosis and growth suppression signalling. Additionally, cancer cells are able to develop vasculature by inducing angiogenesis, allowing a constant supply of nutrients to meet their metabolic

needs, as well as providing them with means to spread to other parts of the body by metastasis (Hanahan and Weinberg, 2011).

Cancer is a leading cause of death worldwide and accounted for 7.6 million deaths (around 13 % of all deaths) in 2008, according to the World Health Organization (WHO, 2013). This means that cancer remains a major public health challenge, although there has been remarkable progress in detection and therapy strategies in the latest years.

Ovarian cancer is a nonspecific term used to designate a variety of cancers that originate in the ovary. It is characterised by an uncontrolled growth of abnormal cells within the ovary, forming a tumour. Cancerous ovarian tumours can spread to nearby structures such as the fallopian tubes and the uterus, or even to other parts of the body such as the liver, lungs and bowel, if not diagnosed and treated. As ovarian cancers display a significant morphological and biological heterogeneity, the WHO categorises most of the human ovarian tumours based on the presumed histogenesis of the normal ovary (Scully, 1987, Serov et al., 1973).

4.1.1.1 Types of ovarian cancer

According to tumour histology, ovarian cancer is classified into three major categories: epithelial ovarian tumours, germ cell tumours and sex-cord stromal tumours. The type of ovarian cancer dictates many aspects of clinical treatment, management and prognosis (Scully, 1987, Serov et al., 1973).

Epithelial ovarian cancer is the most common type of ovarian cancer, corresponding to approximately 90 % of all ovarian cancer cases. It includes serous, the most frequent subtype, endometrioid, clear cell, mucinous and undifferentiated or unclassifiable. Epithelial ovarian tumours develop on the surface layer covering the ovary and so far they have all been treated in a similar way (Kaku et al., 2003). About 10 to 20 % of epithelial ovarian neoplasms are borderline or low malignant potential (LMP) tumours, which are characterised by a higher degree of cellular proliferation than benign tumours, but in the absence of stromal invasion (Scully,

1987, Hart, 1977). Among the invasive epithelial ovarian cancers, about 75 to 80 % are serous, 10 % are endometrioid and 10 % are mucinous (Holschneider and Berek, 2000).

Serous tumours occur most frequently in women aged 40-60 years old and account for 25-40 % of epithelial tumours. Endometrioid tumours are approximately 20 % of epithelial tumours and occur primarily in women who are between 50 and 70 years of age. In these tumours, cells resemble those in endometrial carcinoma, which affects the lining of the uterus (endometrium, womb). About 5 % of endometrioid tumours are connected to endometriosis, a non-cancerous disorder of the endometrium, and around a fifth of the cases occur in women who have also been diagnosed with endometrial carcinoma. Clear cell tumours make up 6 % of epithelial tumours and are mainly diagnosed in women aged 40 to 80. Approximately 50 % of these tumours are associated with endometriosis. Clear cell carcinoma is considered an aggressive form of ovarian cancer. Mucinous tumours are most common in women between 30 and 50 years old and correspond to roughly 1 % of epithelial ovarian tumours. In this subtype of tumour, cells are similar to those of the mucinous membrane of the cervical canal. Undifferentiated tumours are those that do not fit into any of the above categories and represent around 10-15 % of epithelial ovarian malignancies (Serov et al., 1973, Kaku et al., 2003).

Germ cell ovarian cancer is less common, accounting for 5-10 % of all ovarian cancer cases, and is more frequent in younger women. These tumours develop from cells within the ovary that form the eggs. Most germ cell tumours are benign ovarian teratomas. The prognosis of this subtype of ovarian cancer is overall favourable, with 90 % of cases successfully treated, although it depends on the specific histology of germ cell tumour. Types of germ cell tumours include teratomas; dysgerminomas, the most frequent of all germ cell tumours; endodermal sinus tumours; embryonal carcinomas and choriocarcinomas. There are also mixed germ cell tumours, which consist of combinations of germ cell tumours and are rare (Serov et al., 1973, Kaku et al., 2003).

Sex-cord stromal tumours are also less common, affecting 5-10 % of women diagnosed with ovarian cancer, independently of their age group. These originate in the connective tissue that holds the ovaries together and produce female hormones. Most of these tumours are either benign or confined to the ovary when diagnosed. Granulosa cell tumours; thecomas; fibromas, the most common sex-cord tumour; Sertoli-Leydig cell tumours; sex-cord tumours with annular tubules; lipid cell tumours and gynandroblastomas are different types of sex-cord stromal tumours (Serov et al., 1973, Kaku et al., 2003).

4.1.1.2 Stages of ovarian cancer

The stage of a cancer gives an indication of how much the cancer has grown and how far it has spread at the time of diagnosis. Treatment options are influenced by the stage of the cancer. The International Federation of Gynaecological Oncologists created the FIGO staging system for classification of ovarian cancer according to 4 different stages: stage I, stage II, stage III and stage IV. This classification system uses information obtained after surgery (Pecorelli et al., 1999).

Borderline tumours are not included in this classification, as they are not real cancers because they rarely invade deeper layers of tissue. These tumours are made up of abnormal cells formed in the covering of the ovary, which usually grow in a slow and controlled way. They may become cancer, yet most do not. Most women with borderline tumours are diagnosed at an early stage and are generally cured with surgery alone (Yancik, 1993).

In ovarian cancer stage I, the cancer is confined to the ovaries. Stage I is divided into 3 sub-sections: stage Ia, in which the cancer is confined to one ovary, there is no fluid accumulation (ascites) and no tumour on the external surface of the ovary, which is intact; stage Ib, similar to stage Ia, but the cancer is contained inside both ovaries; stage Ic, where the cancer is similar to stages Ia or Ib, though it is also characterised by the presence of cancer cells on the surface of at least one ovary, or in the fluid taken from inside the abdomen during surgery, or there are ovary ruptures before or during surgery (Pecorelli et al., 1999).

Stage II ovarian cancer is characterised by the existence of cancer cells outside the ovaries, although the cancer has not spread further than the pelvic region. There are 3 sub-sections in stage II: stage IIa, in which the cancer has spread into the fallopian tubes or the uterus or both; stage IIb, where the cancer has expanded into other tissues in the pelvis, such as the bladder or rectum; stage IIc, similar to stages IIa or IIb, yet it is also characterised by the presence of cancer cells on the surface of at least one ovary, or in ascites taken from inside the abdomen during surgery, or there are tumour ruptures before or during surgery (Pecorelli et al., 1999).

Ovarian cancer stage III occurs when one or both ovaries are involved and the cancer has spread beyond the pelvic region into the abdominal cavity, excluding the liver, and/or to nearby lymph nodes. In stage III there are also 3 sub-sections: stage IIIa, where tumours are found in one or both ovaries and the pelvis, but cancer cells can be visualised under the microscope in tissue collected from the lining of the abdomen, and lymph nodes are negative for cancer; stage IIIb, similar to stage IIIa, although there are confirmed small tumour growths (with less than 2 cm in diameter) on the lining of the abdomen; stage IIIc, characterised by the presence of tumour growths larger than 2 cm on the lining of the abdomen and/or cancer cells on the lymph nodes, in addition to the aspects mentioned for the previous stages (Pecorelli et al., 1999).

Stage IV ovarian cancer implies that cancer cells have spread to other parts of the body such as the lungs, liver and brain (Pecorelli et al., 1999).

The AJCC/TNM staging system includes 3 categories for ovarian cancer: T, N and M. This system describes the extent of the primary tumour (T), the absence or presence of metastasis to nearby lymph nodes (N), and the presence or absence of distant metastasis (M). The T category is divided into sub-categories, classified according to the place where the tumour has developed and how far it has spread. The N and M categories are also divided into sub-categories, according to the absence or presence of metastasis to nearby lymph nodes and distant metastasis. The AJCC stages correspond to the FIGO stages. For example, stage T1a+N0+M0 in the AJCC system corresponds to stage Ia in the FIGO system; stage T2c+N0+M0 in

the AJCC system corresponds to stage IIc in the FIGO system and Any T+ Any N+M1 in the AJCC system corresponds to stage IV in the FIGO system (Pecorelli et al., 1999).

4.1.1.3 Grades of ovarian cancer

The microscopic visual aspect of cancer cells determines the grading of cancers. The grading gives an indication of how quickly cancer cells are likely to grow and the cancer to develop, by comparison of the tumour cells with normal cells. The more similar cancers are to normal tissue, the less likely to grow and spread quickly they tend to be. Ovarian cancer can be divided into 4 grades: Grade 0 (zero) or borderline, Grade 1 or well differentiated, Grade 2 or moderately differentiated, Grade 3 or poorly or undifferentiated. Treatment options depend on the tumour grade (Pecorelli et al., 1999, Coukos et al., 2008).

Grade 0 tumours are the least aggressive, unlikely to spread, look very much like normal tissue and, thus, are usually easy to treat and cure. They are also known as tumours of low malignant potential and represent around 15 % of epithelial ovarian tumours. Grade 1 tumours also look very similar to normal tissue and tend to grow slowly. They are commonly recognised as low-grade tumours. Grade 2 tumours are often referred to as intermediate grade tumours, because they do not look like normal tissue and grow moderately fast. Grade 3 tumours are the most aggressive; they grow quickly and in a disorganised way and do not look similar to normal tissue (Coukos et al., 2008).

Results of recent molecular genetic studies have suggested that high-grade and low-grade serous ovarian cancers are distinct and have classified them into two categories. Type I cancers are low-grade, slowly developing ovarian carcinomas (including endometrioid, mucinous and low-grade serous carcinomas). These are commonly associated with KRAS, BRAF, PTEN and B-catenin mutations and frequently associated with endometriosis. Type II cancers are high-grade serous carcinomas, which are more aggressive and develop rapidly, and are characterised by TP53 mutations (Gilks, 2010, Kurman and Shih le, 2010).

4.1.1.4 Epidemiology

In 2008, the number of new cases of ovarian cancer worldwide was estimated to be 225,000, accounting for approximately 4 % of all cancers diagnosed in women. The world age-standardised incidence rate for the more developed regions (9 per 100,000) is estimated to be nearly twice as high as the incidence rate for the less developed countries (5 per 100,000). The regions of the world with the highest ovarian cancer incidence rates are Northern, Central and Eastern Europe, followed by Western Europe and Northern America, whereas the lowest incidence rates are recorded in Africa and Asia. In 2008, over 21,500 new cases were estimated to be diagnosed in the USA and more than 65,000 in Europe (Holschneider and Berek, 2000, CRUK, 2013). In terms of mortality, in 2008 more than 140,000 women died from ovarian cancer worldwide (Jemal et al., 2010).

Within Europe, ovarian cancer incidence varies by approximately 40 %, with estimated European age-standardised rates ranging from 17 per 100,000 women in Northern Europe to 12 per 100,000 in Southern Europe, in 2008. The countries with the highest incidence rates were Latvia and Lithuania (19 per 100,000) and the countries with the lowest were Cyprus and Portugal (7 per 100,000). Out of the 27 countries in the European Union, the UK was 7th. In 2008, ovarian cancer caused around 29,000 deaths in Europe (CRUK, 2013).

In 2011, ovarian cancer was the 5th most common cancer among women in the UK and the second most common gynaecological cancer, with around 7,116 women being diagnosed in that year. In the UK, ovarian cancer is responsible for more deaths than all the other gynaecological cancers combined. Yet, ovarian cancer mortality has slightly decreased in the UK, according to the latest statistics. There were 4,272 deaths from ovarian cancer in 2011, accounting for 6 % of all female deaths from cancer. Nevertheless, in the same year, ovarian cancer was still the 4th most common cause of cancer death among females in the UK (CRUK, 2013).

Ovarian cancer is mainly diagnosed in peri-menopausal and post-menopausal women with over 80 % of cases in women over 40 years old. The malignant forms

generally appear after menopause, in the sixth decade, when the ovary has no physiological role and, consequently, its abnormal function causes no symptoms. As a result of this factor, early stages of the disease are difficult to diagnose. Owing to the anatomical location of the ovaries, deep in the pelvis, the symptoms only appear when the tumour reaches a large size or has disseminated (Yancik, 1993, Jacobs and Menon, 2004).

There are very significant differences in the survival data from distinct countries worldwide, including Australia, Canada, Norway, Sweden and the UK. Discrepancies in data quality and coding practices across the world may contribute to some of the variation. Several studies are being undertaken to investigate the factors underlying these differences within Europe (CRUK, 2013).

With respect to survival by age, even after discounting the higher background mortality in older people, relative survival for ovarian cancer is higher in younger women. This is similar to what is observed in other cancers and the reasons for this are likely to comprise a combination of earlier diagnosis, more effective response to treatment and better general health in younger people in general. As an example, the five-year relative survival rates for ovarian cancer in England for the period 2005-2009 ranged from 87 % in the 15-39 age group, 53 % in the 50-59 year olds, to 16 % in the 80-99 age group (CRUK, 2013).

The stage of the disease at diagnosis is one of the most important factors influencing ovarian cancer survival. Data from the Anglia Cancer Network for women diagnosed during 2004-2008 has indicated that five-year relative survival rates are above 90 % for early stage ovarian cancers, but decrease drastically to below 10 % for late stage cases. The majority (60 %) of women are diagnosed with stage III or IV disease, with only around 30 % of women being diagnosed at the earliest stage (CRUK, 2013, Jacobs and Menon, 2004). Another study, conducted in Munich, Germany, has also shown that most of the long-term improvement in ovarian cancer survival has occurred in women diagnosed with stage I or II disease (Engel et al., 2002).

4.1.1.5 Causes and risk factors

The etiology of ovarian cancer is multifactorial, but remains poorly understood until today. In most cases, the exact cause of ovarian cancer remains unknown. It is thought that genetic, environmental and endocrinal factors are directly or indirectly related to carcinogenesis. Based on previous studies, there are several theories regarding this subject.

The incessant ovulation theory, proposed by Fathalla (Fathalla, 1971), hypothesises that the repetitive disruption and repair of the ovarian surface epithelium may lead to a higher probability of spontaneous mutations and, thus, increase the risk of ovarian cancer. However, this model does not explain why infertility, often caused by hypo- or anovulation, is associated with an increased risk of ovarian cancer. This led to the theory that gonadotropin stimulation of the ovary contributes to the ovarian cancer risk (Choi et al., 2007a). A third proposal by Parmley and Woodruff (Parmley and Woodruff, 1974) suggests that epithelial ovarian malignancies might arise from transformation of the surface epithelium of the ovary exposed to pelvic contaminants and carcinogens. This theory has been supported by observations that the use of talc in genital hygiene may increase the risk of ovarian cancer.

Theories apart, nowadays it is known that neoplastic transformation is a product of an accumulation of genetic changes in a variety of different classes of genes, leading to the activation of oncogenes and loss of function of tumour suppressor genes.

At least 15 oncogenes, 16 candidate tumour suppressor genes and more than 7 signalling pathways have been implicated in ovarian cancer. As an example, PI3KCA has been suggested as an oncogene involved in ovarian carcinogenesis (Shayesteh et al., 1999) and K-ras is overexpressed in up to 30 % of tumours, particularly in mucinous tumours (Enomoto et al., 1991). HER-2/neu oncogene is overexpressed in up to 34 % of ovarian cancers (Berchuck et al., 1990).

With respect to tumour suppressor genes, it has been suggested that BRCA1 plays a role in DNA repair. This gene was found to be mutated in 30 % of familial and 10 % of non-familial ovarian cancers. Its loss of function increases the propagation of

DNA errors (Scully et al., 1997). Mutations on the p53 gene are found in about 30 % of human ovarian cancers, with p53 overexpression reported in about 50 % of the cases (Okamoto et al., 1991, Marks et al., 1991). These alterations lead to aberrations in cell proliferation, apoptosis, autophagy and changes in cell adhesion and motility, all contributing to disease development and metastasis.

A number of factors can influence the risk of developing ovarian cancer. The main risk factors include: family history/genetics, age, obesity, reproductive history, hormone replacement therapy (CRUK, 2014).

Ovarian cancer can be hereditary. Over 10 % of ovarian cancers result from an inherited faulty gene (BRCA1 or BRCA2 mutation), which increases a women's risk of developing ovarian and breast cancer. Women who carry this gene mutation have a 35-60 % chance of developing ovarian cancer. Research has shown that women who descend from Dutch, Polish, Ashkenazi Jewish, Pakistani, Norwegian and Icelandic families are more likely to carry this mutation. Thus it is important to know the family's medical history, as women who have two or more relatives on one side of their family with ovarian, or ovarian and breast cancer, may be at higher risk of developing ovarian cancer, when compared to the general population (Risch et al., 2006).

The following factors contribute to a woman having an increased risk of developing ovarian cancer: having a first generation relative (daughter, sister, mother) and a second generation relative (grandmother, aunt) who has had ovarian cancer; having a first generation relative who has suffered from ovarian cancer and a second generation relative (male or female) with breast cancer under the age of 50 or two or more second generation relatives with breast cancer under the age of 60; having relatives who are known BRCA1 or BRCA2 gene carriers; having three or more relatives with either colon, stomach, ovarian, endometrial or small bowel cancer; having a first generation relative with both breast and ovarian cancer (Boyd and Rubin, 1997).

Age is another risk factor for developing ovarian cancer, since the majority of ovarian cancer cases are diagnosed in women over the age of 40. Nevertheless, some types of ovarian cancer do occur in younger women from the age of 20 (CRUK, 2014).

Obesity can also be associated with an increased risk of developing ovarian cancer, as women with a body mass index above 30 may be at an increased risk (CRUK, 2014).

A woman's reproductive history plays an important role in the risk of developing ovarian cancer as well. Women who have never given birth, had their first child after the age of 30, have never taken oral contraceptives, started menstruating at a young age (before 12 years old), experienced menopause at a late age (after 50 years of age), did not breast feed are at an increased risk of developing ovarian cancer. Infertile women and those who suffer from endometriosis are also at an increased risk of developing ovarian cancer (Collaborative Group on Epidemiological Studies of Ovarian et al., 2008, CRUK, 2014).

Hormone replacement therapy can be a risk factor, as women using oestrogen only may have a slightly higher risk of developing ovarian cancer (Collaborative Group on Epidemiological Studies of Ovarian et al., 2008, CRUK, 2014).

4.1.1.6 Symptoms

On early stages of ovarian cancer, signs and symptoms are frequently absent. When existent they may be subtle and usually persist for several months before being recognised and diagnosed. The most common symptoms include: difficulty eating, bloating, abdominal or pelvic pain, and urinary symptoms. If these symptoms have started recently and occur with a frequency over 12 times per month diagnosis should be considered (CRUK, 2014).

Other signs and symptoms comprise abnormal vaginal bleeding, an abdominal mass, accumulation of fluid in the abdominal cavity (ascites), involuntary weigh loss,

back pain, tiredness, constipation and a variety of other non-specific symptoms (CRUK, 2014).

Ovarian cancer is associated with age, family history of ovarian cancer (9.8-fold higher risk), appetite loss (5.2-fold higher risk), weight loss (2-fold higher risk), postmenopausal bleeding (6.6-fold higher risk), rectal bleeding (2-fold higher risk), anaemia (2.3-fold higher risk), abdominal pain (7-fold higher risk) and abdominal distension (23-fold higher risk) (CRUK, 2014).

4.1.1.7 Importance of early diagnosis, prognosis and screening

Ovarian cancer mortality, and cancer mortality in general, can be reduced if cases are detected and treated early. Early diagnosis and screening are the two components of early detection efforts. It is extremely important to pay attention to early signs and symptoms in order to diagnose cancers and treat them before the disease becomes advanced, as early detection is generally associated with improved outcomes. Early diagnosis programmes are particularly significant in low-resource countries in which the majority of diagnoses are made in very late stages and where there is no screening.

According to the WHO, screening is defined as the systematic application of a test in an asymptomatic population in order to identify individuals with abnormalities that suggest a specific cancer or pre-cancer, and refer them promptly for diagnosis and treatment (WHO, 2013). Ovarian cancer fulfils some of the criteria required for the introduction of population screening and tests such as ultrasound and tumour marker detection have demonstrated to be able to detect a significant proportion of ovarian cancers pre-clinically. These screening tools have been shown to extend median survival when used as sequential screening tests. However, potential screening tests for ovarian cancer have not yet been shown to reduce mortality (CRUK, 2014).

In the UK, two population screening studies are currently being conducted. On one hand, the UK Collaborative Trial of Ovarian Cancer Screening (UKCTOCS) is carrying

out a very large randomised controlled trial, aiming to recruit 200,000 post-menopausal women, in order to assess the cost, acceptability and mortality benefit of population screening. In this study women have been randomly assigned to three groups: no treatment (control group); annual multimodal screening (MMS; CA125 followed by transvaginal ultrasound as a second-line test); or annual ultrasound (UUS). Preliminary results show that large scale population screening is viable and does detect ovarian cancer in women without symptoms. The biobank of information collected will help in understanding the natural history of ovarian cancer and assist the search for better biomarkers for early detection. Final results of this study are expected in 2015 (CRUK, 2014).

On the other hand, the UK Familial Ovarian Cancer Screening Study (UKFOCSS) is being conducted with 5,000 women aged over 35 with a significant family history of ovarian cancer. This study assesses the utility of CA125 measurement and ultrasound as annual screening. Furthermore, blood samples are being collected every 4 months for retrospective analysis of existing and novel tumour markers (CRUK, 2014).

4.1.1.8 Treatment strategies

The vast majority of women with diagnosed epithelial ovarian tumours will require a debulking surgery, followed by a chemotherapy combination regimen.

An exploratory laparotomy is usually done for histological confirmation, staging and tumour debulking. The standard surgical approach consists of a total abdominal hysterectomy and bilateral salpingo-oophorectomy along with examination of all peritoneal surfaces, an infracolic omentectomy, biopsies of pelvic and para-aortic lymph nodes and clinically uninvolved areas, and peritoneal washings. The amount of surgery will depend on the stage and type of cancer (CRUK, 2014). For example, patients with LMP ovarian tumours treated with surgical resection do not require chemotherapy. On the other hand, many patients diagnosed with advanced-stage disease require adjuvant chemotherapy after the surgery to destroy the remaining tumour cells. Several studies have been carried out in order to define the standard

regimen in the initial chemotherapeutic management of advanced disease (Skeel, 2007).

Results of clinical trials done over the past thirty years have identified the combination of a platinum drug (carboplatin or cisplatin) and a taxane (paclitaxel/taxol or docetaxel), given intravenously as the best standard treatment (Aabo et al., 1998, Piccart et al., 2000, Neijt et al., 2000, du Bois et al., 2003, Vasey et al., 2004). In 2005, the Gynecologic Cancer Intergroup Consensus Meeting defined the standard of care as carboplatin plus taxol, every 21 days, for 6 to 8 cycles.

4.1.1.8.1 Platinum drugs

The platinum-based compounds have the coordination complex cisplatin, cis-diamminedichloroplatinum(II), as their lead molecule (Figure 4.1). It was discovered in 1845, but only about one century later, some *in vitro* studies conducted in *Escherichia coli* (*E. coli*) demonstrated its cytotoxic effects (Rosenberg et al., 1965, Rosenberg et al., 1969).

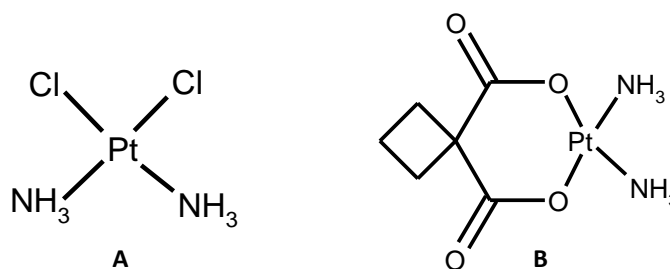


Figure 4.1 Chemical structures of the two most used platinum compounds in ovarian cancer treatment. (A) Cisplatin, (B) Carboplatin.

It is currently known that cisplatin becomes activated intracellularly by the aquation of one of the two chloride leaving groups and covalently binds to DNA, forming DNA adducts. The compound interacts with the major groove of DNA and preferentially

binds to the N7 position of the imidazole ring of the purine bases — guanine and, in a lower extent, adenine — to form either monofunctional (via one leaving group) or bifunctional (via both leaving groups) adducts. Most adducts occur on the same DNA strand, involve bases adjacent to one another and are, therefore, known as intrastrand adducts or crosslinks (Thurston, 2007, Kelland, 2007).

These adducts cause distortions in the DNA around the adduct site, including unwinding and bending, and are recognised by several surveillance enzymes, some of which are involved in DNA-repair pathways (Thurston, 2007).

The final cellular outcome is generally apoptotic cell death, although the pathway(s) through which platinum–DNA binding leads to apoptosis remains incompletely elucidated. The platinum–DNA adducts can impede cellular processes, such as replication and transcription, that require DNA-strand separation in different extents. Signal-transduction pathways that control growth, differentiation and stress responses have also been implicated (Kelland, 2007, Siddik, 2003).

Carboplatin, *cis*-diammine-[1,1-cyclobutanedicarboxylato]platinum(II), is a second-generation analogue of cisplatin. Introduced in the 1980s, it incorporates a cyclobutyl substituted hexa dilactone ring, a more stable leaving group. Carboplatin has the same mechanism of action as cisplatin and a similar spectrum of activity, but is better tolerated in terms of toxic effects. Although myelosuppression (thrombocytopenia) is more pronounced and dose limiting, it is now preferred for the treatment of ovarian cancers (Thurston, 2007, Harrap, 1985).

4.1.1.8.2 Taxanes

Taxol is the most well known molecule of the taxanes group. It is a highly complex tetracyclic diterpene (Figure 4.2) found in the needles and bark of the tree *Taxus brevifolia*. The compound was isolated in 1966 and its structure published in 1971, but it only appeared in clinical practice in the 1990s. Docetaxel is a more recently introduced semi-synthetic analogue with similar therapeutic and toxicological properties (Thurston, 2007).

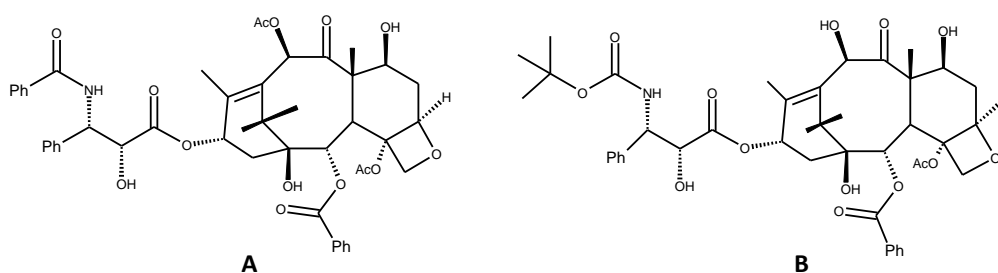


Figure 4.2 Chemical structures of the two most used taxanes in ovarian cancer treatment. (A) Taxol, (B) Docetaxel. Ac, acetyl; Ph, phenyl.

These drugs are antimetabolic agents, but have a mechanism of action distinct from colchicine or vinca alkaloids. It involves the promotion of microtubule assembly by stabilising the microtubule complex and inhibiting their depolymerisation to free tubulin. This action shifts the microtubule equilibrium in favour of the polymeric form (Dumontet and Sikic, 1999).

Taxol has the ability to polymerise tubulin in the absence of guanosine triphosphate (GTP), which under normal conditions is an absolute requirement for microtubule polymerisation. Microtubules formed in the presence of the drug possess unusual stability and resist to depolymerisation by Ca^{2+} , cold temperature and dilution. The drug binds to the β -tubulin subunit in the microtubules, specific and reversibly, and this interferes with the chromosomes ability to separate during cell division. Cells are prevented from progressing from metaphase to anaphase, causing cell cycle arrest and inducing apoptosis (Thurston, 2007, Orr et al., 2003).

4.1.2 Chemoresistance

The effectiveness of many chemotherapeutic agents used in cancer therapy is limited by drug resistance. The acquisition of resistance constitutes a serious impediment to improved healthcare and is one of the biggest challenges in cancer treatment nowadays. The resistance phenomena may be intrinsic or acquired

during the course of treatment. In the case of acquired drug resistance, tumours may become resistant to drugs other than those initiating the resistance, despite the fact that these drugs may have different mechanisms of action and not be structurally related (Fojo and Menefee, 2007).

Tumours usually consist of mixed populations of malignant cells, some of which are drug-sensitive while others are drug-resistant. Chemotherapy kills drug-sensitive cells, but leaves behind a higher proportion of drug-resistant cells. As the tumour begins to grow again, chemotherapy may fail because the remaining tumour cells are now resistant (Gottesman, 2002).

Disease management in patients with ovarian cancer exemplifies this problem: some patients have an excellent response at the beginning of the treatment, followed by the evolution of fatal drug resistance (Kaye, 2008). Following debulking surgery, patients with advanced ovarian cancer generally receive chemotherapy, with response rates of 70-80 %. However, a subset of 20-30 % of patients either progress during chemotherapy or relapse within six months of treatment (ESMO, 2001). These tumours have low response rates to re-challenge with second-line agents and a poor prognosis, with only an approximately 30 % 5-year survival rate (Agarwal and Kaye, 2006, Agarwal and Kaye, 2003).

Varied mechanisms can give rise to the resistance phenomenon. They can be grouped in two classes: non-cellular and cellular mechanisms. Those in the first class are related with factors inherent to the host, the tumour itself or the anticancer drug, such as changes in absorption, distribution, metabolism and excretion of drug or insufficient vascularisation of the tumour cells. The second ones are related to biochemical and molecular changes that occur within tumour cells (Gottesman, 2002).

Since chemoresistance is an extremely complex and vast theme, in this brief introduction only the resistance mechanisms correlated to the drugs used in ovarian cancer treatment will be approached, since they are directly connected with the background of this study.

4.1.2.1 Mechanisms of resistance to platinum drugs

Soon after the initial promising clinical trial data with cisplatin, and later with carboplatin, attention shifted to determining how tumour resistance was acquired during courses of therapy and why some tumours were intrinsically resistant. This knowledge has largely arisen from studies that have been carried out in cell lines. These models have been established, primarily, by repeatedly exposing drug-sensitive cells to chemotherapeutic drugs *in vitro* (Roberts et al., 2005).

Although the molecular basis for platinum resistance remains largely undefined, it is considered multifactorial and numerous mechanisms seem to be involved. They can be divided in two distinct groups: first, an insufficient amount of platinum to reach the DNA, limiting the formation of platinum-DNA adducts, and second, failure to achieve cell death after platinum-DNA adduct formation and drug-induced damage. More specifically, the first group includes decreased drug uptake and increased drug inactivation, while the second group includes increased repair of platinum-DNA adducts and increased platinum-DNA damage tolerance (Siddik, 2003).

Some of these mechanisms may be specific to the type of platinum drug used, whereas others may be pleiotropic, which means they are related to a few drugs of the same class. Many resistant cells show a pleomorphic phenotype, which consists of various altered pathways involving drug uptake, DNA-damage recognition and repair, and apoptosis (Kelland, 2007).

4.1.2.1.1 Resistance through insufficient DNA binding

The formation of DNA adducts by cisplatin can be limited by reduced accumulation of the drug, enhanced drug efflux and cisplatin inactivation by coordination to sulphur-containing proteins, including metallothioneins, whose production may be increased as a result of cisplatin treatment (Brabec and Kasparkova, 2002).

In contrast to the mechanism of multidrug resistance (MDR), which is reported in several natural product-based drugs, it is generally decreased uptake, rather than

increased efflux, that predominates in platinum-drug resistance (Brabec and Kasparkova, 2002).

Mechanisms that reduce drug uptake prevent therapeutic levels of the drug from being reached in the target cells. These include limited blood flow to the site of action, high extracellular pH, binding with plasma proteins and a decrease in transporters (Stewart, 2007).

Platinum might enter cells using either transporters, a significant one being the copper transporter-1 (CTR1), or by passive diffusion. Loss of CTR1 results in less platinum entering cells and, consequently, a decreased cytotoxic effect, leading to drug resistance. Both copper and cisplatin cause a rapid down-regulation of CTR1 expression in human ovarian cancer cell lines. This occurs through the internalisation of CTR1 from the plasma membrane by macropinocytosis, followed by proteasome-based degradation (Holzer and Howell, 2006).

Once inside cells, cisplatin is activated by the addition of water molecules to form chemically reactive aqua species. In the cytoplasm, the activated aqua species preferentially react with species containing high sulphur levels. There is extensive evidence implicating increased levels of cytoplasmic thiol-containing species as causative of acquired and inherited resistance to cisplatin or carboplatin, as well as to other DNA-damaging drugs. These species, such as the tripeptide glutathione (GSH) and metallothioneins, are rich in the sulphur-containing amino acids cysteine and methionine and lead to detoxification. Activated platinum avidly binds to sulphur and is effectively arrested in the cytoplasm before DNA binding can occur, thereby causing resistance (Holzer and Howell, 2006).

Finally, active export of platinum from the cells through the copper exporters 7A/7B (ATP7A and ATP7B), as well as through the glutathione S-conjugate export (GS-X) pump can contribute to platinum drug resistance. The conjugation of cisplatin with GSH might be catalysed by glutathione S-transferases (GSTs), which makes the compound more anionic and more readily exported from cells by the adenosine triphosphate (ATP)-dependent GS-X pump (Kelland, 2007).

The efflux of cisplatin from target cells through transporters such as the lung resistance-related protein (LRP) also confers resistance (Wang et al., 2004b), however unlike the anti-tubulin drugs, there is no cross resistance due to increased expression P-glycoprotein (Kaye, 2008).

4.1.2.1.2 Resistance mediated after DNA binding

After platinum-DNA adducts have been formed, cellular survival, and therefore tumour drug resistance, can occur either by removal of these adducts and DNA repair or by tolerance mechanisms.

An increased repair of platinum-DNA adducts is considered the most significant event of platinum resistance (Thurston, 2007, Brabec and Kasparkova, 2002). Many cisplatin-resistant cell lines derived from various tumour types have shown increased DNA-repair capacity in comparison to their sensitive counterparts (Johnson et al., 1994). Nucleotide-excision repair (NER) is the major pathway known to remove cisplatin lesions from DNA. Increased NER is mainly due to increased activity of the endonuclease protein ERCC1 (excision repair cross-complementing 1), which is considered to be able to remove incorrect nucleotide sequences and thus protect the cell from apoptosis (Kelland, 2007). In ovarian cancer this protein was found overexpressed, increasing the ability of cancer cells to repair DNA damage (Dabholkar et al., 1992).

Increased tolerance to platinum-induced DNA damage can also occur through loss of function of the mismatch repair (MMR) pathway. During MMR, cisplatin-induced DNA adducts are recognised by the MMR proteins MutS homolog 2/3/6 (MSH2, MSH3 and MSH6) (Zdraveski et al., 2002). It is postulated that cells, after undergoing several unsuccessful repair cycles, finally trigger an apoptotic response. Loss of MMR results in reduced apoptosis and, consequently, drug resistance. Another tolerance mechanism involves enhanced replicative bypass, whereby certain DNA polymerases, such as β and η , can bypass cisplatin-DNA adducts by translesion synthesis. Polymerase η has shown to have a role in cellular tolerance to cisplatin and carboplatin (Albertella et al., 2005).

At last, tolerance to platinum might occur through decreased expression or loss of apoptotic signalling pathways, either the mitochondrial or death-receptor pathways, mediated through various proteins such as p53, anti-apoptotic and pro-apoptotic members of the Bcl-2 family, and JNK35 (Kelland, 2007).

The p53 protein is considered to have many important roles including DNA repair in response to damage, functions within the apoptotic pathway and as a transactivator in the expression of the bax gene (Gottlieb and Oren, 1998). Evidence suggests that mutations in the p53 gene result in p53 overexpression, which is related to the development of chemoresistance. There is also a loss of p53 protein function, resulting in a reduction in the expression of bax, a pro-apoptotic protein. These mutations also result in cross-resistance with a number of other cytotoxic agents including melphalan (Perego et al., 1996). Moreover, the expression of the mutant p53 gene may be responsible for resistance to taxol, which is also thought to induce apoptosis through a p53-dependent pathway. The loss of function of the p53 protein therefore compromises this pathway. Nonetheless, the significance of this mechanism is not clear, as taxol is considered to induce apoptosis through a p53-independent pathway as well (Dumontet and Sikic, 1999). This is supported by a study that revealed that taxol was able to induce apoptosis in cisplatin resistant cell lines (Perego et al., 1998).

4.1.2.2 Mechanisms of resistance to taxanes

Since its approval by the Food and Drug Administration in 1992 for the treatment of ovarian cancer, the use of taxol has dramatically increased. Despite the improvement verified in duration and quality of life for some patients, drug resistance represents a major obstacle to improve the overall response and survival (Orr et al., 2003).

In the case of taxol, several potential mechanisms have been proposed to explain the resistance observed in human tumours and tumour cell lines. Drug resistance may occur at the cell level, due to evasion of apoptosis or changes in the target protein. It may also occur as a consequence of poor pharmacologic accessibility of

the drug, due to changes in the rate of transport in and out of the cell or in drug metabolism (Fojo and Menefee, 2007).

Taxanes resistance appears to develop owing to changes in the expression of proteins with important anti-apoptotic effects and roles in stress response. These include certain isoforms of heat shock protein, superoxide dismutase, which is involved in the formation of redox species, and endoplasmic reticulum ATPase. Changes in the β -tubulin binding site prevent the binding of taxol and exertion of its cytotoxic effects, also resulting in resistance (Di Michele et al., 2009).

4.1.2.2.1 Multidrug resistance (MDR)

MDR due to overexpression of the P-glycoprotein (P-gp) pump or multidrug resistant protein 1 is possibly the most extensively researched and well-understood resistance mechanism. P-gp is an ATP-dependent drug transporter located in the cellular membrane and belongs to the ATP-binding cassette (ABC) superfamily. Overexpression of P-gp is often the cause of resistance to antimitotic agents, including the taxanes, as demonstrated *in vitro*, in preclinical models and in patients (Gottesman, 2002).

P-gp works as an efflux pump which actively transports the drugs that reach the intracellular compartment to the extracellular medium (Krishna and Mayer, 2000). By preventing intracellular drug accumulation, its cytotoxic effect is drastically reduced and tumour cells remain viable, instead of being destroyed (Nobili et al., 2006). Among the MDR related proteins, P-gp is arguably the most important of the ABC transporters, since it confers the strongest resistance to the widest variety of compounds.

4.1.2.2.2 Resistance through altered microtubule dynamics

There is another large group of mechanisms directly related to the microtubule and alterations verified in its dynamics. It includes tubulin mutations, that affect either longitudinal or lateral interactions, tubulin isotype selection, altered binding of taxol

to its cellular target, post-translational modifications and altered expression of microtubule-associated proteins (MAPs) (Orr et al., 2003).

Several reports have described tubulin mutations as etiologic in drug resistance. Some of these mutations have shown to alter drug binding or binding of regulatory proteins, while others have been observed to cause shifts in the equilibrium of the tubulin dimer and microtubule polymer. In the latter case, a shift in the equilibrium to a more soluble tubulin dimer and less stable microtubule polymer has shown to result in increased resistance to taxanes (Cabral and Barlow, 1989).

A detailed analysis of class I β -tubulin mutations in taxol-resistant chinese hamster ovary cell line revealed a cluster of mutations at leucines 215, 217 and 228. It was concluded that resistance in these cells was a result of mutations that altered microtubule dynamics by affecting the lateral-longitudinal interactions, important for microtubule assembly. By destabilising the microtubules, these mutations apparently counteract the stabilising effects of taxol (Gonzalez-Garay et al., 1999).

There have been numerous reports of altered expression of individual β -tubulin isotypes, especially class III and IVa, in cells that have been selected for resistance to antimetabolic agents. This hypothesis is supported by the analysis of tubulin isotypes in cells not selected for drug resistance. Altered expression of β -tubulin isotypes confers altered sensitivity to microtubule-targeting agents, with both *in vitro* and clinical data implicating the microtubule composition as important in cell drug sensitivity. Thus, for example, expression of class III β -tubulin in non-small cell lung cancer is correlated with resistance to taxane chemotherapy (Fojo and Menefee, 2007).

Yet, another hypothesis suggests that altered expression of β -tubulin isotypes may not be directly related to the resistant phenotype, but represents a secondary effect that may require the participation of additional isotype-specific regulatory proteins (Orr et al., 2003).

Since it is known that some MAPs bind to the highly divergent, but isotype-specific, C-terminal region of tubulin, it would be expected that such regulatory proteins

exist and are co-ordinately expressed along with their respective isotype upon drug selection. This scenario would explain why simple overexpression of tubulin isoforms in drug-sensitive cells cannot produce a resistance phenotype (Orr et al., 2003).

Proteins that regulate microtubule dynamics, by interacting with tubulin dimers or polymerised microtubules, clearly have the potential to modulate the sensitivity of a cell towards taxol. Stathmin, a microtubule destabiliser, and MAP4, a microtubule stabiliser, represent such proteins (Poruchynsky et al., 2001).

The overexpression or activation of stathmin and/or the down-regulation or inactivation of MAP4 should increase the dynamicity and decrease the stability of microtubules. Such changes in cancer cells could reduce the microtubule-stabilising potency of taxol and confer a mechanism of resistance to the drug. For example, MAP4 phosphorylation and dissociation from microtubules was correlated with a decrease in taxol sensitivity in taxol-resistant ovarian cancer cell lines (Poruchynsky et al., 2001).

4.1.2.2.3 Drug resistance through altered signalling pathways

Key proteins that mediate various signalling pathways are often localised in microtubules (Gundersen and Cook, 1999, Hollenbeck, 2001, Cardone et al., 2002), and microtubule-targeting drugs, such as taxol, have the potential to modulate these pathways.

One well-documented example of a signalling pathway that interacts with microtubules involves the extracellular signal regulated kinases 1/2 (ERK1 and ERK2), components of the mitogen-activated protein kinase (MAPK) family. It has been proposed that MAPK activation inhibits microtubule stabilisation, causing resistance (Shinohara-Gotoh et al., 1991).

A particular challenge in the ovarian cancer therapy will be to identify the different factors related to platinum drugs and taxanes resistance, as it is very likely that they

will not be the same, and modulation approaches will ultimately need to consider that clinical drug resistance is a multifactorial phenomenon (Kaye, 2008).

4.1.2.3 Overcoming drug resistance

The identification of specific genes and pathways involved in chemoresistance will hopefully lead to new strategies to treat platinum and taxane-refractory tumours or prevent resistance from emerging. Clinical investigations are already exploring alternative pharmacologic means of resistance reversal, either that acquired during therapy cycles, as occurs in patients with ovarian cancer, or intrinsic resistance, as that seen in patients with colorectal, prostate, lung or breast cancer (Kelland, 2007).

Considering platinum resistance, the major ongoing strategies to circumvent it are related to improvements in drug delivery, reversal of the phenomenon with resistance modulators and use of new chemotherapeutic drugs, which do not develop resistance.

In order to increase the levels of platinum reaching the tumour, some research groups have tried to use liposomal and co-polymer platinum products. The use of intraperitoneal administration, instead of the conventional intravenous injection, is another approach that was used to improve drug delivery. Other approaches are related to the combination of existing platinum drugs with molecularly targeted drugs, for example, the antibodies bevacizumab and trastuzumab (Kelland, 2007).

The use of platinum resistance modulators, either alone (for example, TLK286) or in combination (for example, decitabine), aims to exploit platinum-mediated resistance mechanisms (Kelland, 2007). Clinical combination studies using platinum drugs with resistance modulators or new molecularly targeted drugs are underway. These include the demethylation approach, which was capable of reversing resistance to carboplatin in an appropriate ovarian cancer xenograft, and is the basis of an ongoing randomised trial involving decitabine. This DNA methyltransferase inhibitor reverses platinum drug resistance by reducing the

methylation of various genes that are silenced by methylation during tumour development (Plumb et al., 2000, Appleton et al., 2007).

With respect to new platinum drugs, oxiplatin, satraplatin and picoplatin are the main examples. They constitute an alternative in cisplatin and carboplatin-resistant tumours, since in some studies it was observed that tumour cells do not seem to develop resistance mechanisms against them (Gore et al., 2002, Treat et al., 2002).

Approaches to overcome taxanes resistance include the use of MDR modulators, if the resistance correlates to P-gp overexpression, molecularly targeted agents and novel cytotoxic molecules, developed on the basis of activity in taxol-resistant models.

A promising strategy to overcome MDR seems to be the use of inhibitors or modulators of the efflux pumps, in conjunction with anticancer therapy. These compounds interact with P-gp and block the transmembrane transport, thus leading to a sufficient intracellular drug accumulation (Wiese and Pajeva, 2001). Combination therapy of cytotoxic agents with MDR modulators results in remission of tumours and increases life expectancy in some animal models. Until now, several compounds that demonstrated MDR modulator activity have been identified. They can be categorised in three generations. The first generation includes lipophilic compounds, which have previously been used in the treatment of distinct diseases, such as verapamil, a known calcium channel blocker (Nobili et al., 2006). The second generation comprises compounds similar to the first generation, but obtained by chemical modification, such as cyclosporin A. They seem to have greater potency and selectivity for MDR, reducing adverse side effects (Wiese and Pajeva, 2001). Finally, the last generation includes molecules rationally developed by combinatorial chemistry with the aid of quantitative structure-activity relationships. These modulators have a higher affinity for their target and less significant pharmacokinetic interactions (Fujimori et al., 2006). The compound tariquidar is an example of this class. It is selective and an extremely potent modulator, having additionally a longer duration of action (Teodori et al., 2006).

With respect to new cytotoxic molecules, the epothilones are the most advanced molecules in development among the microtubule-stabilising agents, with several being investigated in clinical trials. These compounds can be distinguished from the taxanes by several biologic and chemical criteria. The most important is that epothilones are not susceptible to P-gp-mediated efflux. It was demonstrated that P-gp overexpression only minimally affects their *in vitro* cytotoxicity. Hence, epothilones represent a new strategy for overcoming MDR (Larkin and Kaye, 2006). In addition, they are functional and structurally distinct from the taxanes and exhibit a greater potency (Fojo and Menefee, 2007).

In resistance to taxanes, as well as platinum, targets for modulation include components of the PI3K/AKT pathway. Amplification of the gene encoding the key catalytic subunit of AKT, P110 α , is seen in 40 % of ovarian cancers (Shayesteh et al., 1999) and mutations are also present (Campbell et al., 2004). Increased activity of this pathway leads to growth promotion and inhibition of drug-induced apoptosis, with consequent resistance to both taxanes and platinum drugs. Reversal of this resistance pathway may be achieved by various agents, several of which are now in phase I trials. Examples include novel inhibitors of both PI3K and PKB/AKT, as well as established inhibitors of the mammalian target rapamycin and of the molecular chaperone heat shock protein 90 (Hsp90) (Sain et al., 2006). Other relevant targets to overcome taxane resistance include the SRC oncogene (Chen et al., 2005) and the endothelin receptor family (Rosano et al., 2007). In both cases, overexpression in ovarian cancer and experimental reversal of taxane resistance has been reported, and specific inhibitors are now under clinical evaluation.

Phenoxodiol is an inhibitor of the anti-apoptotic XIAP family and experimental reversal of resistance to both platinum and taxanes has been demonstrated with this agent (Mor et al., 2006). A randomised trial involving this drug is ongoing in platinum-resistant ovarian cancer patients.

Other apoptosis regulators, including those of the Bcl-2 family, are promising candidates as targets for resistance modulation and appropriate clinical trials are under consideration.

There has been various and extensive research into the mechanisms of resistance and, increasingly, into identifying potential biomarkers of resistance, which would allow patients to receive more effective treatment faster. However, although various proteins have been identified and many mechanisms, such as those mentioned, hypothesised, the biggest drawback in this area is the lack of clinical evidence. This is because much of the research has been conducted on *in vitro* cell lines rather than on actual tumour tissue (Agarwal and Kaye, 2003). The main reason for this is the difficulty in obtaining large enough tissue samples from patients to be able to derive significant data. There are possible, although not ideal, alternative sources, such as ascitic tumour cells and free tumour DNA and RNA from blood samples (Kaye, 2008). Still, to develop a real understanding of the development of chemoresistance, tissue samples that feature in the actual tumour microenvironment are needed.

Similarly, more research is required into characterising tumour stem cells, in order to better understand their ability to remain dormant and their role in developing drug resistance (Kaye, 2008). This is because many cytotoxic drugs, such as vinblastine, are cell cycle specific, and tumours with a low mitotic index have a greater proportion of cells that are not dividing and, therefore, display chemoresistance. They also appear to reduce the efficacy of some non-cell cycle specific drugs such as cisplatin, possibly owing to an enhanced ability to repair DNA damage. Furthermore, tumour regions occupied by these stem cells tend to have an inadequate blood supply due to their low metabolic demand, thus sub-therapeutic levels of the cytotoxic agents are achieved (Mellor et al., 2005).

There have been impressive advancements in quantifying and analysing proteins. However, whereas with DNA microarray gene expression can be extensively monitored, proteomic technology is limited. As a result, better proteomic methods need to be developed with increased sensitivity (to allow monitoring of low abundance proteins), efficiency and better reproducibility (Kabuyama et al., 2004).

4.2 Aims & Objectives

The first aim of this study was to develop and optimise a proteomics approach for the discovery of protein targets of resistance to chemotherapy in ovarian cancer. This would be achieved by comparing the protein profile of human ovarian cancer cell lines, which are sensitive or resistant to the ovarian anti-cancer chemotherapy of choice – taxol and carboplatin.

The second aim of this study was to apply the same optimised method to compare the protein profile of human ovarian tissue biopsies, including control/non-cancer tissue and ovarian cancer tissues of different histology and their clinical history. The main objective was to confirm the ovarian cancer protein targets of resistance to chemotherapy identified with the previous samples, and to identify ovarian cancer protein targets of diagnosis and histological type.

The third aim of this study was to endeavour to build the *in-vivo/in-vitro* connection, through the analysis and comparison of the proteins identified in each of the previous studies and their relevance.

4.3 Materials & Methods

The supplier of all the chemicals and equipment used in the following experiments is specified after each one of them in the descriptions below, unless mentioned previously. A schematic diagram summarising the experiments carried out in this study is represented in Figure 4.3.

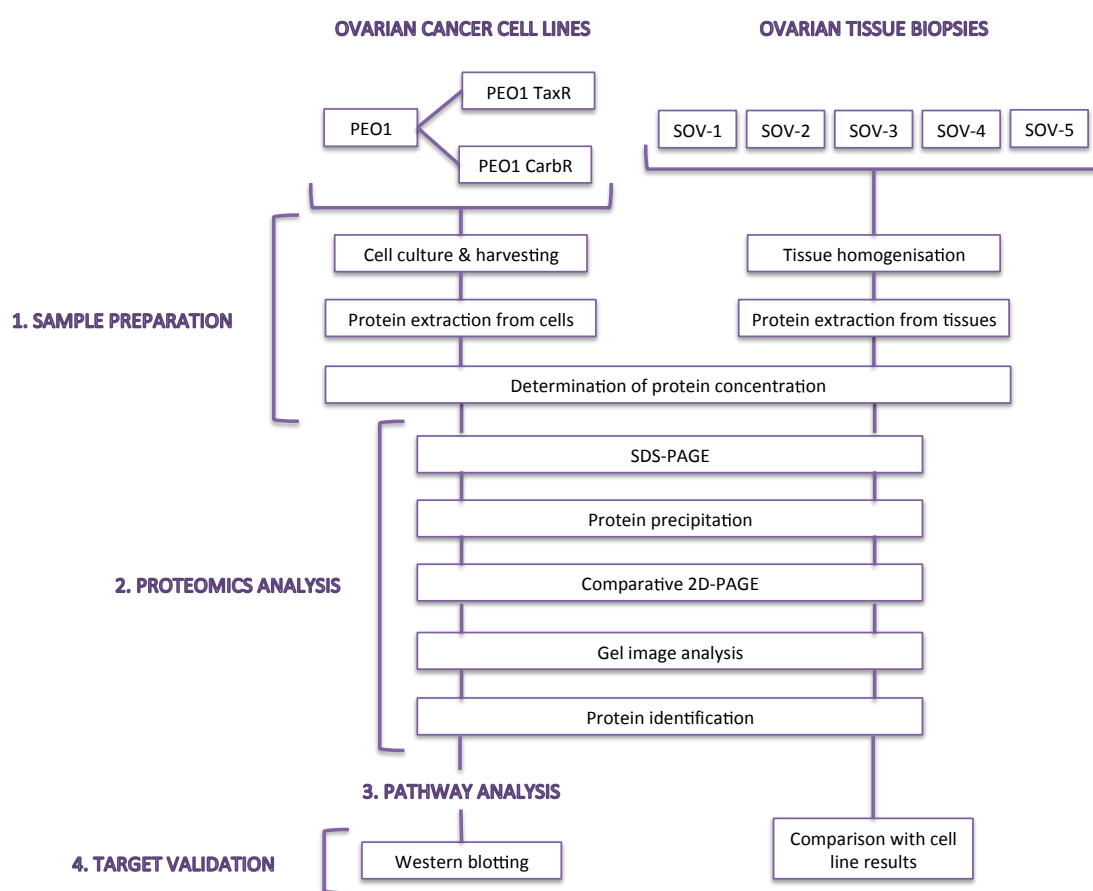


Figure 4.3 Schematic diagram summarising the experiments done in this study.

4.3.1 Biological samples

Ovarian cancer cells and tissues were kindly supplied by Dr. Helen Coley from the Faculty of Health and Medical Sciences, University of Surrey, for the proteomics study of ovarian cancer.

The human epithelial ovarian carcinoma cell line used in this study was PEO1. This cell line was originally developed by Langdon *et al.* and was derived from the ascites of patients with poorly differentiated serous ovarian adenocarcinoma (Langdon *et al.*, 1988).

The parental ovarian cancer cell line model PEO1 was used as drug sensitive reference cell line in this study. Novel drug resistant models, derived from the parental line, with *in vitro* acquired resistance to taxol – PEO1 TaxR – and carboplatin – PEO1 CarbR – were used alongside their respective drug sensitive parental counterparts.

The ovarian tissues – SOV-1, SOV-2, SOV-3, SOV-4, SOV-5 – were obtained by biopsy from 5 different patients, 4 of which were diagnosed with ovarian cancer and 1 suffered from endometriosis, a benign gynaecologic condition. Relevant clinical information about the patients, tissue histology, stage of disease and response to chemotherapy for each sample are shown in Table 4.1.

Table 4.1 Clinical information from 5 different patients and their respective ovarian tissue biopsies.
† denotes death; Pre- or Post-chemotherapy denotes drug therapy timing in relation to sample taken; N/A – not applicable.

Sample	Histology	Stage of Disease	Pre- or Post-Chemotherapy	Response to Chemotherapy	Survival Time	Notes
SOV-1	Endometriosis	N/A	N/A	N/A	Alive & well	Non-malignant condition
SOV-2	Serous adenocarcinoma	IVa	Previously treated – interval debulking sample	No response, progressive disease	38 months †	—
SOV-3	Serous adenocarcinoma	IIIc	No previous chemotherapy, primary surgery	Complete response	60 + (alive & well)	—
SOV-4	Clear cell adenocarcinoma	IVa	No previous chemotherapy, primary surgery	Partial response	34 months †	—
SOV-5	Serous adenocarcinoma	IIb	No previous chemotherapy, primary surgery	Partial response	106 months †	BRCA1 mutant

4.3.2 Sample preparation

Ovarian cancer cell line and tissue samples were subjected to the following sample preparation steps prior to separation and identification of their proteins.

4.3.2.1 Cell culture

PEO1 ovarian cancer cells were cultured by Dr. Helen Coley according to the procedure described in the literature (Coley et al., 2006). Briefly, cells were cultured as monolayers in RPMI-1640 medium supplemented with 10 % fetal calf serum (FCS, heat inactivated; Invitrogen, UK) and 2 mM L-glutamine. Cells were grown at 37 °C in a CO₂ independent incubator and passaged 12 times.

In order to obtain the resistant cell lines PEO1 TaxR and PEO1 CarbR, PEO1 cells were split and grown in the presence of a maintenance dose of 8 nM taxol and 2 µM carboplatin, respectively, until a stable resistance phenotype was acquired. This

resulted in the PEO1 TaxR cell line with approximately 15-fold resistance, which was passaged 42 times, and PEO1 CarbR cell line with approximately 8-fold resistance to both carboplatin and cisplatin, which was passaged 41 times.

4.3.2.2 Cell harvesting

After checking confluence, cells were harvested from the culture flasks as detailed in section 2.3.1.1.

4.3.2.3 Protein extraction from PEO1 ovarian cancer cells

Proteins were extracted from the PEO1 ovarian cancer cells according to the procedures described in sections 2.3.1.2 and 2.3.1.3.

4.3.2.4 Protein extraction from ovarian tissue samples

The complete procedure followed to extract proteins from the ovarian tissue samples can be found in section 2.3.2.3.

4.3.2.5 Protein concentration assay

Protein concentrations of all cell and tissue lysate samples were determined in triplicate using the RCDC Protein Assay Kit (Bio-Rad, UK), according to the description given in section 2.3.3. Before starting the experiment, all cell line protein samples were diluted 2x and all tissue protein samples were diluted 25x to allow them to fit the calibration curve.

4.3.3 Proteomics analysis

Quantified protein mixtures obtained from lysis and homogenisation of the ovarian cancer cells and tissues were then subjected to proteomics analysis in order to separate and identify the proteins.

4.3.3.1 SDS-PAGE

Proteins extracted from the PEO1 cells and the ovarian tissue samples were separated by SDS-PAGE under denaturing and reducing conditions, in the presence of SDS and DTT as described in section 2.4.1. For the PEO1 cells, two different amounts of protein (10 and 20 µg) were tested for each sample. For the ovarian tissue samples, 10 µg of protein were examined for each sample. Precast gels, Mini-Protean TGX Precast Gel, any kD, 10-well comb, 30 µL/well (Bio-Rad, UK) and 12.5 % SDS-PAGE handmade gels were used for the separation of proteins extracted from the PEO1 cell lines. Tissue proteins were separated using 10 % SDS-PAGE handmade gels.

Protein band visualisation was achieved through Coomassie blue staining, as explained in section 2.5.1.

4.3.3.2 Protein precipitation

Prior to 2D-PAGE, cell and tissue lysates (with 50 µg protein per sample) were subjected to treatment with the ReadyPrep 2-D Clean Up Kit (Bio-Rad, UK) to remove interfering agents, such as excess salts, and to concentrate proteins. The comprehensive protocol for the use of the 2D clean-up kit can be found in section 2.3.4.2.

4.3.3.3 2D-PAGE

Proteins extracted from the PEO1 cells and the ovarian tissue samples were also separated by 2D-PAGE, which was performed according to the following steps. To ensure the reproducibility of 2D-PAGE experiments, each cell sample was analysed twice. Unfortunately, this was not possible for the tissue samples, as there was not enough protein.

4.3.3.3.1 First dimension: isoelectric focussing (IEF)

Isoelectric focussing was performed using Protean IEF Cell (Bio-Rad, UK) with 11 cm ReadyStrips, pH 3-10 non-linear (Bio-Rad, UK), according to the description in section 2.4.3.1. Pellets resulting from the treatment with the 2D clean-up kit were resuspended in rehydration buffer II to a total volume of 200 µL. Mixtures were centrifuged and the supernatants were loaded into a focussing tray. The rehydration procedure took place at 50 V (active rehydration) for 12 h (overnight). Focussing was then started and carried out on a rapid ramp according to the following steps: 250 V for 15 min, 8000 V for 2 h, 8000 V until 40 000 V/h (Table 2.3, focussing conditions D).

4.3.3.3.2 Equilibration, reduction & alkylation

After the first dimension separation and before the second dimension separation, proteins were equilibrated, reduced and alkylated in accordance to section 2.4.3.2.

4.3.3.3.3 Second dimension: SDS-PAGE

Each strip was transferred to the top of a precast gel, Criterion TGX Precast Gels, any kD, IPG + 1 well comb, 11 cm IPG strip (Bio-Rad, UK), as described in section 2.4.3.3. A molecular weight marker was loaded into the single well of the precast gel. Electrophoresis was carried out using a Criterion Cell System (Bio-Rad, UK) at 40 V until the blue dye had reached the main gel, and then increased to 150 V until the dye front had reached the bottom of the gel.

4.3.3.3.4 Gel staining: silver staining

Separated proteins were visualised on the 2D gels using the Pierce Silver Stain Kit (Thermo Scientific, UK), according to the details given in section 2.5.2.

4.3.3.4 Gel image analysis

Gel images were obtained with a digital photographic camera and/or using the camera device of EXQuest Spot Cutter (Bio-Rad, UK), and analysed using PDQuest

Advanced software version 8.0.1 (Bio-Rad, UK). The comparative analysis of the spots present on the gels and the selection of the spots of interest was performed either visually or using PDQuest Advanced software.

4.3.3.5 Protein identification

Protein identification was achieved by in-gel trypsin digestion, followed by LC-MS/MS analysis. The respective procedures are depicted in the following sections.

4.3.3.5.1 Spot excision, washing and in-gel trypsin digestion

Spots of interest were excised from the gels and cut into 1-2 mm³ gel pieces, either manually or using an EXQuest Spot Cutter (Bio-Rad, UK) with a picker head of 1.5 mm, and placed into 0.6 mL siliconised tubes or 96-well microplates, for the manual and automated excisions respectively. The subsequent washing steps and in-gel trypsin digestion were performed as described in section 2.6.1.1.

4.3.3.5.2 Peptide extraction from gel pieces

Peptides were extracted from the gel pieces in accordance to the procedure described in section 2.6.1.2.

4.3.3.5.3 MS analysis

LC-MS/MS analysis of the extracted peptide mixtures was performed on a Waters CapLC system coupled to the front end of a Waters Micromass Q-ToF Premier, as described in section 2.6.1.3.

4.3.3.5.4 Data processing and database searching

Raw LC-MS/MS data were processed using MassLynx ProteinLynx version 4.1 (Waters, UK) and searches were done using two online search engines, MASCOT and X!Tandem, as described in section 2.6.1.4. SwissProt databases were chosen to look for human proteins (taxonomy — *Homo sapiens*). The search parameters used were those listed in the same section of Chapter 2.

Scaffold 3 software version 3.6.4 (Proteome Software, USA) was used to confirm protein identifications, combine and compare proteins identified among different biological samples and to group proteins by biological relevance and molecular function. Parameters of analysis using Scaffold 3 can be found in the same section of Chapter 2.

4.3.4 Pathway analysis

Pathway analysis was performed using Ingenuity Pathway Analysis (IPA) software (Ingenuity Systems, Quiagen, CA, USA).

4.3.5 Target validation – Western blotting

A total of 20 µg of protein per well was loaded onto precast gels, Mini-Protean TGX precast gels, any kD, 10-well comb, 30 µL/well (Bio-Rad, UK). Proteins were separated by SDS-PAGE and transferred onto nitrocellulose membranes (Hybond-C Extra, Amersham Biosciences, UK) using a Mini Trans-Blot Transfer Cell (Bio-Rad, UK) for 1 h at 100 V, as described in section 2.6.2.

After blocking with 1 % BSA (Sigma-Aldrich, UK) or 1 % milk (dried skimmed milk, Marvel) in TBS buffer for 1 h at room temperature, the membranes were probed with rabbit polyclonal primary antibodies, diluted in blocking solution, overnight at 4 °C. A list of the primary antibodies used, their supplier and respective product code, as well as the dilution and blocking agent used for each antibody is shown in Table 4.2.

Table 4.2 List of the primary antibodies used for target validation in the ovarian cancer study. The suppliers and respective product codes, dilutions and blocking agents used for each antibody are also shown.

Antibody	Dilution	Blocking Agent	Supplier (UK)	Product Code
Anti-14-3-3 antibody	1:1000	Milk	Abcam	ab9063
Anti-MMS2 antibody	1:100	Milk	Abcam	ab13906
Anti-PGAM1 antibody	1:500	Milk	Abcam	ab96622
Anti-TRX antibody	1:1000	Milk	Abcam	ab86255
Anti-UBE2K antibody	1:1000	Milk	Sigma-Aldrich	SAB2102623-50UG
Anti-Actin antibody (loading control)	1:100	BSA	Abcam	ab1801

The membranes were then washed 4x with TBS buffer containing 0.05 % Tween 20 (Sigma-Aldrich, UK) and subsequently incubated for 1.5 h at room temperature with a horseradish peroxidase (HRP)-conjugated donkey anti-rabbit secondary antibody (ab16284, Abcam, UK) at a dilution of 1:2000, in the same blocking solution as the primary antibody. After incubation with secondary antibody, membranes were washed again with TBS buffer containing 0.05 % Tween 20. Protein bands were developed using a SuperSignal West Pico Chemiluminescent Substrate (Thermo Scientific, UK) and visualised with a Bio-Rad gel imager using Image Lab software (Bio-Rad, UK). The western blot assay was performed at least twice for each antibody.

4.4 Results & Discussion

Ovarian cancer has been studied for many years and the phenomenon of resistance to chemotherapy is widely recognised as one of the main reasons for treatment failure and, as a result, poor prognostic and low survival rates in ovarian cancer. However, the mechanisms underlying drug resistance and the protein targets responsible for such phenomenon are poorly understood and reliable ovarian cancer biomarkers are yet to be identified. Therefore, the main aim of this study was to identify protein targets of resistance to chemotherapy in ovarian cancer through a proteomic approach.

In order to achieve this task, three groups of PEO1 ovarian cancer cells were used in this study: PEO1 sensitive cell line and two resistant counterparts originated from the sensitive cell line, taxol resistant 'PEO1 TaxR' and carboplatin resistant 'PEO1 CarbR'. In addition, five ovarian tissue biopsies, SOV-1, SOV-2, SOV-3, SOV-4 and SOV-5, collected from five different patients with distinct diagnosis and clinical history, were used in this study.

The work was divided in four phases. Firstly, a 2D-PAGE technique to separate the proteins previously extracted from the cells and tissue biopsies was used. Secondly, the gels obtained were compared and some of the spots with different intensities, in at least two of the gels, were selected for further analysis. The isolated spots were analysed using LC-MS/MS and the proteins were identified by comparison with a human protein database. After that, the identified proteins and their differences in expression between samples were used for pathway analysis and the results were compared to the literature, so that possible targets of resistance to chemotherapy could be suggested. Finally, one representative protein from each of the top 6 identified pathways was selected for validation using western blotting.

Furthermore, proteins identified in the tissue samples and their expressions were used not only for confirmation of the results obtained with the PEO1 cell lines, but

they were also compared between the tissue samples themselves, in order to suggest possible protein targets of diagnosis and ovarian cancer histological type.

4.4.1 Preliminary observations and assays

4.4.1.1 Ovarian tissue biopsies

Ovarian tissue biopsies were weighed and visually observed prior to treatment. Visual observations are recorded in Table 4.3.

Table 4.3 Visual observations and weights of ovarian tissue biopsies analysed. The ovarian tissues – SOV-1, SOV-2, SOV-3, SOV-4, SOV-5 – were obtained by biopsy from 5 different patients, 4 of which were diagnosed with ovarian cancer and 1 suffered from endometriosis, a benign gynaecologic condition.

Sample	Histology	Visual Observation	Weight (mg)
SOV-1	Endometriosis (non-cancer)	White-stained tissue, solid, haemorrhagic	700
SOV-2	Serous adenocarcinoma	Bloodstained, flap sample	500
SOV-3	Clear cell adenocarcinoma	White-stained tissue, solid, dense	500
SOV-4	Serous adenocarcinoma	Bloodstained, flap sample	100
SOV-5	Serous adenocarcinoma	Bloodstained, flap sample	100

All ovarian cancer biopsies studied were epithelial ovarian tumours (adenocarcinomas), the most frequent type of ovarian cancer. Ovarian cancer tissues SOV-2/4/5 were all macroscopically similar, described as bloodstained, flap samples, which corroborates the fact that all of them were serous adenocarcinomas, according to the histological classification. SOV-3 was visually different from the other cancer tissues, described as a white-stained, solid, dense tissue, yet it was similar to SOV-1, the non-cancerous tissue sample. This is in line with the fact that SOV-3, according to histology, was categorised as a different type of ovarian cancer, clear cell adenocarcinoma, and this type of ovarian carcinoma is the most related to endometriosis. In fact, approximately 50% of these tumours are associated with endometriosis (Serov et al., 1973, Kaku et al., 2003).

Endometriosis is a gynaecological condition in which cells from the lining of the uterus (endometrium) grow in other areas of the body, most commonly in the pelvic region. These endometrial-like cells respond to hormones in the same way as the cells of the uterine cavity, but with no outlet it can cause inflammation, scarring and adhesions, leading to severe pain and many other symptoms (Brosens and Benagiano, 2011).

The link between endometriosis and ovarian cancer is well recognised and has intrigued physicians for a long time. Epidemiological studies have suggested a specific link with non-serous ovarian carcinomas such as endometrioid and clear-cell carcinomas, however there is no firm evidence supporting endometriosis as an ovarian cancer precursor lesion (Nezhat et al., 2008). A recent study by a team of researchers from the Ovarian Cancer Association Consortium (OCAC) confirmed that women with history of endometriosis have increased reports of clear-cell carcinoma and endometrioid ovarian cancer (Pearce et al., 2012). The study also shows for the first time that endometriosis is associated with low-grade serous ovarian carcinomas, and that its risk is doubled in women who suffer from that condition. Nevertheless, the authors showed no relationship between endometriosis and high-grade serous carcinomas or other subtypes of ovarian cancer.

In addition, endometriosis has been related to a chronic inflammatory state leading to cytokine release, which can lead to unregulated mitotic division, growth and differentiation, and migration or apoptosis similar to malignant mechanisms (Nezhat et al., 2008).

Despite similarities in name and location, endometriosis has not been associated with endometrial cancer to date.

Notwithstanding its limitations, in this study, SOV-1 was used as a non-cancerous control and compared with the ovarian cancer tissues, although the ideal control would be normal ovarian tissue, which for numerous reasons is difficult to obtain for research purposes.

4.4.1.2 Protein concentration assay

Protein concentration of the cells and tissues was tested using a commercial kit. Firstly, a calibration curve was generated with absorbance values versus the corresponding concentrations of the standard bovine plasma γ -globulin, which were prepared by serial dilutions from the initial stock concentration of 1.5 mg/mL. Then, a linear regression was applied to the calibration curve and protein concentrations were calculated using the equation obtained.

4.4.1.2.1 Protein concentration assay of PEO1 cell lines

PEO1 cell line samples were diluted 2x in order to fit the calibration curve. Figure 4.4 illustrates an example of calibration curve used in this experiment and its respective equation. Table 4.4 shows the calculated protein concentrations of the different ovarian cancer cell lines.

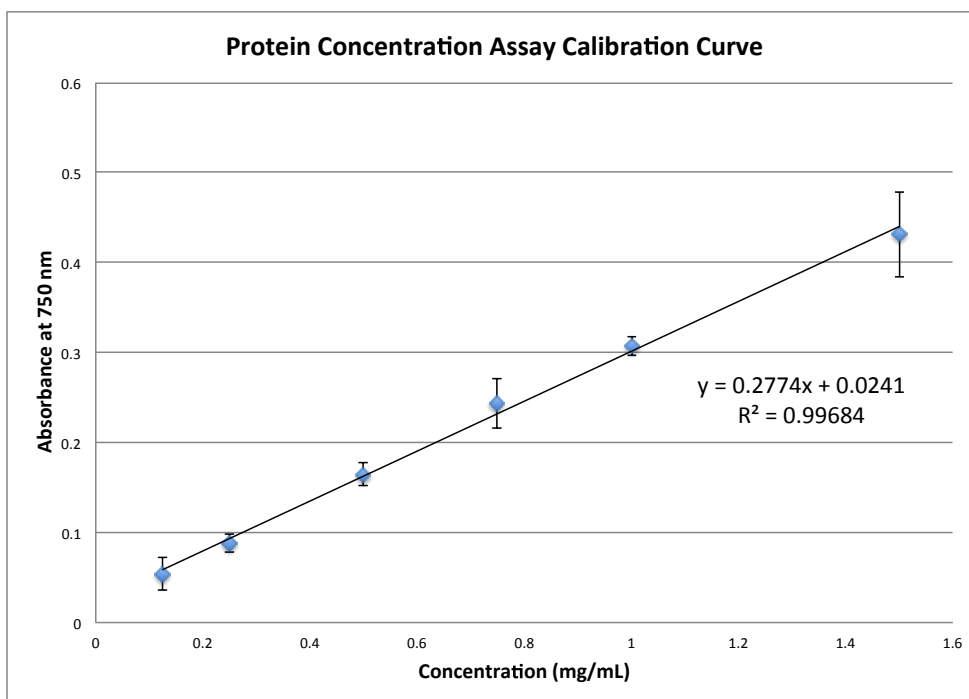


Figure 4.4 Protein concentration assay calibration curve. Protein concentration assay was performed using a commercial kit according to the manufacturer’s instructions. Bovine plasma γ -globulin was used as standard in the following concentrations: 0.125, 0.25, 0.5, 0.75, 1.0, 1.5 mg/mL. Equation of the linear regression is shown in the graph.

Table 4.4 Protein concentration of the three ovarian cancer cell line samples. Protein concentration assay was performed using a commercial kit according to the manufacturer’s instructions. The concentrations were calculated using the equation displayed in Figure 4.4.

Cell line sample	Mean Absorbance at 750 nm	Dilution Factor	Protein Concentration (mg/mL)
PEO1	0.362	X 2	2.44
PEO1 TaxR	0.416		2.83
PEO1 CarbR	0.359		2.42

The calculated concentration values were multiplied by 2 to obtain the protein concentrations of the original cell line samples, since samples had been diluted.

As shown in Table 4.4, all the samples had similar concentrations of protein, with PEO1 TaxR cell line being the most concentrated. For further experiments, similar volumes of sample would be needed, which considerably facilitates sample preparation for gel electrophoresis.

4.4.1.2.2 Protein concentration assay of tissue biopsies

The ovarian tissue samples were diluted 25x in order to fit the calibration curve. Figure 4.5 shows an example of calibration curve used in this experiment and its respective equation. Table 4.5 depicts the calculated protein concentrations of the different ovarian tissue samples.

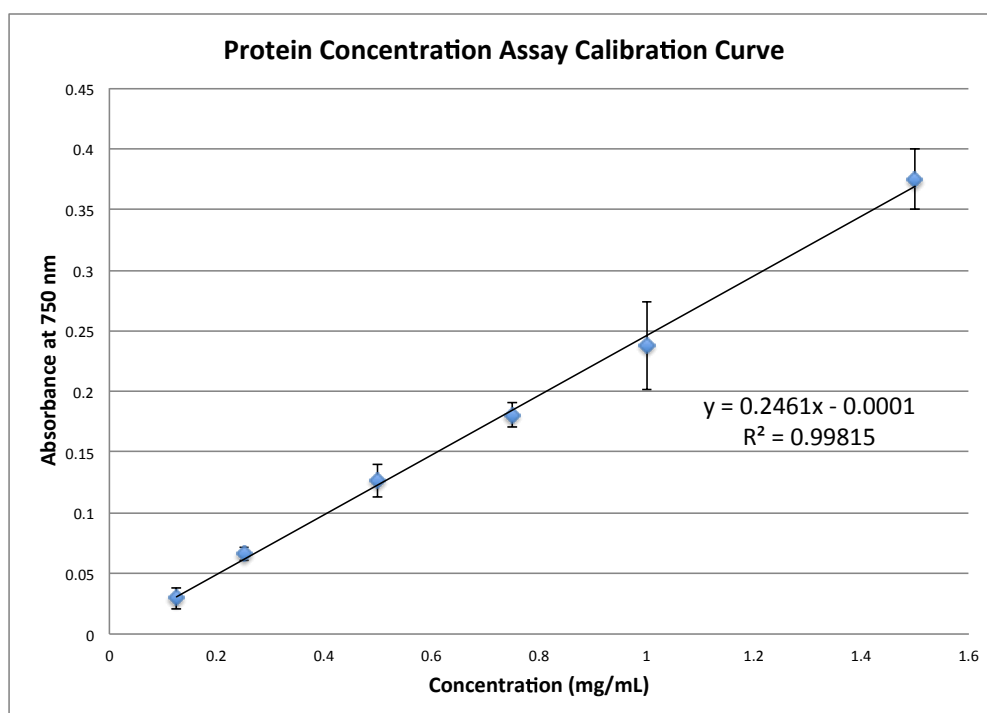


Figure 4.5 Protein concentration assay calibration curve. Protein concentration assay was performed using a commercial kit according to the manufacturer’s instructions. Bovine plasma γ -globulin was used as standard in the following concentrations: 0.125, 0.25, 0.5, 0.75, 1.0, 1.5 mg/mL. Equation of the linear regression is shown in the graph.

Table 4.5 Protein concentration of the five ovarian tissue samples. Protein concentration assay was performed using a commercial kit according to the manufacturer’s instructions. The concentrations were calculated using the equation displayed in Figure 4.5.

Tissue sample	Mean Absorbance at 750 nm	Dilution Factor	Protein Concentration (mg/mL)
SOV-1	0.215	X 25	21.85
SOV-2	0.230		23.34
SOV-3	0.346		35.16
SOV-4	0.191		19.41
SOV-5	0.051		5.23

As samples had been diluted, the calculated concentration values were multiplied by 25 to obtain the protein concentrations of the original tissue samples.

According to the data shown in Table 4.5, all the samples had reasonable and similar concentrations of protein apart from SOV-5, which only had 5.23 mg/mL.

This might be related with the fact that the weight of SOV-5 tissue sample was lower than most of the others, as shown in Table 4.3, resulting in lower protein content after extraction. However, the amount of SOV-4 tissue sample was identical to SOV-5 and SOV-4 did not present such a low protein concentration. Therefore it was imperative to conduct the experiments careful and efficiently in order to minimise any further potential loss of protein. As expected, overall the ovarian tissue samples were significantly more concentrated than the PEO1 cell line samples.

4.4.2 Proteomics analysis

4.4.2.1 SDS-PAGE gels

Protein profiles of PEO1 sensitive and resistant cell lines and the tissue biopsy samples were examined by SDS-PAGE. These experiments aimed to verify the quality of the samples, by confirming the presence of proteins and therefore the success of the extraction procedure, and search for initial protein expression differences between the studied samples. The experiments were performed only once.

4.4.2.1.1 SDS-PAGE gels of the PEO1 cell lines

Approximately 10 and 20 μg of protein for each of the PEO1 cell lines were separated by SDS-PAGE using a 12.5 % handmade SDS-PAGE gel and a precast gel. Gels were stained with Coomassie blue and photographed. Figure 4.6 exhibits two representative images of the obtained gels.

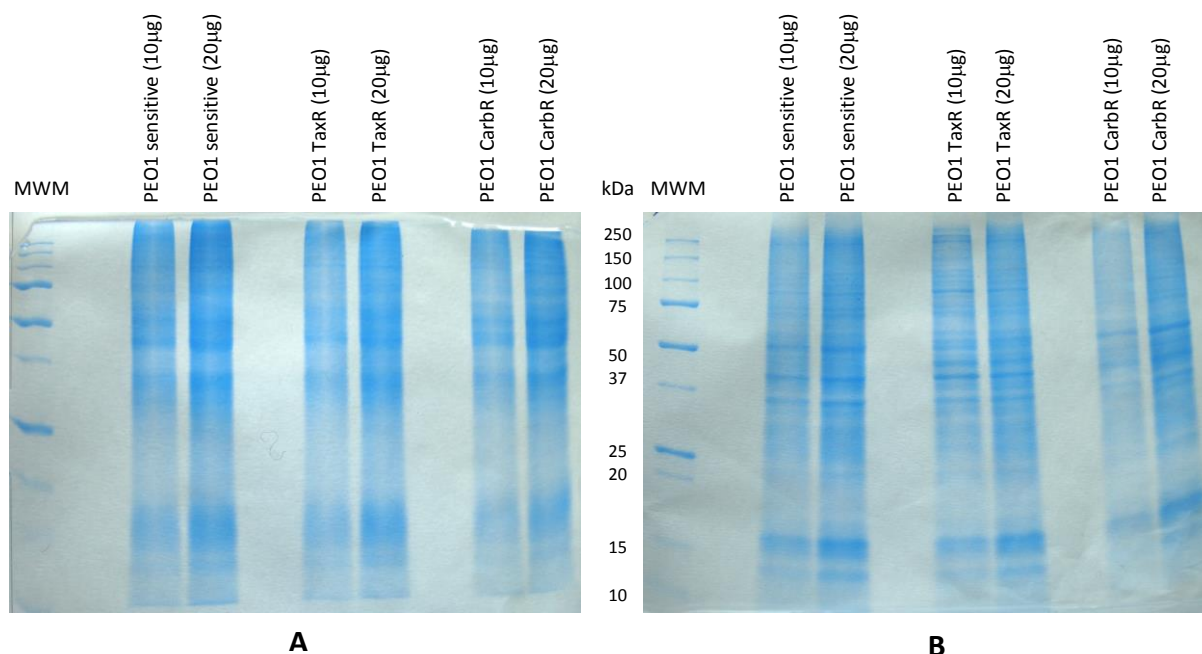


Figure 4.6 SDS-PAGE gel images of PEO1 sensitive, PEO1 TaxR and PEO1 CarbR resistant cell lines. Proteins (10 and 20 μg) extracted from PEO1 sensitive and resistant cell lines were separated by SDS-PAGE at 150 V. The resulting gels were stained with Coomassie blue. (A) 12.5 % SDS-PAGE handmade gel. (B) Mini-Protean TGX Precast Gel, any kD, 10-well comb, 30 μL /well. MWM: molecular weight marker.

In Figure 4.6, it is possible to see the distinct intensity of the sample lanes, as the strongest ones have twice the amount of protein. Additionally, it is possible to observe that protein bands are much better resolved in the precast gel. This fact is probably owing to the existence of a polyacrylamide concentration gradient in that gel, which does not exist in the handmade one. In the precast gel, clear differences in protein band intensity between the sensitive and resistant cell lines or between both resistant cell lines can be visualised. These differences are particularly evident in the range of molecular weights between 37 and 75 kDa.

4.4.2.1.2 SDS-PAGE gels of the tissue biopsies

Approximately 10 µg of protein for each of the five ovarian tissue samples were separated by SDS-PAGE using a 10 % SDS-PAGE handmade gel. The gels was stained with Coomassie blue and photographed. Figure 4.7 displays a representative image of the obtained gel.

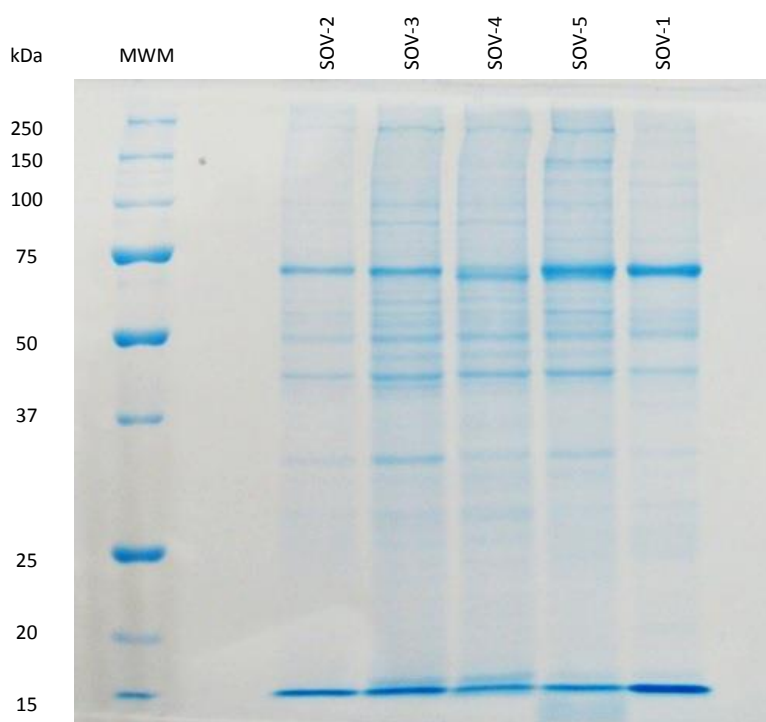


Figure 4.7 SDS-PAGE gel images of SOV-1, SOV-2, SOV-3, SOV-4 and SOV-5 ovarian tissues. Proteins (10 µg) extracted from ovarian tissue biopsies were separated by SDS-PAGE at 150 V on a 10 % SDS-PAGE handmade gel. The resulting gel was stained with Coomassie blue. MWM: molecular weight marker.

The gel illustrated in Figure 4.7 shows well resolved bands, with a particularly strong band between 50 and 75 kDa for all the five tissue samples. This band is probably related to high levels of contamination with human serum albumin, which has a molecular weight of approximately 69 kDa and is abundant in the human serum. Albumin is a common contaminant in the analysis of tissue lysates (Walsh, 2002). Moreover, considering that cancer cells promote angiogenesis and spread through the blood, this high level of contamination by a serum protein was expected. In these cases, the use of protein precipitation techniques prior to protein separation helps remove contaminants such as albumin, which are likely to hide other less abundant proteins.

Interestingly, SOV-5 presents a much stronger band at approximately 150 kDa than the other samples, despite the same amount of protein being loaded for each sample. This possibly indicates differences in the expression of specific proteins among different samples.

As SDS-PAGE only allows separation of proteins according to their molecular weight, the concentrated bands observed at the bottom of the gel may be a mixture of low molecular weight proteins that migrated quickly. These bands could be better separated using 2D-PAGE.

Overall, the 10 % SDS-PAGE handmade gel used in this experiment seemed to resolve the tissue proteins more efficiently than the 12.5 % SDS-PAGE handmade gel used for the separation of the cell line proteins. Gels that are more concentrated in acrylamides have smaller pore size, hindering the migration of proteins and sometimes resulting in poorly separated bands, when complex protein mixtures are under investigation (Hames and Rickwood, 1990).

All samples analysed were pre-treated with the 2D clean-up kit prior to 2D-PAGE in order to remove contaminants and minimise as much as possible the presence of albumin in the tissue samples.

4.4.2.2 2D-PAGE gels

2D-PAGE separation was carried out with protein samples of the three cell lines and five ovarian tissue biopsies in order to obtain a better protein separation, which permitted a more accurate identification of the proteins and the study of potential protein expression differences between samples. Only precast gels were used in these experiments. After silver staining, the gels were photographed, scanned and analysed using PDQuest Advanced software. Gel images were edited to crop out the marker protein bands on the right hand side to facilitate automatic spot selection. The experiments were performed twice for the three PEO1 cell lines and only once for the ovarian tissues, due to insufficient amount of sample.

4.4.2.2.1 2D-PAGE gels of the PEO1 cell lines

Approximately 50 µg of protein for each of the PEO1 cell lines were separated by 2D-PAGE using pH 3-10 non-linear 11 cm IPG strips for the first dimension and precast gels for the second dimension. Gels were stained with silver stain and photographed. Figure 4.8, Figure 4.9 and Figure 4.10 depict representative images of the replicate gels obtained for each of the studied cell lines.

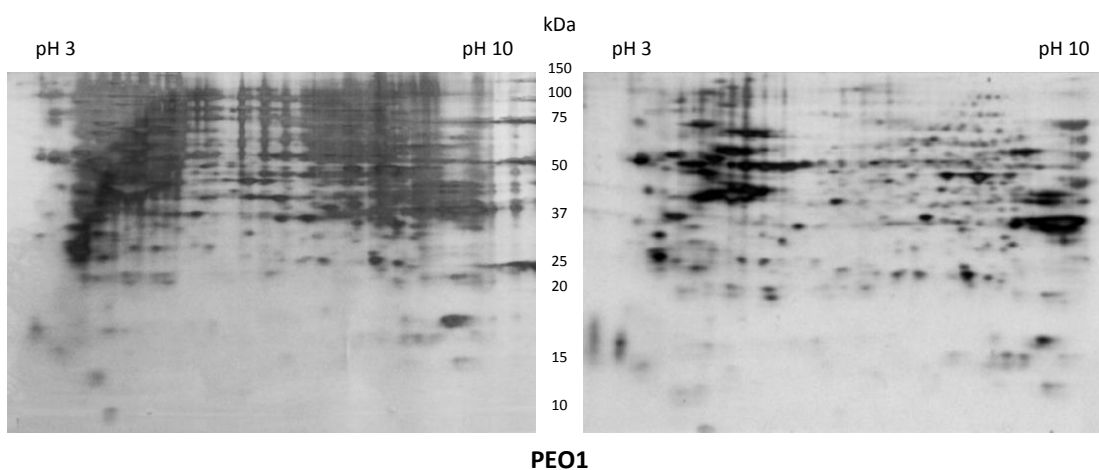


Figure 4.8 Representative 2D-PAGE silver stained gels of the PEO1 sensitive ovarian cancer cell line. Proteins (approximately 50 µg) were separated on pH 3-10 non-linear 11 cm IPG strips in the first dimension (IEF) and by precast gels (Criterion TGX Precast Gels, any kD, IPG + 1 well comb, 11 cm IPG strip) in the second dimension (SDS-PAGE). Resulting gels were silver stained.

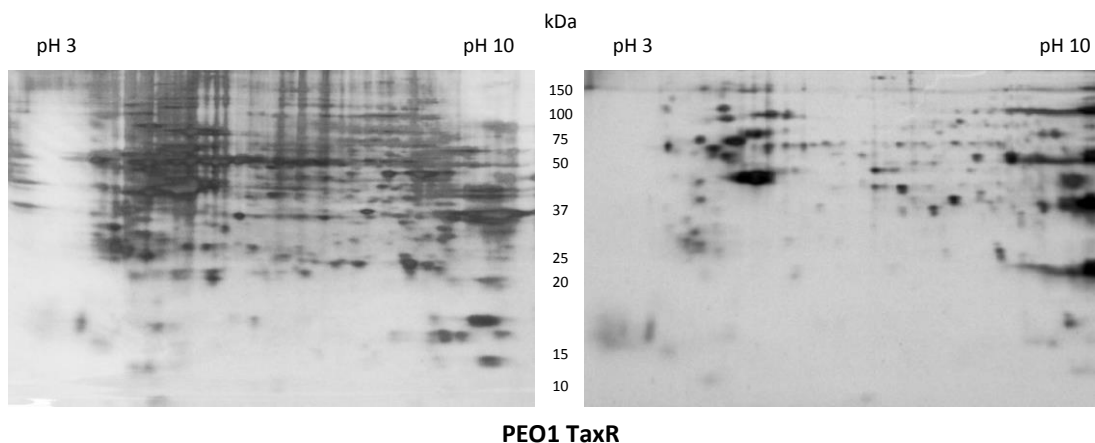


Figure 4.9 Representative 2D-PAGE silver stained gels of the PEO1 TaxR ovarian cancer cell line. Proteins (approximately 50 µg) were separated on pH 3-10 non-linear 11 cm IPG strips in the first dimension (IEF) and by precast gels (Criterion TGX Precast Gels, any kD, IPG + 1 well comb, 11 cm IPG strip) in the second dimension (SDS-PAGE). Resulting gels were silver stained.

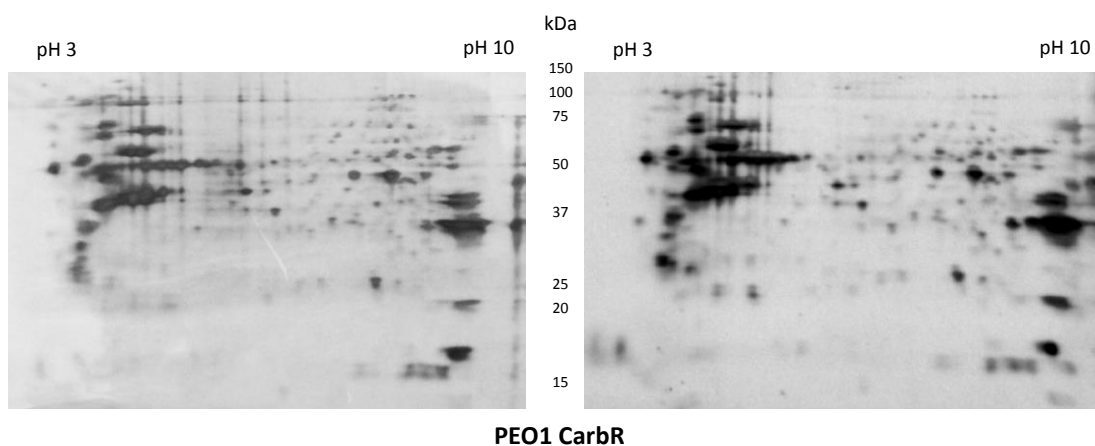


Figure 4.10 Representative 2D-PAGE silver stained gels of the PEO1 CarbR ovarian cancer cell line. Proteins (approximately 50 µg) were separated on pH 3-10 non-linear 11 cm IPG strips in the first dimension (IEF) and by precast gels (Criterion TGX Precast Gels, any kD, IPG + 1 well comb, 11 cm IPG strip) in the second dimension (SDS-PAGE). Resulting gels were silver stained.

One of the limitations of 2D-PAGE is reproducibility, i.e. the difficulty in generating identical gels when replicates of the same sample are analysed (Voss and Haberl, 2000, Lilley et al., 2002, Rabilloud et al., 2010). This is in great part owing to the multiple steps of the technique that are controlled by the operator. Preparation of the second dimension separation, in particular positioning of the IPG strip on the second dimension gel, and silver staining are examples of two steps of the 2D-PAGE

method that heavily influence image quality and are largely dependent on the operator. Most of the times protein spots can still be visible despite eventual streaking defects present on the gels; however, if reproducibility is compromised, the comparative analysis of spot intensity for protein regulation assessment will also be affected.

The PEO1 sensitive and PEO1 TaxR gels, shown in Figure 4.8 and Figure 4.9 respectively, are examples of replicates of the same sample that did not generate identical gels. This was possibly a result of over-staining of the first replicates (on the left), which were run and stained in parallel. The over-staining effect was most probably caused by an excessive colour development time (3 minutes). However, this fact allowed visualisation of some less concentrated protein spots that would not be visible otherwise and, in fact, could not be seen on the second replicate gels, where the colour development time was 2 minutes only. In any case, it is possible to observe individualised protein spots on all four replicate gels.

In the PEO1 sensitive and PEO1 TaxR gels a few horizontal streaks are visible on the right hand side, close to the MWM. This might have been caused by an incorrect loading of the MWM or, more likely, by an excessive volume of MWM loaded into the MWM wells. Probably, during the application of the overlay agarose solution that fixes the IPG strip to the second dimension gel, some MWM solution migrated out of its well and ran in the same well as the sample, creating this effect.

With respect to the PEO1 TaxR cell line, the number of spots present on the second replicate gel (on the right) seems to be significantly lower than on the first replicate gel obtained with the same sample. This fact can be justified by an incomplete solubilisation of the pellet after the protein precipitation assay, which may have resulted in less amount of protein loaded on the first dimension strip. Ideally, protein concentration should be confirmed after the precipitation assay and before starting IEF to prevent these situations. However, in practical terms, this is not possible for several reasons. Firstly, a larger amount of sample would have to be used to allow for the determination of its protein concentration. Secondly, the protein pellet would have to be resuspended in a different buffer, since the

constituents of the rehydration buffer severely interfere with the usual methods to assess protein concentration (Olson and Markwell, 2007). Yet, a different resuspension buffer would compromise the success of the first dimension separation. Even using the rehydration buffer to resuspend the protein pellet and then diluting it, so that the interference would be minimal, would also dilute the proteins in the sample to a level where they would be difficult to quantify.

In turn, the PEO1 CarbR gels, portrayed in Figure 4.10, represent replicate similarity that is closer to the ideal situation. The two replicates of the same sample depict many well-individualised protein spots and are similar, although some differences can still be observed. The staining development time in this case was 2 minutes for both replicates. It is possible to observe that the right hand side horizontal streaking caused by the MWM is less apparent on these gels than on the gels of the other cell lines. It is so, because a lower volume of MWM was loaded into the MWM wells in order to avoid the horizontal streaks previously observed.

All the gels show consistent horizontal streaking on the far left and right hand sides, generally more evident on the left hand side. This may be a result of inadequate focussing of the proteins, preventing efficient transfer of proteins to the second dimension gel. Additionally, it could suggest that too much sample was loaded onto the strip, overloading it, or that the proteins had not been adequately solubilised due to inadequate pellet resuspension or incorrectly prepared buffers. Protein absorption into the IPG strip gel matrix may also have been hindered by the presence of bound nucleic acids, which require digestion with an endonuclease and should have been removed by the 2D clean-up kit. There is also some background vertical streaking, more visible in the first replicate gels than the others, which suggests contamination of the gel or sample with dust or some particles present in the water supply (Garfin and Heerdt, 2001, Rabilloud, 2000).

The lack of reproducibility of 2D gels has been widely recognised to the point of affecting the credibility of 2D-PAGE applications in the field of proteomics. As a result, in an effort to restore credibility, Bio-Rad Laboratories, Novartis Institutes for BioMedical Research and Nonlinear Dynamics coordinated an initiative called the

'Fixing Proteomics Campaign', initiated during the 6th HUPO (Human Proteome Organization) Annual World Congress in Korea in October 2007. The main goal of this initiative was to develop standards and validated protocols that ensure reproducibility of 2D gel experiments. After Phase I and II of the campaign, participant laboratories proved that it was possible to generate gel images that fell within a 95 % confidence level in an inter-laboratory study (Bio-Rad, 2009).

In order to evaluate the level of reproducibility of an experiment, a number of replicates of the same sample are needed, so that a statistical test can be applied and the similarity/difference between replicates can be quantified. In the particular case of 2D-PAGE, a large number of replicate gels should be generated due to the great variation observed between gels. Unfortunately, in this experiment it was not possible to produce enough replicate gels to allow statistical evaluation of reproducibility, owing to the limited amount of samples available.

Nonetheless, after visual comparison of the 2D gels obtained for PEO1 sensitive and resistant cell lines, gels images were analysed using PDQuest Advanced software and spots relative abundance was compared between gels.

4.4.2.2.2 2D-PAGE gels of the tissue biopsies

Approximately 50 µg of protein for each of the five ovarian tissue biopsies were separated by 2D-PAGE using pH 3-10 non-linear 11 cm IPG strips for the first dimension and precast gels for the second dimension. Gels were stained with silver stain and photographed. Figure 4.11 displays representative images of the replicate gels obtained for each of the studied tissue samples.

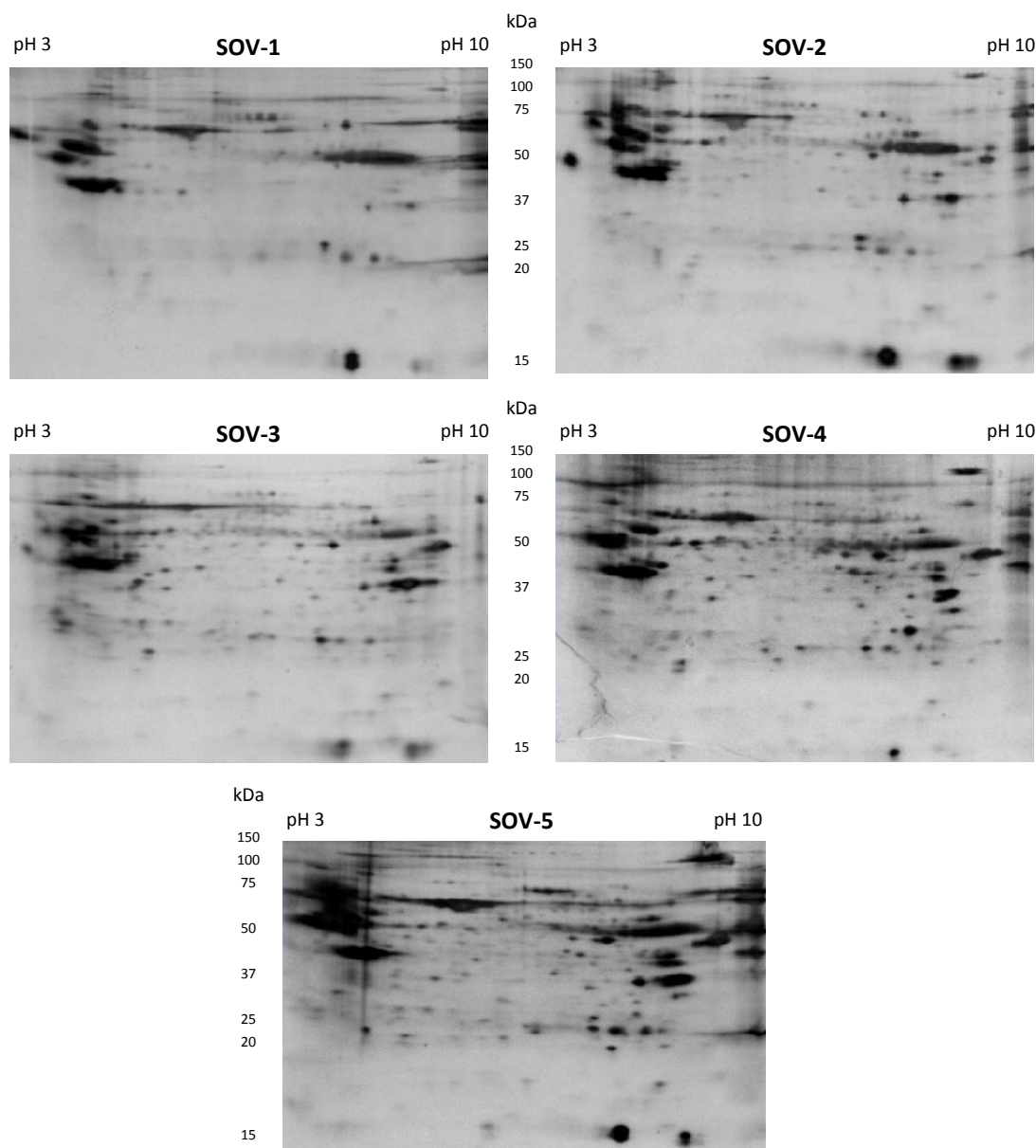


Figure 4.11 Representative 2D-PAGE silver stained gels of the five ovarian tissue biopsies. Proteins (approximately 50 µg) were separated on pH 3-10 non-linear 11 cm IPG strips in the first dimension (IEF) and by precast gels (Criterion TGX Precast Gels, any kD, IPG + 1 well comb, 11 cm IPG strip) in the second dimension (SDS-PAGE). Resulting gels were silver stained.

In all tissue gels represented in Figure 4.11 it is possible to visualise a vast number of well-resolved protein spots and the gel images show good quality overall, evidencing a successful separation of the tissue protein mixtures by 2D-PAGE.

As for the ovarian cancer cell line gels, all the tissue gels in Figure 4.11 display consistent horizontal streaking on the far left and right hand sides, as well as some

faint background vertical streaking. The reasons that could explain these effects were mentioned earlier. Nonetheless, when compared to the cell line gels as a whole, tissue gels display improved image quality, demonstrating a better technical control of the 2D-PAGE technique.

SOV-1 gel shows fewer spots than the other gels and this could have been due to a number of procedural errors, since the same amount of protein was loaded onto all gels. Proteins from SOV-1 tissue sample may have been unable to migrate into the IPG strip gel matrix during rehydration, because they were not adequately solubilised, owing to the reasons previously mentioned. Since SOV-1 and SOV-5 2D gels were run simultaneously and SOV-5 gel shows a greater number of spots, the problems in SOV-1 gel are most likely caused by inadequate rehydration, rather than IPG strip orientation or ineffective staining (Garfin and Heerdt, 2001, Rabilloud, 2000).

SOV-2 and SOV-3 gels depict a large number of clearly visible spots throughout the gels with some degree of streaking as previously described. These two gels look very similar, which is in line with the fact that they both result from serous epithelial ovarian cancer samples.

SOV-4 and SOV-5 gels also show a great number of well-resolved protein spots. These gels present a slightly darker background than the other gels and this may be due to an increased incubation time during the colour development step of the silver stain, which is a very precise technique.

SOV-5 gel displays the greatest degree of streaking of all tissue gels, which could be caused by the reasons previously given. Its spots also appear to show greater intensity than the other spots on the other gels, despite the same amount of protein being loaded onto all gels. This is most likely owing to the increased incubation time during the colour development step of the silver stain mentioned above.

As mentioned before for the cell line gels, the reproducibility of the technique should have been assessed by means of a statistical test to quantify the

similarity/difference between gels. If a greater amount of sample had been available for each one of the ovarian tissues analysed, all gels should have been repeated at least twice more, in order to increase reliability on the 2D gels obtained and evaluate the reproducibility of this experiment. This would be particularly advantageous for SOV-1 tissue sample, to allow better analysis and evaluation, as SOV-1 gel was the most defective of the gels.

4.4.2.3 Gel image analysis

After visual comparison of the 2D gels obtained for the PEO1 sensitive and resistant cell lines and for the ovarian tissues, gel images were analysed using PDQuest Advanced software and spots' presence and relative abundance was compared between gels. This would ultimately allow the study of differences in regulation of the proteins identified after this stage.

Spot intensity was the method of semi-quantitation (relative quantitation) used. This method compares the intensity of the spots in which a specific protein was identified among the different gels that correspond to different samples. The size (area and intensity) of protein spots changes in parallel with the expression level of proteins, thus 2D-PAGE can achieve quantitative comparison between multiple samples (Palagi et al., 2006).

The background was subtracted and resolved protein spots were located and quantified. The total gel image optical density (OD) and the total number of spots were used to normalise individual protein abundance, allowing the quantity of each protein to be defined as ppm of the total integrated OD. A master image containing a match-set of all the 2D gel images was created after constructing a reference pattern, and pattern matching was achieved by landmarking prominent protein spots represented in each gel pattern. This enabled qualitative and quantitative analysis of differentially expressed proteins through parameters set within the PDQuest software and fold changes (Bio-Rad, 2004).

For each gel obtained, more than 200 spots could be individually visualised. In order to facilitate analysis and focus on relevant proteins, spots were selected according to the following criteria: exclusive presence in only one gel, 2-fold and 5-fold change in intensity in at least one of the gels when compared to the others. Spots located in the same place on different gels were assigned the same SSP number, which is a unique sample spot protein number assigned by the PDQuest software.

In Figure 4.12, two examples of the spot selection process using PDQuest Advanced software are given. The histogram graphs can be used to quickly compare spot

quantity among gels. A brief look at a histogram can give a sense of the general trends in spot quantitation. They are also useful as tools for detecting problems such as mismatched spots and spots whose quantitation is suspiciously off the average.

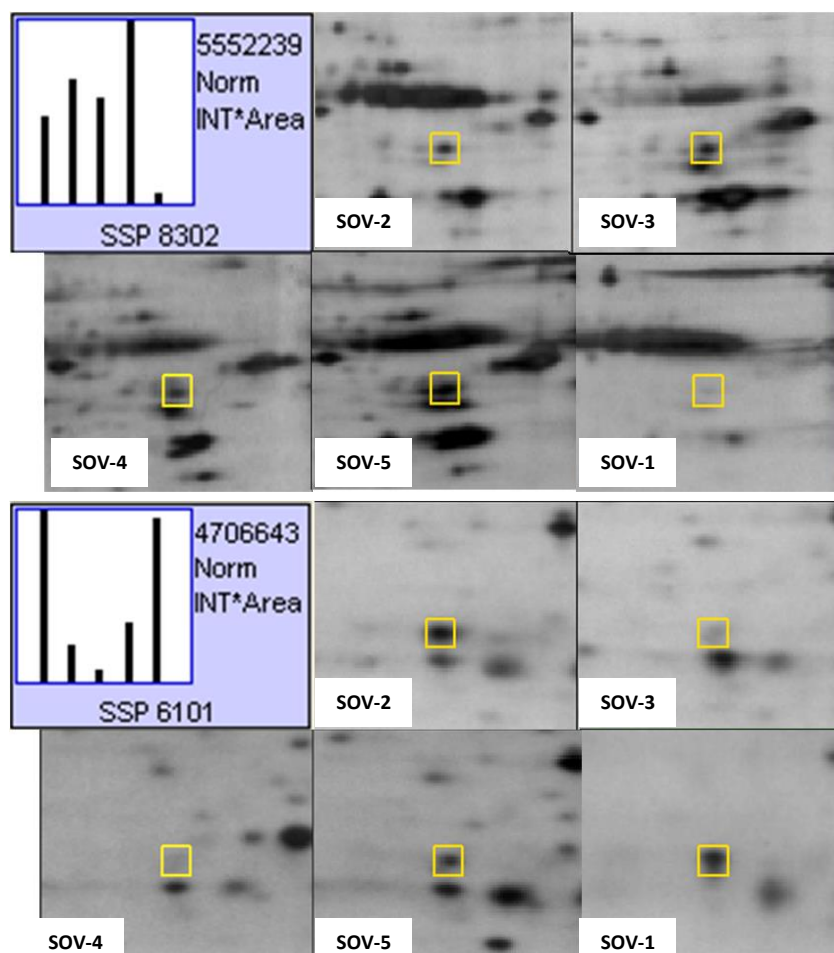


Figure 4.12 Examples of spot selection using PDQuest Advanced 8.0.1. Histograms on the upper left show quantity bars for the corresponding spot in each of the different gels, SOV-2/3/4/5/1 (bars from left to right).

Each bar on a spot histogram represents the spot's quantity in a gel. In Figure 4.12, the bars from the left to the right represent SOV-2/3/4/5/1 gels, respectively. The Standard Spot (SSP) number is displayed beneath the histogram. The number in the upper right of the histogram is the quantitation of the maximum bar in the graph. The other bars are drawn in proportion to the highest bar. The normalisation units are displayed below the maximum quantitation. Normalisation is a process by which quantitative data from different gels are adjusted so that different samples can be compared to one another (Bio-Rad, 2004).

4.4.2.3.1 Gel image analysis of the PEO1 cell lines

PDQuest software was not available when the first replicates of the cell line gels were analysed. Therefore, all well-resolved protein spots on those gels were excised for further analysis to avoid misjudging of spot intensity differences. For the second replicate, spot intensity analysis was performed for spot selection and only the spots that followed the selection criteria (exclusive presence, 2-fold and 5-fold change in intensity) were excised. Spots in the PEO1 sensitive and resistant cell line gels that were selected for excision and further analysis by LC-MS/MS with the aim of identifying the proteins are highlighted in Figure 4.13.

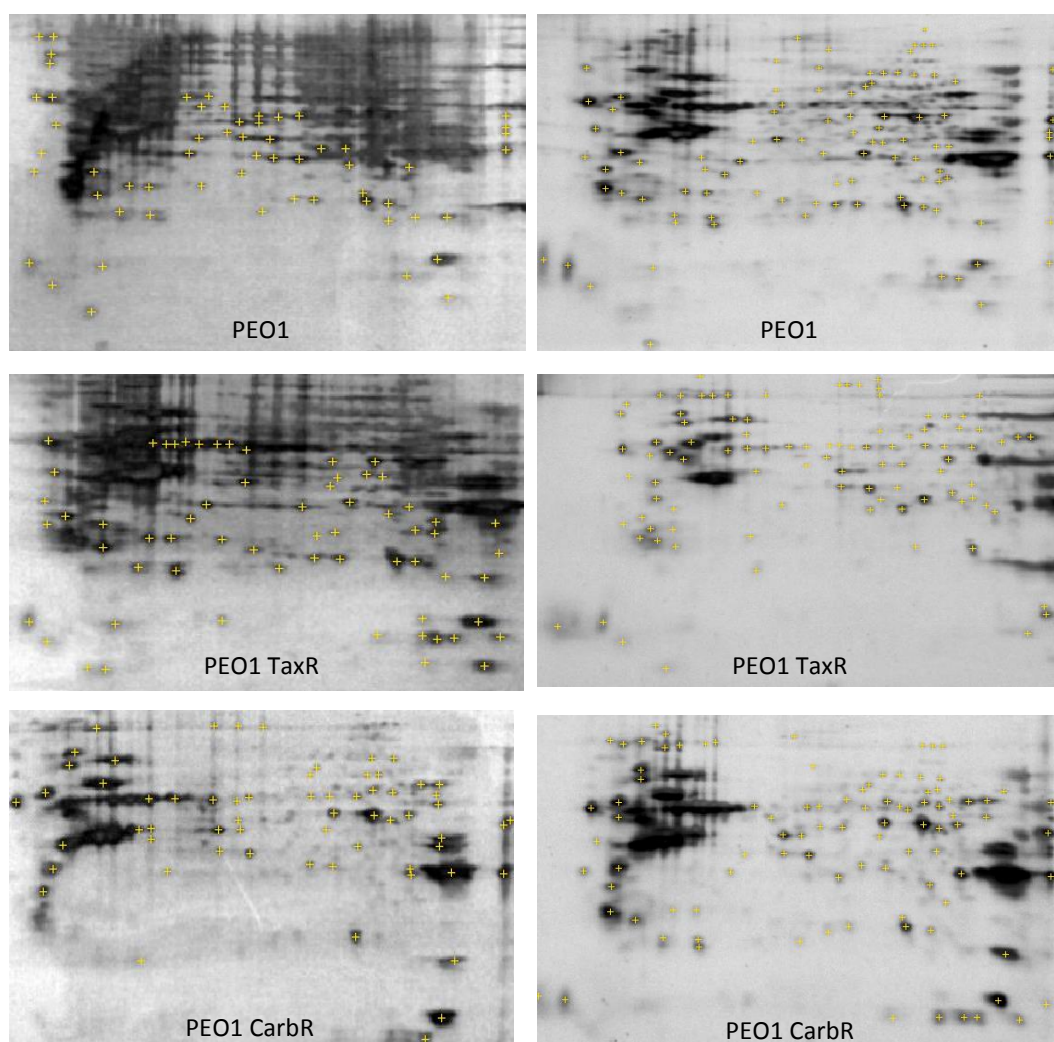


Figure 4.13 Spots in the ovarian cancer cell line gels that were selected for excision and further analysis by LC-MS/MS. All well-resolved protein spots on the first replicates (left) were excised for further analysis. For the second replicate, spot intensity analysis was performed for spot selection and only the spots that followed the selection criteria (exclusive presence, 2-fold and 5-fold change in intensity) were excised.

4.4.2.4 Selection of protein hits

Mass spectrometry data were used for the protein identification searches in two ways. Firstly, database searches were performed manually using two online search engines, MASCOT (Matrix Science) (Perkins et al., 1999) and X!Tandem (The GPM) (Craig and Beavis, 2004). In order to minimise the chances of false-positive identification of contaminant proteins, protein hits were accepted if:

MASCOT protein score > 100 and at least one of the theoretical MW and pI values matched the experimental value. Experimental MW and pI were estimated based on relative positions to MW markers and corresponding vertical alignment to pI values on 2D gels.

OR

MASCOT protein score < 100 and the theoretical MW and pI values were both similar to the experimental values.

OR

MASCOT protein score < 100 and at least one of the theoretical MW and pI values was similar to the experimental values.

AND

First hits in the MASCOT search result corresponded to the same first hits in the X!Tandem search results or the protein identified belonged to the same family (isoforms).

For all the selected protein hits Min # Peptides identified was ≥ 2 . This generated a focused list of 151 proteins reliably identified.

Secondly, searches and analysis were performed using Scaffold 3 (Proteome Software), and the criteria used for protein hit selection was: Min Peptide – 95 %, Min # Peptides – 2, Min Protein – 99 % and 1 % false discovery rate (FDR) (Keller et

al., 2002, Nesvizhskii et al., 2003). This search method resulted in a list of 189 proteins reliably identified.

In both sets of results, two very common contaminants abundantly seen in proteomics analysis were removed from the hits list of each spot – keratin and trypsin (Keller et al., 2008).

Two protein lists were then generated and checked for proteins that were present in both and proteins that were absent from one of the lists. A total of 25 proteins were found in the 151-manual-protein-list but not in the 189-Scaffold-3-protein-list (Figure 4.15). The majority of proteins missing from the 189-Scaffold-3-protein-list are proteins with low confidence identification (% coverage < 20), and/or they belong to the same family or are similar to the ones found in the mentioned list (isoforms). A total of 63 proteins were found in the 189-Scaffold-3-protein-list but not in the 151-manual-protein-list. The criteria used for accepting a protein hit in the manual searches case, which generated the 151-manual-protein-list, were stricter than the criteria used for the other list. In fact, most of those 63 missing proteins are indeed present in the data; however they were not selected, as they do not comply with the criteria previously mentioned.

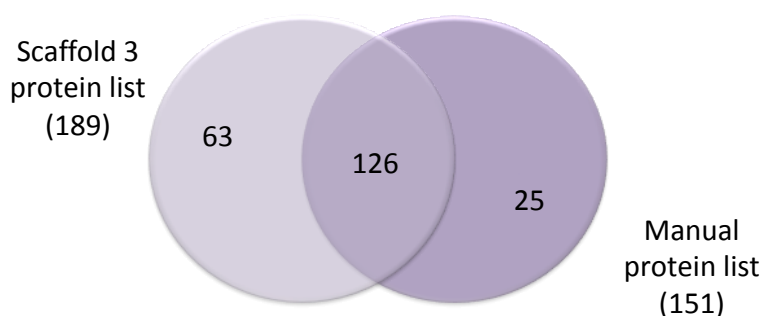


Figure 4.15 Venn diagram of the protein lists generated using the two protein database search approaches: manual search and Scaffold 3 software search.

For the above reasons, the list with more protein hits, 189-Scaffold-3-protein-list, was the one used for further analysis and is shown in Table 4.6.

Table 4.6 Proteins identified in the ovarian cancer cell lines (sensitive – PEO1 and resistant – PEO1 TaxR, PEO1 CarbR) and/or in the ovarian tissue biopsies (control – SOV-1 and cancer – SOV-2/3/4/5). Proteins shown in the table (189) were identified by LC-MS/MS after in-gel trypsin digestion of the selected protein spots. Criteria used for protein hit selection was Min Peptide – 95 %, Min # Peptides – 2, Min Protein – 99 % (Scaffold 3 Software, version 3.6.4). SSP, sample spot protein number; MW, molecular weight; pI, isoelectric point; N/A, not applicable; R, resistant; S, sensitive; P, partially resistant/sensitive.

Protein Name	Accession Number	MW (kDa)	pI	% Coverage									
				Ovarian Tissue Biopsies					Ovarian Cancer Cell Lines				
				N/A	R	S	P	P	S	R	R		
				SOV-1	SOV-2	SOV-3	SOV-4	SOV-5	PEO1	PEO1 TaxR	PEO1 CarbR		
14-3-3 protein beta/alpha	1433B_HUMAN	28	4.76									17%	
14-3-3 protein theta	1433T_HUMAN	28	4.68							4.90%	7.30%		
14-3-3 protein zeta/delta	1433Z_HUMAN	28	4.73							4.90%	17%		
26S protease regulatory subunit 4	PRS4_HUMAN	49	5.87							5.00%	2.70%	13%	
60 kDa heat shock protein, mitochondrial	CH60_HUMAN	61	5.24			9.90%	8.20%	16%			2.10%	36%	
60S acidic ribosomal protein P0	RLA0_HUMAN	34	5.7							23%	17%		
78 kDa glucose-regulated protein	GRP78_HUMAN	72	5.01										28%
Abhydrolase domain-containing protein 10, mitochondrial	ABHDA_HUMAN	34	6.29							8.50%			
Actin, cytoplasmic 1	ACTB_HUMAN	42	5.29			5.60%				14%	15%	16%	
Adenosylhomocysteinase	SAHH_HUMAN	48	5.92							2.50%		6.20%	
Adenylosuccinate synthetase isozyme 2	PURA2_HUMAN	50	6.13							4.80%			
Adenylyl cyclase-associated protein 1	CAP1_HUMAN	52	8.26										26%
ADP-sugar pyrophosphatase	NUDT5_HUMAN	24	4.87							12%			
A-kinase anchor protein 12	AKA12_HUMAN	191	4.37							1.50%			
Alcohol dehydrogenase 1B	ADH1B_HUMAN	40	8.63					6.10%					
Aldehyde dehydrogenase family 1	AL1A3_HUMAN	56	7.12										21%

Protein Name	Accession Number	MW (kDa)	pI	% Coverage									
				Ovarian Tissue Biopsies				Ovarian Cancer Cell Lines					
				N/A	R	S	P	P	S	R	R		
				SOV-1	SOV-2	SOV-3	SOV-4	SOV-5	PEO1	PEO1 TaxR	PEO1 CarbR		
member A3													
Aldehyde dehydrogenase X, mitochondrial	AL1B1_HUMAN	57	5.96										14%
Alpha-1-antichymotrypsin	AACT_HUMAN	48	5.32	4.50%									
Alpha-actinin-4	ACTN4_HUMAN	105	5.27										5.70%
Alpha-enolase	ENOA_HUMAN	47	6.99			6.20%	6.50%	9.20%	6.50%	35%	57%		
Annexin A1	ANXA1_HUMAN	39	6.64			3.20%	7.80%		29%	29%	44%		
Annexin A11	ANX11_HUMAN	54	7.53										5.00%
Annexin A2	ANXA2_HUMAN	39	7.56	17%	10%	17%	18%	42%		6.20%	39%		
Annexin A3	ANXA3_HUMAN	36	5.63							28%			
Annexin A5	ANXA5_HUMAN	36	4.93						14%	2.80%			
Apolipoprotein A-I	APOA1_HUMAN	31	5.27					9.40%					8.60%
Aspartate aminotransferase, mitochondrial	AATM_HUMAN	48	8.98						6.70%				
ATP synthase subunit alpha, mitochondrial	ATPA_HUMAN	60	8.28										29%
Bifunctional purine biosynthesis protein PURH	PUR9_HUMAN	65	6.27										9.00%
C-1-tetrahydrofolate synthase, cytoplasmic	C1TC_HUMAN	102	6.89										2.10%
Calreticulin	CALR_HUMAN	48	4.29						13%	18%	21%		
Calumenin	CALU_HUMAN	37	4.46						23%	13%			
Caprin-1	CAPR1_HUMAN	78	5.14										9.30%
Cathepsin D	CATD_HUMAN	45	5.6						4.60%	2.20%			

Protein Name	Accession Number	MW (kDa)	pI	% Coverage								
				Ovarian Tissue Biopsies					Ovarian Cancer Cell Lines			
				N/A	R	S	P	P	S	R	R	
				SOV-1	SOV-2	SOV-3	SOV-4	SOV-5	PEO1	PEO1 TaxR	PEO1 CarbR	
Chloride intracellular channel protein 4	CLIC4_HUMAN	29	5.45							13%	6.30%	
Cofilin-1	COF1_HUMAN	19	8.26							26%	18%	36%
Coiled-coil-helix-coiled-coil-helix domain-containing protein 3, mitochondrial	CHCH3_HUMAN	26	8.5								8.40%	
Complement component 1 Q subcomponent-binding protein, mitochondrial	C1QBP_HUMAN	31	4.32							5.00%	5.00%	
Cytosol aminopeptidase	AMPL_HUMAN	56	8.03									27%
D-3-phosphoglycerate dehydrogenase	SERA_HUMAN	57	6.31									12%
Delta(3,5)-Delta(2,4)-dienoyl-CoA isomerase, mitochondrial	ECH1_HUMAN	36	5.99								7.60%	
Desmoplakin	DESP_HUMAN	250	6.44							0.80%		
Dihydrolipoylysine-residue succinyltransferase component of 2-oxoglutarate dehydrogenase complex, mitochondrial	ODO2_HUMAN	49	5.9							6.80%	3.10%	7.30%
DnaJ homolog subfamily C member 9	DNJC9_HUMAN	30	5.58								13%	
EF-hand domain-containing protein D2	EFHD2_HUMAN	27	5.15							22%		
Elongation factor 1-alpha 1	EF1A1_HUMAN	50	9.1		2.40%	5.00%	5.00%	12%		5.80%		8.40%
Elongation factor 1-delta	EF1D_HUMAN	31	4.9							8.50%		12%
Elongation factor 1-gamma	EF1G_HUMAN	50	6.27							7.60%		
Elongation factor Tu, mitochondrial	EFTU_HUMAN	50	6.31			2.70%	5.80%	2.70%			20%	24%
Endoplasmic	ENPL_HUMAN	92	4.73									4.40%

Protein Name	Accession Number	MW (kDa)	pI	% Coverage								
				Ovarian Tissue Biopsies					Ovarian Cancer Cell Lines			
				N/A	R	S	P	P	S	R	R	
				SOV-1	SOV-2	SOV-3	SOV-4	SOV-5	PEO1	PEO1 TaxR	PEO1 CarbR	
Enoyl-CoA hydratase, mitochondrial	ECHM_HUMAN	31	5.88								15%	
Eukaryotic initiation factor 4A-I	IF4A1_HUMAN	46	5.32							2.50%		11%
Eukaryotic translation initiation factor 5A-1	IF5A1_HUMAN	17	5.08							26%		
F-actin-capping protein subunit beta	CAPZB_HUMAN	31	5.36								14%	
Far upstream element-binding protein 1	FUBP1_HUMAN	68	7.33									20%
Fatty acid-binding protein, epidermal	FABP5_HUMAN	15	6.82	26%						6.70%	24%	
Fructose-bisphosphate aldolase A	ALDOA_HUMAN	39	8.39			6.90%	6.90%	19%		3.80%		36%
Fumarate hydratase, mitochondrial	FUMH_HUMAN	55	6.99									11%
Galectin-1	LEG1_HUMAN	15	5.3							5.90%	21%	
Galectin-7	LEG7_HUMAN	15	7.02	12%						10%	22%	
GIPC PDZ domain containing family, member 1	GIPC1_HUMAN	36	5.9							11%		
Glucosidase 2 subunit beta	GLU2B_HUMAN	59	4.33							18%		
Glutathione S-transferase omega-1	GSTO1_HUMAN	28	6.23							17%	14%	
Glutathione S-transferase P	GSTP1_HUMAN	23	5.44					9.00%		15%	15%	
Glyceraldehyde-3-phosphate dehydrogenase	G3P_HUMAN	36	8.58	8.70%	14%	13%	14%	27%	8.70%	8.70%	8.70%	50%
G-rich sequence factor 1	GRSF1_HUMAN	53	5.11								4.00%	
GTP-binding nuclear protein Ran	RAN_HUMAN	24	7.2							10%	6.00%	
Guanine nucleotide-binding protein subunit beta-2-like 1	GBLP_HUMAN	35	7.6							8.50%	35%	

Protein Name	Accession Number	MW (kDa)	pI	% Coverage														
				Ovarian Tissue Biopsies					Ovarian Cancer Cell Lines									
				N/A	R	S	P	P	S	R	R							
				SOV-1	SOV-2	SOV-3	SOV-4	SOV-5	PEO1	PEO1 TaxR	PEO1 CarbR							
Heat shock 70 kDa protein 1A/1B	HSP71_HUMAN	70	5.48															14%
Heat shock cognate 71 kDa protein	HSP7C_HUMAN	71	5.37															39%
Heat shock protein beta-1	HSPB1_HUMAN	23	5.98															8.80%
Hemoglobin subunit beta	HBB_HUMAN	16	6.81	67%	46%	8.80%	8.80%	51%	28%									
Heterogeneous nuclear ribonucleoprotein D0	HNRPD_HUMAN	38	7.61							2.80%								6.80%
Heterogeneous nuclear ribonucleoprotein F	HNRPF_HUMAN	46	5.37															6.50%
Heterogeneous nuclear ribonucleoprotein H	HNRH1_HUMAN	49	5.89							28%	13%							6.00%
Heterogeneous nuclear ribonucleoprotein H3	HNRH3_HUMAN	38	6.37							8.40%	2.60%							3.50%
Heterogeneous nuclear ribonucleoprotein K	HNRPK_HUMAN	51	5.39				2.60%			8.90%	13%							37%
Heterogeneous nuclear ribonucleoprotein L	HNRPL_HUMAN	64	8.46															15%
Heterogeneous nuclear ribonucleoprotein Q	HNRPQ_HUMAN	70	8.68							11%								
Heterogeneous nuclear ribonucleoproteins A2/B1	ROA2_HUMAN	37	8.97				7.40%			9.90%								22%
Heterogeneous nuclear ribonucleoproteins C1/C2	HNRPC_HUMAN	34	4.95							13%	2.90%							10%
High mobility group nucleosome-binding domain-containing protein 5	HMG5_HUMAN	32	4.5							3.50%	1.60%							4.10%

Protein Name	Accession Number	MW (kDa)	pI	% Coverage							
				Ovarian Tissue Biopsies					Ovarian Cancer Cell Lines		
				N/A	R	S	P	P	S	R	R
				SOV-1	SOV-2	SOV-3	SOV-4	SOV-5	PEO1	PEO1 TaxR	PEO1 CarbR
Histidine-tRNA ligase, cytoplasmic	SYHC_HUMAN	57	5.73						14%	7.10%	19%
Histone H2B type 1-M	H2B1M_HUMAN	14	10.32								6.70%
Hypoxanthine-guanine phosphoribosyltransferase	HPRT_HUMAN	25	6.24						12%	17%	
Ig gamma-1 chain C region	IGHG1_HUMAN	36	8.46	8.80%						13%	
Inosine-5'-monophosphate dehydrogenase 2	IMDH2_HUMAN	56	6.46								7.80%
Isoform 2 of Shootin-1	A0MZ66-2 SHOT1_HUMAN	53	5.27								4.60%
Lactoylglutathione lyase	LGUL_HUMAN	21	5.12						14%	16%	
Lamin-B1	LMNB1_HUMAN	66	5.11								7.80%
Leukocyte elastase inhibitor	ILEU_HUMAN	43	5.9							10%	
LIM and SH3 domain protein 1	LASP1_HUMAN	30	6.61								8.80%
L-lactate dehydrogenase A chain	LDHA_HUMAN	37	8.46								30%
L-lactate dehydrogenase B chain	LDHB_HUMAN	37	5.72						15%	43%	20%
Macrophage-capping protein	CAPG_HUMAN	38	5.82						14%	8.00%	3.70%
Malate dehydrogenase, cytoplasmic	MDHC_HUMAN	36	6.89							8.70%	
Malate dehydrogenase, mitochondrial	MDHM_HUMAN	36	8.54			13%		16%	5.60%		19%
Microtubule-associated protein 4	MAP4_HUMAN	121	5.32						3.40%		
Microtubule-associated protein RP/EB family member 1	MARE1_HUMAN	30	5.02						10%		

Protein Name	Accession Number	MW (kDa)	pI	% Coverage								
				Ovarian Tissue Biopsies					Ovarian Cancer Cell Lines			
				N/A	R	S	P	P	S	R	R	
				SOV-1	SOV-2	SOV-3	SOV-4	SOV-5	PEO1	PEO1 TaxR	PEO1 CarbR	
Myosin light polypeptide 6	MYL6_HUMAN	17	4.56						21%	22%		
Myristoylated alanine-rich C-kinase substrate	MARCS_HUMAN	32	4.46						19%			
Nascent polypeptide-associated complex subunit alpha	NACA_HUMAN	23	4.52						13%	26%		
Neutral alpha-glucosidase AB	GANAB_HUMAN	107	5.58									3.50%
Nitrilase homolog 1	NIT1_HUMAN	36	7.91							6.40%		
Nuclear autoantigenic sperm protein	NASP_HUMAN	85	4.26									2.30%
Nucleolin	NUCL_HUMAN	77	4.6							1.30%	5.90%	
Nucleophosmin	NPM_HUMAN	33	4.64							3.10%	29%	
Nucleoporin p54	NUP54_HUMAN	55	6.53									5.70%
Nucleoside diphosphate kinase A	NDKA_HUMAN	17	5.82							47%		
Nucleosome assembly protein 1-like 1	NP1L1_HUMAN	45	4.34						5.60%	2.60%	5.40%	
Paraspeckle component 1	PSPC1_HUMAN	59	6.26									7.50%
PDZ and LIM domain protein 1	PDLI1_HUMAN	36	6.55									39%
Peptidyl-prolyl cis-trans isomerase A	PPIA_HUMAN	18	7.68						33%	28%	45%	
Peptidyl-prolyl cis-trans isomerase FKBP4	FKBP4_HUMAN	52	5.35							17%		
Peroxiredoxin-1	PRDX1_HUMAN	22	8.27					5.50%	11%	18%	22%	
Peroxiredoxin-2	PRDX2_HUMAN	22	5.67		9.10%		9.10%	9.10%	19%	19%	15%	
Peroxiredoxin-5, mitochondrial	PRDX5_HUMAN	22	6.73							8.90%		
Peroxiredoxin-6	PRDX6_HUMAN	25	6.02						8.50%	31%		

Protein Name	Accession Number	MW (kDa)	pI	% Coverage							
				Ovarian Tissue Biopsies					Ovarian Cancer Cell Lines		
				N/A	R	S	P	P	S	R	R
				SOV-1	SOV-2	SOV-3	SOV-4	SOV-5	PEO1	PEO1 TaxR	PEO1 CarbR
Phosphoglycerate kinase 1	PGK1_HUMAN	45	8.3			12%	3.60%	20%	12%		34%
Phosphoglycerate mutase 1	PGAM1_HUMAN	29	6.75						27%	7.10%	13%
Platelet-activating factor acetylhydrolase IB subunit gamma	PA1B3_HUMAN	26	6.33						7.80%	7.40%	
Poly(rC)-binding protein 1	PCBP1_HUMAN	37	6.66							3.10%	11%
Poly(rC)-binding protein 2	PCBP2_HUMAN	39	6.33							9.90%	
Polymerase I and transcript release factor	PTRF_HUMAN	43	5.5							6.70%	
Prelamin-A/C	LMNA_HUMAN	74	6.57								16%
Profilin-1	PROF1_HUMAN	15	8.47						20%	53%	
Prohibitin	PHB_HUMAN	30	5.57						34%	11%	
Prohibitin-2	PHB2_HUMAN	33	9.83						7.70%		
Proliferating cell nuclear antigen	PCNA_HUMAN	29	4.57							29%	12%
Proliferation-associated protein 2G4	PA2G4_HUMAN	44	6.12						8.40%		3.00%
Proteasome subunit alpha type-1	PSA1_HUMAN	30	6.15							16%	
Proteasome subunit alpha type-3	PSA3_HUMAN	28	5.19						7.50%	4.70%	
Proteasome subunit alpha type-6	PSA6_HUMAN	27	6.34						14%	12%	
Proteasome subunit alpha type-7	PSA7_HUMAN	28	8.6							27%	
Proteasome subunit beta type-3	PSB3_HUMAN	23	6.12						7.80%	4.40%	
Proteasome subunit beta type-6	PSB6_HUMAN	25	4.91							13%	
Proteasome subunit beta type-7	PSB7_HUMAN	30	5.61						7.90%	7.20%	
Protein disulfide-isomerase	PDIA1_HUMAN	57	4.69								29%

Protein Name	Accession Number	MW (kDa)	pI	% Coverage							
				Ovarian Tissue Biopsies					Ovarian Cancer Cell Lines		
				N/A	R	S	P	P	S	R	R
				SOV-1	SOV-2	SOV-3	SOV-4	SOV-5	PEO1	PEO1 TaxR	PEO1 CarbR
Protein disulfide-isomerase A3	PDIA3_HUMAN	57	5.61			2.20%		6.90%	14%	21%	29%
Protein DJ-1	PARK7_HUMAN	20	6.32						9.00%	16%	
Protein S100-A7	S10A7_HUMAN	11	6.26	38%			20%	11%	11%	11%	
Protein S100-A8	S10A8_HUMAN	11	6.5	12%					25%	31%	12%
Protein S100-A9	S10A9_HUMAN	13	5.71	13%			25%		45%	31%	28%
Protein SET	SET_HUMAN	33	4.22						7.20%	3.80%	
Purine nucleoside phosphorylase	PNPH_HUMAN	32	6.45							9.70%	
Pyruvate kinase isozymes M1/M2	KPYM_HUMAN	58	7.95								54%
Ran-specific GTPase-activating protein	RANG_HUMAN	23	5.19						11%	5.50%	
Rho GDP-dissociation inhibitor 1	GDIR1_HUMAN	23	5.01						22%	18%	
Serine hydroxymethyltransferase, mitochondrial	GLYM_HUMAN	56	8.11								20%
Serine protease HTRA2, mitochondrial	HTRA2_HUMAN	49	6.12						9.80%		
Serine/arginine-rich splicing factor 1	SRSF1_HUMAN	28	10.37						9.30%	4.80%	
Serpin B3	SPB3_HUMAN	45	6.35	6.90%					9.50%	5.10%	
Serpin B4	SPB4_HUMAN	45	5.86	6.90%					6.90%	9.70%	
Serpin B5	SPB5_HUMAN	42	5.72						2.40%	5.60%	
Serum albumin	ALBU_HUMAN	69	5.67	2.50%	2.30%	2.30%	5.90%	2.50%	4.90%	7.40%	9.00%
Serum deprivation-response protein	SDPR_HUMAN	47	5.14								7.10%
Single-stranded DNA-binding protein, mitochondrial	SSBP_HUMAN	17	8.24						16%		

Protein Name	Accession Number	MW (kDa)	pI	% Coverage									
				Ovarian Tissue Biopsies				Ovarian Cancer Cell Lines					
				N/A	R	S	P	P	S	R	R		
				SOV-1	SOV-2	SOV-3	SOV-4	SOV-5	PEO1	PEO1 TaxR	PEO1 CarbR		
Stress-70 protein, mitochondrial	GRP75_HUMAN	74	5.44				3.70%						18%
Stress-induced-phosphoprotein 1	STIP1_HUMAN	63	6.4										18%
Superoxide dismutase [Mn], mitochondrial	SODM_HUMAN	25	6.86					17%	10%				
T-complex protein 1 subunit beta	TCPB_HUMAN	57	6.02										5.80%
T-complex protein 1 subunit eta	TCPH_HUMAN	59	7.55										16%
T-complex protein 1 subunit theta	TCPQ_HUMAN	60	5.41									1.80%	5.80%
Thioredoxin	THIO_HUMAN	12	4.82							12%	21%		
Thymidylate kinase	KTHY_HUMAN	24	8.43									14%	5.20%
Transgelin-2	TAGL2_HUMAN	22	8.45							6.00%			31%
Transitional endoplasmic reticulum ATPase	TERA_HUMAN	89	5.14										28%
Translationally-controlled tumor protein	TCTP_HUMAN	20	4.84									22%	
Trifunctional enzyme subunit beta, mitochondrial	ECHB_HUMAN	51	9.24				2.70%	6.10%					
Triosephosphate isomerase	TPIS_HUMAN	31	5.65			10%	23%	29%	40%	51%	53%		
tRNA-splicing ligase RtcB homolog	RTCB_HUMAN	55	6.77										5.00%
Tropomyosin alpha-1 chain	TPM1_HUMAN	33	4.69									3.50%	19%
Tropomyosin alpha-3 chain	TPM3_HUMAN	33	4.68									12%	
Tryptophan-tRNA ligase, cytoplasmic	SYWC_HUMAN	53	5.83										5.70%
Tubulin alpha-1A chain	TBA1A_HUMAN	50	4.94							7.30%	25%	14%	
Tubulin alpha-1B chain	TBA1B_HUMAN	50	4.94								31%	20%	

Protein Name	Accession Number	MW (kDa)	pI	% Coverage								
				Ovarian Tissue Biopsies					Ovarian Cancer Cell Lines			
				N/A	R	S	P	P	S	R	R	
				SOV-1	SOV-2	SOV-3	SOV-4	SOV-5	PEO1	PEO1 TaxR	PEO1 CarbR	
Tubulin alpha-4A chain	TBA4A_HUMAN	50	4.93								29%	20%
Tubulin beta chain	TBB5_HUMAN	50	4.78							4.30%	30%	17%
Tubulin beta-6 chain	TBB6_HUMAN	50	4.77								15%	
Ubiquitin-conjugating enzyme E2 K	UBE2K_HUMAN	22	5.33							24%	5.00%	
Ubiquitin-conjugating enzyme E2 variant 2	UB2V2_HUMAN	16	8.05							6.90%	13%	6.90%
UDP-glucose 6-dehydrogenase	UGDH_HUMAN	55	6.73									4.00%
UMP-CMP kinase	KCY_HUMAN	22	5.44							11%	6.60%	
Uroporphyrinogen decarboxylase	DCUP_HUMAN	41	5.77							12%		
UV excision repair protein RAD23 homolog B	RD23B_HUMAN	43	4.77							2.20%	2.20%	20%
Vimentin	VIME_HUMAN	54	5.05							2.40%	15%	5.20%
Voltage-dependent anion-selective channel protein 1	VDAC1_HUMAN	31	8.63				11%	4.20%				
Voltage-dependent anion-selective channel protein 2	VDAC2_HUMAN	32	7.66							12%	22%	
Xaa-Pro dipeptidase	PEPD_HUMAN	55	5.64							1.80%	7.10%	7.10%

A common observation in 2D-PAGE separations is the presence of a protein in more than one spot of the same 2D gel. In this study, this was no exception, as it was observed that several of the proteins shown in Table 4.6 were identified in a few spots belonging to the same gel. Two examples of this are illustrated in Figure 4.16.

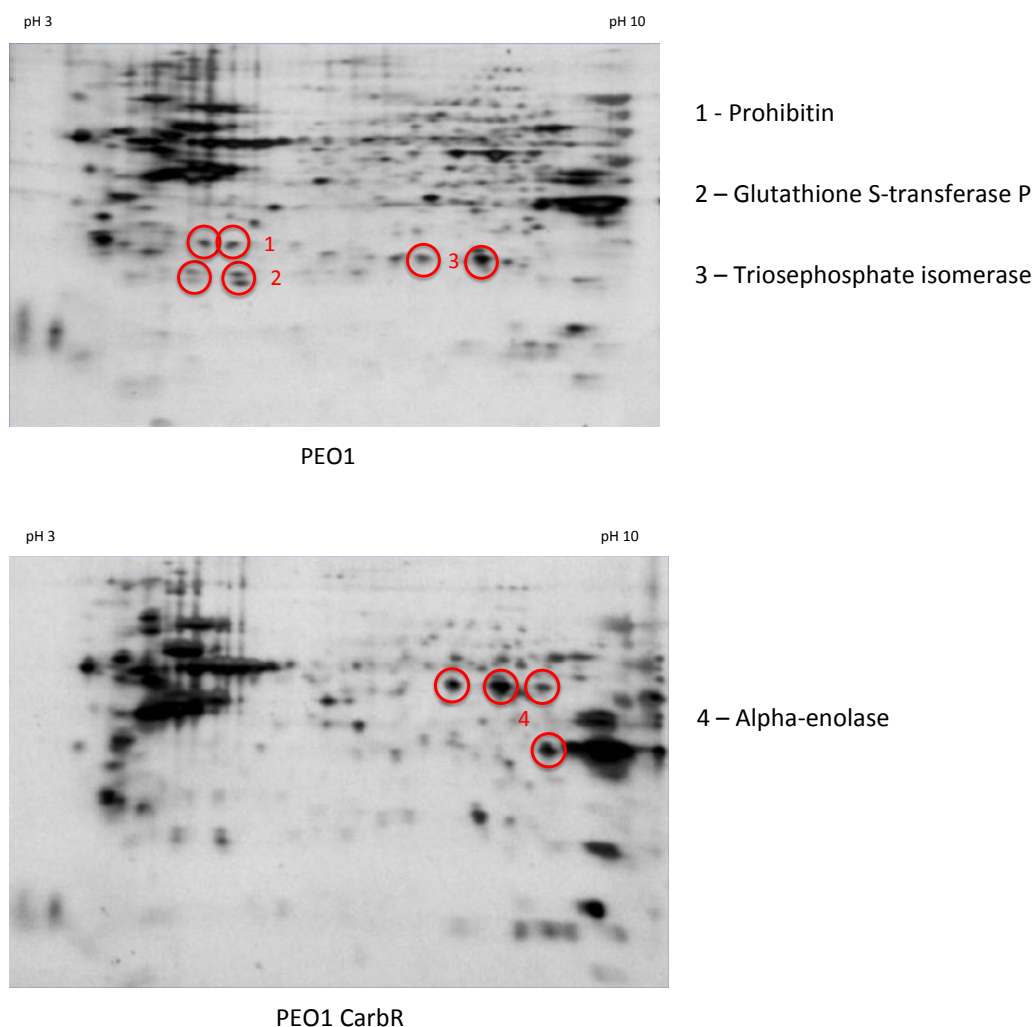


Figure 4.16 Examples of proteins that were identified in more than one spot on the same gel and the respective spots where they were identified.

Identification of a single protein in different spots of the same gel might be a result of cross-contamination (handling errors, very abundant protein that binds to other proteins, carry over during LC-MS/MS run); poor gel resolution resulting from inefficient separation of the protein mixture; or post-translational modifications,

which might change the MW (for example glycosylation) and/or pI (for example phosphorylation) of the proteins, as explained in Chapter 3. Further studies would be necessary in order to investigate the cause of this problem.

To avoid errors in the interpretation of spot intensity data, which would influence the analysis of differences in protein expression between distinct samples, spot intensity was studied using two different approaches. Firstly, considering the spot position on the gel, where only spots located in the same position on different gels, in which a certain protein was identified, were used for quantitative purposes. Theoretically, spots located in the same place on different gels correspond to the same protein and are given the same SSP number. In this case, only spots with the same SSP number were compared between samples.

Secondly, ignoring the spot position on the gel, where all the spots on one gel, in which a certain protein was identified, were considered for quantitation purposes. In this case, the total presence of a protein in a gel or sample was considered as a sum of the intensities of all the spots in which this protein was identified. The total intensity values were then compared between samples.

With the aim of identifying differentially expressed proteins that could possibly be related to resistance, for either of the semi-quantitative approaches described, fold regulation was calculated for each protein using the corresponding spot intensity data as follows:

$$\frac{\text{Quantity value of the spot/protein in the resistant sample}}{\text{Quantity value of the spot/protein in the sensitive (control) sample}}$$

Five results were possible:

Fold regulation = -1000 (or 0) – not found in the resistant sample considered

Fold regulation < 0 (or >0, <1) – down-regulated in the resistant sample

Fold regulation = 1 – no change in expression or not found in any of the samples considered

Fold regulation > 1 – up-regulated in the resistant sample

Fold regulation = +1000 – not found in the sensitive sample

Fold regulation was validated by confirmation with the gel images. As an example, for a protein identified in the three cell line samples, if that protein was up-regulated in the resistant cell lines (TaxR and CarbR), then the corresponding spots on the resistant gels should be more intense than the one on the sensitive gel. Nevertheless, for proteins that were identified in many spots on the same gel/sample, this confirmation was not possible.

Table 4.7 shows the number of up-regulated, down-regulated and unchanged/inexistent proteins in the resistant samples, when compared to the sensitive samples, for the cell line and tissue proteins. This determination was done using spot intensity data considering and ignoring the spot position on the gel.

Table 4.7 Protein fold regulation using two methods of spot intensity analysis. Spot intensities considering and ignoring the spot position on the gel were used to determine the number of up-regulated, down-regulated and unchanged/inexistent proteins in the resistant samples, when compared to the sensitive samples.

Fold Regulation		Considering Spot Position			Ignoring Spot Position		
		TaxR/ Sens	CarbR/ Sens	SOV-2/ SOV-3	TaxR/ Sens	CarbR/ Sens	SOV-2/ SOV-3
Not found in resistant	-1000	33	63	10	31	59	10
Down-regulated in resistant	< 0	5	6	2	6	7	4
No change/Not found	1	42	24	21	42	24	21
Up-regulated in resistant	> 1	65	34	3	69	40	1
Not found in sensitive	+1000	40	58	2	37	55	2
Total		185	185	38	185	185	38

Regarding the tissue samples, SOV-1, SOV-4 and SOV-5 were not used in the primary analysis of protein targets of resistance owing to the fact that SOV-1 was a non-cancerous sample, and SOV-4 and SOV-5 were described as partially

resistant/sensitive, which would make them less suitable for comparison with the resistant cell lines.

Proteins in the cell line and tissue samples that were found differentially regulated, or only present in the sensitive or resistant samples were the possible targets of resistance to chemotherapy. Therefore, those were the proteins further analysed.

Proteins that were reported as 'not found' in one or more of the samples might have been missed, because the gel was not excised in that specific place (not a well resolved spot, smearing/streaking area), or they were not present in a high enough concentration for the mass spectrometer to detect them. However, this does not mean that these proteins were not present in the sample at all.

Despite not hugely significant, there were a few differences in the number of up-regulated, down-regulated and not found proteins when spot intensity was calculated considering or ignoring the spot position on the gel. This was only observed for the proteins that were identified in more than one spot. One way of overcoming this problem would be to analyse more replicates of the same sample, to check if the same proteins would be identified in more than one spot and decide upon the best method to calculate their fold regulation. As in this study it was not possible to analyse more replicates, another method of validation for the protein identification and fold regulation would be needed.

A literature review on proteins reported with an association with ovarian cancer or ovarian cancer resistance was performed. The information collected was compared to the identifications and fold regulation data obtained for the proteins in this study. A summary of the literature review can be found in Table 4.8.

Table 4.8 Results of a literature review on proteins reported with an association with ovarian cancer or ovarian cancer resistance. The information collected was compared to the identifications and fold regulation data obtained for the proteins in this study.

Protein Accession Number	SwissProt ID	References					
		Up-regulated in ovarian cancer			Down-regulated in ovarian cancer		
		TaxR Cells	CarbR Cells	Tissue	TaxR Cells	CarbR Cells	Tissue
1433B_HUMAN	P31946						4*
1433T_HUMAN	P27348					4	
1433Z_HUMAN	P63104		4	9			
PRS4_HUMAN	P62191	10*	4		10*	4	
CH60_HUMAN	P10809	10	1, 4*	11*			
RLA0_HUMAN	P05388				10*		
GRP78_HUMAN	P11021			9		4*	
ABHDA_HUMAN	Q9NUJ1						
ACTB_HUMAN	P60709	10	1				5*, 6
SAHH_HUMAN	P23526						
PURA2_HUMAN	P30520						
CAP1_HUMAN	Q01518		4				
NUDT5_HUMAN	Q9UKK9						
AKA12_HUMAN	Q02952						
ADH1B_HUMAN	P00325						11*
AL1A3_HUMAN	P47895	10*					
AL1B1_HUMAN	P30837						
AACT_HUMAN	P01011						
ACTN4_HUMAN	O43707		4*			4*	
ENOA_HUMAN	P06733	10	1, 4*	11*		1, 4*	
ANXA1_HUMAN	P04083		4				
ANX11_HUMAN	P50995				10	4	
ANXA2_HUMAN	P07355		1				11
ANXA3_HUMAN	P12429						
ANXA5_HUMAN	P08758		4				11
APOA1_HUMAN	P02647			6*, 9			5*, 11
AATM_HUMAN	P00505	10					
ATPA_HUMAN	P25705	10*					
PUR9_HUMAN	P31939						
C1TC_HUMAN	P11586						
CALR_HUMAN	P27797			11			
CALU_HUMAN	O43852						
CAPR1_HUMAN	Q14444						
CATD_HUMAN	P07339	10		11*		4*	9
CLIC4_HUMAN	Q9Y696		1*				
COF1_HUMAN	P23528			11			
CHCH3_HUMAN	Q9NX63						
C1QBP_HUMAN	Q07021	10		9*, 11*			9*, 11*
AMPL_HUMAN	P28838			11*			
SERA_HUMAN	O43175					4	
ECH1_HUMAN	Q13011						
DESP_HUMAN	P15924						
ODO2_HUMAN	P36957	10*					
DNJC9_HUMAN	Q8WXX5	10*	4*				
EFHD2_HUMAN	Q96C19						
EF1A1_HUMAN	P68104		4	11			
EF1D_HUMAN	P29692			11*	10*		
EF1G_HUMAN	P26641						
EFTU_HUMAN	P49411			11			
ENPL_HUMAN	P14625	10					
ECHM_HUMAN	P30084	10					

Protein Accession Number	SwissProt ID	References					
		Up-regulated in ovarian cancer			Down-regulated in ovarian cancer		
		TaxR Cells	CarbR Cells	Tissue	TaxR Cells	CarbR Cells	Tissue
IF4A1_HUMAN	P60842		4				
IF5A1_HUMAN	P63241	10*			10*	4*	
CAPZB_HUMAN	P47756						
FUBP1_HUMAN	Q96AE4		1			1	
FABP5_HUMAN	Q01469			11			
ALDOA_HUMAN	P04075			9			
FUMH_HUMAN	P07954						
LEG1_HUMAN	P09382		4				11
LEG7_HUMAN	P47929		1				
GIPC1_HUMAN	Q14908						
GLU2B_HUMAN	P14314		4			4	
GSTO1_HUMAN	P78417						11*
GSTP1_HUMAN	P09211				10		
G3P_HUMAN	P04406			9, 11			
GRSF1_HUMAN	Q12849						
RAN_HUMAN	P62826						
GBLP_HUMAN	P63244	10*	1*			1*	
HSP71_HUMAN	P08107		4		10*	1, 4	11*
HSP7C_HUMAN	P11142		4	11*		4	
HSPB1_HUMAN	P04792		4			4	
HBB_HUMAN	P68871	10*					5*, 11
HNRPD_HUMAN	Q14103						11*
HNRPF_HUMAN	P52597						
HNRH1_HUMAN	P31943					1	
HNRH3_HUMAN	P31942	10					
HNRPK_HUMAN	P61978		4			4	
HNRPL_HUMAN	P14866						
HNRPQ_HUMAN	O60506						
ROA2_HUMAN	P22626		1*, 4*	11*	10*	4*	11*
HNRPC_HUMAN	P07910						
HMGNS5_HUMAN	P82970						11*
SYHC_HUMAN	P12081						
H2B1M_HUMAN	Q99879	10*	4*			4*	11*
HPRT_HUMAN	P00492						
IGHG1_HUMAN	P01857						
IMDH2_HUMAN	P12268						
SHOT1_HUMAN	A0MZ66						
LGUL_HUMAN	Q04760						11
LMNB1_HUMAN	P20700		1*			4	11*
ILEU_HUMAN	P30740						
LASP1_HUMAN	Q14847				10	1	
LDHA_HUMAN	P00338		1	11*		1	
LDHB_HUMAN	P07195			11			
CAPG_HUMAN	P40121						
MDHC_HUMAN	P40925					4	
MDHM_HUMAN	P40926	10					
MAP4_HUMAN	P27816		1*		10*		
MARE1_HUMAN	Q15691				10		
MYL6_HUMAN	P60660		4*		10*		5*, 11*
MARCS_HUMAN	P29966						
NACA_HUMAN	Q13765						
GANAB_HUMAN	Q14697						
NIT1_HUMAN	Q86X76						
NASP_HUMAN	P49321					1*	
NUCL_HUMAN	P19338						
NPM_HUMAN	P06748		4	11*		4	
NUP54_HUMAN	Q7Z3B4		1			1	
NDKA_HUMAN	P15531		4			4	
NP1L1_HUMAN	P55209		4*			4*	

Protein Accession Number	SwissProt ID	References					
		Up-regulated in ovarian cancer			Down-regulated in ovarian cancer		
		TaxR Cells	CarbR Cells	Tissue	TaxR Cells	CarbR Cells	Tissue
PSPC1_HUMAN	Q8WXF1						
PDL1_HUMAN	O00151						
PPIA_HUMAN	P62937	10*			10*	4	
FKBP4_HUMAN	Q02790	10*				4*	
PRDX1_HUMAN	Q06830				10		
PRDX2_HUMAN	P32119			9			
PRDX5_HUMAN	P30044	10*					
PRDX6_HUMAN	P30041						
PGK1_HUMAN	P00558					1, 4	
PGAM1_HUMAN	P18669				10		
PA1B3_HUMAN	Q15102				10		
PCBP1_HUMAN	Q15365			11			
PCBP2_HUMAN	Q15366						
PTRF_HUMAN	Q6NZI2						11*
LMNA_HUMAN	P02545						
PROF1_HUMAN	P07737			11			
PHB_HUMAN	P35232		4			4	
PHB2_HUMAN	Q99623			11*			
PCNA_HUMAN	P12004		4		10		
PA2G4_HUMAN	Q9UQ80						
PSA1_HUMAN	P25786						5*, 11*
PSA3_HUMAN	P25788						
PSA6_HUMAN	P60900						
PSA7_HUMAN	O14818						
PSB3_HUMAN	P49720	10*					
PSB6_HUMAN	P28072						
PSB7_HUMAN	Q99436					1*	
PDIA1_HUMAN	P07237			11		4*	
PDIA3_HUMAN	P30101	10*		11		4*	
PARK7_HUMAN	Q99497						
S10A7_HUMAN	P31151			11*			
S10A8_HUMAN	P05109			9			
S10A9_HUMAN	P06702			9			
SET_HUMAN	Q01105						
PNPH_HUMAN	P00491						
KPYM_HUMAN	P14618			11*			
RANG_HUMAN	P43487						
GDIR1_HUMAN	P52565	10		7		4	
GLYM_HUMAN	P34897	10	4*			4*	
HTRA2_HUMAN	Q43464					12*	
SRSF1_HUMAN	Q07955	10*					
SPB3_HUMAN	P29508						
SPB4_HUMAN	P48594						
SPB5_HUMAN	P36952		4*			4*	
ALBU_HUMAN	P02768						9, 11*
SDPR_HUMAN	O95810						
SSBP_HUMAN	Q04837						
GRP75_HUMAN	P38646	10		11			
STIP1_HUMAN	P31948						
SODM_HUMAN	P04179		2, 4, 8				11*
TCPB_HUMAN	P78371			11*			
TCPH_HUMAN	Q99832						
TCPQ_HUMAN	P50990	10					
THIO_HUMAN	P10599	10*	4		10	1*	
KTHY_HUMAN	P23919						
TAGL2_HUMAN	P37802		4*				
TERA_HUMAN	P55072						
TCTP_HUMAN	P13693						
ECHB_HUMAN	P55084	10					11*

Protein Accession Number	SwissProt ID	References					
		Up-regulated in ovarian cancer			Down-regulated in ovarian cancer		
		TaxR Cells	CarbR Cells	Tissue	TaxR Cells	CarbR Cells	Tissue
TPIS_HUMAN	P60174		4	9, 11*		1*, 4	
RTCB_HUMAN	Q9Y310						
TPM1_HUMAN	P09493						
TPM3_HUMAN	P06753		4*			1*	
SYWC_HUMAN	P23381						
TBA1A_HUMAN	Q71U36	10*	3, 4*				
TBA1B_HUMAN	P68363						
TBA4A_HUMAN	P68366						
TBB5_HUMAN	P07437						
TBB6_HUMAN	Q9BUF5						
UBE2K_HUMAN	P61086						
UB2V2_HUMAN	Q15819				10*		
UGDH_HUMAN	O60701						
KCY_HUMAN	P30085			11*			
DCUP_HUMAN	P06132					1	
RD23B_HUMAN	P54727						
VIME_HUMAN	P08670	10	1				11
VDAC1_HUMAN	P21796						
VDAC2_HUMAN	P45880						
PEPD_HUMAN	P12955						

	Consistent to what was observed in this study
	Contrary to what was observed in this study
	Not found in this study
*	Different isoform or similar protein
1	(Brown et al., 2007)
2	(Brown et al., 2009)
3	(Burkhardt et al., 2001)
4	(Fitzpatrick et al., 2007)
5	(Huang et al., 2012b)
6	(Huang et al., 2012a)
7	(Jones et al., 2002)
8	(Kim et al., 2010)
9	(Kristjansdottir et al., 2013)
10	(Tian et al., 2009)
11	(Wang et al., 2012b)
12	(Yang et al., 2005)

It is worth noting that not all the papers searched reflect studies done with the same cell line/tissue histology, chemotherapeutic agent and experimental conditions as those in this study. As a result, the information on this protein literature review (if the protein is either up or down-regulated) is just an indication to allow comparison between this study and what has been done.

4.4.3 Pathway analysis

Fold regulation data obtained using spot intensity calculated considering and ignoring the spot position on the gel were used for pathway analysis. Only fold regulation data obtained for the ovarian cancer cell lines was used for pathway analysis, as the number of proteins identified for these samples was greater than the number of proteins identified for the tissue samples, increasing, this way, the chance of finding a relevant pathway. All proteins identified in the tissue samples were also identified in the cell line samples, with the exception of 4 proteins.

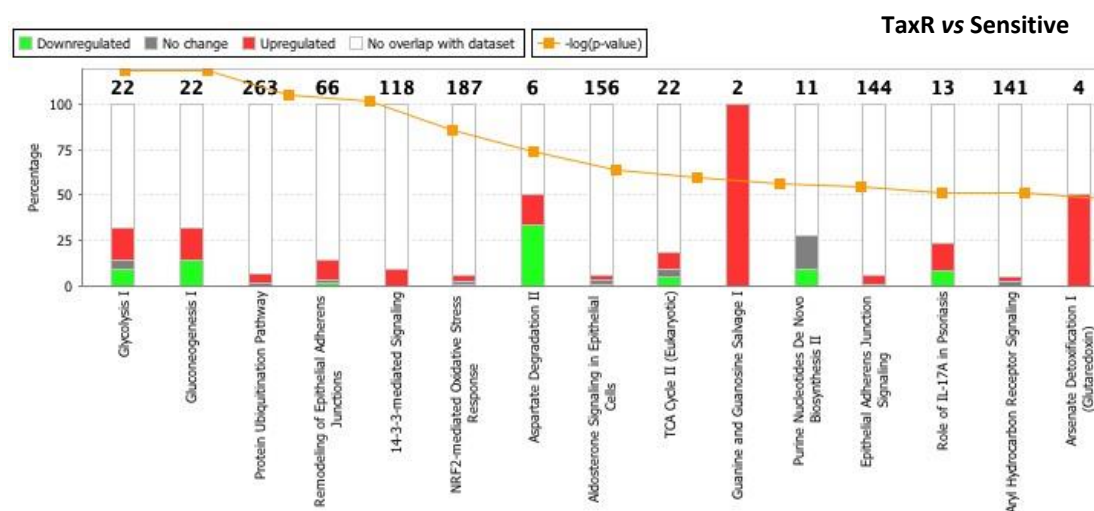
Pathway analysis was performed with Ingenuity Pathway Analysis (IPA) software and the fold regulation data uploaded can be found in Appendix.

IPA helps understand complex 'omics data at multiple levels by integrating data from a variety of experimental platforms and providing insight into the molecular and chemical interactions, cellular phenotypes, and disease processes. It helps discover hidden causal connections in a dataset by delivering a rapid assessment of the signalling and metabolic pathways, molecular networks, and biological processes that are most significantly perturbed in a dataset of interest (Ingenuity, 2013).

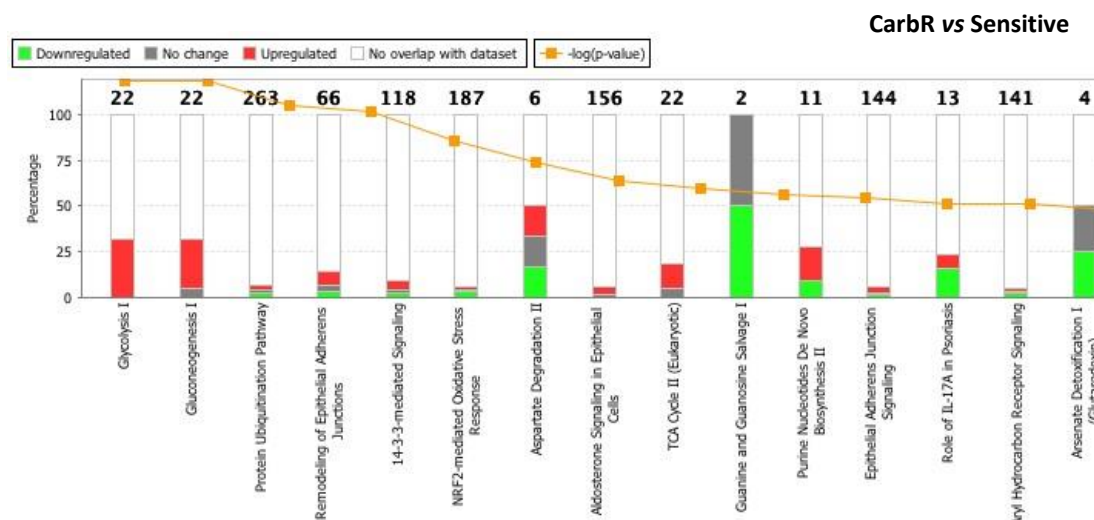
In IPA, relationships between molecules are represented by canonical pathways, which display the molecules of interest within well-established signalling or metabolic pathways. Each relationship between molecules is created using scientific information contained in the Ingenuity Knowledge Base and molecules of interest are related to known biological functions and disease states (Ingenuity, 2013).

The stacked bar charts displayed in Figure 4.17 illustrate the pathways most associated with the genes that codify for the proteins in the analysed datasets. The canonical pathways involved in this analysis are displayed along the x-axis. The y-axis displays the percentage of the number of molecules identified in a given pathway, relative to the total number of molecules that make up that pathway. The line graph shows $-\log(p\text{-value})$, which indicates the overlap of the analysis with the canonical pathway. The graph exhibits the various pathways presented from

smallest p-value to largest p-value. The colours of the bars display the number of up-regulated (red), down-regulated (green), and unchanged molecules (grey) in each canonical pathway for the TaxR vs Sensitive and CarbR vs Sensitive datasets, respectively (Ingenuity, 2013).



© 2000–2014 Ingenuity Systems, Inc. All rights reserved.



© 2000–2014 Ingenuity Systems, Inc. All rights reserved.

Figure 4.17 Stacked bar charts illustrating the pathways most associated with the genes that codify for the proteins in the analysed datasets. Canonical pathways are displayed along the x-axis. The y-axis displays the percentage of the number of molecules identified in a given pathway, relative to the total number of molecules that make up that pathway. The line graph shows $-\log(p\text{-value})$, indicating the overlap of the analysis with the canonical pathway. The colours of the bars display the number of up-regulated (red), down-regulated (green), and unchanged molecules (grey) in each canonical pathway for the TaxR vs Sensitive and CarbR vs Sensitive datasets, respectively. Pathway analysis was performed using IPA software.

Results of this analysis revealed that there were not many changes in fold regulation for the proteins involved in the 10 canonical pathways most related to the genes that codify for the proteins in the datasets, when fold regulation was calculated considering or ignoring the spot position on the gel. As a result, the pathway analysis results shown are related to the fold change data obtained considering the spot position on the gel.

In Figure 4.17, it is possible to observe that the main pathways are common to both datasets used for the analysis (ratio TaxR/Sensitive and ratio CarbR/Sensitive). However, the regulation of most genes/proteins is different; the number of up-regulated, down-regulated and unchanged molecules in each canonical pathway is distinct between the two datasets. This indicates that possibly the mechanisms of resistance, developed by these cancer cell lines against the two chemotherapeutic agents, are not the same and do not involve the same genes/proteins.

Table 4.9 contains the 5 canonical pathways most related to the genes that codify for the proteins in the analysed datasets, which could possibly be involved in the phenomenon of resistance to chemotherapy.

Table 4.9 Top 5 canonical pathways most related to the genes that codify for the proteins in the analysed datasets. Protein fold change was calculated using spot intensity data of the proteins identified in the sensitive and resistant ovarian cancer cell lines. Pathway analysis was performed using IPA software. Statistical significance was determined by using Fisher’s exact test ($P < 0.001$). Arrows next to each gene name indicate up- or down-regulation, = indicates no change or not found.

Ingenuity Canonical Pathway	P-value	Ratio	Proteins	
			TaxR	CarbR
Glycolysis I	< 0.001	7/22 (0.318)	ALDOA↓, TPIS↑, G3P↑, PGK1↓, PGAM1↑, ENOA↑, KPYM=	ALDOA↑, TPIS↑, G3P↑, PGK1↑, PGAM1↑, ENOA↑, KPYM↑
Gluconeogenesis I	< 0.001	7/22 (0.318)	MDHC↑, MDHM↓, ENOA↑, PGAM1↑, PGK1↓, G3P↑, ALDOA↓	MDHC=, MDHM↑, ENOA↑, PGAM1↑, PGK1↑, G3P↑, ALDOA↑
Protein Ubiquitination Pathway	< 0.001	16/263 (0.061)	UB2V2↑, DNJC9↑, ENPL=, CH60↑, GRP75=, GRP78=, HSPB1↑, HSP7C=, PSA1↑, PSA3↑, PSA6↑, PSA7↑, PSB3↑, PSB6↑, PSB7↑, PRS4↑	UB2V2↑, DNJC9=, ENPL↑, CH60↑, GRP75↑, GRP78↑, HSPB1=, HSP7C↑, PSA1=, PSA3↓, PSA6↓, PSA7=, PSB3↓, PSB6=, PSB7↓, PRS4↓
Remodelling of Epithelial Adherens Junctions	< 0.001	9/66 (0.136)	TBA1A↑, TBA1B↑, TBA4A↑, TBB5↑, TBB6↑, ACTB↑, ACTN4=, NDKA↑, MARE1↓	TBA1A↑, TBA1B↑, TBA4A↑, TBB5↑, TBB6=, ACTB↓, ACTN4↑, NDKA=, MARE1↓
14-3-3-mediated Signalling	< 0.001	10/118 (0.085)	PDIA3↑, VIME↑, 1433B↑, 1433T↑, 1433Z↑, TBA1A↑, TBA1B↑, TBA4A↑, TBB5↑, TBB6↑	PDIA3↑, VIME↑, 1433B=, 1433T↓, 1433Z↓, TBA1A↑, TBA1B↑, TBA4A↑, TBB5↑, TBB6=

It is worth noting that some of the up-regulated proteins were defined as up-regulated, because the protein was not found in the sensitive cell line. In a similar way, some of the down-regulated proteins were not found in the resistant cell line. Moreover, most of the ‘not changed’ or ‘not found’ proteins, identified with ‘=’ in Table 4.9, were not found in both the sensitive and resistant cell lines under comparison. As explained earlier, the fact that these proteins were not found does not necessarily indicate they were truly absent, but rather that they were not identified in this study.

In the top 5 canonical pathways, only two proteins presented a change in fold regulation, when this was calculated considering or ignoring the spot position on the gel. Those proteins were Actin cytoplasmic 1 (ACTB), involved in the

Remodelling of Epithelial Adherens Junctions pathway, and 26S protease regulatory subunit 4 (PRS4), involved in the Protein Ubiquitination pathway. When fold regulation was calculated ignoring the spot position on the gel, ACTB and PRS4 appeared up-regulated in both resistant cell lines. Hence, there was a change from down-regulated (not found) in the CarbR cell line to up-regulated. This can be explained by the fact that these proteins were identified in matching spots present in the sensitive and TaxR gels (SSP 3001 – ACTB and SSP 3604 – PRS4), but these spots were not seen in the CarbR gel. Yet, ACTB and PRS4 were identified in other non-matching spots of the CarbR gel. Therefore, when fold regulation was calculated considering matching spots, these proteins were not found in the CarbR cell line; while when other non-matching spots were used for the same calculation, ACTB and PRS4 were found up-regulated in the same cell line.

Prior to drawing any conclusion on the possible involvement of these pathways and their respective genes/proteins in ovarian cancer resistance to taxol and carboplatin, the presence and expression of a few of the proteins associated with the top pathways identified was validated.

4.4.4 Target validation

4.4.4.1 Western blotting assay

Western blotting was used to validate some of the possible protein targets of drug resistance identified in the ovarian cancer cell lines by 2D-PAGE and LC-MS/MS. Validation was considered fundamental as a result of the lack of reproducibility of the 2D gel system, which could have generated results with questionable reliability. For this analysis, proteins for validation were chosen from the group of proteins involved in the pathways mostly associated with the evaluated dataset.

Proteins were selected to be validated through Western blotting on the basis of two main criteria. Firstly, if no study had been found reporting the relationship of that protein with ovarian cancer or resistance in ovarian cancer. Secondly, if that protein had already been connected to ovarian cancer or resistance in ovarian cancer, but the information reported was contradictory to what was found in this study.

Accordingly, for the glycolysis I and gluconeogenesis I pathways, which share a similar group of proteins identified in the cell line dataset, PGAM1 was the selected protein. All the 7 proteins in the group have already been described in association with ovarian cancer and/or ovarian cancer resistance. Furthermore, the majority of them presented fold regulation results in this study that are comparable to what was found in the literature, although these particular resistant cell lines have never been studied in a similar approach. However, PGAM1 was found up-regulated in both resistant cell lines in this study, while it has been reported down-regulated in taxol resistant cell lines (Tian et al., 2009).

In the protein ubiquitination pathway, among the 16 proteins linked to this pathway, UB2V2 was selected for further investigation. This protein has been reported to be down-regulated in taxol resistant ovarian cancer cell lines (Tian et al., 2009). Nevertheless, in this study it was found up-regulated both in PEO1 TaxR and PEO1 CarbR. Most of the remaining 15 proteins presented similar fold regulation results to the findings reported in the literature. In addition, UBE2K was

also tested, since it is another ubiquitin-conjugating enzyme that belongs to the same family as UB2V2 and the antibody was available.

In the remodelling of epithelial adherens junctions pathway, the fold regulation changes observed for most of the 9 proteins in this study that matched this pathway were confirmed with literature findings. The only two exceptions were NDKA, for which the reports found were not conclusive, and ACTB. As explained earlier, ACTB was one of the proteins for which fold regulation changed according to the method used for its calculation, owing to the fact that it was identified in several non-matching spots. For this reason, ACTB was a good target for validation and, therefore, it was selected.

In the 14-3-3-mediated signalling pathway, the only proteins from the matched dataset (10 proteins) whose fold regulation was conflicting to what was found in the literature were the 14-3-3 proteins. As a result, they were scrutinised through Western blotting, using an antibody that recognised all 14-3-3 protein forms.

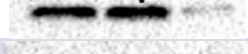
A final protein from the NRF2-mediated oxidative stress response pathway was chosen for validation. This protein was THIO and it was selected for having shown fold regulation results (up-regulated in PEO1 TaxR and down-regulated in PEO1 CarbR), which were totally inconsistent to literature reports (Fitzpatrick et al., 2007, Tian et al., 2009).

The choice of a loading control proved to be a challenge in this experiment. Proteins that had been identified only in matching spots and that presented similar expression among the sensitive and both resistant cell lines were rare. Therefore, despite its variation in fold regulation, actin was chosen as the loading control, mainly because it is one of the most widely used loading controls for Western blotting and it has been vastly used in that role in ovarian cancer studies (Altomare et al., 2004, Gritsko et al., 2003, Yuan et al., 2000). Additionally, actin was the representative protein selected for the remodelling of epithelial adherens junctions pathway for having shown controversial results.

A preliminary test with anti-actin antibody was conducted, in order to confirm the suitability of this protein as a loading control in this experiment. The result revealed that there was no apparent change in expression for the three cell lines used, and consequently, actin was adopted as loading control. The differences in fold regulation previously observed were probably not large enough to be detected on a Western blot, which is not more than a semi-quantitative method.

After the choice of proteins for evaluation, a Western blotting assay was performed using a new batch of protein lysates extracted from freshly cultured PEO1 ovarian cancer cell lines. The results of this experiment are presented in Table 4.10.

Table 4.10 Results of target validation through Western blotting assay. Ovarian cancer cell line proteins (20 µg per well from PEO1, PEO1 TaxR and PEO1 CarbR) were separated by SDS-PAGE using precast gels and transferred onto nitrocellulose membranes. Membranes were blocked, probed with primary and secondary antibodies and developed using a chemiluminescent substrate. A list of the antibodies, supplier, product code, dilution and blocking agent used is shown in Table 4.2. The experiment was carried out at least twice for each antibody. +, presence; ++, up-regulation; -, absence; --, down-regulation.

Protein (Antibody)	MW (kDa)	Spot Intensity/MS Results						WB Results				
		Considering Spot Position on the Gel			Ignoring Spot Position on the Gel			PEO1	PEO1 TaxR	PEO1 CarbR	Blots	
		PEO1	PEO1 TaxR	PEO1 CarbR	PEO1	PEO1 TaxR	PEO1 CarbR					
PGAM1 (Anti-PGAM1)	29	-	+	+	+	++	++	+	++	++		~29 kDa
UBE2K (Anti-UBE2K)	22	+	++	-	+	++	-	+	+	-		~30 kDa
UB2V2 (Anti-MMS2)	16	+	++	++	+	++	++	+	++	++		~22 kDa
1433B 1433T 1433Z (Anti-14-3-3)	28	-	+	-	-	+	-	+	++	++		~28 kDa
THIO (Anti-TRX)	12	+	++	-	+	++	-	+	++	--		~22 kDa
ACTB (Anti-Actin, loading control)	42	+	++	-	+	++	++	+	+	+		~12 kDa
												~42 kDa

Overall, WB results confirmed the results obtained by MS and spot intensity, in terms of the presence and expression of the selected proteins. WB is characterised by its high level of specificity, for recognising specific proteins among complex protein mixtures. In this study, it also proved to be more sensitive than MS in some cases, where the protein had not been found using MS but it was found using WB. This might as well have been a result of the amount of protein present on the WB membrane, when compared to the amount present on the sample that was analysed by MS. The number of fractionation steps carried out from the original cell lysate until the peptides are solubilised and ready to be identified by MS is a lot higher than this number for the WB procedure. Consequently, it is likely that the concentration of protein found in the blots was higher than the concentration of protein in the MS run.

In the WB results, PGAM1 appeared up-regulated in both ovarian cancer cell lines, confirming the previous MS/spot intensity results. The blot probed with anti-UBE2K antibody presented two sets of bands, probably owing to cross-reaction with another ubiquitin-conjugating enzyme in the samples. In any case, the bands with approximately 22 kDa, which should correspond to UBE2K, confirmed the results obtained with MS/spot intensity. UB2V2 was no exception, as its up-regulation in the resistant cell lines shown in the blots also corroborated the MS/spot intensity results previously obtained.

The anti-14-3-3 antibody used could recognise any 14-3-3 protein isoform. In fact, two sets of bands appeared in the blots and they possibly correspond to the three different forms identified by MS, 1433B, 1433T and 1433Z. According to the fold regulation, the top bands at approximately 28 kDa could correspond to either or both the 1433T and/or 1433Z, as they showed up-regulation in the resistant cell lines. In turn, the bottom bands at approximately 22 kDa could relate to 1433B, as they showed up-regulation in PEO1 TaxR and down-regulation in PEO1 CarbR.

Finally, the presence and fold regulation of THIO was also confirmed by the WB results. It had been identified in the PEO1 and PEO1 TaxR cell lines, where it was up-

regulated. WB results revealed its presence in all three cell lines, and its up-regulation in PEO1 TaxR and down-regulation in PEO1 CarbR.

4.4.5 Protein targets of chemoresistance in ovarian cancer

4.4.5.1 Proteins identified in the ovarian cancer cell lines

The main classes of proteins identified in this study are related to cytoskeleton and cell structure, detoxification and stress response, and cellular metabolism, such as several enzymes involved in the glycolytic pathway and nucleic acid synthesis.

Some of these proteins were common to all the cell lines, others only appeared in the sensitive or resistant cell lines, and finally, a few specific proteins were present in only one of the three cell lines. Some of the most relevant proteins in line with the aims of this study are grouped according to their major function and discussed in the following sections. The majority of them were found over 10-fold up or down-regulated at least in one of the resistant cell lines. The information in the sections ahead may be supplemented with the literature review table found in Table 4.8.

Cellular metabolism

Over several decades, it has been shown that tumours have altered metabolic profiles, displaying high rates of glucose uptake and glycolysis to generate ATP. Although these metabolic changes are not the fundamental defects that cause cancer, they might confer a common advantage on many different types of cancers, which allows the cells to survive and invade (Dang and Semenza, 1999). Warburg (1956) observed that cancer cells depend largely on the glycolytic metabolic pathway to achieve their required energy levels. This metabolic alteration was attributed to malfunction of mitochondrial respiration and to hypoxia in tumour environment, and is frequently associated with resistance to therapeutic agents.

The glycolysis I and gluconeogenesis I pathways have been extensively described to be connected to cancer (Hanahan and Weinberg, 2011, Bongaerts et al., 2006). Targeting glycolysis has proven to be an attractive way for therapeutic intervention in cancer and several preclinical investigations have indeed demonstrated the effectiveness of this therapeutic approach (Ganapathy-Kanniappan and Geschwind, 2013). These pathways have also been particularly associated with ovarian cancer,

and there are even studies reporting ways of inhibiting glycolysis and improving the results obtained with the standard treatment regimen in advanced ovarian cancer (De Lena et al., 2001).

Triosephosphate isomerase is a glycoprotein involved in the glycolytic pathway. It catalyses the reversible interconversion of the triose phosphate isomers dihydroxyacetone phosphate and D-glyceraldehyde 3-phosphate (Wierenga et al., 2010). Alterations in cell metabolism, mostly consisting in an increase in glycolysis and an enhanced lactate production have been described in cancer cells. These changes include an altered expression of metabolic enzymes, such as triosephosphate isomerase. In fact, this protein was found to be modulated in ovarian (Alaiya et al., 1997) and other types of tumour, such as breast (Zhang et al., 2005) and pancreatic cancer (Mori-Iwamoto et al., 2007). Overexpression of this enzyme may also be related to the increased requirements of both energy and protein synthesis/degradation pathways in rapidly growing tumours. Furthermore, triosephosphate isomerase has already been found to be modulated in resistance to several chemotherapeutic agents. The protein showed to be down-regulated in vincristine-resistant gastric cancer cell lines (Wang et al., 2008), whereas it was up-regulated in taxol-resistant A2780 ovarian cancer cell line, when compared to the sensitive counterpart (Cicchillitti et al., 2009).

In the present study, triosephosphate isomerase was identified in all three ovarian cancer cell lines and it was found up-regulated in PEO1 TaxR and PEO1 CarbR cell lines, when compared to its sensitive counterpart. These results confirm the taxol-resistant A2780 ovarian cancer cell line study previously described.

Lactate dehydrogenase (LDH) is the enzyme responsible for the NADPH-dependent conversion of pyruvate to lactate in the last step of the cellular glycolytic process. This reaction mainly takes place in the absence of oxygen.

It has been shown that LDHA plays a key role in glycolysis, growth properties and tumour maintenance of breast cancer cells (Zhou et al., 2010). With respect to non-small cell lung cancer, the overexpression of LDH5 was reported in cancer tissues

and was suggested to be linked to tumour hypoxia, angiogenic factors production and poor prognosis (Koukourakis et al., 2003).

In the present study, L-lactate dehydrogenase A chain was identified in the resistant cell lines, but not in the sensitive PEO1 cell line. On the other hand, L-lactate dehydrogenase B chain was identified in the three ovarian cancer cell lines and showed up-regulation in PEO1 TaxR and down-regulation in PEO1 CarbR. Literature findings are controversial for this protein, as LDHA is reported up- and down-regulated in the same study, in two distinct 2D gel spots (Brown et al., 2007).

4.4.5.1.1 Cytoskeleton and cell structure

Actin constitutes a framework of the cytoskeletal machinery and plays an important role in apoptosis. This protein is degraded by caspases during the execution phase of apoptosis, thus promoting disruption of required mechanical tension and leading to signals that may facilitate cell detachment (White et al., 2001). There has been increasing evidence that a decrease in actin turnover triggers cell death through an apoptosis-like pathway, accompanied by an increase of caspase-3 activation (Posey and Bierer, 1999). Actin has also been involved in resistance to taxol and other microtubule agents (Verrills et al., 2006). Di Michele and co-workers (2009) described that actin was down-regulated in resistant A2780 ovarian cancer cell lines, and this protein has also been found up-regulated in vinblastine-resistant SKOV-3 cell line (Brown et al., 2007). Nonetheless, there are no studies about actin expression in platinum-resistant cell lines.

In the present study, actin was identified in all three cell lines. However, this protein was found in several spots on the same gel, making it difficult to determine its fold change between resistant and sensitive cell lines. In turn, the WB results revealed similar protein expression among the three cell lines. For this reason, it is not possible to draw further conclusions about actin's expression in the studied cell lines, as more research would be needed to confirm these results.

Cofilin-1 is an intracellular actin regulatory protein, which depolymerises filamentous actin and inhibits the polymerisation of monomeric actin (Bamburg,

1999). Cofilin has also been found to play a key role in apoptosis. A study showed that the active form of this protein (dephosphorylated) is targeted to mitochondria after initiation of apoptosis and induces cytochrome C release from the mitochondria (Chua et al., 2003).

Yan et al. (2007) described the overexpression of cofilin-1 in cisplatin- and carboplatin-resistant A2780 ovarian cancer cell lines, while the same protein was down-regulated in SKOV-3 cell lines, when selected against the same agents and compared with their respective sensitive counterparts. Another study revealed that cofilin was down-regulated in taxol-resistant A2780 cell line (Cicchillitti et al., 2009). It is speculated that cofilin may exert its platinum-resistance role through modulating actin turnover and inhibiting apoptosis, in response to chemotherapeutic agents.

In the present study, cofilin-1 was identified in all the studied cell lines. Fold regulation analysis revealed that this protein was up-regulated in PEO1 TaxR and PEO1 CarbR. This could mean that cofilin-1 might be involved in a resistance mechanism that is not drug specific, but rather related to both taxol and carboplatin resistance.

Profilin-1 is a small ubiquitous protein that regulates actin polymerisation by binding to and sequestering the monomeric actin. This protein has already been described as involved in the tumourigenesis process of renal cell carcinoma, where it appeared overexpressed (Minamida et al., 2011), and has been identified in the ascites of patients with ovarian cancer (Gortzak-Uzan et al., 2008).

In this study, profilin-1 was identified in PEO1 and PEO1 TaxR cell lines, and it was found up-regulated in the latter. In PEO1 CarbR, this protein was not found, suggesting a possible down-regulation.

Tropomyosins are a family of proteins that participates in the regulation of the vertebrate skeletal muscle. Tropomyosin physically blocks the myosin binding site of actin in the absence of Ca^{2+} , avoiding the contraction of muscle cells (Chalovich et al., 1981).

Suppression or down-regulation of tropomyosins is a prominent feature of many transformed cells. Raval et al. (2003) reported the suppression of tropomyosin-1 in human breast carcinoma and suggested its involvement in the neoplastic transformations that cells undergo during tumourigenesis. However, the pathway involved is barely known.

Tropomyosin has been suggested as a biomarker of oesophageal squamous carcinoma and appeared down-regulated in both adenoma and colorectal cancer (CRC) tissues (Luo et al., 2009). Although tropomyosin-3 was reported as overexpressed in cisplatin-resistant ovarian cancer cell lines (Fitzpatrick et al., 2007), the same protein was found down-regulated in vinblastine-resistant SKOV-3 cell line (Brown et al., 2007). The pathway by which this protein family could lead to drug resistance remains poorly understood.

In the present study, tropomyosin alpha-1 chain was identified in PEO1 TaxR and PEO1 CarbR cell lines and tropomyosin alpha-3 chain was only identified in PEO1 TaxR cell line.

Myosins are actin-dependent Mg^{2+} ATPases that use the energy derived from ATP hydrolysis to move along the actin filaments within the cell (Berg et al., 2001).

The overexpression of myosin VI was reported in prostate cancer cells and it is believed that it enhances prostate specific antigen and vascular endothelial growth factor secretion (Puri et al., 2010). Yoshida et al. (2004) described the involvement of myosin VI in migration of ovarian cancer cells. In a *Drosophila* model, they observed that the inhibition of this protein prevented ovarian cancer cells from migrating and invading surrounding tissues. Yet, no additional relationship with chemoresistance mechanisms has already been described for this protein.

In this study, myosin light chain polypeptide 6 was identified in PEO1 and PEO1 TaxR, but not in PEO1 CarbR. Moreover, the protein was found up-regulated in PEO1 TaxR.

4.4.5.1.2 Detoxification and stress response

Glutathione S-transferase P (GSTP) was identified in PEO1 and PEO1 TaxR cell lines. This protein is related with the cell response to stress. GST is a family of phase II detoxification enzymes that catalyse the conjugation of GSH with a wide variety of xenobiotics and noxious compounds. It has already been described that, in KB carcinoma and leukemia cells, the conjugation with GSH inhibits the formation of cisplatin-DNA adducts, leading to drug resistance. This happens because GSH covalently binds to platinum agents and the conjugate formed is transported out of the cell by the ATP-dependent pump (Kelland, 2007, Chen et al., 1998, Ishikawa and Ali-Osman, 1993). This type of proteins also inhibit the conversion of monoadducts to crosslinks, thereby reducing the cytotoxic potential of cisplatin adducts.

The overexpression of GSTO1-1, a member of the omega class, was reported as being involved in drug resistance. Cicchillitti et al. (2009) studied SKOV-3 and A2780 platinum-resistant cell lines, against cisplatin and carboplatin, and described the overexpression of GSTO1-1 in both cisplatin-resistant cell lines, but not in SKOV-3 carboplatin resistant cell line.

This fact contradicts the results obtained in the present study, since GSTP1 and GSTO1 were both not identified in the PEO1 CarbR cell line. In turn, these two proteins were found up-regulated in the taxol resistant cell line. Nevertheless, another study has revealed that GSTP1 was down-regulated in SKOV-3 taxol resistant cell line (Tian et al., 2009).

Peroxiredoxin-1, 2, 5 and 6 were also identified in this study. The peroxiredoxin family is associated with cellular detoxification as well. Its function is related to the protection against oxidative stress. Proteins such as peroxiredoxin-2, 3 and -6 have already been identified in taxol resistant ovarian cancer cell lines (Di Michele et al., 2009). The hypoxia observed in cancer cells may explain their changed expression. Hypoxia environment tends to originate a high number of reactive species. In normal cells, the increase of cellular stress usually triggers an apoptotic cell death.

However, the increased expression of detoxification proteins helps the tumour cells to survive, by removing those reactive species.

The presence of peroxiredoxin-2, as well as other members of the same family, was described in sensitive to chemotherapy IGROV1 ovarian cancer cell line (Le Moguen et al., 2006).

In this study, peroxiredoxin-1 and 2 were identified in all three ovarian cancer cell lines studied and appeared up-regulated in PEO1 TaxR and PEO1 CarbR. Peroxiredoxin-5 was only found in the PEO1 TaxR cell line, and peroxiredoxin-6 was also found in the sensitive and taxol resistant cell lines, but not in the carboplatin resistant cell line. Peroxiredoxin-6 showed up-regulation in PEO1 TaxR as well.

As suggested before for cofilin-1, peroxiredoxin-1 and 2 seem not to be specific resistance markers, as they are likely to be involved in a common pathway present in sensitive, as well as in resistant PEO1 ovarian cancer cell lines. This pathway is possibly altered in the resistant cells.

4.4.5.1.3 Multifunctional proteins

Three isoforms of the 14-3-3 protein were identified in the ovarian cancer cell lines, 1433B, 1433T and 1433Z. They belong to the 14-3-3 class of proteins and fit into a number of functional categories (Hodgkinson et al., 2012). This is a class of multifunctional, acidic proteins, which act as regulators of a vast array of cellular pathways, including cell growth and neuronal development. Although they were initially thought to be found only in the brain, it has now been established that they are present in almost every tissue, and in eukaryotes are found largely in the cytoplasm (Fu et al., 2000).

There are seven isoforms of the 14-3-3 proteins and all undergo dimerisation to form a cleft, which recognises and binds, although not exclusively, to phosphorylated residues of 14-3-3 ligands (Robinson, 2010). There is a great degree of cross over between the isoforms, with a number of ligands being able to bind to more than one isoform (Fu et al., 2000).

An important pathway that these proteins regulate is that of apoptosis, by binding to the proapoptotic protein BAD. BAD causes apoptosis by inhibiting antiapoptotic proteins, including Bcl-2; however when it is bound to 14-3-3 in the cytosol, it is unable to bind to its target proteins in the mitochondria and is, therefore, inactivated (Zha et al., 1996). Another 14-3-3 target protein involved in apoptosis is apoptosis signal-regulating kinase 1 (ASK1). This protein is an important component of a signal transduction pathway, which can be activated by tumour necrosis factor α (TNF- α), Fas, oxidative stress (Ichijo et al., 1997) and the cytotoxic drugs cisplatin and taxol (Zhang et al., 1999). The binding of ASK1 to different isoforms of 14-3-3 proteins has been shown to inhibit its proapoptotic activity (Zhang et al., 1999) and, thus, it can be inferred that it reduces the cytotoxic activity of the drugs cisplatin and taxol.

Additionally, the isoform 14-3-3 theta was found to be up-regulated in chemotherapy resistant breast cancer cells (Hodgkinson et al., 2012). The same isoform also has a stabilising effect by binding to some proapoptotic proteins, such as E2F1, which is important when DNA damage has occurred. Thus, the down-regulation of 14-3-3 protein theta results in a loss of proapoptotic proteins and promotes cell survival. As drugs such as cisplatin induce apoptosis through DNA damage, this suggests that down-regulation may also infer resistance (Wang et al., 2004a). In fact, 14-3-3 protein theta was found down-regulated in cisplatin resistant ovarian cancer cells in a previous proteomics study (Fitzpatrick et al., 2007).

This is supported by the cell line results, as one of the three 14-3-3 protein isoforms was found down-regulated in the PEO1 CarbR cell line, possibly 1433B. Moreover, all three isoforms identified were found up-regulated in PEO1 TaxR. This different behaviour for different chemotherapy agents suggests distinct mechanisms of drug resistance for the two drugs.

Nucleoside diphosphate kinase A was identified only in the PEO1 TaxR cell line, suggesting that this protein is related to drug resistance mechanisms that are present/activated specifically in taxol resistant cell lines, while they are possibly absent/repressed in the other two cell lines.

These proteins have several biological functions and play important roles in cell differentiation, regulation of signal transduction, cell survival, DNA recombination and cell transformation (Fitzpatrick et al., 2007). The isoform A is associated with nucleic acid synthesis, where it is responsible for the synthesis of most non-ATP nucleoside triphosphates. Nucleoside diphosphate kinase is encoded by the NM23 gene, known as an antimetastatic factor, whose expression is correlated inversely with tumour metastatic potential in murine melanoma cell lines (Steeg et al., 1988). In addition to the antimetastatic property, this gene has been shown to be associated with sensitivity to cisplatin in breast and ovarian carcinomas (Scambia et al., 1996).

Nucleoside diphosphate kinase A was described as overexpressed in taxol resistant ovarian cancer cell lines (Cicchillitti et al., 2009). It is thought that it can modulate taxol resistance in tumour cells, allowing faster DNA repair. Its increased expression is associated with resistance to initial chemotherapy, but further studies are required to confirm this hypothesis.

Eukaryotic transcription is regulated predominantly by the PTM of the participating components. One such modification is the cis-trans isomerisation of peptidyl-prolyl bonds, which results in a conformational change in the protein involved. The enzyme responsible for this reaction is peptidyl-prolyl cis-trans isomerase (Shaw, 2007).

Peptidyl-prolyl cis-trans isomerase A, also known as cyclophilin A, belongs to the family of peptidyl-prolyl cis-trans isomerase proteins (PPIases). Found mainly in the cytoplasm, they are ubiquitous, multifunctional proteins, which are thought to be involved in protein folding, transport, cell adhesion and signalling (Galat, 1993). Cyclophilin A is also a well known cytokine, which activates the CD147 receptor, and is secreted from cells in response to environmental stresses (Obchoei et al., 2009). It is inhibited by the immunosuppressant drug cyclosporine A, which is administered to prevent graft rejection following transplant surgery (Gothel and Marahiel, 1999).

Owing to its multifunctional and ubiquitous nature, there is not yet a complete understanding of all cyclophilin A's substrates and actions (Obchoei et al., 2009). Various proteomic studies have shown it to be over-expressed in a number of cancers, including pancreatic adenocarcinoma (Mikuriya et al., 2007), lung cancer (Campa et al., 2003) and endometrial carcinoma (Li et al., 2008b). Cyclophilin A has been found to promote cell proliferation, protect against apoptosis (Li et al., 2008b) and contribute to the metastatic activity of cancer cells (Zhang et al., 2011).

Nevertheless, cyclophilin A is also thought to have pro-apoptotic activity, which therefore makes it a candidate for down-regulation in resistant cancer cells (Obchoei et al., 2009). Although the mechanism is not clearly understood, it is known that cyclophilin A is modulated in cancer drug resistance. Overexpression of cyclophilin A has been found to confer cisplatin resistance to a number of different cancer cells, including prostate carcinoma and cervical carcinoma cells (Choi et al., 2007b). The down-regulation of this protein was reported in taxol resistant BT549 breast cancer cells (Balasubramani et al., 2011), as well as in cisplatin resistant ovarian cancer cell lines (Fitzpatrick et al., 2007). Cyclophilin A was also found to be down-regulated in cisplatin resistant cervix squamous carcinoma (Castagna et al., 2004). Though, it was found to be up-regulated in a gemcitabine resistant human pancreatic adenocarcinoma cell line (Kuramitsu et al., 2010).

Peptidyl-prolyl cis-trans isomerase A was identified in all three ovarian cancer cell lines studied and was found markedly up-regulated in PEO1 TaxR and PEO1 CarbR cell lines. The results obtained do not corroborate those previously described for taxol resistant breast cancer cell lines and cisplatin resistant ovarian cancer cell lines. Additional studies are, therefore, required in order to confirm these results and further understand the mechanism by which peptidyl-prolyl cis-trans isomerase leads to drug resistance.

Nucleophosmin was present in both resistant cell lines in this study and absent from the sensitive cell line. This protein is an abundant multifunctional phosphoprotein present in the nucleoli. Nucleophosmin is also active in many cellular functions, including ribosome biogenesis, histone assembly, regulation of DNA integrity, cell

proliferation, and regulation of tumour suppressors (Park et al., 2009). In normal cells, it plays an essential role in embryonic development and, particularly, in the control of centrosome duplication and genomic stability (Grisendi et al., 2006). However, nucleophosmin is frequently overexpressed, mutated, rearranged and deleted in human cancer. Traditionally regarded as a tumour marker and a putative proto-oncogene, it has now also been attributed with tumour-suppressor functions, contributing to the tumourigenesis process through many mechanisms (Grisendi et al., 2006). It has been suggested that nucleophosmin has an anti-apoptotic function via BAX binding and that its polymerisation, by transglutaminase-2, can also be correlated with the drug resistance of cancer cells (Park et al., 2009).

Wang et al. (2009) reported the expression of nucleophosmin in both cisplatin sensitive (COC1) and resistant (COC1/DDP) ovarian cancer cell lines. These findings corroborate the results obtained in the present study, where nucleophosmin was identified in a carboplatin resistant cell line, a therapeutic agent structural and functionally related to cisplatin.

4.4.5.2 Proteins confirmed in the tissue biopsies

According to the clinical information provided for each tissue sample, SOV-2 was described as resistant to the standard drug treatment for ovarian cancer. In turn, SOV-3 was described as sensitive, as it showed a complete response to treatment. SOV-4 and SOV-5 behaved as partially resistant/sensitive, as they showed only a partial response to chemotherapy.

In order to identify the un-regulated proteins in the resistant tissue samples, fold regulation was calculated in a similar way as for the resistant cell lines. In this case, spot intensities in the SOV-2 resistant tissue gel were directly compared with the corresponding spot intensities in the SOV-3 sensitive tissue gel. In addition, spot intensities in the SOV-4 and SOV-5 partially resistant tissue gels were compared with the corresponding spot intensity values in the sensitive tissue gel. When fold regulation of the tissue proteins was known, it was compared to the same information on the cell line proteins. The results of this comparison revealed a

group of un-regulated proteins in the cell line samples that were similarly un-regulated in the tissue samples. This group of proteins includes potential protein targets of chemoresistance confirmed in the clinical samples and is shown in Table 4.11.

Table 4.11 Possible protein targets of chemoresistance in ovarian cancer. Un-regulated proteins identified in the ovarian cancer cell line resistant samples (PEO1 TaxR and PEO1 CarbR) that were found similarly un-regulated in the resistant (SOV-2) and partially resistant (SOV-4 and SOV-5) tissue samples.

Un-regulated proteins confirmed in the clinical samples			
Resistant/Sensitive		Partially resistant/Sensitive	
SOV-2/SOV-3 vs TaxR/Sens, CarbR/Sens		SOV-4/SOV-3, SOV-5/SOV-3 vs TaxR/Sens, CarbR/Sens	
Up-regulated	Down-regulated	Up-regulated	Down-regulated
ANXA2, PRDX2, SPB4 (TaxR), ALBU	ANXA1 (CarbR), ALDOA (TaxR), MDHM (TaxR), PGK1 (TaxR)	CH60, ENOA, ANXA2, APOA1 (CarbR), CATD (TaxR), EFTU, ALDOA (CarbR), GSTP1 (TaxR), G3P, HNRPK, ROA2 (CarbR), MDHC (TaxR), MDHM (CarbR), PRDX1, PRDX2, PGK1 (CarbR), RANG (TaxR), GRP75 (CarbR)	MDHM (TaxR), PGK1 (CarbR)

A great number of the un-regulated proteins confirmed in the clinical samples are involved in the glycolysis I and gluconeogenesis I pathways, which supports the pathway analysis results obtained in this study. It is also in line with previous studies, which have demonstrated that chemoresistant cell lines have elevated aerobic glycolysis, indicating a biochemical link between resistance and glycolysis (Zhou et al., 2012).

Most of the un-regulated proteins confirmed in the clinical samples were up-regulated in the resistant or partially resistant samples. The up-regulation of CH60, ENOA, CATD, EFTU, G3P and GRP75 was also reported in a quantitative proteome analysis of ovarian cancer and normal ovarian epithelial tissues using an iTRAQ

approach (Wang et al., 2012b). APOA1 and PRDX2 have also been found up-regulated in ovarian cyst fluid of patients diagnosed with advanced serous ovarian adenocarcinoma (Kristjansdottir et al., 2013).

Additionally, studies conducted in taxol and platinum resistant ovarian cancer cell lines have reported CH60, ENOA, ANXA2, CATD, HNRPK and ROA2 to be up-regulated in the resistant cells, when compared to their sensitive counterparts (Brown et al., 2007, Fitzpatrick et al., 2007, Tian et al., 2009). These studies further support the claim that the un-regulated proteins confirmed using clinical samples could be potential targets of resistance in ovarian cancer.

Comparing the tissue sample results with the cell line results has provided some interesting conclusions. The clinical information allowed a better understanding of these findings, since each sample could be related to a specific response to chemotherapy, allowing more effective and accurate comparisons. Furthermore, the comparison with the proteins identified in the tissue samples has brought a much higher impact to the cell line results, as the majority of findings on chemoresistance in ovarian cancer are based on research that has been conducted on cell lines.

Therefore, to have these findings confirmed in ovarian cancer tissue samples provides more solid clinical evidence, which can then be used for further research into the development of chemoresistance. In addition, even for the up and down-regulation confirmed in cancer tissue, there will inevitably be differences in the degree of differentiation, owing to the heterogeneity of cancer tissue and the tumour microenvironment, when compared to the homogeneity of cancer cell lines. The list of proteins presented is a good starting point for further studies on specific protein targets of chemoresistance in ovarian cancer.

4.4.6 Other protein targets in ovarian cancer

4.4.6.1 Protein targets of ovarian cancer diagnosis

Early detection remains the most promising approach to improve long-term survival of patients with ovarian cancer. As a result, biomarkers for the detection of early stage ovarian cancer are the most sought by the scientific community.

Taking advantage of the availability of a non-cancerous tissue sample among the samples analysed in this study, the presence of un-regulated proteins between the SOV-1 non-cancerous tissue and SOV-2, SOV-3, SOV-4 and SOV-5 ovarian cancer tissues was evaluated. For that matter, fold regulation was calculated using the ratios SOV-2/SOV-1, SOV-3/SOV-1, SOV-4/SOV-1 and SOV-5/SOV-1. Only proteins that were similarly un-regulated in the four ovarian cancer tissues were accepted as potential protein targets of ovarian cancer diagnosis.

Nine proteins in total were found differentially regulated in a similar way among the four ovarian tissues. Out of those 9 proteins, 6 (AACT, FABP5, LEG7, HBB, IGHG1 and SPB3) were down-regulated in the cancer tissues. The other 3 proteins (EF1A1, G3P, ALBU) were up-regulated in cancer.

Wang and co-workers (2012b) have reported EF1A1 and G3P to be up-regulated in a quantitative proteome analysis of ovarian cancer tissues, while HBB was down-regulated. Their results strongly support the results of this study and suggest that a potential biomarker of diagnosis in ovarian cancer might be among them.

Other studies have been carried out with the aim of discovering novel biomarkers for the diagnosis of ovarian cancer. Several biomarkers have been suggested, including haptoglobin and transferrin (Ahmed et al., 2005), kallikrein 10 (Luo et al., 2003), osteopontin (Kim et al., 2002), apolipoprotein A1, truncated form of transthyretin and cleavage fragment of inter- α -trypsin inhibitor heavy chain H4 (Zhang et al., 2004).

4.4.6.2 Protein targets of ovarian cancer histologic subtype

Research has suggested that the association of biomarker expression with survival varies substantially between subtypes of epithelial ovarian cancer. Some scientists even say that ovarian carcinoma subtypes are different diseases and, therefore, should be reflected in clinical research study design.

A retrospective study assessed the protein expression of 21 candidate tissue-based biomarkers (CA 125, CRABP-II, EpCam, ER, F-Spondin, HE4, IGF2, K-Cadherin, Ki-67, KISS1, Matriptase, Mesothelin, MIF, MMP7, p21, p53, PAX8, PR, SLPI, TROP2, WT1) and reported that, when analysed by subtype, only 3 of the candidates (MMP7, WT1, Ki-67) remained prognostic indicators in the serous and none in the clear cell subtype (Kobel et al., 2008).

A study by Cloven et al. (2004) to determine whether there is a relationship between histologic subtype of epithelial ovarian cancer and chemoresistance, detected a significantly higher expression of HER-2 neu in clear cell carcinomas and higher expression of mP53 in papillary serous carcinomas.

In the present study, despite the limited number of samples, there was a possibility of investigating the existence of un-regulated proteins between the SOV-4 clear cell ovarian carcinoma tissue and SOV-2, SOV-3 and SOV-5 serous ovarian cancer tissues. For this purpose, fold regulation was calculated using the ratios SOV-2/SOV-4, SOV-3/SOV-4 and SOV-5/SOV-4. Only proteins that were similarly un-regulated in the three serous carcinoma tissues were accepted as potential protein targets of ovarian cancer subtype.

A total of 12 proteins were found differentially regulated in a similar way among the three serous tissues. Out of those 12 proteins, 11 (CH60, ENOA, EF1A1, EFTU, HNRPK, ROA2, PRDX2, RANG, GRP75, ECHB and VDAC1) were down-regulated in the serous tissues. The only up-regulated protein was ANXA2.

Although the un-regulated proteins identified have not yet been particularly associated with a specific ovarian carcinoma subtype, they might still be useful as

the basis of further studies aiming the discovery of new biomarkers of ovarian cancer subtype.

Another interesting study would be the investigation of potential protein targets of disease stage, in order to understand the molecular basis of metastasis. However, in this study, it was not possible to undertake such analysis, since the ovarian cancer samples studied were all from an advanced stage of the disease.

4.5 Conclusions & Future Work

4.5.1 Conclusions

Proteomics has proven to be a powerful approach to better understand the complex signalling pathways involved in drug resistance of ovarian cancer cells and tissues, and to identify potential resistance biomarkers.

In this study, taxol and carboplatin resistance-associated proteins were identified by MS, after comparing the protein expression profile of sensitive and resistant cell lines and different ovarian cancer tissues, through 2D-PAGE. The 2D gels clearly showed a large number of protein spots and allowed comparison between all the samples. The PDQuest software aided this comparison, proving particularly helpful in the comparison between the cell line and the tissue results, which gave an indication of the clinical relevance of the cell line findings.

A total of 189 proteins were identified with high confidence in at least one of the three cell lines or five tissues studied. Among them were proteins belonging to different classes and responsible for distinct functions within the cell, such as cytoskeleton and cell structure, detoxification and stress response and cellular metabolism. This demonstrated that the development of resistance is indeed a multi-factorial process, involving various biological pathways.

The pathways most highly associated with the un-regulated proteins identified were also discovered in this study, using fold regulation data calculated with the spot intensity for each of the proteins identified.

Furthermore, validation of a few key proteins that participate in the top pathways and presented fold regulation results conflicting with the literature, was undertaken using a Western blotting assay, and their identities and fold regulations were confirmed.

Similar studies have been carried out by other groups. However, they only provide the resistance profile of one chemotherapeutic drug or two that are structural and functionally related. This work shows promising utility, as it was the first time cell lines that are resistant to two non-related drugs, carboplatin and taxol, were studied in parallel. Apart from the proteins that were differentially expressed in one resistant cell line, this work also aimed to identify common targets and pathways involved in both types of resistance.

One of the biggest limitations of research into the development of chemoresistance in ovarian cancer is that the majority of studies has been conducted on cell lines rather than actual human tissue. This was the first study of its kind, which analysed protein expression in different samples of ovarian cancer tissue. Therefore, it has great potential for determining the significance of data obtained from cell line research in human ovarian cancer tissue.

Ultimately, significant differences in the expression of certain proteins in both the cell lines and tissues may lead to the discovery of specific resistance biomarkers. In addition, significant similarities may lead to better understanding of resistance biomarkers, which confer resistance to both classes of drugs and may play a role in the development of cross-resistance. As carboplatin and taxol constitute the first-line treatment for advanced-stage ovarian cancer patients, the results obtained in this study can be useful in the prognostic of treatment response to both agents simultaneously, and for further studies of resistance mechanisms.

The clinical data regarding the ovarian tissue samples, allowed a more in depth and accurate analysis, as samples corresponded to different histological subtypes and stages of ovarian cancer, apart from having shown distinct responses to treatment. Discrepancies in protein expression among the tissue samples have revealed a relationship between the different subtypes and stages and chemoresistance. Furthermore, possible protein targets of ovarian cancer diagnosis and subtype have also been suggested in this study.

Nevertheless, the results obtained in this study should only be regarded as a starting point for more studies in this field, as the main aim was to screen for possible protein targets of chemoresistance in ovarian cancer. Moreover, the limitations of this study, mainly related to the insufficient number of samples that did not permit the creation of a reproducible 2D gel system, must be overcome by extensive validation of the suggested protein targets. Further studies are also required in order to better understand the altered pathways and the mechanisms involved in the development of the resistance phenomenon, as well as to confirm the potential targets of ovarian cancer diagnosis and histologic subtype suggested.

Key Findings				
Protein targets of chemoresistance	2D-PAGE + LC-MS/MS + spot intensity analysis	PEO1 ovarian cancer cell lines		Ovarian cancer tissues
		Over 70 % proteins un-regulated in PEO1 TaxR	Over 80 % proteins un-regulated in PEO1 CarbR	Over 40 % proteins un-regulated in resistant tissue (SOV-2)
	Pathway analysis	Top 6 altered pathways: glycolysis I, gluconeogenesis I, protein ubiquitination pathway, remodelling of epithelial adherens junctions, 14-3-3-mediated signalling, NRF2-mediated oxidative stress response		
	WB Validation	ID and fold regulation reported for 6 key proteins associated with top 6 pathways confirmed by WB		
	Clinical Validation	Subset of un-regulated proteins confirmed in the tissue samples are potential protein targets of chemoresistance		
Protein targets of diagnosis and subtype	Potential protein targets of ovarian cancer diagnosis and subtype suggested. Further studies needed.			

4.5.2 Future work

Many of the identified proteins have already been related to cancer development and/or drug resistance. Some of them have already been associated with resistance pathways in other ovarian cancer cell lines, which means they have a great potential of becoming resistance biomarkers in the near future. These proteins could have an important application in screening, early diagnosis and prognosis of the disease through the design of marker panels. Other interesting applications for these markers are related to personalised treatment, by choosing an appropriate and individualised treatment for each cancer patient, and discovery of new molecular targets and alternative treatments, by identifying disruptive cellular pathways.

It would be interesting to compare the protein profile of the resistant cell lines used in this study, which were derived from the sensitive PEO1 cell line, with resistant cell lines that are actually isolated from patients. For example, the known PEO4 and PEO6 cell lines (Langdon et al., 1988), which are both resistant to chemotherapy, could be a good option.

Another useful comparison in the study of ovarian chemoresistance would be against a cell line that is simultaneously resistant to carboplatin and taxol. This would allow a more accurate comparison with the resistant ovarian tissues, since it is very likely that the same tumour contains some cells resistant to taxol and others resistant to carboplatin. In addition, this would allow the study of cross-resistance.

The resistance profile of the cell lines used in this study could also be analysed against other combinations of chemotherapeutic drugs involved in ovarian cancer treatment, such as cisplatin-taxol, cisplatin-docetaxel and carboplatin-docetaxel, with the aim of identifying simultaneous or exclusive abnormal protein expression and altered molecular pathways.

Another interesting approach could be the use of different ovarian cancer resistant cell lines, perhaps in other stages of the disease or with a distinct degree of differentiation (for example, PEO1, PEO4 and PEO6), in order to investigate if the

differentially expressed proteins identified in this study are similarly altered in those conditions.

A further option would be to use the same proteomic approach to compare ovarian cancer cell lines with acquired and innate resistance.

A different approach for further experiments with these cell lines would be to conduct pathway inhibition studies, in order to investigate the possibility of inhibiting one or more of the top pathways identified. This would not only validate the pathway previously found, but would also provide additional information on the behaviour of resistant cells in the presence of an inhibitor and the therapeutic agent. A quick way of testing this would be the use of MTT assays, for example.

An important limitation of this study was the small number of ovarian cancer tissue samples analysed. In general, it is difficult to obtain cancer tissue samples from patients, owing to the related ethical issues, and when available they are usually very small in size. This significantly limits the number of experiments that can be conducted with the tissues. Nevertheless, although the results demonstrated that cancer cell lines are good models to study cancer, it is essential to confirm findings obtained with cell lines using tissue samples, since there might be differences between what occurs in the cancer tissue microenvironment and what is found in cell lines.

**Chapter 5 – FUNCTIONAL CHARACTERISATION OF HEAT SHOCK
PROTEIN 90 TARGETED COMPOUNDS**

5.1 Introduction

5.1.1 Heat shock proteins (Hsps)

In 1962, an Italian geneticist Ferruccio Ritossa took the first step in the identification of the heat shock proteins (Hsps), when he reported that heat and the metabolic uncoupler 2,4-dinitrophenol induced a characteristic puffing pattern in the chromosomes of *Drosophila melanogaster* (Ritossa, 1962). Increased synthesis of selected proteins in *Drosophila* cells as a result of stresses such as heat shock was first reported in 1974 (Tissieres et al., 1974).

Since then, a great number of researchers have demonstrated that the heat shock response is ubiquitous and highly conserved, as it is present in all organisms from bacteria to plants and animals. The heat shock response is an essential defence mechanism existent in cells for their protection against a wide variety of harmful environmental conditions, such as heat shock, oxidative stress, heavy metals, or pathological conditions, including inflammation, tissue damage, infection, and mutant proteins associated with genetic diseases (Lindquist, 1986).

Exposure of cells to acute and chronic stress results in the inducible expression of Hsps. However, some Hsps are constitutive and are expressed in non-stress conditions. These are involved in protein folding and translocation of polypeptides across membranes and, therefore, have been named molecular chaperones. Molecular chaperones are a family of proteins that function in protein folding, translocation and refolding of intermediates, which are generated during cell stress, to prevent misfolded or damaged molecules. This way, Hsps contribute to restore protein homeostasis and promote cell survival by repairing damaged proteins or by degrading them (Georgopoulos and Welch, 1993).

There are several methods of classification for Hsps; one of the most widely used is according to their molecular weight (De Maio, 1999). Heat shock protein 90 (Hsp90) is named as such owing to its molecular weight being approximately 90 kDa.

5.1.2 Hsp90 characteristics and functions

As the majority of Hsps, Hsp90 plays a key role in cellular stress response, assisting the folding of nascent polypeptides and assembly of multimeric protein complexes. Nevertheless, Hsp90 also has an important regulatory role in normal physiological conditions. Hence, Hsp90 is responsible for the stabilisation and maturation of over 100 proteins, which are called Hsp90 client proteins (Stravopodis et al., 2007). These can be divided into three groups: steroid hormone receptors, serine/threonine or tyrosine kinases, and other apparently unrelated proteins such as mutant p53 and the catalytic subunit of telomerase hTERT. All mentioned proteins play key regulatory roles in many physiological and biochemical processes in the cell (Maloney and Workman, 2002).

In humans, four genes compose the highly conserved Hsp90 family: the cytosolic HSP90 α and HSP90 β isoforms (Hickey et al., 1989), GRP94 in the endoplasmic reticulum (Argon and Simen, 1999) and HSP75/tumour necrosis factor receptor associated protein 1 (TRAP1) in the mitochondrial matrix (Felts et al., 2000). All genes share a similar mode of action, but bind to different client proteins according to their localisation within the cell.

Three domains form the Hsp90 monomer: a 25 kDa amino terminal region (N-terminal), a charged linker region (M-domain) and a 55 kDa carboxyl terminal (C-terminal). All three termini are reported to bind to substrate polypeptides, including client proteins and co-chaperones. The N-terminal contains the ATP-binding pocket, where ATP hydrolysis occurs, and a drug-binding site with co-chaperone-interacting motifs. The M-domain participates in forming the active ATPase. The C-terminal contains a second drug-binding region and mediates the formation of dimers, which are the dominant Hsp90 forms in physiological conditions (Pearl and Prodromou, 2000).

Research revealed that Hsp90 is an ATP-dependent molecular chaperone (Prodromou et al., 1997) and that dimerisation of the nucleotide-binding domains is

vital for ATP hydrolysis, which in turn is necessary for chaperone function (Prodromou et al., 2000, Wayne and Bolon, 2007).

Although some facts about Hsp90 remain unclear, it is undisputed that the ATP binding site localised at the N-terminal plays an essential role in Hsp90's function. It is believed that ATP binding and hydrolysis offer energy to cells and trigger substantial conformational changes in Hsp90 caused by binding of client proteins. Consequently, the majority of studies aim at ATP binding towards Hsp90.

The following model (Figure 5.1) represents the Hsp90 chaperone cycle, showing the conformational changes that result from ATP binding.

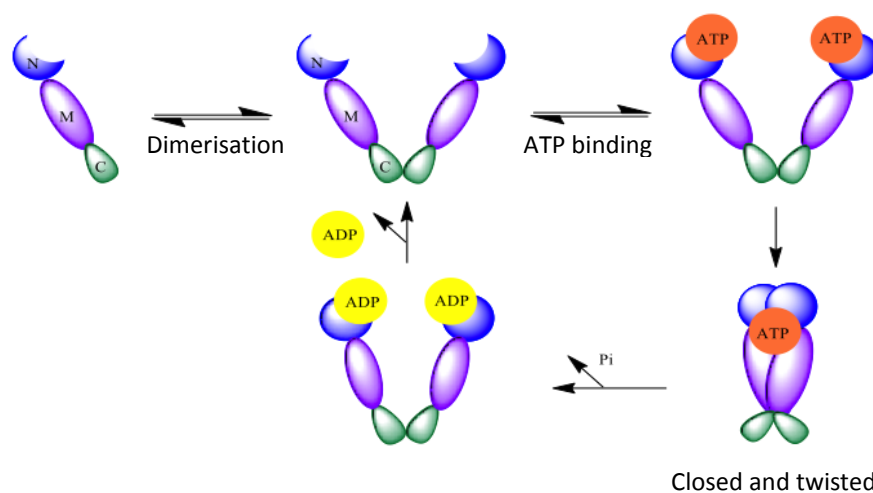


Figure 5.1 Hsp90 chaperone cycle. ATP binding triggers the Hsp90 chaperone cycle. Hsp90 starts as a monomer and when ATP binds to the N-terminal there is a structural rearrangement, leading to dimerisation and the 'closed and twisted' conformation of Hsp90. After ATP hydrolysis, Pi (inorganic phosphate) and ADP are released, and Hsp90 returns to its initial open structure. N, amino-terminal domain; M, middle domain; C, carboxy-terminal domain. Adapted from (Trepel et al., 2010).

5.1.3 Hsp90's role in cancer

Cell stress and cell death are connected, such that molecular chaperones induced in response to stress appear to have a key regulatory function in the control of apoptosis. As a result, it is not surprising that the heat shock response and molecular chaperones have been implicated in the control of cell growth and, therefore, are seen as potential targets for cancer diagnosis and treatment (Jolly and Morimoto, 2000).

Owing to its protective role, Hsp90 is overexpressed in the stressful environment characteristic of tumour cells (Neckers, 2007). Hsp90 is responsible for the conformational maturation of a number of enzymes involved in many different cancer pathways often referred to as the six hallmarks of cancer (Hanahan and Weinberg, 2000). In addition, research suggests that Hsp90 may also play a role in buffering against the effects of mutation, by correcting the inappropriate folding of mutant proteins, helping them to survive (Rutherford and Lindquist, 1998). Therefore, targeting Hsp90 represents a powerful tool against a broad array of cancers. A few specific examples of how Hsp90 assists cancerous cells in becoming self-sufficient and promoting genetic variation are described ahead.

Hsp90 is accountable for stabilising the structure and maintaining the active conformation of proteins such as EGFR (epidermal growth factor receptor) and signal transduction proteins PI3K and Akt, which are found overexpressed in cancer cells (Sawai et al., 2008, Basso et al., 2002). The PI3k/Akt/mTOR pathway is responsible for cellular survival, proliferation and mobility of tumour cells. Research has proved that inhibition of proteins involved in this pathway may trigger apoptosis (Morgensztern and McLeod, 2005). One of the reasons why these proteins are able to preserve their functions when they are overexpressed is that Hsp90 contributes to the stability of their structure (Zhang et al., 2012). Consequently, Hsp90 inhibition is associated with cancer cells apoptosis (Saturno et al., 2013).

During the process of tumour growth, oxygen often becomes insufficient in cancer tissues. When this occurs, the *de novo* angiogenesis process is initiated by the activation of several proteins, including vascular endothelial growth factor (VEGF) and nitric oxide synthase (NOS). It has been shown that Hsp90 contributes to this activation, helping tumours to become self-sufficient, and that when Hsp90 is inhibited, VEGF and NOS expression is also suppressed (Garcia-Cardena et al., 1998, Pritchard et al., 2001, Sun and Liao, 2004).

Numerous proteins participate in cell transformation and mutation. Products of oncogenes *BCR/ABL*, *SRC*, mutant *p53* are examples of mutant proteins involved in

cell transformation, which are stabilised by Hsp90 (Lee et al., 2010, Whitesell et al., 1994). The tumour suppressor protein p53, for example, is found mutated in about 55 % of tumour cells, resulting in the loss of its function. Previous studies suggest that mutant p53 remains extremely stable when binding to Hsp90 and that inhibition of Hsp90 leads to degradation of this mutant protein (Peng et al., 2001).

Tumour cells exhibit higher Hsp90 activity and accumulate Hsp90 inhibitors to a larger extent than normal cells, which may allow targeting of this protein by tumour-selective inhibitors (Kamal et al., 2003, Porter et al., 2010).

In summary, inhibition of Hsp90 has been shown to cause selective degradation of key signalling proteins involved in cell proliferation, cell cycle regulation and apoptosis, which are fundamentally important processes that are frequently deregulated in cancer (Isaacs, 2005, Powers and Workman, 2006). In contrast to traditional cancer therapeutics directed against one molecular target, disruption of the Hsp90 machinery is thought to simultaneously inhibit multiple therapeutic targets and pathways critical to tumour survival. This is why evaluation of Hsp90 inhibitors is a current focus of drug discovery.

5.1.4 Hsp90 inhibitors

5.1.4.1 Hsp90 N-terminal inhibitors

The search for new anticancer drugs that interact with Hsp90 identified the benzoquinone ansamycin family of antibiotics, which act by inhibiting cell proliferation and reversing oncogenic transformation (Whitesell et al., 1992, Uehara et al., 1986). These compounds are natural products and were isolated for the first time in the 1970s from actinomycete broths (DeBoer et al., 1970).

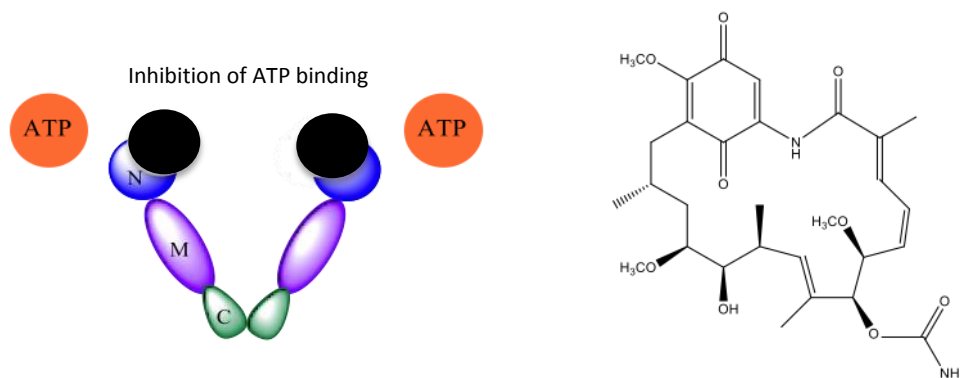


Figure 5.2 Hsp90 N-terminal inhibitors. Model of Hsp90 N-terminal inhibition: inhibitor represented in black preventing ATP binding. Example of an N-terminal inhibitor: geldanamycin. Adapted from (Trepel et al., 2010).

Geldanamycin (Figure 5.2), a well-characterised member of the ansamycins, targets the amino-terminal ATP-binding domain of Hsp90, resulting in the competitive inhibition of ATPase activity (Prodromou et al., 1997, Stebbins et al., 1997). This prevents the formation of mature multimeric Hsp90 complexes capable of chaperoning client proteins, which in turn are targeted for degradation *via* the ubiquitin proteasome pathway. Although geldanamycin presented activity in human tumour xenograft models, unacceptable levels of hepatotoxicity at doses required for therapeutic activity stopped the progression of this compound to clinical trials (Supko et al., 1995).

In an effort to overcome geldanamycin drawbacks, a range of analogues was screened and 17-AAG was discovered. This compound showed significantly less hepatotoxicity than geldanamycin (Page et al., 1997), yet retaining the property of Hsp90 inhibition, which resulted in client protein depletion and anti-tumour activity in cell culture and xenograft models (Schulte and Neckers, 1998, Kelland et al., 1999). While 17-AAG appeared to be the most promising member of the benzoquinone ansamycin family, continuous efforts have been made to develop additional analogues with improved pharmaceutical properties, such as solubility and oral bioavailability, and different pharmacological behaviour (Drysdale et al., 2002).

Radicicol is an antifungal agent that also binds to Hsp90's N-terminal domain, inhibiting chaperone activity and suppressing transformation by the *SRC* and *RAS* oncogenes (Sharma et al., 1998). The potency to inhibit Hsp90 ATPase activity is higher for radicicol than for geldanamycin and 17-AAG, even though they have similar growth inhibitory effects on tumour cells (Roe et al., 1999). This compound binds to all Hsp90 family members, although it has higher binding affinity to the cytosolic Hsp90 isoforms than to GRP94 or TRAP1 (Schulte et al., 1999). Similarly to 17-AAG, the structure of radicicol has been subjected to some changes in order to eliminate undesirable features that could lead to unfavourable metabolism, without losing the important interactions required for Hsp90 inhibition. The unstable chemical nature of radicicol results in lack of anti-tumour activity *in vivo*. However, a few derivatives of this compound have been synthesised, which retain the Hsp90 inhibitory activity and exhibit *in vivo* anti-tumour activity in human tumour xenograft models (Soga et al., 1999).

5.1.4.2 Hsp90 C-terminal inhibitors

Despite the majority of Hsp90 inhibitors under clinical evaluation disrupts the chaperone cycle by replacing ATP in the N-terminal domain nucleotide-binding pocket, the Hsp90 C-terminal domain can also be targeted by drugs (Figure 5.3).

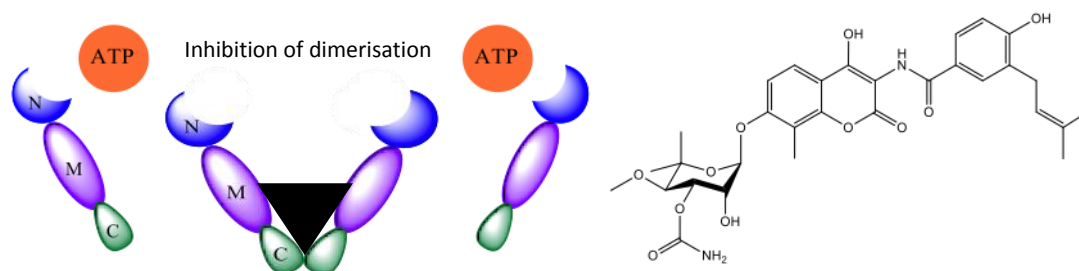


Figure 5.3 Hsp90 C-terminal inhibitors. Model of Hsp90 C-terminal inhibition: inhibitor represented in black preventing dimerisation. Example of a C-terminal inhibitor: novobiocin. Adapted from (Trepel et al., 2010).

As mentioned previously, the C-terminal domain of Hsp90 is involved in the formation of dimers, which is crucial for promoting changes at the N-terminal and consequent ATP binding and hydrolysis. Therefore, inhibition of the C-terminal

results in reduced ATPase activity, as well as failure of client proteins' folding and subsequent ubiquitination and degradation (Donnelly and Blagg, 2008).

Compounds from the coumarin family of antibiotics, such as novobiocin, clorobiocin and coumermycin A1, are known to bind to the C-terminal of Hsp90 (Marcu et al., 2000a). This has resulted in inhibition of Hsp90 function and degradation of Hsp90-chaperone signalling proteins (Marcu et al., 2000b).

An example of the therapeutic importance of inhibiting the C-terminal of Hsp90 is in hormone-dependent breast and prostate cancers. Research has revealed that the level of glucocorticoid receptor protein in HeLa cells may be effectively reduced by novobiocin and its family derivative coumermycin A1. Furthermore, the same study has shown that TPR immunophilins may be influenced by novobiocin, as their receptor, MEEVD, is located at the C-terminal of Hsp90 (Allan et al., 2006).

Initially, these compounds were not seen as clinically useful Hsp90 inhibitors, due to their poor affinity for Hsp90 and their higher affinity for type II topoisomerases (Donnelly and Blagg, 2008). Additionally, poor water solubility and absorption contributed to their poor bioavailability. However, recent advances have been made to improve their properties. Compound F-4 is an example, which demonstrated superior efficacy to 17-AAG in inducing apoptosis in prostate cancer cell lines (Matthews et al., 2010). Another novobiocin derivative, KU135, also proved more potent than 17-AAG in inhibiting cell proliferation and promoting apoptosis (Shelton et al., 2009). Other studies have evaluated a set of novobiocin derivatives and have identified various promising compounds with anti-proliferative activity in several cancer cell lines (Radanyi et al., 2009). Glycosylation has recently proved to be an effective method to enhance inhibitory activity and increase selectivity. Glycosylated analogues of novobiocin exhibited 100-fold improved activity against breast, brain, pancreatic, lung and ovarian cancers as well as an increase in selectivity (Patel et al., 2011).

These findings strongly support further medicinal chemistry development and preclinical evaluation of C-terminal Hsp90 inhibitors in cancer.

Although Hsp90 has emerged as a promising target for anticancer therapy, its presence in normal cells under physiological conditions may present a disadvantage, as it is expected that drugs targeting Hsp90 will have side effects on normal cellular function. This issue of therapeutic selectivity can only be resolved by evaluating Hsp90 inhibitors in preclinical models and ultimately in clinical trials.

To date, there are 17 Hsp90 inhibitors undergoing clinical evaluation for multiple cancer indications (Barrott and Haystead, 2013). Although there are currently no approved Hsp90-targeted drugs, there has been considerable progress on several areas. One of the most important advances has been in the drug design, for example, 17-AAG started Phase III evaluation with an improved formulation that overcomes several toxicity problems common in earlier trials (Kim et al., 2009). Other chemically distinct Hsp90 inhibitors have also entered clinical evaluation with improved properties, including oral bioavailability. Another field of advance is the choice of the appropriate indication, in which recent studies have enlightened some key points to take into account in the future development of Hsp90 inhibitors (Workman et al., 2007).

5.1.5 Methods to study Hsp90 inhibition

Although there are various assays to test Hsp90 activity, there is no standardised method to ascertain Hsp90 inhibition (Jhaveri et al., 2012). There is also no standard assay to specifically distinguish a C- or N-terminal inhibitor. Research has previously demonstrated a combined enzymatic/chemical glycosylation strategy for the discovery of Hsp90 inhibitor analogues with a 2.7×10^4 increased selectivity of anticancer activity compared with the antimicrobial effect (Patel et al., 2011). While formerly reported Western blot methods (Burlison et al., 2006) are able to demonstrate general Hsp90 binding of such candidates, they do not allow the pharmacologically critical distinction between inhibition of the C- and N-terminal domains.

The few currently available methods developed to determine whether a drug is a C- or N-terminal inhibitor have significant limitations. The original affinity gel method

(Marcu et al., 2000a, Marcu et al., 2000b) is not convenient and the cytotoxicity test (Burlison et al., 2006) is convenient, but only an indirect test.

In this chapter, a native gel binding assay (nGBA) that not only allows qualitative distinction of the C- and N-terminal inhibitors, but also permits full quantitative characterisation with reliable binding constants is reported. Furthermore, an Hsp90 ATPase assay is used in combination with the nGBA to analyse the inhibition pattern of each inhibitor and calculate the inhibitors' dissociation constants.

Native gel electrophoresis, or non-denaturing electrophoresis, is the technique behind the nGBA. It is a type of electrophoresis used for separating and analysing proteins that is similar to SDS-PAGE, but performed under non-denaturing conditions, i.e. in the absence of SDS, DTT and heat. Under such conditions proteins keep their original structure and properties, which means the mobility of proteins in native gels will depend on both the protein's charge and its hydrodynamic size. The main advantage of this separation technology is that it allows the study of the structure and conformational changes of proteins (Robyt and White, 1987). Therefore, this was the method chosen to distinguish C- and N-terminal inhibitors of Hsp90, as they may lead to changes in Hsp90's structure when interacting with it.

As mentioned before, Hsp90 hydrolyses ATP, functioning like an ATPase. As a consequence of this behaviour, Hsp90 and the effect of its inhibitors can be studied in the same way enzymes are, according to enzyme kinetics and enzyme inhibition patterns. A section on enzyme kinetics and enzyme inhibition patterns can be found in Appendix.

5.2 Aims & Objectives

The main aim of this study was to develop and optimise a robust method for anti-cancer drug discovery, which allowed rapid screening and functional characterisation of heat shock protein 90 targeted compounds.

On one hand, the chosen approach should allow qualitative distinction between C- and N-terminal inhibitors of Hsp90.

On the other hand, the method should also permit full quantitative characterisation of each inhibitor with reliable binding constants.

Moreover, the technique should be relatively easy to master to facilitate reproducibility, suitable for the chemical properties of the majority of inhibitors, and as rapid and inexpensive as possible.

With the previous key points in mind, a native gel binding assay was developed and optimised. This method was then used in combination with an ATPase activity assay to fully characterise known C- and N-terminal inhibitors of Hsp90, as well as a novel novobiocin glycosylated derivative – glucosyl-novobiocin.

5.3 Materials & Methods

The source of all the chemicals and equipment used in the following experiments is specified after each one of them in the descriptions below, unless mentioned previously. A schematic diagram summarising the experiments carried out in this study is represented in Figure 5.4.

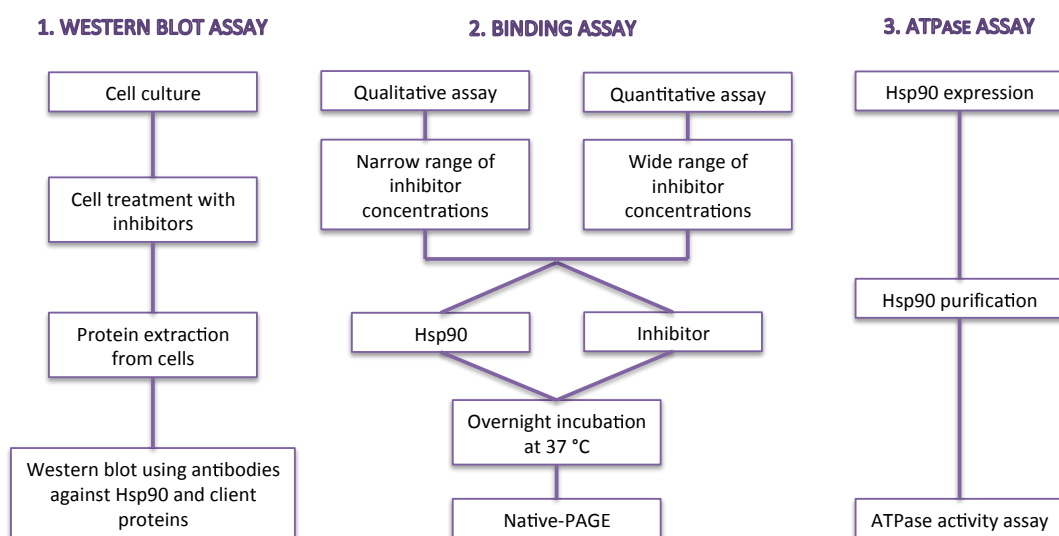


Figure 5.4 Schematic diagram summarising the experiments conducted in this study.

5.3.1 Western blot study of MCF-7 breast cancer cells treated with novobiocin analogues

5.3.1.1 Cell culture, treatment with novobiocin analogues and harvesting

These experiments were done with the collaboration of Dr. Schatzlein's group from the Department of Pharmaceutical and Biological Chemistry of the UCL School of Pharmacy. MCF-7 breast cancer cells (Human Caucasian breast adenocarcinoma) were obtained from the European Collection of Cell Cultures (ECACC) and cultured in Dulbecco's Modified Eagle Medium (DMEM, Gibco, Invitrogen, USA) supplemented with 10 % fetal bovine serum (Biosera, UK), 2 mM L-glutamine and 1

% non-essential amino acids (Gibco, Invitrogen, USA). Cells were grown at 37 °C in a 5 % CO₂, 95 % humidity incubator and passaged 2-3 times a week.

The day before the experiment, cells were seeded in 25 cm² flasks (4x10⁴ cells/cm²) to a total volume of 5 mL. The growing medium was then replaced by 1 mL of fresh culture medium and 50 µL of the compound of interest (previously dissolved in methanol) were subsequently added to each flask. Considering the dose-dependent activity of the compounds, concentrations were selected based on the previously reported IC₅₀ values (Patel et al., 2011). Cells were exposed to increasing concentrations of novobiocin (Nov, Calbiochem, USA), glucosyl-novobiocin (Glc-Nov) and galactosyl-novobiocin (Gal-Nov), 0.1, 1, 5, 10 and 40 µM. Glc-Nov and Gal-Nov were synthesised by a colleague in our group. A batch of non-treated cells was used as control. After 24 h of continuous drug exposure, cells were washed and harvested for total protein extraction.

5.3.1.2 Protein extraction from cells

Cells were harvested and their protein content was extracted as described in section 2.3.1.2.

Protein concentrations of all cell lysate samples were determined using the RCDC Protein Assay Kit (Bio-Rad, UK), according to the description in section 2.3.3.

5.3.1.3 Western blot assay

A total of 10 µg of protein per well was loaded onto precast gels, Mini-Protean TGX precast gels, any kD, 10-well comb, 30 µL/well (Bio-Rad, UK). Proteins were separated by SDS-PAGE and transferred onto nitrocellulose membranes (Hybond-C Extra, Amersham Biosciences, UK) using a Mini Trans-Blot Transfer Cell (Bio-Rad, UK) for 1 h at 100 V, as described in section 2.6.2.

After blocking with 1 % BSA (Sigma-Aldrich, UK) in TBS buffer for 1 h at room temperature, the membranes were probed with rabbit polyclonal primary antibodies against Hsp90 (ab13495, Abcam, UK), diluted 1:1000; Raf1 (SAB4300291,

Sigma-Aldrich, UK), diluted 1:100; and Actin (A2066, Sigma-Aldrich, UK), diluted 1:100, in blocking solution overnight at 4 °C. The membranes were washed 4x with TBS buffer containing 0.05 % Igepal (Sigma-Aldrich, UK) and subsequently incubated for 1.5 h at room temperature with a horseradish peroxidase (HRP)-conjugated anti-rabbit secondary antibody (NA934, GE Healthcare, UK) at a dilution of 1:2000, in blocking solution. After incubation with secondary antibody, membranes were washed again with TBS buffer containing 0.05 % Igepal. Protein bands were developed using a Pierce ECL Western Blotting Substrate (Thermo Scientific, UK) and visualised with the GeneGnome chemiluminescence imaging system, using the GeneSnap software (SynGene Bio Imaging, UK). The western blot assay was performed at least three times for each antibody.

5.3.2 Hsp90 binding assay – native-PAGE

Prior to incubation of Hsp90 with the various inhibitors at different concentrations, the purity of the commercially acquired protein was tested by SDS-PAGE and native-PAGE. For SDS-PAGE, three amounts of protein were used (2.5, 1.25, 0.625 µg) and for native-PAGE 1.25 µg of protein were tested. Both techniques were performed according to sections 2.4.1 and 2.4.2. Protein band visualisation was achieved through Coomassie blue staining, as described in section 2.5.1.

5.3.2.1 Qualitative assay

Hsp90 protein (1 mg/mL, 1.25 µg, Abcam, UK) was incubated with novobiocin, glucosyl-novobiocin and geldanamycin (InvivoGen, UK) at 1/10, 1 and 10 times the IC₅₀, i.e. 70 µM, 700 µM and 7 mM for novobiocin; 1 µM, 10 µM and 100 µM for glucosyl-novobiocin; 5 nM, 50 nM and 500 nM for geldanamycin. The total mixture volume was 5 µL. Suitable stock solutions were prepared so that the volume added of each of the inhibitors at different concentrations was 3.75 µL. The same volume of distilled water was added to the control without inhibitor. Samples were incubated overnight at 37 °C before analysis by native polyacrylamide gel electrophoresis.

5.3.2.2 Quantitative assay

Hsp90 protein (1 mg/mL, 1.25 µg, Abcam, UK) was incubated with novobiocin at 0, 70, 140, 350, 700, 1400, 3500 and 7000 µM. The total mixture volume was 5 µL. Suitable stock solutions were prepared so that the volume added of each of the inhibitors at different concentrations was 3.75 µL. The same volume of distilled water was added to the control without inhibitor. Samples were incubated overnight at 37 °C before analysis by native-PAGE.

The same procedure was followed using glucosyl-novobiocin, for 9 different concentrations at 0, 0.1, 1, 2, 5, 10, 20, 50 and 100 µM. Furthermore, 8 different concentrations of geldanamycin at 0, 0.5, 5, 10, 25, 50, 100 and 250 nM; and 9 different concentrations of geldanamycin at 0, 1 nM, 10 nM, 50 nM, 100 nM, 500 nM, 1 µM, 5 µM, and 10 µM were incubated with Hsp90 as described above.

5.3.2.3 Native-PAGE

After incubating all the controls and mixtures of Hsp90 + inhibitor overnight at 37 °C, 2x native sample buffer was added to each sample tube and the mixtures were loaded into the wells of 8 % native polyacrylamide gels, without stacking gel. All gels were prepared and run in triplicate. Proteins were separated in the absence of SDS by native gel electrophoresis and visualised with Coomassie Blue stain (Instant Blue, Expedeon, UK) followed by silver stain (Pierce Silver Stain Kit, Thermo Scientific, UK), as described in sections 2.4.2, 2.5.1 and 2.5.2.

5.3.3 Hsp90 ATPase assay

The following experiments were performed by Miss Yixi Zhang, an MRes student at the time in our group.

5.3.3.1 Protein expression and purification

Human Hsp90α was a generous gift from Prof. Houry in the University of Toronto, Canada. The procedure was followed according to the literature (Zhao et al., 2010,

Panaretou et al., 1998). Briefly, the plasmid was transformed in *E. coli* strain BL21-CodonPlus (DE3)-RIL (Agilent Technologies, UK). A single colony was grown at 37 °C until OD600 reached 0.4-0.7. Proteins were induced for 5 h at 30 °C by adding 0.1 mM isopropyl β -D-1-thiogalactopyranoside (IPTG, Sigma-Aldrich, UK). Cells were harvested by centrifugation and broken by sonication. Proteins were purified using HisTrap FastFlow crude columns (GE Healthcare, UK) and were stored in storage buffer (25 mM Tris-HCl, pH7.5; 150 mM KCl; 10 % glycerol; 0.5 mM DTT).

5.3.3.2 ATPase activity assay

The ATPase activity assay was based on a coupled enzyme assay, where the ADP hydrolysed by Hsp90 is regenerated by phosphokinase in the presence of phosphoenolpyruvate. The reaction was monitored through the disappearance of NADH at 340 nm (Zhao et al., 2010, Panaretou et al., 1998). The reaction mixture was set up in a final volume of 100 μ L containing 100 mM Tris-HCl pH 7.4 (Sigma-Aldrich, UK), 20 mM KCl (Sigma-Aldrich, UK), 6 mM MgCl₂ (Fisher Scientific, UK), 3 mM phosphoenolpyruvate acid monopotassium salt (Sigma-Aldrich, UK), 0.2 mM β -nicotinamide-adenine dinucleotide disodium salt (Fisher Scientific, UK), 18-28 U/mL lactate dehydrogenase (Sigma-Aldrich, UK), 12-20 U/mL pyruvate kinase (Sigma-Aldrich, UK) and 10 μ L of Hsp90. The concentrations of ATP (Sigma-Aldrich, UK) and inhibitors varied in different experiments, which are illustrated respectively below. The decrease in NADH absorbance at 340 nm was recorded continuously for 1 h using a spectrophotometer (Pherastar, BMGLabtech, UK).

ATP concentrations were fixed at 0, 10, 20, 50, 100 and 250 μ M. Novobiocin concentrations varied at 0, 100, 300, 500 and 700 μ M. Glucosyl-novobiocin concentrations varied at 0, 1, 5, 10, 20, 50, and 100 μ M. Geldanamycin concentrations varied at 0, 10 and 20 nM. Native hydrolysis of ATP was measured under the same conditions, but without Hsp90 and inhibitors.

5.4 Results & Discussion

This study was divided in three parts: western blot assay, binding assay and ATPase assay. The first part was a preliminary experiment, which consisted in a western blot assay using a cancer cell line and appropriate antibodies to detect Hsp90 and one of its client proteins, Raf-1. Prior to the assay, cells were treated with increasing concentrations of different Hsp90 inhibitors, namely novobiocin and two derivatives, glucosyl-novobiocin and galactosyl-novobiocin. The aim of this experiment was to demonstrate the binding of these two novobiocin analogues to Hsp90, similarly to novobiocin itself, resulting in inhibition of Raf-1. This proof of inhibitory activity would support the use of the analogues in the subsequent experiments.

The second part included the Hsp90 binding assay, through which it was possible to distinguish the binding site of inhibitors interacting with Hsp90, and accordingly differentiate C-terminal from N-terminal inhibitors. The use of a wide range of inhibitor concentrations also allowed to calculate the IC_{50} value of each inhibitor using their dose-response curves.

Finally, in the third part of this study, the Hsp90 ATPase assay was performed to characterise the inhibition pattern of the C- and N-terminal inhibitors tested by comparison with known inhibition patterns. The inhibition constant, K_i , of each inhibitor was also calculated in this experiment using their Lineweaver-Burk plots.

Detailed results and discussion of the mentioned three parts are presented in the following sections.

5.4.1 Western blot study of MCF-7 breast cancer cells treated with novobiocin analogues

Western blot is a technique used to detect specific proteins in a given sample of cell/tissue homogenate. In the first stage, it involves gel electrophoresis to separate proteins either in their native state or denatured; then the proteins are transferred to a membrane; and finally, antibodies specific to the target proteins are used to detect the protein bands (Renart et al., 1979, Towbin et al., 1979). Usually, the detection process occurs with a modified antibody, which is linked to a reporter enzyme; when exposed to an appropriate substrate, this enzyme drives a colorimetric, chemiluminescent or fluorimetric reaction, producing a colour or fluorescence (Hames and Rickwood, 1990). The intensity of the protein bands can then be compared among different samples for relative quantitative purposes.

In order to relatively quantify the abundance of a specific protein among distinct samples, it is crucial to make sure the disparities in the intensity of the bands visualised on the blots are due to different amounts of that protein in those samples, and not due to loading differences. To guarantee that the same total protein amount for each sample was loaded into the wells of the SDS-PAGE gel, prior to protein separation and Western blot assay, each protein homogenate was subjected to a protein concentration assay.

5.4.1.1 Protein concentration assay

Protein concentration was tested using a commercial kit. Firstly, a calibration curve was generated with absorbance values versus the corresponding concentrations of the standard bovine plasma γ -globulin, which were prepared by serial dilutions from the initial stock concentration of 1.5 mg/mL. Then, a linear regression was applied to the calibration curve and protein concentrations were calculated using the equation. Figure 5.5 displays an example of calibration curve used in this experiment and its respective equation. Table 5.1 shows the calculated protein concentrations of the various MCF-7 breast cancer cell line samples treated with the three inhibitors in different concentrations.

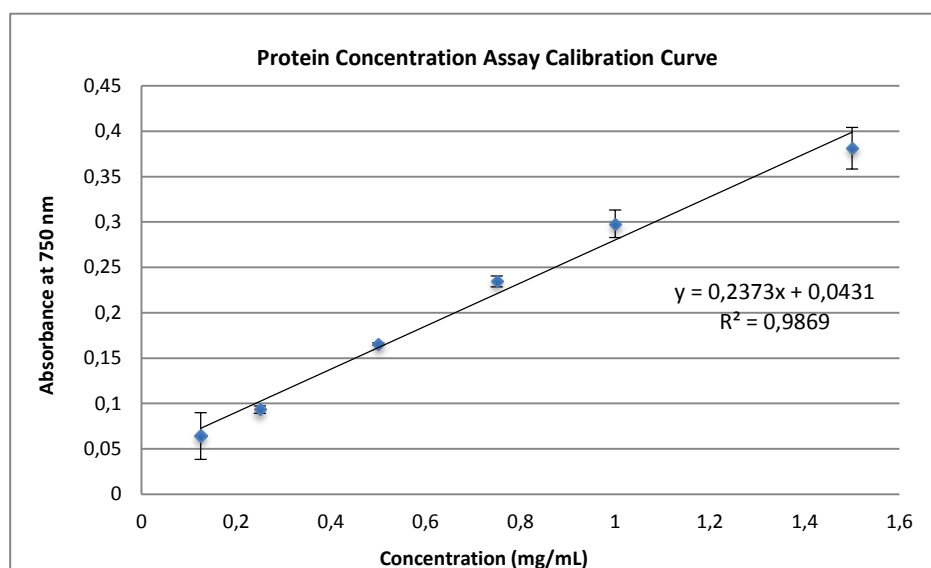


Figure 5.5 Protein concentration assay calibration curve. Protein concentration assay was performed using a commercial kit according to the manufacturer's instructions. Bovine plasma γ -globulin was used as standard in the following concentrations: 0.125, 0.25, 0.5, 0.75, 1.0, 1.5 mg/mL. Equation of the linear regression is shown in the graph.

Table 5.1 Protein concentration of the various MCF-7 breast cancer cell line samples treated with the three inhibitors in different concentrations. Protein concentration assay was performed using a commercial kit according to the manufacturer's instructions. The concentrations were calculated using the equation displayed in Figure 5.5.

Inhibitor	Inhibitor Concentration (μM)	Protein Concentration (mg/mL)
Control (no inhibitor)	—	0.354
Novobiocin	0.1	0.139
	1	0.233
	5	0.185
	10	0.185
	40	0.305
Glucosyl-novobiocin	0.1	0.126
	1	0.113
	5	0.181
	10	0.105
	40	0.168
Galactosyl-novobiocin	0.1	0.147
	1	0.143
	5	0.229
	10	0.231
	40	0.065

5.4.1.2 Western blot assay

Previously developed assays for the characterisation of Hsp90 inhibitors include a Western blot assay, which has been able to demonstrate general binding of the inhibitors to Hsp90 (Burlison et al., 2006). Based on that, the present experiment was designed to test Hsp90 binding of a known and two novel Hsp90 inhibitors.

In this experiment, three Hsp90 inhibitors were used: novobiocin (Nov), which is a known inhibitor of Hsp90, and the two derivatives glucosyl-novobiocin (Glc-Nov) and galactosyl-novobiocin (Gal-Nov), obtained by modification of novobiocin's structure. These analogues have been enzymatically/chemically synthesised through the addition of sugars to the coumarin core of novobiocin with the aim of improving their physicochemical properties and their anti-cancer effect (Patel et al., 2011).

MCF-7 is a widely studied breast cancer cell line isolated from a 69-year-old Caucasian woman in 1970. The origin of the cells was a pleural effusion from an invasive breast ductal carcinoma. They possess oestrogen and progesterone receptors and present a proliferative response to oestrogen (Soule et al., 1973, Levenson and Jordan, 1997). This particular cell line was selected for the Western blot assay owing to results obtained in previous studies, in which the anti-cancer activity of novobiocin and the analogues mentioned above was tested using various cancer cell lines. The results revealed that among all the cancer cell lines tested, glucosyl-novobiocin and galactosyl-novobiocin exhibited the highest anti-proliferative activity against the MCF-7 breast cancer cell line (Patel et al., 2011).

Hsp90 appears to be crucial for the correct folding, stability, localisation and function of a subset of proteins that are heavily involved in creating and maintaining the malignant phenotype. These include Raf-1, which is a key player in the Ras-Raf-MEK-ERK signalling pathway (Schulte et al., 1996), among others such as Akt (Basso et al., 2002), EGFR (Sawai et al., 2008), HER-2 (Solit et al., 2002), v-Src (Whitesell et al., 1994). Depletion of these oncogenic kinases is readily seen with Hsp90 inhibitors. In this experiment, Hsp90 client Raf-1 was chosen to confirm the efficacy of the inhibitors under assessment.

After exposing MCF-7 breast cancer cells to increasing concentrations of the three inhibitors, 0 (control), 0.1, 1, 5, 10 and 40 μM , their total protein content was extracted and Western blot assays were performed, using an anti-Hsp90 antibody and an anti-Raf-1 antibody to assess the abundance of these proteins in each cell lysate. An anti-Actin antibody was used as control. The results are shown in Figure 5.6.

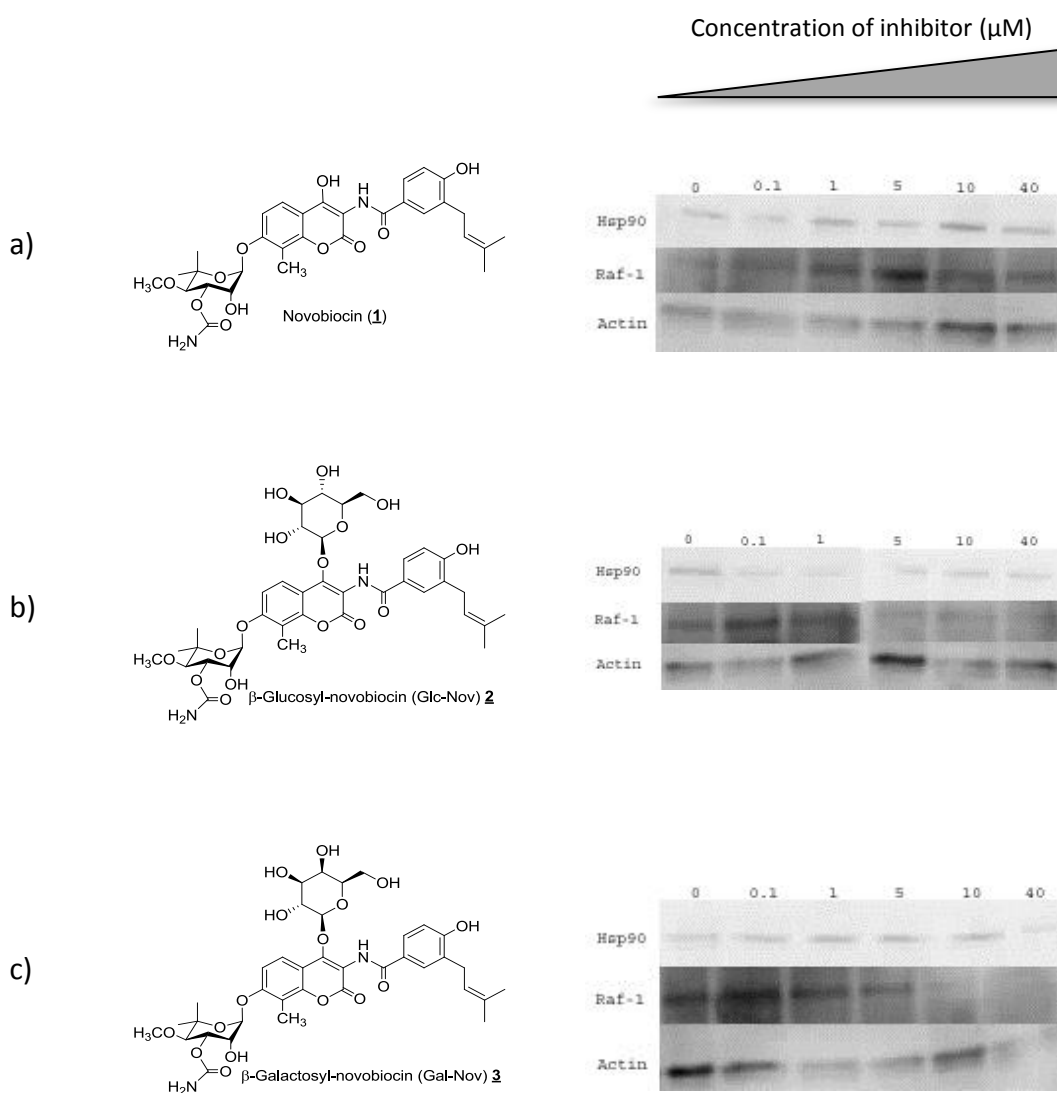


Figure 5.6 Western blot study of MCF-7 breast cancer cells treated with novobiocin analogues. a) Novobiocin, b) Glucosyl-novobiocin (Glc-Nov), c) Galactosyl-novobiocin (Gal-Nov). Unit: μM . Expression of Hsp90 dependent Raf-1 protein reduced at 5 μM (Glc-Nov) and 10 μM (Gal-Nov), but not Hsp90 itself and Hsp90 independent Actin. This indicates that both Glc-Nov and Gal-Nov bind to Hsp90 as novobiocin does.

The analysis of the Western blot assay results revealed that the expression of Hsp90 dependent Raf-1 protein reduced at 5 μ M, when MCF-7 breast cancer cell lines were treated with glucosyl-novobiocin, and 10 μ M, when they were treated with galactosyl-novobiocin. However, no change in expression of Raf-1 was observed when the breast cancer cells were treated with novobiocin. These results are all consistent with the IC_{50} values calculated for these inhibitors in a former study, based on which the range of inhibitor concentrations used in this experiment was established (Patel et al., 2011).

In addition, neither Hsp90 itself nor Hsp90 independent Actin showed a reduction in expression. This indicates that both glucosyl-novobiocin and galactosyl-novobiocin bind to Hsp90 as novobiocin does, resulting in inhibition of Hsp90 client protein Raf-1.

Hsp90 inhibition induces degradation of Hsp90 client proteins, leading to a combinatorial inhibition of multiple oncogenic signalling pathways with consecutive growth arrest and apoptosis. A study done in various cell lines has demonstrated the efficacy of the Hsp90 inhibitor SNX-2112, which led to degradation of several Hsp90 client proteins and abrogation of Ras/Raf/MEK/MAPK and PI3K/Akt signalling, also using a Western blot assay (Bachleitner-Hofmann et al., 2011).

5.4.2 Hsp90 binding assay – native-PAGE

The method chosen to analyse the interaction between Hsp90 and different inhibitors, allowing distinction of the binding site (C- or N-terminal) of the inhibitors was a native gel binding assay (nGBA). Native-PAGE is an electrophoretic technique that is performed under non-denaturing conditions, i.e. in the absence of denaturing agents such as SDS, DTT and heat, unlike what happens in SDS-PAGE. Proteins in their denatured state assume a primary, linear structure, making it impossible to study conformational changes.

In native-PAGE, proteins keep their original structure and are separated on the basis of their size, shape and charge. While native-PAGE does not provide direct measurement of molecular weight, the technique can provide useful information about protein charge, conformation, self-association or aggregation, and the binding of other proteins or compounds. Since the protein retains its folded conformation, its size and mobility on a native gel will also vary with the nature of this conformation; more compact conformations will show higher mobility and larger structures will move slower (Robyt and White, 1987).

Thus, native-PAGE allows the visualisation of Hsp90's different structures. As mentioned in the introduction of this chapter, Hsp90 exists in two forms: monomer (84 kDa) and dimer (168 kDa), which may be separated on native gels, since the monomer migrates faster than the dimer. In line with the fact that the C-terminal domain of Hsp90 is responsible for its dimerisation, incubation of Hsp90 with C-terminal inhibitors leads to an increase in intensity of the monomer band. In opposition, incubation of Hsp90 with N-terminal inhibitors does not result in a change of intensity of the monomer band. Moreover, for C-terminal inhibitors and using the intensity of the monomer bands and the concentration of inhibitor, it is possible to build dose-response curves, through which the IC₅₀ value for each inhibitor can be determined.

In this experiment, Hsp90 was incubated overnight at 37 °C with different concentrations of a known C-terminal inhibitor, novobiocin (Nov), and a known N-

presence of SDS, DTT and heat characteristic of SDS-PAGE, no dimer was present. The native-PAGE gel, b), confirmed the presence of the Hsp90 monomer, between 75 and 100 kDa, and the Hsp90 dimer, between 150 and 250 kDa. In the absence of SDS, DTT and heat, proteins retained their native conformations. These results ratified the purity of the commercial Hsp90 and its suitability for the nGBA, as no other bands were visible on the gels.

In addition, the use of three different Hsp90 loading amounts for SDS-PAGE, made it possible to conclude that 1.25 μg was the most appropriate loading amount to carry out the nGBA.

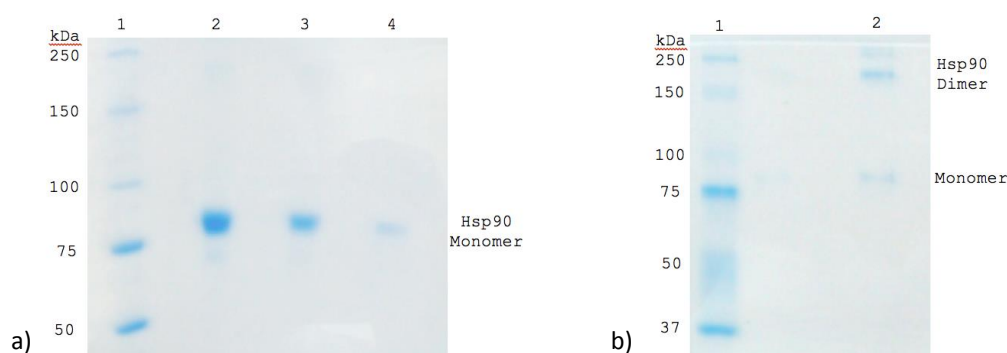


Figure 5.8 Commercial Hsp90 gel analysis. a) 5 % SDS-PAGE gel. 1, marker. 2-4, commercial Hsp90 (1 mg/mL) 2.5 μg , 1.25 μg and 0.625 μg , respectively. b) 10 % Native-PAGE gel. 1, marker. 2, commercial Hsp90 (1 mg/mL) 1.25 μg . Gels were stained by Coomassie stain. The SDS-PAGE gel showed a single band between 75 and 100 kDa, which corresponds to the Hsp90 monomer. No dimer was present when the protein was denatured. The native-PAGE gel confirmed the presence of the Hsp90 monomer, between 75 and 100 kDa, and the Hsp90 dimer, between 150 and 250 kDa.

5.4.2.2 Qualitative assay

Firstly, a qualitative assay was designed with a narrow range of inhibitor concentrations to test the inhibitor binding site. The three inhibitors studied were incubated with Hsp90 in the following concentrations: 1/10, 1 and 10 times the IC_{50} . Reported IC_{50} values are 700 μM for novobiocin (Burlison et al., 2006), 10 μM for glucosyl-novobiocin (Patel et al., 2011) and 50 nM for geldanamycin (Patel et al., 2004).

According to the mechanism by which the C-terminal inhibitors interact with Hsp90, darker monomer bands were expected to be observed when increasing concentrations of novobiocin and glucosyl-novobiocin were incubated with Hsp90.

On the contrary, no change in the intensity of the monomer bands was expected for the incubation of Hsp90 with geldanamycin.

Figure 5.9 shows the native gel obtained with protein-inhibitor mixtures after overnight incubation at 37 °C. Hsp90 monomer bands are represented on the gel at a molecular weight between 75 and 100 kDa, and the dimer bands between 150 and 250 kDa. Regardless of the inhibitor concentration, there was clearly higher abundance of Hsp90 dimer than monomer, as the dimer bands were much darker than the monomer bands, which is in line with the fact that the dimer corresponds to the most common form of Hsp90 in physiological conditions (Wayne and Bolon, 2007). As expected, it was possible to visualise an increase in intensity of the monomer bands with increasing concentrations of the C-terminal inhibitors novobiocin and glucosyl-novobiocin. No change in the relative intensity of the monomer bands could be observed for the N-terminal inhibitor geldanamycin.

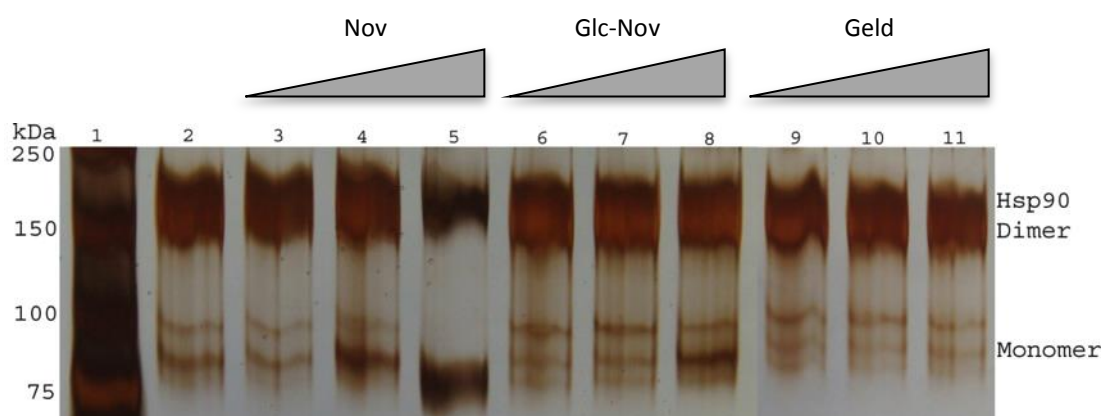


Figure 5.9 Native polyacrylamide gel analysis to probe Hsp90 C- and N-terminal binding targets. 1, marker. 2-11, commercial Hsp90 with different concentrations of inhibitors. 2, control (no inhibitor); 3-5, with novobiocin at 1/10, 1 and 10 times the IC₅₀ (700 μM), respectively; 6-8, with Glc-Nov at 1/10, 1 and 10 times the IC₅₀ (10 μM), respectively; 9-11, with geldanamycin at 1/10, 1 and 10 times the IC₅₀ (50 nM), respectively. Protein-inhibitor mixtures were analysed by native gel electrophoresis after overnight incubation at 37 °C. Gel was stained by silver stain.

5.4.2.3 Quantitative assay

In order to verify the results of the qualitative assay and have enough data to build dose-response curves to determine the IC₅₀ values of the inhibitors, a wider range of inhibitor concentrations was used in the quantitative assay.

This time, novobiocin was incubated with Hsp90 under the same conditions used in the qualitative assay, but at 0, 1/10 (70 μM), 1/5 (140 μM), 1/2 (350 μM), 1 (700 μM), 2 (1400 μM), 5 (3500 μM) and 10 (7000 μM) times the IC_{50} (700 μM). The native gel obtained and the corresponding response curve are depicted in Figure 5.10.

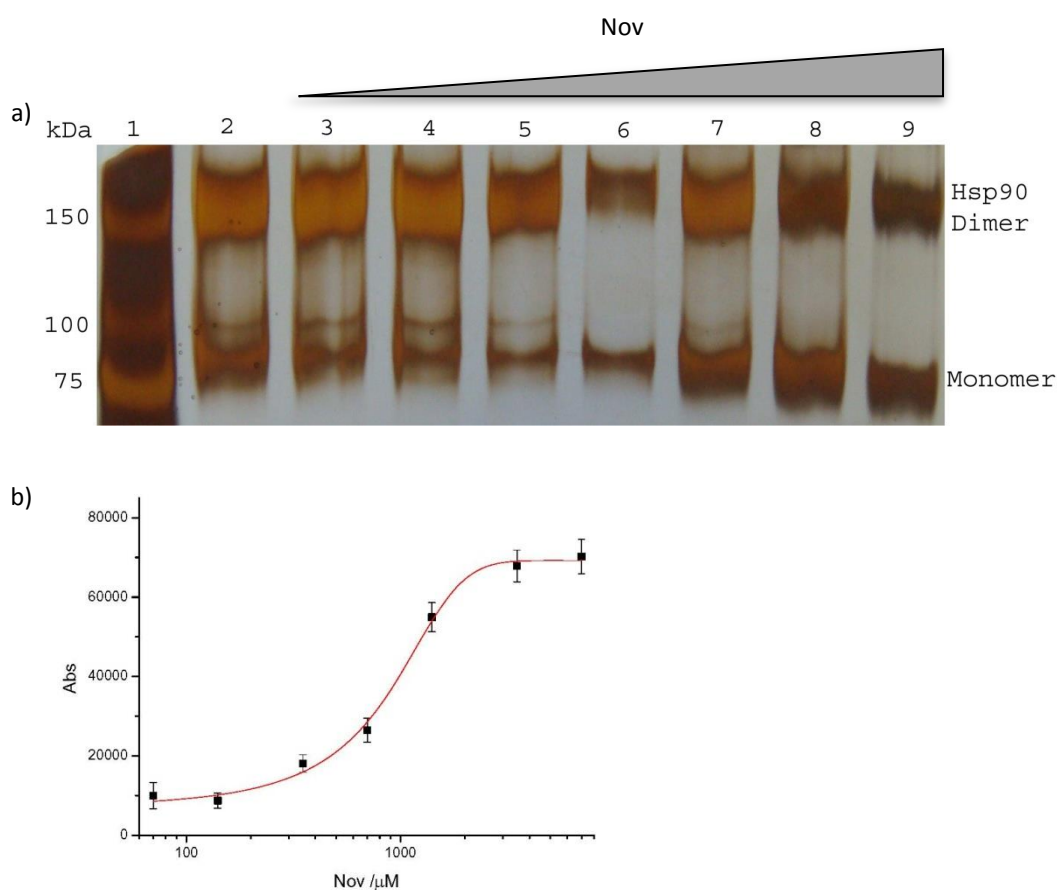


Figure 5.10 Native polyacrylamide gel analysis to probe novobiocin IC_{50} . a) Hsp90 binding assay. 1, marker. 2-9, commercial Hsp90 with different concentrations of novobiocin. 2, control (no inhibitor); 3-9, novobiocin at 1/10, 1/5, 1/2, 1, 2, 5 and 10 times the IC_{50} (700 μM), respectively. Protein-inhibitor mixtures were analysed by native gel electrophoresis after overnight incubation at 37 $^{\circ}\text{C}$. Gel was stained by silver stain. b) Response curve of novobiocin. Abs was obtained from gel a). This aligned with the fact that novobiocin is an Hsp90 C-terminal inhibitor. $\text{IC}_{50} = 813 \pm 149 \mu\text{M}$.

Once more, it could be observed that the monomer bands became darker with increasing concentrations of inhibitor. Therefore, it could be confirmed that novobiocin influenced Hsp90 dimerisation, as it prevented the formation of dimers, supporting the fact that novobiocin is a C-terminal inhibitor of Hsp90.

IC₅₀ determination from the dose-response curve was $813 \pm 149 \mu\text{M}$, which was similar to the IC₅₀ value previously reported for novobiocin ($700 \mu\text{M}$) (Burlison et al., 2006). This result proved that the quantitative assay was reliable.

As a novobiocin derivative, glucosyl-novobiocin was anticipated to share similar inhibition mechanism as novobiocin and be a C-terminal inhibitor. Thus, an increase in intensity of the monomer bands was predicted for higher concentrations of inhibitor. In addition, when the intensity of the monomer bands remained constant, it could be concluded that the inhibitory concentration had achieved its maximum, allowing the determination of the IC₅₀ value through the dose-response curve.

In fact, darker monomer bands were seen for increasing concentrations of glucosyl-novobiocin, after overnight incubation at 37 °C of Hsp90 with that inhibitor at 0, 1/100 (0.1 μM), 1/10 (1 μM), 1/5 (2 μM), 1/2 (5 μM), 1 (10 μM), 2 (20 μM), 5 (50 μM) and 10 (100 μM) times the IC₅₀ (10 μM). The results are illustrated in Figure 5.11. From the native gel analysis it could be inferred that glucosyl-novobiocin shared the same binding site as novobiocin, i.e. the Hsp90 C-terminal domain.

Moreover, the IC₅₀ value calculated from the dose-response curve was $34.7 \pm 2.8 \mu\text{M}$, which is approximate to the value reported in the literature for glucosyl-novobiocin (10 μM) (Patel et al., 2011). This IC₅₀ value proved that glucosyl-novobiocin has stronger binding ability to Hsp90 than novobiocin, whose IC₅₀ is much higher, also confirming the results of previous research (Patel et al., 2011).

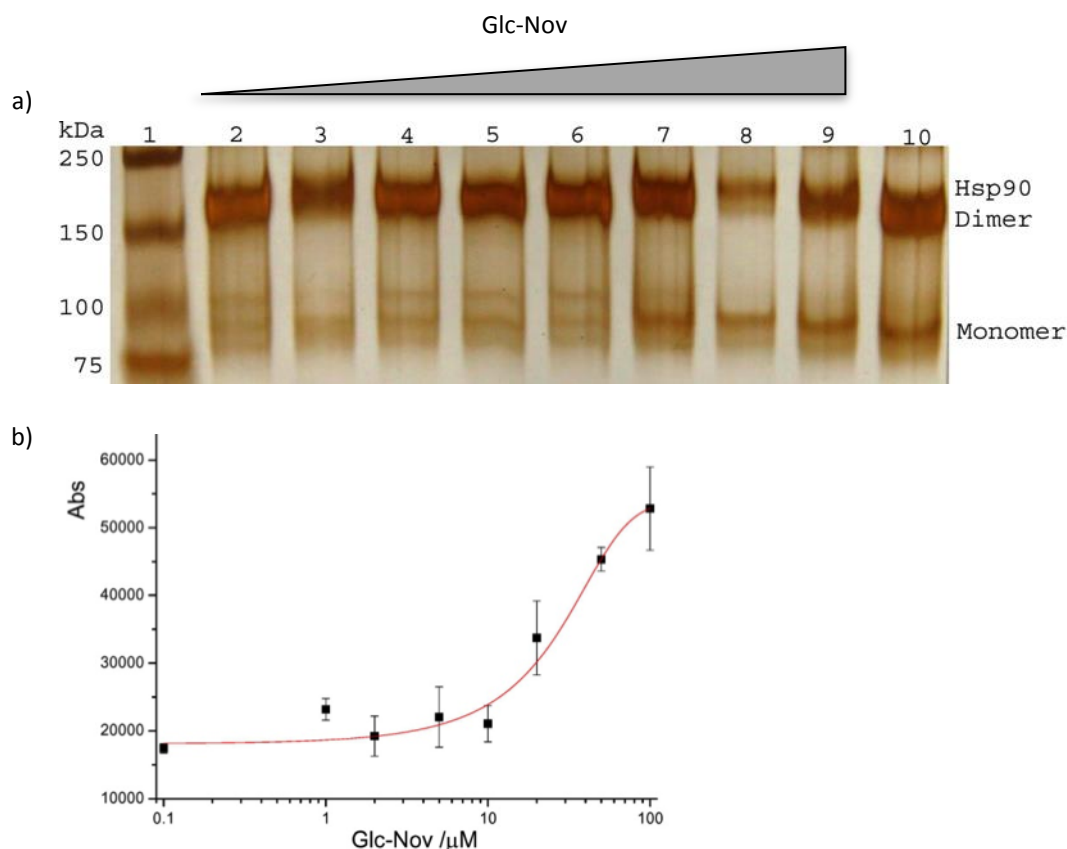
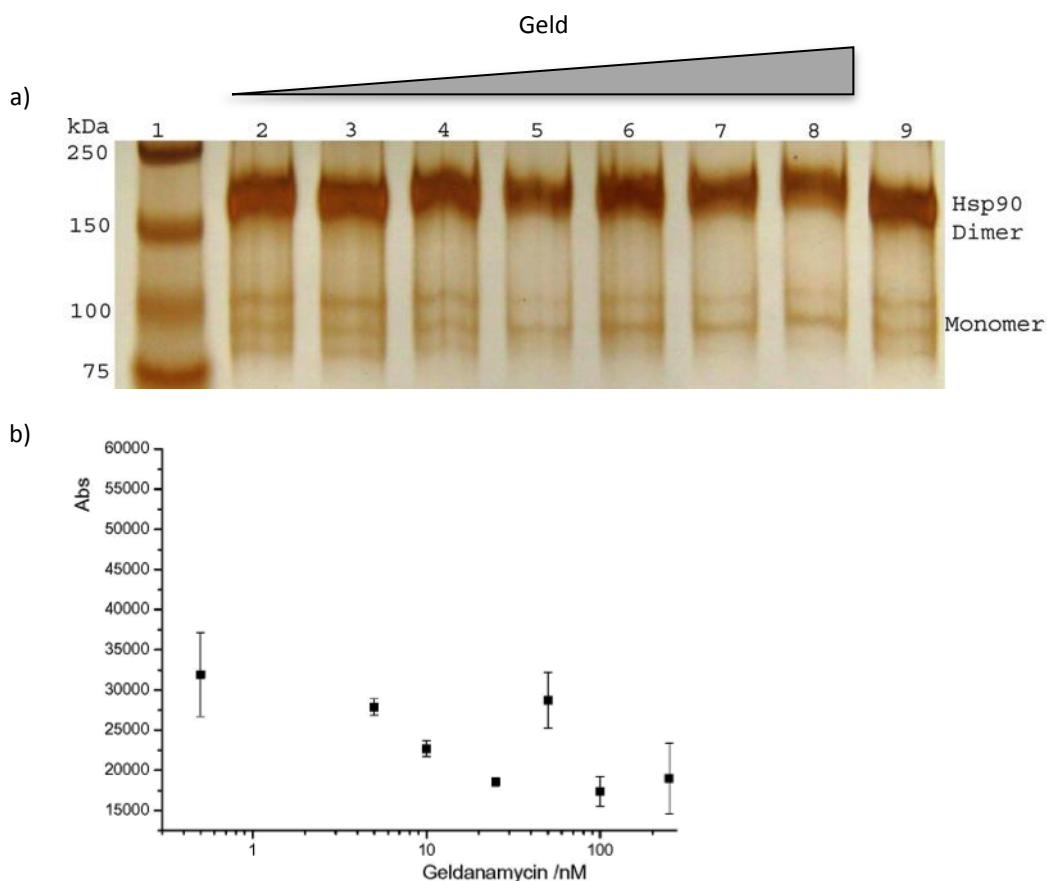


Figure 5.11 Native polyacrylamide gel analysis to probe glucosyl-novobiocin IC_{50} . a) Hsp90 binding assay. 1, marker. 2-10, commercial Hsp90 with different concentrations of Glc-Nov. 2-9, Glc-Nov at 1/100, 1/10, 1/5, 1/2, 1, 2, 5 and 10 times the IC_{50} (10 μM), respectively; 10, control (no inhibitor). Protein-inhibitor mixtures were analysed by native gel electrophoresis after overnight incubation at 37 °C. Gel was stained by silver stain. b) Response curve of glucosyl-novobiocin. Abs was obtained from gel a). This proved that Glc-Nov is an Hsp90 C-terminal inhibitor. $\text{IC}_{50} = 34.7 \pm 2.8 \mu\text{M}$.

As mentioned earlier, geldanamycin is a known N-terminal inhibitor that interacts with Hsp90 at the ATP binding pocket, having little or no effect on dimerisation. Hence, the intensity of Hsp90 monomer bands on a native gel should be constant and independent of the concentration of inhibitor.

The native gels presented in Figure 5.12 were obtained after overnight incubation at 37 °C of Hsp90 with geldanamycin at 0, 1/100 (0.5 nM), 1/10 (5 nM), 1/5 (10 nM), 1/2 (25 nM), 1 (50 nM), 2 (100 nM) and 5 (250 nM) times the IC_{50} (50 nM) and at 1, 10, 50, 100, 500, 1000, 5000 and 10000 nM. Either representing a narrower (a)) or a broader (c)) range of inhibitor concentrations, both gels show that the intensity of the monomer bands remained relatively constant.

Nonetheless, in gel c), lane 2 (1 nM) showed a different pattern probably due to experimental error. Lane 10 (control, no inhibitor) also performed differently as observed previously. The maximum concentration of geldanamycin (10 μ M) nearly reached its maximum solubility in water (20 μ M). In summary, it could be concluded that geldanamycin did not bind the C-terminal domain to mediate the formation of Hsp90 dimers, which corroborates that it is an N-terminal inhibitor.



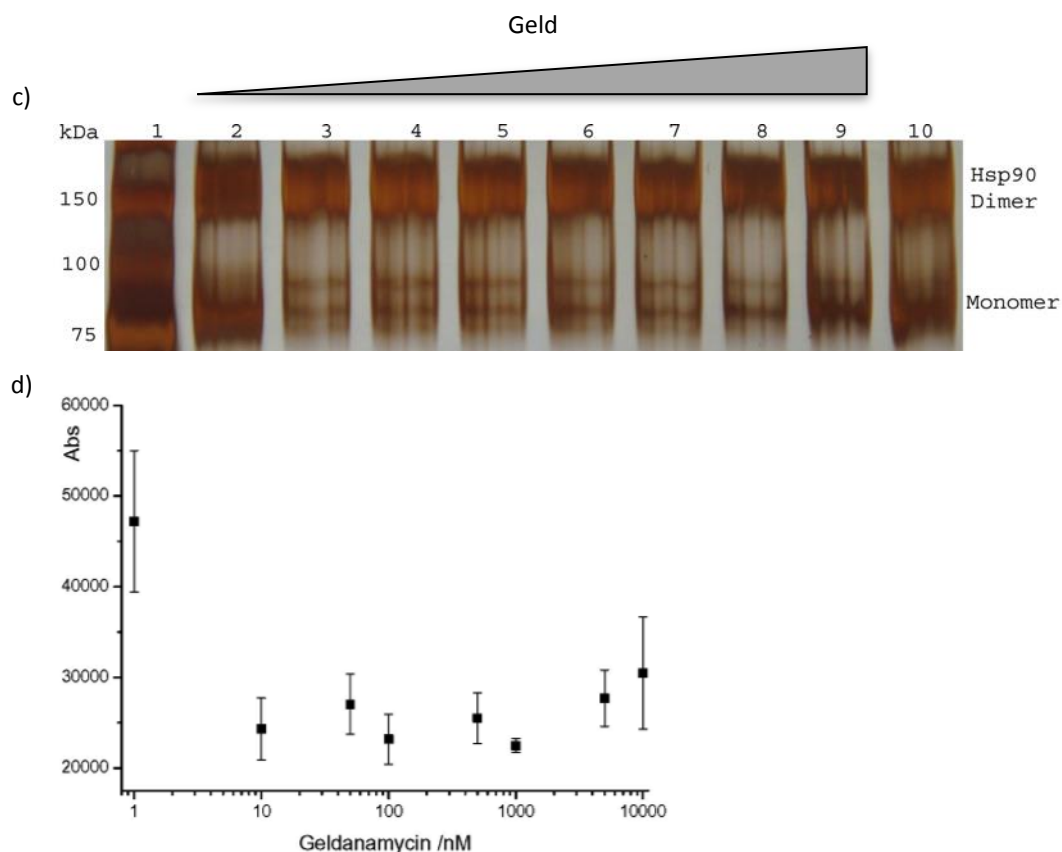


Figure 5.12 Native polyacrylamide gel analysis to probe geldanamycin IC_{50} . a) Hsp90 binding assay. 1, marker. 2-9, commercial Hsp90 with different concentrations of geldanamycin. 2-8, geldanamycin at 1/100, 1/10, 1/5, 1/2, 1, 2, 5 times the IC_{50} (50 nM), respectively; 9, control (no inhibitor). Protein-inhibitor mixtures were analysed by native gel electrophoresis after overnight incubation at 37 °C. Gel was stained by silver stain. b) Response curve of geldanamycin. Data showed that monomer stayed relatively stable. Abs was obtained from gel a). c) The same experiment with broader geldanamycin concentrations. 1, marker, 2-9, geldanamycin at 1, 10, 50, 100, 500, 1000, 5000 and 10000 nM, respectively; 10, control (no inhibitor). No obvious increase of monomer observed. Lane 2 (1 nM) showed a different pattern probably due to experimental error. Control (lane 10) also performed differently as observed previously. The maximum concentration of geldanamycin (10 μ M) nearly reached its maximum solubility in water. This proved that geldanamycin is an N-terminal inhibitor.

In conclusion, the nGBA demonstrated to be a convenient, robust approach, which not only allowed distinction of the C- or N-terminal binding site of the inhibitors, but also permitted the IC_{50} value calculation for each individual inhibitor. Although a variety of assays have been reported to test Hsp90 activity in previous research, up until now there was no standardised method to ascertain Hsp90 inhibition. nGBA offers a reliable alternative for overcoming the problem of the study of Hsp90 inhibitors.

However, the nGBA presents a weakness in the fact that it does not allow the determination of the IC_{50} value for an N-terminal inhibitor, since there is no real dose-response curve, as a result of the relatively constant intensity of the monomer bands.

Furthermore, glucosyl-novobiocin proved to be a C-terminal inhibitor with higher affinity for Hsp90 than novobiocin and, thus, a potentially better anti-cancer drug candidate. This illustrates the importance of glycosylation in drug discovery. Glycosylated derivatives exhibit good clinical use, as carbohydrate moieties affect drugs' physicochemical properties, thermal stability and reactivity with receptors. Consequently, glycosylation represents an effective route for modification and optimisation of compounds (Kawasaki et al., 2009).

5.4.3 Hsp90 ATPase assay

Unlike for the nGBA, the Hsp90 used in the ATPase assay was expressed from Human Hsp90 α plasmid, pProEX HTa Hsp90 α , a kind gift from Prof. Houry in the University of Toronto. This was owing to the fact that the commercial Hsp90 presented very low activity when tested and, thus, there would be a need for very high amounts of protein to carry out the ATPase assay, which would become extremely costly.

In the process of purification of the expressed Hsp90, the elution buffer used contained imidazole, which is known to block Hsp90 activity. As a result, it was necessary to change the buffer and Hsp90 was finally stored in a storage buffer (25 mM Tris-HCl, pH7.5; 150 mM KCl; 10 % glycerol; 0.5 mM DTT) used in previous research (Zhao et al., 2010).

As for the commercial Hsp90 used in the nGBA, this expressed and purified Hsp90 was analysed by SDS-PAGE prior to its use in the ATPase activity assay.

5.4.3.1 Expressed Hsp90 purity test

Figure 5.13 illustrates the SDS-PAGE analysis of the expressed and purified Hsp90. Lanes 5, 6 and 7 of the SDS-PAGE gel showed a stronger band between 75 and 100 kDa, which corresponds to the Hsp90 monomer. Fractions matching these lanes were then combined for the ATPase activity assay. It could be clearly seen that there was more than one band in the lanes containing purified Hsp90. This might be a result of protein degradation during SDS-PAGE and/or, more likely, low purification efficiency. For improved purification efficiency, size-exclusion chromatography could be used to purify proteins according to their molecular weight, as previously reported (Zhao et al., 2010). Although not 100 % pure, these results confirmed the suitability of the expressed Hsp90 for the ATPase activity assay.

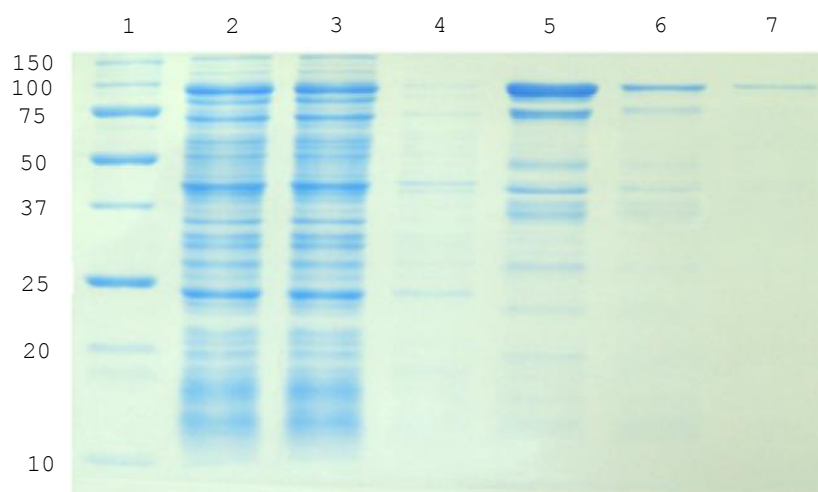


Figure 5.13 Expressed Hsp90 SDS-PAGE analysis. 1, marker. 2, protein mixture before purification. 3, proteins in the flow-through fraction after washing with binding buffer. 4, proteins in the flow-through fraction after washing with wash buffer. 5-7, purified Hsp90 protein. 10 % SDS-PAGE gel. Gel was stained by Coomassie stain. The SDS-PAGE gel showed a stronger band between 75 and 100 kDa, which corresponds to the Hsp90 monomer.

5.4.3.2 ATPase activity assay

Dimerisation, ATP binding and hydrolysis are essential to Hsp90's function (Panaretou et al., 1998). Previously developed assays for the characterisation of Hsp90 inhibitors include a high-throughput firefly luciferase assay (Galam et al., 2007), a Western blot assay (Burlison et al., 2006), and an ATPase assay (Wayne and Bolon, 2007, Zhao et al., 2010, Richter et al., 2006). Quantification of the inhibition of the ATPase activity provides direct information not only on the type of binding, but also on the inhibitor's dissociation constant (K_i).

In this particular study, ATPase assay was considered a suitable method for testing the inhibition pattern of Hsp90 inhibitors, because by hydrolysing ATP, Hsp90 mimics the effect of ATPase in this coupled assay. If inhibitors are added into the mixture, a slow change in NADH absorbance will be observed. Subsequently, the NADH depletion curve can be used for the analysis of Hsp90 kinetics. Additionally, as the ATP binding site, the N-terminal domain of Hsp90 is seen as an active site. Therefore, if an N-terminal inhibitor is used, it will compete against ATP for the same binding site, resulting in a competitive inhibition pattern. On the other hand,

if a C-terminal inhibitor is used, it will affect Hsp90's structure, preventing dimerisation and making it impossible for ATP to bind to its pocket. However, it will not compete directly to the same binding site as ATP, resulting in a non-competitive inhibition pattern.

In Lineweaver-Burk plots, a competitive inhibition pattern is characterised by an intersection on the same point of the y-axis of the curves obtained with different concentrations of an inhibitor. When the curves intersect on the same point of the x-axis, the inhibitor tested is a non-competitive inhibitor.

So far, only Sti1 has been identified as a non-competitive inhibitor using an Hsp90 ATPase assay (Richter et al., 2003). Nevertheless, a corresponding Lineweaver-Burk plot has not been previously published.

Before studying the inhibition patterns of the chosen inhibitors, Hsp90's kinetics was firstly tested without inhibitor. In order to do so, Hsp90 was incubated with different concentrations of substrate (ATP) and the decrease in the concentration of NADH was plotted over time. The reaction rate of Hsp90 was then plotted against different concentrations of substrate and, finally, Lineweaver-Burk plots were obtained.

It is worth noting that the substrate ATP suffers spontaneous hydrolysis, causing NADH consumption. This hydrolysis was measured in the control group, which contained no inhibitor and no Hsp90, and subtracted from the concentration of NADH in each experiment.

After the first test without inhibitor, the same procedure was applied for Hsp90 with the various inhibitors in different concentrations. For each specific concentration of a certain inhibitor, a Lineweaver-Burk plot was obtained. In the end, all plots for that inhibitor were combined, analysed and the inhibitor constants were calculated.

Similarly to what was done in the nGBA, Hsp90 was incubated with different concentrations of three inhibitors: a known C-terminal inhibitor, novobiocin (Nov); a

novobiocin derivative, glucosyl-novobiocin (Glc-Nov); and a known N-terminal inhibitor, geldanamycin (Geld).

ATP concentrations were fixed at 0, 10, 20, 50, 100 and 250 μM for all inhibitors. For the C-terminal inhibitor novobiocin, concentrations varied within the following range: 0, 100, 300, 500 and 700 μM . Figure 5.14 represents the combination of the Lineweaver-Burk plots obtained for novobiocin.

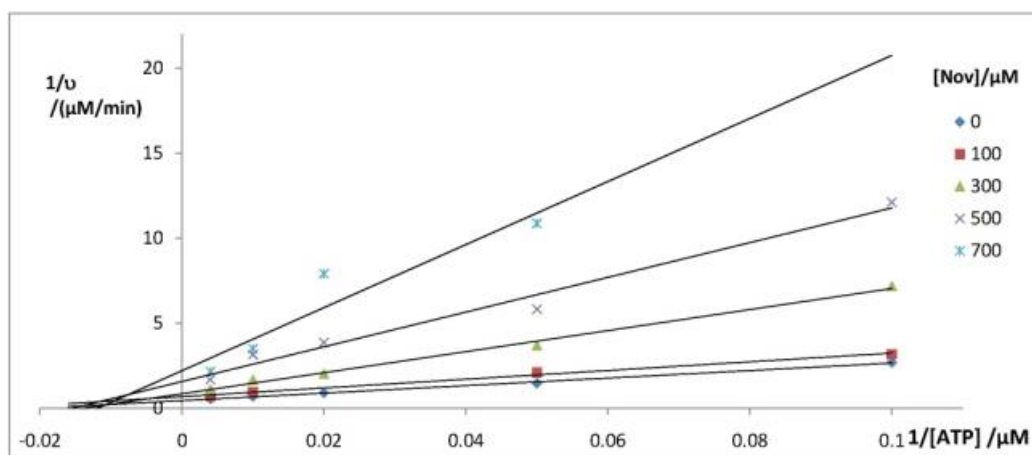


Figure 5.14 Inhibition of novobiocin (Nov) to Hsp90. The pattern showed that novobiocin is a non-competitive inhibitor, which aligns with the fact that it binds to the Hsp90 C-terminal domain. $K_i = 226 \pm 71 \mu\text{M}$.

For the novobiocin derivative glucosyl-novobiocin, concentrations varied within the following range: 0, 1, 5, 10, 20, 50, and 100 μM . Figure 5.15 illustrates the inhibition pattern of glucosyl-novobiocin.

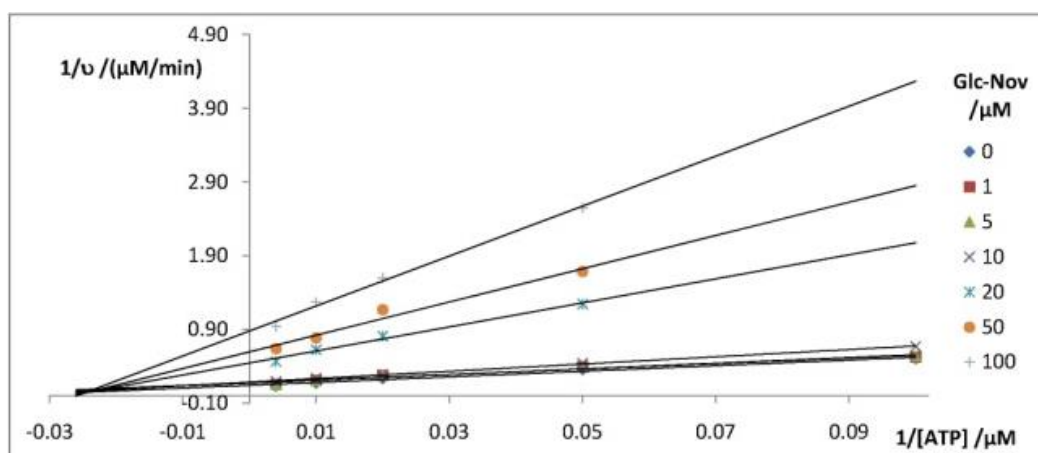


Figure 5.15 Inhibition of glucosyl-novobiocin (Glc-Nov) to Hsp90. The pattern showed that glucosyl-novobiocin is a non-competitive inhibitor, which aligns with the fact that it binds to the Hsp90 C-terminal domain. $K_i = 18.5 \pm 12.9 \mu\text{M}$.

For the N-terminal inhibitor geldanamycin, concentrations varied within the following range: 0, 10 and 20 nM. Figure 5.16 elucidates the inhibition pattern of geldanamycin.

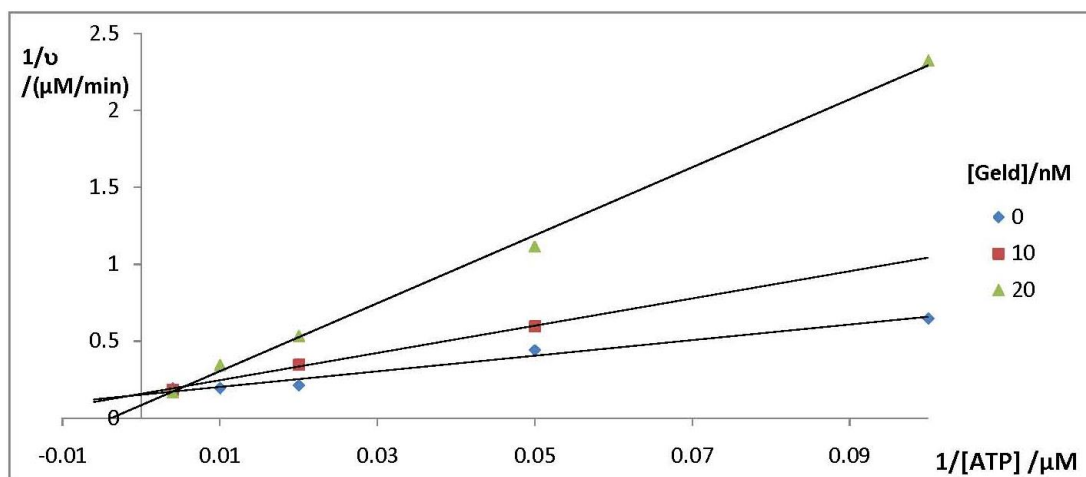


Figure 5.16 Inhibition of geldanamycin (Geld) to Hsp90. The pattern showed that geldanamycin is a competitive inhibitor, which aligns with the fact that it binds to the Hsp90 N-terminal ATP hydrolysis pocket. $K_i = 10 \pm 6.5$ nM.

From the analysis of the above figures, it is possible to conclude that novobiocin presented a non-competitive inhibition pattern, which is consistent with the fact that it is a C-terminal inhibitor. Novobiocin's glycosylated derivative, glucosyl-novobiocin, revealed a similar inhibition pattern to novobiocin, confirming its characteristics of C-terminal inhibitor as well. The known N-terminal inhibitor geldanamycin exhibited the expected competitive inhibition pattern, corroborating the suitability of this ATPase assay for the study of the inhibition pattern of Hsp90 inhibitors.

Although the possibility that glucosyl-novobiocin could bind allosterically on Hsp90 cannot be fully excluded, owing to the fact that it is an analogue of a known C-terminal inhibitor and it behaved similarly to novobiocin, one may conclude that it functions as a C-terminal inhibitor.

The Hsp90 ATPase assay also allowed the calculation of the inhibitor constant, K_i , for each inhibitor from its Lineweaver-Burk plots. The K_i value is related to the dissociation between the enzyme and the inhibitor, thus, lower K_i values correspond to higher affinity of the inhibitor for the enzyme and vice versa (Roberts, 1977). In

this experiment, the K_i values obtained for each inhibitor studied were K_i (Nov) = $226 \pm 71 \mu\text{M}$, K_i (Glc-Nov) = $18.5 \pm 12.9 \mu\text{M}$ and K_i (Geld) = $10 \pm 6.5 \text{ nM}$, which were similar to those reported in the literature (Burlison et al., 2008, Patel et al., 2004). Glucosyl-novobiocin showed a more powerful inhibition effect than novobiocin, as its K_i value was much lower than novobiocin's, offering another proof that glycosylation plays an important role in the enhancement of anti-cancer drug effect.

In conclusion, the Hsp90 ATPase assay developed in this study presented a new method for the analysis of Hsp90 inhibition patterns. Previous research has demonstrated that inhibitors influence Hsp90's ATPase properties (Zhao et al., 2010), however no accurate quantitative analysis of that effect has been proposed. This approach has permitted to overcome those pitfalls. Furthermore, since this assay may be performed in a micro scale, using micro plates containing a vast number of samples in different conditions that can be analysed simultaneously, this method may be used as high-throughput screening of Hsp90 target inhibitors in the future.

5.5 Conclusions & Future Work

5.5.1 Conclusions

Hsp90 has become a very attractive target in anti-cancer drug discovery and, as a result, many inhibitors have been suggested. By simultaneously tackling all the hallmark traits of cancer cells, Hsp90 inhibitors have the potential to deliver a one-step combinatorial attack on multistep oncogenesis. This offers the ability for a powerful anti-tumour effect across a broad range of cancers and may make it more difficult for a cancer cell to develop drug resistance.

Both strategies – aiming to inhibit ATPase activity at the N-terminal domain and targeting Hsp90 dimerisation via the C-terminal domain – have yielded promising drug candidates. Yet, to fully explore the potential of compounds for Hsp90 inhibition, convenient and robust assays are required to allow qualitative and quantitative characterisation of C- or N-terminal inhibition potential.

This study aimed to develop a reliable and reproducible method capable of analysing Hsp90's inhibition patterns. Two methods used in combination were reported in this chapter: native gel binding assay (nGBA) and Hsp90 ATPase assay.

The nGBA was used to distinguish C-terminal and N-terminal inhibitors of Hsp90, through the observation of conformational changes of the protein caused by the binding of an inhibitor, which could be visualised on a native gel. This not only provided qualitative information about the inhibitors, but also quantitative, as their IC_{50} values could be obtained from the dose-response curves.

On the other hand, the Hsp90 ATPase assay was used to qualitatively predict the inhibition pattern of an inhibitor through the study of its Lineweaver-Burk plot, also distinguishing C- and N-terminal inhibitors. In terms of quantitative information, this technique allowed to calculate the K_i value for each inhibitor.

In conclusion, the combined use of these two methods proved to be a convenient and robust approach to characterise Hsp90 inhibitors and will aid the development of Hsp90 targeted anti-cancer drugs.

Moreover, the analysis of a novel novobiocin analogue, glucosyl-novobiocin, through these techniques showed improved anti-cancer activity for the analogue when compared with novobiocin, demonstrating that glycosylation is a good way to enhance the anti-cancer properties of compounds.

The work reported in this chapter has been published (Cruz et al., 2013b) and the article can be found in Appendix.

Key Findings			
Development of a new screening method for Hsp90 inhibitors	nGBA	Qualitative assay	Binding site: distinction between C- and N-terminal inhibitors
		Quantitative assay	IC ₅₀ value of each inhibitor
	ATPase assay	Qualitative assay	Inhibition pattern
		Quantitative assay	K _i value of each inhibitor
Confirmation of improved anti-cancer activity for glucosyl-novobiocin when compared with novobiocin			

5.5.2 Future work

The developed native nGBA combined with the Hsp90 ATPase assay can be used to screen more Hsp90 possible inhibitors, which will present a new prospect to the study of Hsp90, making it possible to create libraries of fully characterised compounds. Information in these libraries will then help to predict the behaviour of these drugs in the human body, facilitating metabolic studies and the anticipation of possible side effects.

An important step further would be to discover the exact binding site of the inhibitors in the Hsp90 structure. For that purpose, a new PhD project undergoing in

our group combines protease fingerprinting and photo-affinity labelling utilising LC-MS/MS to further identify and reveal Hsp90 C-terminal binding site of novobiocin and its derivatives. Photo-reactive azide moieties placed in the p-, o- or m- positions are used in the Tolyl side chain to mimic the sugar group, which is present in 4-position of the coumarin ring in novobiocin and its analogues. A recombinant His-tagged Hsp90 C-terminal construct will be incubated in the presence or absence of these compounds followed by UV-irradiation. Subsequent MALDI-TOF analysis will give information on the exact binding area. The identified site will then be characterised by molecular modelling and molecular dynamics to give a computational model of bioactive conformation. On the other hand, the comparison within different modifications of novobiocin will also enlighten upon optimisation of novobiocin's structure to achieve enhanced efficiency.

Further optimisation might allow some of the limitations identified so far in the inhibitors to be overcome. Structure-activity relationships with the known drug analogues will shed more light on the chemical features required for Hsp90 inhibitory activity. Gene expression profiling of Hsp90 inhibitors from the different chemical classes may be used to distinguish target-specific molecular effects from changes uniquely due to the chemical backbone of these compounds.

In the development of novel Hsp90 inhibitors, an option is to discover completely new chemical classes of Hsp90 inhibitors, which can be identified by high-throughput screening of diverse compound libraries using both cell-free biochemical assays and also cell-based methods. Another interesting possibility would be to design compounds that introduce a higher degree of molecular selectivity to the Hsp90 inhibitory activity in terms of the client proteins affected, by targeting specific co-chaperones, or specific members of the Hsp90 family.

**Chapter 6 – SUMMARY AND GENERAL DISCUSSION &
CONCLUSIONS**

The use of proteomics proved to be a powerful approach to identify un-regulated proteins and to help decipher the complex signalling circuitry or pathways involved in various biological processes. In particular, the use of 2D-PAGE allowed the identification and analysis of various proteins simultaneously, with the advantage of enabling their immediate visualisation, through separation and staining. This not only allowed the comparison of protein expression between pairs of samples with different characteristics, i.e. non-enriched/enriched, sensitive/resistant, non-cancer/cancer, it also allowed patterns in expression to be identified.

Nevertheless, the use of 2D-PAGE would not be as valuable without the complement of MS techniques capable of identifying the differentially expressed proteins. Recent technical advances in MS-based proteomics have made it possible to identify proteins with greater ease and sensitivity than previously. Subcellular organellar proteomic studies have further provided detailed mapping of the constituent proteins of various organelles. Therefore, protein spots showing different intensities between samples of the same pair are the most likely to contain proteins of interest. These protein spots should then be excised, digested and identified by MS, aiming the discovery of protein biomarkers, which can be targets for future medicines or help in the diagnosis and prognosis of diseases.

In this project, as part of a target discovery approach, proteomics was fundamental for the identification of protein targets in two distinct studies.

The first study used the archetypal glycomimetic iminosugar and therapeutic NB-DNJ/miglustat/Zavesca in a glyco-A^eP strategy to elucidate a focused subsection of the proteome, hypothetically relevant to mammalian reproduction. The discovered binding partners and the associated genomic analysis implicate a subset of proteins as important in male fertility. These new interactions would not have been readily predicted and might define the mechanisms by which NB-DNJ causes male infertility. Since miglustat passed the safety tests to be approved for the treatment of Gaucher disease in humans, and is already available on the market, it might lead to the discovery of a male birth control pill. However, further studies in humans are needed.

In the second study, taxol and carboplatin resistance-associated proteins were identified by MS, after comparing the protein expression profile of sensitive and resistant cell lines and different ovarian cancer tissues, through 2D-PAGE. A number of proteins, belonging to different classes and responsible for distinct functions within the cell, such as cytoskeleton and cell structure, detoxification and stress response and cellular metabolism, were identified in at least one of the three cell lines or five tissues studied. This demonstrated that the development of resistance is indeed a multi-factorial process, involving various biological pathways. The pathways most highly associated with the un-regulated proteins identified were also discovered in this study and validation of a few key proteins undertaken.

Despite its numerous advantages, proteomics also presents limitations. Ideally, proteomics should allow the identification of an entire proteome with 100 % protein sequence coverage. In reality, the large dynamic range and complexity of cellular proteomes results in over-sampling of abundant proteins, while peptides from low abundance proteins appear under-sampled or remain undetected.

Mechanisms that contribute to increase the quantity of peptides identified and the quality of MS/MS spectra acquired have long been a challenge and are currently under development. Proteome equalisation technology has proven to be a promising methodology to improve low abundance protein identification confidence, reproducibility, and sequence coverage in proteomics experiments. This important step opened a new avenue of research for improving proteome coverage (Fonslow et al., 2011).

A study by Di Michele et al. (2010) used multiplexed proteomics technology, whereby 2D separation was followed by sequential staining with two different dyes (2D-DIGE), allowing both the glycoprotein expression profile as well as the total protein expression profile to be obtained. This was combined with Multi-lectin Affinity Chromatography (MAC) to allow detection of low-abundance glycoproteins by removing larger non-glycosylated proteins. It, therefore, resulted in the identification of chemoresistant biomarkers, which could not be observed by standard analysis due to their low concentration.

Just as the previously mentioned study used dyes that bind specifically to sugar residues on the proteins, ICAT (isotope-coded affinity tag) labelling, which labels specific amino acid residues on protein lysates, can also be used to reduce the complexity of samples and allow the quantification of low abundance proteins, without limiting the sample to a small population (Stewart et al., 2006).

Any proteome has a highly dynamic nature. It may vary in different cells and tissue types of the same organism and in different growth and developmental stages. It is also dependent on environmental factors, disease, drugs and stress conditions. Even small changes in experimental conditions can have significant effects on the expression, folding and activity of proteins (Taylor et al., 2008). This might affect reproducibility, which represents another limitation of proteomics. In order to minimise it, a sufficient number of sample replicates should be used in each experiment to ensure, as much as possible, that the detected changes are indeed related to the condition under analysis, and not a result of intra-sample variation.

One of the greatest challenges in the diagnosis and treatment of human disease is the identification of biomarkers for disease detection at an early and still treatable stage, and for the molecular definition of disease progression, to allow for implementation of more effective treatments. Numerous gene expression array and proteomic studies on cells and tissues have shown, over the years, that such markers do exist and can be associated with pathological changes in the disease and its prognosis.

However, the fact that most tissues are not readily accessible for routine screening, often requiring invasive procedures for sample collection, and that the affected cells/tissue segments might be difficult to identify in the first place, are just some of the drawbacks of using cells and tissues.

Therefore, it has been observed a rising interest in blood plasma as a potentially rich source of biomarkers, since this body fluid is readily accessible and thought to acquire proteins secreted, shed, or otherwise released from the tissues through which blood circulates. Biomarkers identified in plasma give an indication of the

status of the different organs and tissues in our body, making it interesting to identify and quantify them (Omenn et al., 2005).

To this end, recent substantial efforts in technology development, especially MS-based analytical methodologies, have significantly increased the ability to investigate the plasma proteome. Nevertheless, a major obstacle for the success of efforts to discover cell and/or tissue-derived changes in the blood plasma protein profile has been its extreme complexity. Blood plasma consists of tens of thousands of different molecular species that span a concentration of at least 10 orders of magnitude, being dominated by highly abundant proteins such as albumin (Anderson and Anderson, 2002).

Still part of the target discovery approach embraced by this project (but with a completely different purpose), a reliable and reproducible assay was developed for the screening of Hsp90 targeted compounds. In this study, a method able to qualitatively and quantitatively distinguish C-terminal and N-terminal inhibitors of Hsp90 (nGBA), and a method capable of analysing Hsp90's inhibition patterns (Hsp90 ATPase assay) were developed. The combined use of these two methods proved to be a convenient and robust approach to characterise Hsp90 inhibitors and will aid the development of Hsp90 targeted anti-cancer drugs.

The development of assays for the screening of inhibitors of proteins that have already been recognised as important drug targets, such as the anti-cancer drug target Hsp90, is of extreme importance for the progress of these targets in the drug discovery process.

References

- The global proteome machine organization proteomics database and open source software* [Online]. GPM. Available: <http://www.thegpm.org/> 2011-2013].
- MASCOT [Online]. Matrix Science. Available: <http://www.matrixscience.com> 2011-2013].
- AABO, K., ADAMS, M., ADNITT, P., ALBERTS, D. S., ATHANAZZIOU, A., BARLEY, V., BELL, D. R., BIANCHI, U., BOLIS, G., BRADY, M. F., BRODOVSKY, H. S., BRUCKNER, H., BUYSE, M., CANETTA, R., CHYLAK, V., COHEN, C. J., COLOMBO, N., CONTE, P. F., CROWTHER, D., EDMONSON, J. H., GENNATAS, C., GILBEY, E., GORE, M., GUTHRIE, D., YEAP, B. Y. & ET AL. 1998. Chemotherapy in advanced ovarian cancer: four systematic meta-analyses of individual patient data from 37 randomized trials. Advanced Ovarian Cancer Trialists' Group. *Br J Cancer*, 78, 1479-87.
- AEBERSOLD, R. & MANN, M. 2003. Mass spectrometry-based proteomics. *Nature*, 422, 198-207.
- AERTS, J. M., DONKER-KOOPMAN, W. E., KOOT, M., BARRANGER, J. A., TAGER, J. M. & SCHRAM, A. W. 1986. Deficient activity of glucocerebrosidase in urine from patients with type 1 Gaucher disease. *Clin Chim Acta*, 158, 155-63.
- AERTS, J. M., DONKER-KOOPMAN, W. E., VAN DER VLIET, M. K., JONSSON, L. M., GINNS, E. I., MURRAY, G. J., BARRANGER, J. A., TAGER, J. M. & SCHRAM, A. W. 1985. The occurrence of two immunologically distinguishable beta-glucocerebrosidases in human spleen. *Eur J Biochem*, 150, 565-74.
- AGARWAL, R. & KAYE, S. B. 2003. Ovarian cancer: strategies for overcoming resistance to chemotherapy. *Nat Rev Cancer*, 3, 502-16.
- AGARWAL, R. & KAYE, S. B. 2006. Expression profiling and individualisation of treatment for ovarian cancer. *Curr Opin Pharmacol*, 6, 345-9.
- AHMED, N., OLIVA, K. T., BARKER, G., HOFFMANN, P., REEVE, S., SMITH, I. A., QUINN, M. A. & RICE, G. E. 2005. Proteomic tracking of serum protein isoforms as screening biomarkers of ovarian cancer. *Proteomics*, 5, 4625-36.
- ALAIYA, A. A., FRANZEN, B., FUJIOKA, K., MOBERGER, B., SCHEDVINS, K., SILFVERSVARD, C., LINDER, S. & AUER, G. 1997. Phenotypic analysis of ovarian carcinoma: polypeptide expression in benign, borderline and malignant tumors. *Int J Cancer*, 73, 678-83.
- ALBERTELLA, M. R., GREEN, C. M., LEHMANN, A. R. & O'CONNOR, M. J. 2005. A role for polymerase eta in the cellular tolerance to cisplatin-induced damage. *Cancer Res*, 65, 9799-806.
- ALBERTS, B., JOHNSON, A., LEWIS, J., RAFF, M., ROBERTS, K. & WALTER, P. 2002. *Molecular biology of the cell*, New York, Garland Science.
- ALBROW, V. E., FERNANDES, C., BEAL, D. M., SELBY, M. D., FERNANDEZ-OCANA, M., RUMPEL, K. C. & JONES, L. H. 2012. Quantitative affinity-based chemical proteomics of TrkA inhibitors. *MedChemComm*, 3, 322-325.
- ALFONSO, P., PAMPIN, S., ESTRADA, J., RODRIGUEZ-REY, J. C., GIRALDO, P., SANCHO, J. & POCOVI, M. 2005. Miglustat (NB-DNJ) works as a chaperone for mutated acid beta-glucosidase in cells transfected with several Gaucher disease mutations. *Blood Cells Mol Dis*, 35, 268-76.
- ALLAN, R. K., MOK, D., WARD, B. K. & RATAJCZAK, T. 2006. Modulation of chaperone function and cochaperone interaction by novobiocin in the C-terminal domain of Hsp90: evidence that coumarin antibiotics disrupt Hsp90 dimerization. *J Biol Chem*, 281, 7161-71.

- ALTOMARE, D. A., WANG, H. Q., SKELE, K. L., DE RIENZO, A., KLEIN-SZANTO, A. J., GODWIN, A. K. & TESTA, J. R. 2004. AKT and mTOR phosphorylation is frequently detected in ovarian cancer and can be targeted to disrupt ovarian tumor cell growth. *Oncogene*, 23, 5853-7.
- AMORY, J. K., MULLER, C. H., PAGE, S. T., LEIFKE, E., PAGEL, E. R., BHANDARI, A., SUBRAMANYAM, B., BONE, W., RADLMAIER, A. & BREMNER, W. J. 2007. Miglustat has no apparent effect on spermatogenesis in normal men. *Hum Reprod*, 22, 702-7.
- ANDERSON, N. L. & ANDERSON, N. G. 2002. The human plasma proteome: history, character, and diagnostic prospects. *Mol Cell Proteomics*, 1, 845-67.
- APPLETON, K., MACKAY, H. J., JUDSON, I., PLUMB, J. A., MCCORMICK, C., STRATHDEE, G., LEE, C., BARRETT, S., READE, S., JADAYEL, D., TANG, A., BELLENGER, K., MACKAY, L., SETANOIANS, A., SCHATZLEIN, A., TWELVES, C., KAYE, S. B. & BROWN, R. 2007. Phase I and pharmacodynamic trial of the DNA methyltransferase inhibitor decitabine and carboplatin in solid tumors. *J Clin Oncol*, 25, 4603-9.
- ARDEKANI, A. M., AKHONDI, M. M. & SADEGHI, M. R. 2008. Application of genomic and proteomic technologies to early detection of cancer. *Arch Iran Med*, 11, 427-34.
- ARGON, Y. & SIMEN, B. B. 1999. GRP94, an ER chaperone with protein and peptide binding properties. *Semin Cell Dev Biol*, 10, 495-505.
- ASADOLLAHI, R., HYDE, C. A. & ZHONG, X. Y. 2010. Epigenetics of ovarian cancer: from the lab to the clinic. *Gynecol Oncol*, 118, 81-7.
- ASANO, N., NASH, R. J., MOLYNEUX, R. J. & FLEET, G. W. J. 2000. Sugar-mimic glycosidase inhibitors: natural occurrence, biological activity and prospects for therapeutic application. *Tetrahedron: Asymmetry*, 11, 1645-1680.
- AYE, T. T., MOHAMMED, S., VAN DEN TOORN, H. W., VAN VEEN, T. A., VAN DER HEYDEN, M. A., SCHOLTEN, A. & HECK, A. J. 2009. Selectivity in enrichment of cAMP-dependent protein kinase regulatory subunits type I and type II and their interactors using modified cAMP affinity resins. *Mol Cell Proteomics*, 8, 1016-28.
- AZAD, N. S., RASOOL, N., ANNUNZIATA, C. M., MINASIAN, L., WHITELEY, G. & KOHN, E. C. 2006. Proteomics in clinical trials and practice: present uses and future promise. *Mol Cell Proteomics*, 5, 1819-29.
- BACHLEITNER-HOFMANN, T., SUN, M. Y., CHEN, C. T., LISKA, D., ZENG, Z., VIALE, A., OLSHEN, A. B., MITTLBOECK, M., CHRISTENSEN, J. G., ROSEN, N., SOLIT, D. B. & WEISER, M. R. 2011. Antitumor activity of SNX-2112, a synthetic heat shock protein-90 inhibitor, in MET-amplified tumor cells with or without resistance to selective MET inhibition. *Clin Cancer Res*, 17, 122-33.
- BALASUBRAMANI, M., NAKAO, C., UECHI, G. T., CARDAMONE, J., KAMATH, K., LESLIE, K. L., BALACHANDRAN, R., WILSON, L., DAY, B. W. & JORDAN, M. A. 2011. Characterization and detection of cellular and proteomic alterations in stable stathmin-overexpressing, taxol-resistant BT549 breast cancer cells using offgel IEF/PAGE difference gel electrophoresis. *Mutat Res*, 722, 154-64.
- BAMBURG, J. R. 1999. Proteins of the ADF/cofilin family: essential regulators of actin dynamics. *Annu Rev Cell Dev Biol*, 15, 185-230.
- BARROTT, J. J. & HAYSTEAD, T. A. 2013. Hsp90, an unlikely ally in the war on cancer. *FEBS J*, 280, 1381-96.
- BASSO, A. D., SOLIT, D. B., CHIOSIS, G., GIRI, B., TSICHLIS, P. & ROSEN, N. 2002. Akt forms an intracellular complex with heat shock protein 90 (Hsp90) and Cdc37 and is destabilized by inhibitors of Hsp90 function. *J Biol Chem*, 277, 39858-66.
- BECK, J. A., LLOYD, S., HAFEZPARAST, M., LENNON-PIERCE, M., EPPIG, J. T., FESTING, M. F. & FISHER, E. M. 2000. Genealogies of mouse inbred strains. *Nat Genet*, 24, 23-5.
- BEERE, H. M., WOLF, B. B., CAIN, K., MOSSER, D. D., MAHBOUBI, A., KUWANA, T., TAILOR, P., MORIMOTO, R. I., COHEN, G. M. & GREEN, D. R. 2000. Heat-shock protein 70

- inhibits apoptosis by preventing recruitment of procaspase-9 to the Apaf-1 apoptosome. *Nat Cell Biol*, 2, 469-75.
- BERCHUCK, A., KAMEL, A., WHITAKER, R., KERNS, B., OLT, G., KINNEY, R., SOPER, J. T., DODGE, R., CLARKE-PEARSON, D. L., MARKS, P. & ET AL. 1990. Overexpression of HER-2/neu is associated with poor survival in advanced epithelial ovarian cancer. *Cancer Res*, 50, 4087-91.
- BERG, J. S., POWELL, B. C. & CHENEY, R. E. 2001. A millennial myosin census. *Mol Biol Cell*, 12, 780-94.
- BERNOTAS, R. C. & GANEM, B. 1990. Easy assembly of ligands for glycosidase affinity chromatography. *Biochem J*, 270, 539-40.
- BIO-RAD 2004. PDQuest: user guide. Bio-Rad Laboratories.
- BIO-RAD. 2009. *Bio-Rad Coordinates Proteomics Initiative Focused on Standardization of Methods* [Online]. Hercules, CA, USA: Bio-Rad. Available: <http://www.bio-rad.com/en-uk/corporate/newsroom/2d-gel-reproducibility-study-in-phase-two> [Accessed May 2014 2014].
- BJELLQVIST, B., EK, K., RIGHETTI, P. G., GIANAZZA, E., GORG, A., WESTERMEIER, R. & POSTEL, W. 1982. Isoelectric focusing in immobilized pH gradients: principle, methodology and some applications. *J Biochem Biophys Methods*, 6, 317-39.
- BJELLQVIST, B., SANCHEZ, J. C., PASQUALI, C., RAVIER, F., PAQUET, N., FRUTIGER, S., HUGHES, G. J. & HOCHSTRASSER, D. 1993. Micropreparative two-dimensional electrophoresis allowing the separation of samples containing milligram amounts of proteins. *Electrophoresis*, 14, 1375-8.
- BLAKE, D. J., WEIR, A., NEWEY, S. E. & DAVIES, K. E. 2002. Function and genetics of dystrophin and dystrophin-related proteins in muscle. *Physiol Rev*, 82, 291-329.
- BLUM, H., BEIER, H. & GROSS, H. 1987. Improved silver staining of plant proteins, RNA and DNA in polyacrylamide gels. *Electrophoresis*, 8, 93-99.
- BOGDANOV, B. & SMITH, R. D. 2005. Proteomics by FTICR mass spectrometry: top down and bottom up. *Mass Spectrom Rev*, 24, 168-200.
- BONE, W., WALDEN, C. M., FRITSCH, M., VOIGTMANN, U., LEIFKE, E., GOTTWALD, U., BOOMKAMP, S., PLATT, F. M. & VAN DER SPOEL, A. C. 2007. The sensitivity of murine spermiogenesis to miglustat is a quantitative trait: a pharmacogenetic study. *Reprod Biol Endocrinol*, 5, 1.
- BONGAERTS, G. P., VAN HALTEREN, H. K., VERHAGEN, C. A. & WAGENER, D. J. 2006. Cancer cachexia demonstrates the energetic impact of gluconeogenesis in human metabolism. *Med Hypotheses*, 67, 1213-22.
- BOYD, J. & RUBIN, S. C. 1997. Hereditary ovarian cancer: molecular genetics and clinical implications. *Gynecol Oncol*, 64, 196-206.
- BRABEC, V. & KASPARKOVA, J. 2002. Molecular aspects of resistance to antitumor platinum drugs. *Drug Resist Updat*, 5, 147-61.
- BROOKES, A. J. 1999. The essence of SNPs. *Gene*, 234, 177-86.
- BROSENS, I. & BENAGIANO, G. 2011. Endometriosis, a modern syndrome. *The Indian journal of medical research*, 133, 581-93.
- BROWN, D. P., CHIN-SINEX, H., NIE, B., MENDONCA, M. S. & WANG, M. 2009. Targeting superoxide dismutase 1 to overcome cisplatin resistance in human ovarian cancer. *Cancer Chemother Pharmacol*, 63, 723-30.
- BROWN, D. P. G., GOKMEN-POLAR, Y., JIANG, L., TAN, J., RINGHAM, H., JANECKI, D. J., OI, G. H., WITZMANN, F. A., SLEDGE, G. W. & WANG, M. 2007. A comparative proteomic study to characterize the vinblastine resistance in human ovarian cancer cells. *Proteomics Clinical Applications*, 1, 18-31.
- BRUNI, S., LOSCHI, L., INCERTI, C., GABRIELLI, O. & COPPA, G. V. 2007. Update on treatment of lysosomal storage diseases. *Acta Myol*, 26, 87-92.

- BURKHART, C. A., KAVALLARIS, M. & BAND HORWITZ, S. 2001. The role of beta-tubulin isotypes in resistance to antimetabolic drugs. *Biochim Biophys Acta*, 1471, O1-9.
- BURLINGAME, A. L. (ed.) 2005. *Biological Mass Spectrometry*, London: Elsevier Academic Press.
- BURLISON, J. A., AVILA, C., VIELHAUER, G., LUBBERS, D. J., HOLZBEIERLEIN, J. & BLAGG, B. S. 2008. Development of novobiocin analogues that manifest anti-proliferative activity against several cancer cell lines. *J Org Chem*, 73, 2130-7.
- BURLISON, J. A., NECKERS, L., SMITH, A. B., MAXWELL, A. & BLAGG, B. S. 2006. Novobiocin: redesigning a DNA gyrase inhibitor for selective inhibition of hsp90. *Journal of the American Chemical Society*, 128, 15529-36.
- BUTTERS, T. D., MELLOR, H. R., NARITA, K., DWEK, R. A. & PLATT, F. M. 2003. Small-molecule therapeutics for the treatment of glycolipid lysosomal storage disorders. *Philos Trans R Soc Lond B Biol Sci*, 358, 927-45.
- BUTTERS, T. D., VAN DEN BROEK, L. A. G. M., FLEET, G. W. J., KRULLE, T. M., WORMALD, M. R., DWEK, R. A. & PLATT, F. M. 2000. Molecular requirements of imino sugars for the selective control of N-linked glycosylation and glycosphingolipid biosynthesis. *Tetrahedron: Asymmetry*, 11, 113-124.
- CABRAL, F. & BARLOW, S. B. 1989. Mechanisms by which mammalian cells acquire resistance to drugs that affect microtubule assembly. *FASEB J*, 3, 1593-9.
- CAMPA, M. J., WANG, M. Z., HOWARD, B., FITZGERALD, M. C. & PATZ, E. F., JR. 2003. Protein expression profiling identifies macrophage migration inhibitory factor and cyclophilin a as potential molecular targets in non-small cell lung cancer. *Cancer Res*, 63, 1652-6.
- CAMPBELL, I. G., RUSSELL, S. E., CHOONG, D. Y., MONTGOMERY, K. G., CIAVARELLA, M. L., HOOI, C. S., CRISTIANO, B. E., PEARSON, R. B. & PHILLIPS, W. A. 2004. Mutation of the PIK3CA gene in ovarian and breast cancer. *Cancer Res*, 64, 7678-81.
- CANTAREL, B. L., COUTINHO, P. M., RANCUREL, C., BERNARD, T., LOMBARD, V. & HENRISSAT, B. 2009. The Carbohydrate-Active EnZymes database (CAZy): an expert resource for Glycogenomics. *Nucleic Acids Res*, 37, D233-8.
- CARDONE, L., DE CRISTOFARO, T., AFFAITATI, A., GARBI, C., GINSBERG, M. D., SAVIANO, M., VARRONE, S., RUBIN, C. S., GOTTESMAN, M. E., AVVEDIMENTO, E. V. & FELICIELLO, A. 2002. A-kinase anchor protein 84/121 are targeted to mitochondria and mitotic spindles by overlapping amino-terminal motifs. *J Mol Biol*, 320, 663-75.
- CASTAGNA, A., ANTONIOLI, P., ASTNER, H., HAMDAN, M., RIGHETTI, S. C., PEREGO, P., ZUNINO, F. & RIGHETTI, P. G. 2004. A proteomic approach to cisplatin resistance in the cervix squamous cell carcinoma cell line A431. *Proteomics*, 4, 3246-67.
- CHAIT, B. T. 2006. Chemistry. Mass spectrometry: bottom-up or top-down? *Science*, 314, 65-6.
- CHALOVICH, J. M., CHOCK, P. B. & EISENBERG, E. 1981. Mechanism of action of troponin . tropomyosin. Inhibition of actomyosin ATPase activity without inhibition of myosin binding to actin. *J Biol Chem*, 256, 575-8.
- CHEN, T., PENGETNZE, Y. & TAYLOR, C. C. 2005. Src inhibition enhances paclitaxel cytotoxicity in ovarian cancer cells by caspase-9-independent activation of caspase-3. *Mol Cancer Ther*, 4, 217-24.
- CHEN, Z. S., MUTOH, M., SUMIZAWA, T., FURUKAWA, T., HARAGUCHI, M., TANI, A., SAIJO, N., KONDO, T. & AKIYAMA, S. 1998. An active efflux system for heavy metals in cisplatin-resistant human KB carcinoma cells. *Exp Cell Res*, 240, 312-20.
- CHEVALIER, F. 2010. Highlights on the capacities of "Gel-based" proteomics. *Proteome Sci*, 8, 23.
- CHOI, J. H., WONG, A. S., HUANG, H. F. & LEUNG, P. C. 2007a. Gonadotropins and ovarian cancer. *Endocr Rev*, 28, 440-61.

- CHOI, K. J., PIAO, Y. J., LIM, M. J., KIM, J. H., HA, J., CHOE, W. & KIM, S. S. 2007b. Overexpressed cyclophilin A in cancer cells renders resistance to hypoxia- and cisplatin-induced cell death. *Cancer Res*, 67, 3654-62.
- CHUA, B. T., VOLBRACHT, C., TAN, K. O., LI, R., YU, V. C. & LI, P. 2003. Mitochondrial translocation of cofilin is an early step in apoptosis induction. *Nat Cell Biol*, 5, 1083-9.
- CHUANG, C. C. 2010. *Mechanism of miglustat-induced infertility in male mice*. PhD, University of Oxford.
- CICCHILLITTI, L., DI MICHELE, M., URBANI, A., FERLINI, C., DONAT, M. B., SCAMBIA, G. & ROTILIO, D. 2009. Comparative proteomic analysis of paclitaxel sensitive A2780 epithelial ovarian cancer cell line and its resistant counterpart A2780TC1 by 2D-DIGE: the role of ERp57. *J Proteome Res*, 8, 1902-12.
- CLOVEN, N. G., KYSHTOOBAYEVA, A., BURGER, R. A., YU, I. R. & FRUEHAUF, J. P. 2004. In vitro chemoresistance and biomarker profiles are unique for histologic subtypes of epithelial ovarian cancer. *Gynecol Oncol*, 92, 160-6.
- COLEY, H. M., SHOTTON, C. F., AJOSE-ADEOGUN, A., MODJTAHEDI, H. & THOMAS, H. 2006. Receptor tyrosine kinase (RTK) inhibition is effective in chemosensitising EGFR-expressing drug resistant human ovarian cancer cell lines when used in combination with cytotoxic agents. *Biochem Pharmacol*, 72, 941-8.
- COLLABORATIVE GROUP ON EPIDEMIOLOGICAL STUDIES OF OVARIAN, C., BERAL, V., DOLL, R., HERMON, C., PETO, R. & REEVES, G. 2008. Ovarian cancer and oral contraceptives: collaborative reanalysis of data from 45 epidemiological studies including 23,257 women with ovarian cancer and 87,303 controls. *Lancet*, 371, 303-14.
- COUKOS, G., BERCHUCK, A. & OZOLS, R. (eds.) 2008. *Ovarian cancer: state of the art and future directions in translational research*, New York, USA: Springer.
- COUTINHO, P. M., DELEURY, E., DAVIES, G. J. & HENRISSAT, B. 2003. An evolving hierarchical family classification for glycosyltransferases. *J Mol Biol*, 328, 307-17.
- COX, T. M., AERTS, J. M., ANDRIA, G., BECK, M., BELMATOUG, N., BEMBI, B., CHERTKOFF, R., VOM DAHL, S., ELSTEIN, D., ERIKSON, A., GIRALT, M., HEITNER, R., HOLLAK, C., HREBICEK, M., LEWIS, S., MEHTA, A., PASTORES, G. M., ROLFS, A., MIRANDA, M. C. & ZIMRAN, A. 2003. The role of the iminosugar N-butyldeoxynojirimycin (miglustat) in the management of type I (non-neuronopathic) Gaucher disease: a position statement. *J Inherit Metab Dis*, 26, 513-26.
- CRAIG, R. & BEAVIS, R. C. 2004. TANDEM: matching proteins with tandem mass spectra. *Bioinformatics*, 20, 1466-7.
- CRUK. 2013. *Ovarian cancer statistics* [Online]. Cancer Research UK. Available: <http://www.cancerresearchuk.org/cancer-info/cancerstats/types/ovary/> [Accessed Dec 2013].
- CRUK. 2014. *Cancer help UK: ovarian cancer* [Online]. Cancer Research UK. Available: <http://www.cancerresearchuk.org/cancer-help/type/ovarian-cancer/> [Accessed Jan 2014].
- CRUZ, I. N., BARRY, C. S., KRAMER, H. B., CHUANG, C. C., LLOYD, S., VAN DER SPOEL, A. C., PLATT, F. M., YANG, M. & DAVIS, B. G. 2013a. Glycomimetic affinity-enrichment proteomics identifies partners for a clinically-utilized iminosugar. *Chemical Science*, 4, 3442-3446.
- CRUZ, I. N., ZHANG, Y., DE LA FUENTE, M., SCHATZLEIN, A. & YANG, M. 2013b. Functional characterization of heat shock protein 90 targeted compounds. *Anal Biochem*, 438, 107-9.
- CUATRECASAS, P. 1970. Protein purification by affinity chromatography. Derivatizations of agarose and polyacrylamide beads. *J Biol Chem*, 245, 3059-65.

- DABHOLKAR, M., BOSTICK-BRUTON, F., WEBER, C., BOHR, V. A., EGWUAGU, C. & REED, E. 1992. ERCC1 and ERCC2 expression in malignant tissues from ovarian cancer patients. *J Natl Cancer Inst*, 84, 1512-7.
- DADVAR, P., O'FLAHERTY, M., SCHOLTEN, A., RUMPEL, K. & HECK, A. J. 2009. A chemical proteomics based enrichment technique targeting the interactome of the PDE5 inhibitor PF-4540124. *Mol Biosyst*, 5, 472-82.
- DANG, C. V. & SEMENZA, G. L. 1999. Oncogenic alterations of metabolism. *Trends Biochem Sci*, 24, 68-72.
- DE LENA, M., LORUSSO, V., LATORRE, A., FANIZZA, G., GARGANO, G., CAPORUSSO, L., GUIDA, M., CATINO, A., CRUCITTA, E., SAMBIASI, D. & MAZZEI, A. 2001. Paclitaxel, cisplatin and lonidamine in advanced ovarian cancer. A phase II study. *Eur J Cancer*, 37, 364-8.
- DE MAIO, A. 1999. Heat shock proteins: facts, thoughts, and dreams. *Shock*, 11, 1-12.
- DEBOER, C., MEULMAN, P. A., WNUK, R. J. & PETERSON, D. H. 1970. Geldanamycin, a new antibiotic. *J Antibiot (Tokyo)*, 23, 442-7.
- DI MICHELE, M., DELLA CORTE, A., CICCHILLITTI, L., DEL BOCCIO, P., URBANI, A., FERLINI, C., SCAMBIA, G., DONATI, M. B. & ROTILIO, D. 2009. A proteomic approach to paclitaxel chemoresistance in ovarian cancer cell lines. *Biochim Biophys Acta*, 1794, 225-36.
- DI MICHELE, M., MARCONE, S., CICCHILLITTI, L., DELLA CORTE, A., FERLINI, C., SCAMBIA, G., DONATI, M. B. & ROTILIO, D. 2010. Glycoproteomics of paclitaxel resistance in human epithelial ovarian cancer cell lines: towards the identification of putative biomarkers. *J Proteomics*, 73, 879-98.
- DIX, D. J., ALLEN, J. W., COLLINS, B. W., MORI, C., NAKAMURA, N., POORMAN-ALLEN, P., GOULDING, E. H. & EDDY, E. M. 1996. Targeted gene disruption of Hsp70-2 results in failed meiosis, germ cell apoptosis, and male infertility. *Proc Natl Acad Sci U S A*, 93, 3264-8.
- DOMINGUEZ, D. C., LOPES, R. & TORRES, M. L. 2007. Proteomics: clinical applications. *Clin Lab Sci*, 20, 245-8.
- DONNELLY, A. & BLAGG, B. S. 2008. Novobiocin and additional inhibitors of the Hsp90 C-terminal nucleotide-binding pocket. *Current medicinal chemistry*, 15, 2702-17.
- DREWS, J. 2000. Drug discovery: a historical perspective. *Science*, 287, 1960-4.
- DRYSDALE, M. J., DYMOCK, B. W., BARRIL-ALONSO, X., WORKMAN, P., PEARCE, L. H., PRODROMOU, C. & MACDONALD, E. 2002. *3-(2,4)Dihydroxyphenyl-4-phenylpyrazoles and their medical use*. Great Britain patent application 02805823.8.
- DU BOIS, A., LUCK, H. J., MEIER, W., ADAMS, H. P., MOBUS, V., COSTA, S., BAUKNECHT, T., RICHTER, B., WARM, M., SCHRODER, W., OLBRICHT, S., NITZ, U., JACKISCH, C., EMONS, G., WAGNER, U., KUHN, W., PFISTERER, J. & ARBEITSGEMEINSCHAFT GYNAKOLOGISCHE ONKOLOGIE OVARIAN CANCER STUDY, G. 2003. A randomized clinical trial of cisplatin/paclitaxel versus carboplatin/paclitaxel as first-line treatment of ovarian cancer. *J Natl Cancer Inst*, 95, 1320-9.
- DUCRET, A., BRUUN, C. F., BURES, E. J., MARHAUG, G., HUSBY, G. & AEBERSOLD, R. 1996. Characterization of human serum amyloid A protein isoforms separated by two-dimensional electrophoresis by liquid chromatography/electrospray ionization tandem mass spectrometry. *Electrophoresis*, 17, 866-76.
- DUMONTET, C. & SIKIC, B. I. 1999. Mechanisms of action of and resistance to antitubulin agents: microtubule dynamics, drug transport, and cell death. *J Clin Oncol*, 17, 1061-70.
- DUNN, M. J. 2011. Proteomics - Clinical Applications Reviews 2011. *Proteomics Clin Appl*, 5, 4-6.
- EDDY, E. M. 1999. Role of heat shock protein HSP70-2 in spermatogenesis. *Rev Reprod*, 4, 23-30.

- ELBEIN, A. D. 1987. Inhibitors of the biosynthesis and processing of N-linked oligosaccharide chains. *Annu Rev Biochem*, 56, 497-534.
- ENGEL, J., ECKEL, R., SCHUBERT-FRITSCHLE, G., KERR, J., KUHN, W., DIEBOLD, J., KIMMIG, R., REHBOCK, J. & HOLZEL, D. 2002. Moderate progress for ovarian cancer in the last 20 years: prolongation of survival, but no improvement in the cure rate. *Eur J Cancer*, 38, 2435-45.
- ENOMOTO, T., WEGHORST, C. M., INOUE, M., TANIZAWA, O. & RICE, J. M. 1991. K-ras activation occurs frequently in mucinous adenocarcinomas and rarely in other common epithelial tumors of the human ovary. *Am J Pathol*, 139, 777-85.
- ESMO 2001. ESMO minimum clinical recommendations for diagnosis, treatment and follow-up of ovarian cancer. *Ann Oncol*, 12, 1205-7.
- FARIDMOAYER, A. & SCAMAN, C. H. 2004. An improved purification procedure for soluble processing alpha-glucosidase I from *Saccharomyces cerevisiae* overexpressing CWH41. *Protein Expr Purif*, 33, 11-8.
- FATHALLA, M. F. 1971. Incessant ovulation--a factor in ovarian neoplasia? *Lancet*, 2, 163.
- FELTS, S. J., OWEN, B. A., NGUYEN, P., TREPEL, J., DONNER, D. B. & TOFT, D. O. 2000. The hsp90-related protein TRAP1 is a mitochondrial protein with distinct functional properties. *J Biol Chem*, 275, 3305-12.
- FENG, H. L., SANDLOW, J. I. & SPARKS, A. E. 2001. Decreased expression of the heat shock protein hsp70-2 is associated with the pathogenesis of male infertility. *Fertil Steril*, 76, 1136-9.
- FENN, J. B., MANN, M., MENG, C. K., WONG, S. F. & WHITEHOUSE, C. M. 1989. Electrospray ionization for mass spectrometry of large biomolecules. *Science*, 246, 64-71.
- FITZPATRICK, D. P. G., YOU, J. S., BEMIS, K. G., WERY, J. P., LUDWIG, J. R. & WANG, M. 2007. Searching for potential biomarkers of cisplatin resistance in human ovarian cancer using a label-free LC/MS-based protein quantification method. *Proteomics Clinical Applications*, 1, 246-263.
- FOJO, T. & MENEFFEE, M. 2007. Mechanisms of multidrug resistance: the potential role of microtubule-stabilizing agents. *Ann Oncol*, 18 Suppl 5, v3-8.
- FONSLOW, B. R., CARVALHO, P. C., ACADEMIA, K., FREEBY, S., XU, T., NAKORCHEVSKY, A., PAULUS, A. & YATES, J. R., 3RD 2011. Improvements in proteomic metrics of low abundance proteins through proteome equalization using ProteoMiner prior to MudPIT. *J Proteome Res*, 10, 3690-700.
- FU, H., SUBRAMANIAN, R. R. & MASTERS, S. C. 2000. 14-3-3 proteins: structure, function, and regulation. *Annu Rev Pharmacol Toxicol*, 40, 617-47.
- FUJIMORI, S., HINOI, E., TAKARADA, T., IEMATA, M., TAKAHATA, Y. & YONEDA, Y. 2006. Possible expression of a particular gamma-aminobutyric acid transporter isoform responsive to upregulation by hyperosmolarity in rat calvarial osteoblasts. *Eur J Pharmacol*, 550, 24-32.
- GALAM, L., HADDEN, M. K., MA, Z., YE, Q. Z., YUN, B. G., BLAGG, B. S. & MATTS, R. L. 2007. High-throughput assay for the identification of Hsp90 inhibitors based on Hsp90-dependent refolding of firefly luciferase. *Bioorganic & medicinal chemistry*, 15, 1939-46.
- GALAT, A. 1993. Peptidylproline cis-trans-isomerases: immunophilins. *Eur J Biochem*, 216, 689-707.
- GANAPATHY-KANNIAPPAN, S. & GESCHWIND, J. F. 2013. Tumor glycolysis as a target for cancer therapy: progress and prospects. *Mol Cancer*, 12, 152.
- GAO, Y., THOMAS, J. O., CHOW, R. L., LEE, G. H. & COWAN, N. J. 1992. A cytoplasmic chaperonin that catalyzes beta-actin folding. *Cell*, 69, 1043-50.
- GARCIA-CARDENA, G., FAN, R., SHAH, V., SORRENTINO, R., CIRINO, G., PAPAPETROPOULOS, A. & SESSA, W. C. 1998. Dynamic activation of endothelial nitric oxide synthase by Hsp90. *Nature*, 392, 821-4.

- GARFIN, D. & HEERDT, L. (eds.) 2001. *2-D electrophoresis for proteomics. A methods and products manual*: Bio-Rad.
- GATTEGNO, L., RAMDANI, A., JOUAULT, T., SAFFAR, L. & GLUCKMAN, J. C. 1992. Lectin-carbohydrate interactions and infectivity of human immunodeficiency virus type 1 (HIV-1). *AIDS Res Hum Retroviruses*, 8, 27-37.
- GEORGOPOULOS, C. & WELCH, W. J. 1993. Role of the major heat shock proteins as molecular chaperones. *Annu Rev Cell Biol*, 9, 601-34.
- GILKS, C. B. 2010. Molecular abnormalities in ovarian cancer subtypes other than high-grade serous carcinoma. *Journal of oncology*, 2010, 740968.
- GINSBURG, G. S. & MCCARTHY, J. J. 2001. Personalized medicine: revolutionizing drug discovery and patient care. *Trends Biotechnol*, 19, 491-6.
- GONZALEZ-GARAY, M. L., CHANG, L., BLADE, K., MENICK, D. R. & CABRAL, F. 1999. A beta-tubulin leucine cluster involved in microtubule assembly and paclitaxel resistance. *J Biol Chem*, 274, 23875-82.
- GORE, M. E., ATKINSON, R. J., THOMAS, H., CURE, H., RISCHIN, D., BEALE, P., BOUGNOUX, P., DIRIX, L. & SMIT, W. M. 2002. A phase II trial of ZD0473 in platinum-pretreated ovarian cancer. *Eur J Cancer*, 38, 2416-20.
- GORG, A., OBERMAIER, C., BOGUTH, G., HARDER, A., SCHEIBE, B., WILDGRUBER, R. & WEISS, W. 2000. The current state of two-dimensional electrophoresis with immobilized pH gradients. *Electrophoresis*, 21, 1037-53.
- GORG, A., WEISS, W. & DUNN, M. J. 2004. Current two-dimensional electrophoresis technology for proteomics. *Proteomics*, 4, 3665-85.
- GORTZAK-UZAN, L., IGNATCHENKO, A., EVANGELOU, A. I., AGOCHIYA, M., BROWN, K. A., STONGE, P., KIREEVA, I., SCHMITT-ULMS, G., BROWN, T. J., MURPHY, J., ROSEN, B., SHAW, P., JURISICA, I. & KISLINGER, T. 2008. A proteome resource of ovarian cancer ascites: integrated proteomic and bioinformatic analyses to identify putative biomarkers. *J Proteome Res*, 7, 339-51.
- GOTHEL, S. F. & MARAHIEL, M. A. 1999. Peptidyl-prolyl cis-trans isomerases, a superfamily of ubiquitous folding catalysts. *Cell Mol Life Sci*, 55, 423-36.
- GOTTESMAN, M. M. 2002. Mechanisms of cancer drug resistance. *Annu Rev Med*, 53, 615-27.
- GOTTLIEB, T. M. & OREN, M. 1998. p53 and apoptosis. *Semin Cancer Biol*, 8, 359-68.
- GRAVES, P. R. & HAYSTEAD, T. A. 2002. Molecular biologist's guide to proteomics. *Microbiol Mol Biol Rev*, 66, 39-63; table of contents.
- GRISENDI, S., MECUCCI, C., FALINI, B. & PANDOLFI, P. P. 2006. Nucleophosmin and cancer. *Nat Rev Cancer*, 6, 493-505.
- GRITSKO, T. M., COPPOLA, D., PACIGA, J. E., YANG, L., SUN, M., SHELLEY, S. A., FIORICA, J. V., NICOSIA, S. V. & CHENG, J. Q. 2003. Activation and overexpression of centrosome kinase BTAK/Aurora-A in human ovarian cancer. *Clin Cancer Res*, 9, 1420-6.
- GRUBER, M., MATHEW, L. K., RUNGE, A. C., GARCIA, J. A. & SIMON, M. C. 2010. EPAS1 Is Required for Spermatogenesis in the Postnatal Mouse Testis. *Biol Reprod*, 82, 1227-36.
- GUNDERSEN, G. G. & COOK, T. A. 1999. Microtubules and signal transduction. *Curr Opin Cell Biol*, 11, 81-94.
- HAGE, D. S. 1999. Affinity chromatography: a review of clinical applications. *Clin Chem*, 45, 593-615.
- HAMES, B. D. & RICKWOOD, D. (eds.) 1990. *Gel electrophoresis of proteins: a practical approach*, Oxford: IRL Press.
- HANAHAHAN, D. & WEINBERG, R. A. 2000. The hallmarks of cancer. *Cell*, 100, 57-70.
- HANAHAHAN, D. & WEINBERG, R. A. 2011. Hallmarks of cancer: the next generation. *Cell*, 144, 646-74.

- HARRAP, K. R. 1985. Preclinical studies identifying carboplatin as a viable cisplatin alternative. *Cancer Treat Rev*, 12 Suppl A, 21-33.
- HART, W. R. 1977. Ovarian epithelial tumors of borderline malignancy (carcinomas of low malignant potential). *Hum Pathol*, 8, 541-9.
- HEGDE, N. S., SANDERS, D. A., RODRIGUEZ, R. & BALASUBRAMANIAN, S. 2011. The transcription factor FOXM1 is a cellular target of the natural product thiostrepton. *Nat Chem*, 3, 725-31.
- HEINEMANN, K., SAAD, F., WIESEMES, M., WHITE, S. & HEINEMANN, L. 2005. Attitudes toward male fertility control: results of a multinational survey on four continents. *Hum Reprod*, 20, 549-56.
- HICKEY, E., BRANDON, S. E., SMALE, G., LLOYD, D. & WEBER, L. A. 1989. Sequence and regulation of a gene encoding a human 89-kilodalton heat shock protein. *Mol Cell Biol*, 9, 2615-26.
- HODGKINSON, V. C., D, E. L., AGARWAL, V., GARIMELLA, V., RUSSELL, C., LONG, E. D., FOX, J. N., MCMANUS, P. L., MAHAPATRA, T. K., KNEESHAW, P. J., DREW, P. J., LIND, M. J. & CAWKWELL, L. 2012. Proteomic identification of predictive biomarkers of resistance to neoadjuvant chemotherapy in luminal breast cancer: a possible role for 14-3-3 theta/tau and tBID? *J Proteomics*, 75, 1276-83.
- HOFFMANN, E. & STROOBANT, V. 2007. *Mass spectrometry : principles and applications*, Chichester, West Sussex, England, J. Wiley.
- HOLLENBECK, P. 2001. Cytoskeleton: Microtubules get the signal. *Curr Biol*, 11, R820-3.
- HOLSCHNEIDER, C. H. & BEREK, J. S. 2000. Ovarian cancer: epidemiology, biology, and prognostic factors. *Semin Surg Oncol*, 19, 3-10.
- HOLZER, A. K. & HOWELL, S. B. 2006. The internalization and degradation of human copper transporter 1 following cisplatin exposure. *Cancer Res*, 66, 10944-52.
- HUANG, H., LI, Y., LIU, J., ZHENG, M., FENG, Y., HU, K., HUANG, Y. & HUANG, Q. 2012a. Screening and identification of biomarkers in ascites related to intrinsic chemoresistance of serous epithelial ovarian cancers. *PLoS One*, 7, e51256.
- HUANG, Y., ZHANG, X., JIANG, W., WANG, Y., JIN, H., LIU, X. & XU, C. 2012b. Discovery of serum biomarkers implicated in the onset and progression of serous ovarian cancer in a rat model using iTRAQ technique. *Eur J Obstet Gynecol Reprod Biol*, 165, 96-103.
- ICHIJO, H., NISHIDA, E., IRIE, K., TEN DIJKE, P., SAITOH, M., MORIGUCHI, T., TAKAGI, M., MATSUMOTO, K., MIYAZONO, K. & GOTOH, Y. 1997. Induction of apoptosis by ASK1, a mammalian MAPKKK that activates SAPK/JNK and p38 signaling pathways. *Science*, 275, 90-4.
- INGENUITY. 2013. *Ingenuity Pathway Analysis (IPA)* [Online]. Ingenuity Systems. Available: <http://www.ingenuity.com/products/ipa> [Accessed Jul 2013].
- INOUE, S., TSURUOKA, T. & NIDA, T. 1966. The structure of nojirimycin, a piperidinose sugar antibiotic. *J Antibiot (Tokyo)*, 19, 288-92.
- INSTRUMENTS, H. S. (ed.) 1994. *Protein electrophoresis - applications guide*, San Francisco: Hoefer Scientific Instruments.
- ISAACS, J. S. 2005. Heat-shock protein 90 inhibitors in antineoplastic therapy: is it all wrapped up? *Expert Opin Investig Drugs*, 14, 569-89.
- ISHIKAWA, T. & ALI-OSMAN, F. 1993. Glutathione-associated cis-diamminedichloroplatinum(II) metabolism and ATP-dependent efflux from leukemia cells. Molecular characterization of glutathione-platinum complex and its biological significance. *J Biol Chem*, 268, 20116-25.
- JACOBS, I. J. & MENON, U. 2004. Progress and challenges in screening for early detection of ovarian cancer. *Mol Cell Proteomics*, 3, 355-66.
- JAMES, P. 1997. Protein identification in the post-genome era: the rapid rise of proteomics. *Q Rev Biophys*, 30, 279-331.

- JEMAL, A., SIEGEL, R., XU, J. & WARD, E. 2010. Cancer statistics, 2010. *CA Cancer J Clin*, 60, 277-300.
- JHAVERI, K., TALDONE, T., MODI, S. & CHIOSIS, G. 2012. Advances in the clinical development of heat shock protein 90 (Hsp90) inhibitors in cancers. *Biochimica et biophysica acta*, 1823, 742-55.
- JOHNSON, S. W., SWIGGARD, P. A., HANDEL, L. M., BRENNAN, J. M., GODWIN, A. K., OZOLS, R. F. & HAMILTON, T. C. 1994. Relationship between platinum-DNA adduct formation and removal and cisplatin cytotoxicity in cisplatin-sensitive and -resistant human ovarian cancer cells. *Cancer Res*, 54, 5911-6.
- JOLLY, C. & MORIMOTO, R. I. 2000. Role of the heat shock response and molecular chaperones in oncogenesis and cell death. *J Natl Cancer Inst*, 92, 1564-72.
- JONES, M. B., KRUTZSCH, H., SHU, H., ZHAO, Y., LIOTTA, L. A., KOHN, E. C. & PETRICOIN, E. F., 3RD 2002. Proteomic analysis and identification of new biomarkers and therapeutic targets for invasive ovarian cancer. *Proteomics*, 2, 76-84.
- JOSHI, S., TIWARI, A. K., MONDAL, B. & SHARMA, A. 2011. Oncoproteomics. *Clin Chim Acta*, 412, 217-26.
- KABUYAMA, Y., RESING, K. A. & AHN, N. G. 2004. Applying proteomics to signaling networks. *Curr Opin Genet Dev*, 14, 492-8.
- KAJIMOTO, T. & NODE, M. 2009. Inhibitors against glycosidases as medicines. *Curr Top Med Chem*, 9, 13-33.
- KAKU, T., OGAWA, S., KAWANO, Y., OHISHI, Y., KOBAYASHI, H., HIRAKAWA, T. & NAKANO, H. 2003. Histological classification of ovarian cancer. *Med Electron Microsc*, 36, 9-17.
- KAMAL, A., THAO, L., SENSINTAFFAR, J., ZHANG, L., BOEHM, M. F., FRITZ, L. C. & BURROWS, F. J. 2003. A high-affinity conformation of Hsp90 confers tumour selectivity on Hsp90 inhibitors. *Nature*, 425, 407-10.
- KANNAGI, R., IZAWA, M., KOIKE, T., MIYAZAKI, K. & KIMURA, N. 2004. Carbohydrate-mediated cell adhesion in cancer metastasis and angiogenesis. *Cancer Sci*, 95, 377-84.
- KARAS, M. & HILLENKAMP, F. 1988. Laser desorption ionization of proteins with molecular masses exceeding 10,000 daltons. *Anal Chem*, 60, 2299-301.
- KATO, K., OKUWAKI, M. & NAGATA, K. 2011. Role of Template Activating Factor-I as a chaperone in linker histone dynamics. *J Cell Sci*, 124, 3254-65.
- KAWASAKI, N., ITOH, S., HASHII, N., TAKAKURA, D., QIN, Y., HUANG, X. & YAMAGUCHI, T. 2009. The significance of glycosylation analysis in development of biopharmaceuticals. *Biol Pharm Bull*, 32, 796-800.
- KAYE, S. B. 2008. Reversal of drug resistance in ovarian cancer: Where do we go from here? *Journal of Clinical Oncology*, 26, 2616-2618.
- KELLAND, L. 2007. The resurgence of platinum-based cancer chemotherapy. *Nat Rev Cancer*, 7, 573-84.
- KELLAND, L. R., SHARP, S. Y., ROGERS, P. M., MYERS, T. G. & WORKMAN, P. 1999. DT-Diaphorase expression and tumor cell sensitivity to 17-allylamino, 17-demethoxygeldanamycin, an inhibitor of heat shock protein 90. *J Natl Cancer Inst*, 91, 1940-9.
- KELLEHER, N. L. 2004. Top-down proteomics. *Anal Chem*, 76, 197A-203A.
- KELLER, A., NESVIZHSKII, A. I., KOLKER, E. & AEBERSOLD, R. 2002. Empirical statistical model to estimate the accuracy of peptide identifications made by MS/MS and database search. *Anal Chem*, 74, 5383-92.
- KELLER, B. O., SUI, J., YOUNG, A. B. & WHITTAL, R. M. 2008. Interferences and contaminants encountered in modern mass spectrometry. *Anal Chim Acta*, 627, 71-81.

- KIM, J. H., SKATES, S. J., UEDE, T., WONG, K. K., SCHORGE, J. O., FELTMATE, C. M., BERKOWITZ, R. S., CRAMER, D. W. & MOK, S. C. 2002. Osteopontin as a potential diagnostic biomarker for ovarian cancer. *JAMA*, 287, 1671-9.
- KIM, J. W., NIE, B., SAHM, H., BROWN, D. P., TEGELER, T., YOU, J. S. & WANG, M. 2010. Targeted quantitative analysis of superoxide dismutase 1 in cisplatin-sensitive and cisplatin-resistant human ovarian cancer cells. *J Chromatogr B Analyt Technol Biomed Life Sci*, 878, 700-4.
- KIM, Y. S., ALARCON, S. V., LEE, S., LEE, M. J., GIACCONE, G., NECKERS, L. & TREPEL, J. B. 2009. Update on Hsp90 inhibitors in clinical trial. *Curr Top Med Chem*, 9, 1479-92.
- KLOSE, J. 1975. Protein mapping by combined isoelectric focusing and electrophoresis of mouse tissues. A novel approach to testing for induced point mutations in mammals. *Humangenetik*, 26, 231-43.
- KOBAYASHI, T. & OHTA, Y. 2005. 150-kD oxygen-regulated protein is an essential factor for insulin release. *Pancreas*, 30, 299-306.
- KOBEL, M., KALLOGER, S. E., BOYD, N., MCKINNEY, S., MEHL, E., PALMER, C., LEUNG, S., BOWEN, N. J., IONESCU, D. N., RAJPUT, A., PRENTICE, L. M., MILLER, D., SANTOS, J., SWENERTON, K., GILKS, C. B. & HUNTSMAN, D. 2008. Ovarian carcinoma subtypes are different diseases: implications for biomarker studies. *PLoS Med*, 5, e232.
- KOENIG, T., MENZE, B. H., KIRCHNER, M., MONIGATTI, F., PARKER, K. C., PATTERSON, T., STEEN, J. J., HAMPRECHT, F. A. & STEEN, H. 2008. Robust prediction of the MASCOT score for an improved quality assessment in mass spectrometric proteomics. *J Proteome Res*, 7, 3708-17.
- KOLKER, E., HIGDON, R. & HOGAN, J. M. 2006. Protein identification and expression analysis using mass spectrometry. *Trends Microbiol*, 14, 229-35.
- KOUKOURAKIS, M. I., GIATROMANOLAKI, A., SIVRIDIS, E., BOUGIOUKAS, G., DIDILIS, V., GATTER, K. C., HARRIS, A. L., TUMOUR & ANGIOGENESIS RESEARCH, G. 2003. Lactate dehydrogenase-5 (LDH-5) overexpression in non-small-cell lung cancer tissues is linked to tumour hypoxia, angiogenic factor production and poor prognosis. *Br J Cancer*, 89, 877-85.
- KOWALCZYK, A. P., NAVARRO, P., DEJANA, E., BORNSLAEGER, E. A., GREEN, K. J., KOPP, D. S. & BORGWARDT, J. E. 1998. VE-cadherin and desmoplakin are assembled into dermal microvascular endothelial intercellular junctions: a pivotal role for plakoglobin in the recruitment of desmoplakin to intercellular junctions. *J Cell Sci*, 111 (Pt 20), 3045-57.
- KRISHNA, R. & MAYER, L. D. 2000. Multidrug resistance (MDR) in cancer. Mechanisms, reversal using modulators of MDR and the role of MDR modulators in influencing the pharmacokinetics of anticancer drugs. *Eur J Pharm Sci*, 11, 265-83.
- KRISTJANSDOTTIR, B., LEVAN, K., PARTHEEN, K., CARLSOHN, E. & SUNDFELDT, K. 2013. Potential tumor biomarkers identified in ovarian cyst fluid by quantitative proteomic analysis, iTRAQ. *Clin Proteomics*, 10, 4.
- KURAMITSU, Y., TABA, K., RYOZAWA, S., YOSHIDA, K., ZHANG, X., TANAKA, T., MAEHARA, S., MAEHARA, Y., SAKAIDA, I. & NAKAMURA, K. 2010. Identification of up- and down-regulated proteins in gemcitabine-resistant pancreatic cancer cells using two-dimensional gel electrophoresis and mass spectrometry. *Anticancer Res*, 30, 3367-72.
- KURMAN, R. J. & SHIH IE, M. 2010. The origin and pathogenesis of epithelial ovarian cancer: a proposed unifying theory. *The American journal of surgical pathology*, 34, 433-43.
- LAEMMLI, U. K. 1970. Cleavage of structural proteins during the assembly of the head of bacteriophage T4. *Nature*, 227, 680-5.
- LAMPIAO, F., AGARWAL, A. & DU PLESSIS, S. S. 2009. The role of insulin and leptin in male reproduction. *Arch Med Sci*, 5, S48-S54.

- LANGDON, S. P., LAWRIE, S. S., HAY, F. G., HAWKES, M. M., MCDONALD, A., HAYWARD, I. P., SCHOL, D. J., HILGERS, J., LEONARD, R. C. & SMYTH, J. F. 1988. Characterization and properties of nine human ovarian adenocarcinoma cell lines. *Cancer Res*, 48, 6166-72.
- LARKIN, J. M. & KAYE, S. B. 2006. Etoposides in the treatment of cancer. *Expert Opin Investig Drugs*, 15, 691-702.
- LE MOGUEN, K., LINCET, H., DESLANDES, E., HUBERT-ROUX, M., LANGE, C., POULAIN, L., GAUDUCHON, P. & BAUDIN, B. 2006. Comparative proteomic analysis of cisplatin sensitive IGROV1 ovarian carcinoma cell line and its resistant counterpart IGROV1-R10. *Proteomics*, 6, 5183-92.
- LEE, C. F., GRIFFITHS, S., RODRIGUEZ-SUAREZ, E., PIERCE, A., UNWIN, R. D., JAWORSKA, E., EVANS, C. A., S, J. G. & WHETTON, A. D. 2010. Assessment of downstream effectors of BCR/ABL protein tyrosine kinase using combined proteomic approaches. *Proteomics*, 10, 3321-42.
- LEVENSON, A. S. & JORDAN, V. C. 1997. MCF-7: the first hormone-responsive breast cancer cell line. *Cancer Res*, 57, 3071-8.
- LI, H., LIU, T., ZHANG, Y., FAVRE, S., BELLO, C., VOGEL, P., BUTTERS, T. D., OIKONOMAKOS, N. G., MARROT, J. & BLERIOT, Y. 2008a. New synthetic seven-membered 1-azasugars displaying potent inhibition towards glycosidases and glucosylceramide transferase. *Chembiochem*, 9, 253-60.
- LI, M., MAKINJE, A. & DAMUNI, Z. 1996. The myeloid leukemia-associated protein SET is a potent inhibitor of protein phosphatase 2A. *J Biol Chem*, 271, 11059-62.
- LI, Z., ZHAO, X., BAI, S., WANG, Z., CHEN, L., WEI, Y. & HUANG, C. 2008b. Proteomics identification of cyclophilin a as a potential prognostic factor and therapeutic target in endometrial carcinoma. *Mol Cell Proteomics*, 7, 1810-23.
- LILLELUND, V. H., JENSEN, H. H., LIANG, X. & BOLS, M. 2002. Recent developments of transition-state analogue glycosidase inhibitors of non-natural product origin. *Chem Rev*, 102, 515-53.
- LILLEY, K. S., RAZZAQ, A. & DUPREE, P. 2002. Two-dimensional gel electrophoresis: recent advances in sample preparation, detection and quantitation. *Curr Opin Chem Biol*, 6, 46-50.
- LIN, C. H., LIN, C. W. & KHOO, K. H. 2008. Proteomic identification of specific glycosyltransferases functionally implicated for the biosynthesis of a targeted glyco-epitope. *Proteomics*, 8, 475-83.
- LIN, D., TABB, D. L. & YATES, J. R. 2003. Large-scale protein identification using mass spectrometry. *Biochim Biophys Acta*, 1646, 1-10.
- LINDQUIST, S. 1986. The heat-shock response. *Annu Rev Biochem*, 55, 1151-91.
- LUBEC, G., NONAKA, M., KRAPPENBAUER, K., GRATZER, M., CAIRNS, N. & FOUNTOULAKIS, M. 1999. Expression of the dihydropyrimidinase related protein 2 (DRP-2) in Down syndrome and Alzheimer's disease brain is downregulated at the mRNA and dysregulated at the protein level. *J Neural Transm Suppl*, 57, 161-77.
- LUDERS, J., DEMAND, J. & HOHFELD, J. 2000. The ubiquitin-related BAG-1 provides a link between the molecular chaperones Hsc70/Hsp70 and the proteasome. *J Biol Chem*, 275, 4613-7.
- LUO, L. Y., KATSAROS, D., SCORILAS, A., FRACCHIOLI, S., BELLINO, R., VAN GRAMBEREN, M., DE BRUIJN, H., HENRIK, A., STENMAN, U. H., MASSOBRIO, M., VAN DER ZEE, A. G., VERGOTE, I. & DIAMANDIS, E. P. 2003. The serum concentration of human kallikrein 10 represents a novel biomarker for ovarian cancer diagnosis and prognosis. *Cancer Res*, 63, 807-11.
- LUO, Y. X., CUI, J., WANG, L., CHEN, D. K., PENG, J. S., LAN, P., HUANG, M. J., HUANG, Y. H., CAI, S. R., HU, K. H., LI, M. T. & WANG, J. P. 2009. Identification of cancer-associated

- proteins by proteomics and downregulation of beta-tropomyosin expression in colorectal adenoma and cancer. *Proteomics Clin Appl*, 3, 1397-406.
- LYSIAK, J. J., NGUYEN, Q. A. & TURNER, T. T. 2000. Fluctuations in rat testicular interstitial oxygen tensions are linked to testicular vasomotion: persistence after repair of torsion. *Biol Reprod*, 63, 1383-9.
- MAHMOOD, T. & YANG, P. C. 2012. Western blot: technique, theory, and trouble shooting. *N Am J Med Sci*, 4, 429-34.
- MALONEY, A. & WORKMAN, P. 2002. HSP90 as a new therapeutic target for cancer therapy: the story unfolds. *Expert Opin Biol Ther*, 2, 3-24.
- MANN, M. & JENSEN, O. N. 2003. Proteomic analysis of post-translational modifications. *Nat Biotechnol*, 21, 255-61.
- MARCU, M. G., CHADLI, A., BOUHOUCHE, I., CATELLI, M. & NECKERS, L. M. 2000a. The heat shock protein 90 antagonist novobiocin interacts with a previously unrecognized ATP-binding domain in the carboxyl terminus of the chaperone. *The Journal of biological chemistry*, 275, 37181-6.
- MARCU, M. G., SCHULTE, T. W. & NECKERS, L. 2000b. Novobiocin and related coumarins and depletion of heat shock protein 90-dependent signaling proteins. *Journal of the National Cancer Institute*, 92, 242-8.
- MARKS, J. R., DAVIDOFF, A. M., KERNS, B. J., HUMPHREY, P. A., PENCE, J. C., DODGE, R. K., CLARKE-PEARSON, D. L., IGLEHART, J. D., BAST, R. C., JR. & BERCHUCK, A. 1991. Overexpression and mutation of p53 in epithelial ovarian cancer. *Cancer Res*, 51, 2979-84.
- MATERN, H., HEINEMANN, H., LEGLER, G. & MATERN, S. 1997. Purification and characterization of a microsomal bile acid beta-glucosidase from human liver. *J Biol Chem*, 272, 11261-7.
- MATTHEWS, S. B., VIELHAUER, G. A., MANTHE, C. A., CHAGUTURU, V. K., SZABLA, K., MATTS, R. L., DONNELLY, A. C., BLAGG, B. S. & HOLZBEIERLEIN, J. M. 2010. Characterization of a novel novobiocin analogue as a putative C-terminal inhibitor of heat shock protein 90 in prostate cancer cells. *The Prostate*, 70, 27-36.
- MCCAW, D. L., CHAN, A. S., STEGNER, A. L., MOONEY, B., BRYAN, J. N., TURNQUIST, S. E., HENRY, C. J., ALEXANDER, H. & ALEXANDER, S. 2007. Proteomics of canine lymphoma identifies potential cancer-specific protein markers. *Clin Cancer Res*, 13, 2496-503.
- MELLOR, H. R., FERGUSON, D. J. & CALLAGHAN, R. 2005. A model of quiescent tumour microregions for evaluating multicellular resistance to chemotherapeutic drugs. *Br J Cancer*, 93, 302-9.
- MELLOR, H. R., NOLAN, J., PICKERING, L., WORMALD, M. R., PLATT, F. M., DWEK, R. A., FLEET, G. W. & BUTTERS, T. D. 2002. Preparation, biochemical characterization and biological properties of radiolabelled N-alkylated deoxynojirimycins. *Biochem J*, 366, 225-33.
- METCALF, B. & DILLON, S. (eds.) 2006. *Target validation in drug discovery*: Academic Press.
- MIKURIYA, K., KURAMITSU, Y., RYOZAWA, S., FUJIMOTO, M., MORI, S., OKA, M., HAMANO, K., OKITA, K., SAKAIDA, I. & NAKAMURA, K. 2007. Expression of glycolytic enzymes is increased in pancreatic cancerous tissues as evidenced by proteomic profiling by two-dimensional electrophoresis and liquid chromatography-mass spectrometry/mass spectrometry. *Int J Oncol*, 30, 849-55.
- MINAMIDA, S., IWAMURA, M., KODERA, Y., KAWASHIMA, Y., IKEDA, M., OKUSA, H., FUJITA, T., MAEDA, T. & BABA, S. 2011. Profilin 1 overexpression in renal cell carcinoma. *Int J Urol*, 18, 63-71.
- MOR, G., FU, H. H. & ALVERO, A. B. 2006. Phenoxodiol, a novel approach for the treatment of ovarian cancer. *Curr Opin Investig Drugs*, 7, 542-8.

- MORANO, K. A. 2007. New tricks for an old dog: the evolving world of Hsp70. *Ann N Y Acad Sci*, 1113, 1-14.
- MORGENSZTERN, D. & MCLEOD, H. L. 2005. PI3K/Akt/mTOR pathway as a target for cancer therapy. *Anticancer Drugs*, 16, 797-803.
- MORI-IWAMOTO, S., KURAMITSU, Y., RYOZAWA, S., MIKURIA, K., FUJIMOTO, M., MAEHARA, S., MAEHARA, Y., OKITA, K., NAKAMURA, K. & SAKAIDA, I. 2007. Proteomics finding heat shock protein 27 as a biomarker for resistance of pancreatic cancer cells to gemcitabine. *Int J Oncol*, 31, 1345-50.
- MRUK, D. D., WONG, C. H., SILVESTRINI, B. & CHENG, C. Y. 2006. A male contraceptive targeting germ cell adhesion. *Nat Med*, 12, 1323-8.
- NACHMAN, M. W. 2001. Single nucleotide polymorphisms and recombination rate in humans. *Trends Genet*, 17, 481-5.
- NECKERS, L. 2007. Heat shock protein 90: the cancer chaperone. *Journal of biosciences*, 32, 517-30.
- NEIJT, J. P., ENGELHOLM, S. A., TUXEN, M. K., SORENSEN, P. G., HANSEN, M., SESSA, C., DE SWART, C. A., HIRSCH, F. R., LUND, B. & VAN HOUWELINGEN, H. C. 2000. Exploratory phase III study of paclitaxel and cisplatin versus paclitaxel and carboplatin in advanced ovarian cancer. *J Clin Oncol*, 18, 3084-92.
- NESVIZHSKII, A. I., KELLER, A., KOLKER, E. & AEBERSOLD, R. 2003. A statistical model for identifying proteins by tandem mass spectrometry. *Anal Chem*, 75, 4646-58.
- NEZHAT, F., DATTA, M. S., HANSON, V., PEJOVIC, T., NEZHAT, C. & NEZHAT, C. 2008. The relationship of endometriosis and ovarian malignancy: a review. *Fertility and Sterility*, 90, 1559-1570.
- NOBILI, S., LANDINI, I., GIGLIONI, B. & MINI, E. 2006. Pharmacological strategies for overcoming multidrug resistance. *Curr Drug Targets*, 7, 861-79.
- O'FARRELL, P. H. 1975. High resolution two-dimensional electrophoresis of proteins. *J Biol Chem*, 250, 4007-21.
- OBCHOEI, S., WONGKHAN, S., WONGKHAM, C., LI, M., YAO, Q. & CHEN, C. 2009. Cyclophilin A: potential functions and therapeutic target for human cancer. *Med Sci Monit*, 15, RA221-32.
- OBERMAIR, A., OBRUCA, A., POHL, M., KAIDER, A., VALES, A., LEODOLTER, S., WOJTA, J. & FEICHTINGER, W. 1999. Vascular endothelial growth factor and its receptors in male fertility. *Fertil Steril*, 72, 269-75.
- OKAMOTO, A., SAMESHIMA, Y., YOKOYAMA, S., TERASHIMA, Y., SUGIMURA, T., TERADA, M. & YOKOTA, J. 1991. Frequent allelic losses and mutations of the p53 gene in human ovarian cancer. *Cancer Res*, 51, 5171-6.
- OLSON, B. J. & MARKWELL, J. 2007. Assays for determination of protein concentration. *Curr Protoc Protein Sci*, Chapter 3, Unit 3 4.
- OMENN, G. S., STATES, D. J., ADAMSKI, M., BLACKWELL, T. W., MENON, R., HERMJAKOB, H., APWEILER, R., HAAB, B. B., SIMPSON, R. J., EDDES, J. S., KAPP, E. A., MORITZ, R. L., CHAN, D. W., RAI, A. J., ADMON, A., AEBERSOLD, R., ENG, J., HANCOCK, W. S., HEFTA, S. A., MEYER, H., PAIK, Y. K., YOO, J. S., PING, P., POUNDS, J., ADKINS, J., QIAN, X., WANG, R., WASINGER, V., WU, C. Y., ZHAO, X., ZENG, R., ARCHAKOV, A., TSUGITA, A., BEER, I., PANDEY, A., PISANO, M., ANDREWS, P., TAMMEN, H., SPEICHER, D. W. & HANASH, S. M. 2005. Overview of the HUPO Plasma Proteome Project: results from the pilot phase with 35 collaborating laboratories and multiple analytical groups, generating a core dataset of 3020 proteins and a publicly-available database. *Proteomics*, 5, 3226-45.
- ONG, S. E., SCHENONE, M., MARGOLIN, A. A., LI, X., DO, K., DOUD, M. K., MANI, D. R., KUAI, L., WANG, X., WOOD, J. L., TOLLIDAY, N. J., KOEHLER, A. N., MARCAURELLE, L. A., GOLUB, T. R., GOULD, R. J., SCHREIBER, S. L. & CARR, S. A. 2009. Identifying the

- proteins to which small-molecule probes and drugs bind in cells. *Proc Natl Acad Sci U S A*, 106, 4617-22.
- OPAL, P., GARCIA, J. J., MCCALL, A. E., XU, B., WEEBER, E. J., SWEATT, J. D., ORR, H. T. & ZOGHBI, H. Y. 2004. Generation and characterization of LANP/pp32 null mice. *Mol Cell Biol*, 24, 3140-9.
- ORNSTEIN, D. K. & TYSON, D. R. 2006. Proteomics for the identification of new prostate cancer biomarkers. *Urol Oncol*, 24, 231-6.
- ORR, G. A., VERDIER-PINARD, P., MCDAID, H. & HORWITZ, S. B. 2003. Mechanisms of Taxol resistance related to microtubules. *Oncogene*, 22, 7280-95.
- PAGE, J., HEATH, J., FULTON, R., YALKOWSKY, E., TABIBI, E., TOMASZEWSKI, J. & AL., E. 1997. Comparison of geldanamycin (NSC- 122750) and 17-allylaminogeldanamycin (NSC-330507D) toxicity in rats. *Proc Am Assoc Cancer Res*, 38, 308.
- PALAGI, P. M., HERNANDEZ, P., WALTHER, D. & APPEL, R. D. 2006. Proteome informatics I: bioinformatics tools for processing experimental data. *Proteomics*, 6, 5435-44.
- PANARETOU, B., PRODROMOUC, C., ROE, S. M., O'BRIEN, R., LADBURY, J. E., PIPER, P. W. & PEARL, L. H. 1998. ATP binding and hydrolysis are essential to the function of the Hsp90 molecular chaperone in vivo. *The EMBO journal*, 17, 4829-36.
- PARK, K. S., HAN, B. G., LEE, K. H., KIM, D. S., KIM, J. M., JEON, H., KIM, H. S., SUH, S. W., LEE, E. H., KIM, S. Y. & LEE, B. I. 2009. Depletion of nucleophosmin via transglutaminase 2 cross-linking increases drug resistance in cancer cells. *Cancer Lett*, 274, 201-7.
- PARMLEY, T. H. & WOODRUFF, J. D. 1974. The ovarian mesothelioma. *Am J Obstet Gynecol*, 120, 234-41.
- PASTORES, G. M., WEINREB, N. J., AERTS, H., ANDRIA, G., COX, T. M., GIRALT, M., GRABOWSKI, G. A., MISTRY, P. K. & TYLKI-SZYMANSKA, A. 2004. Therapeutic goals in the treatment of Gaucher disease. *Semin Hematol*, 41, 4-14.
- PATEL, K., PIAGENTINI, M., RASCHER, A., TIAN, Z. Q., BUCHANAN, G. O., REGENTIN, R., HU, Z., HUTCHINSON, C. R. & MCDANIEL, R. 2004. Engineered biosynthesis of geldanamycin analogs for Hsp90 inhibition. *Chem Biol*, 11, 1625-33.
- PATEL, S. M., DE LA FUENTE, M., KE, S., GUIMARAES, A. M., OLIYIDE, A. O., JI, X., STAPLETON, P., OSBOURN, A., PAN, Y., BOWLES, D. J., DAVIS, B. G., SCHATZLEIN, A. & YANG, M. 2011. High throughput discovery of heteroaromatic-modifying enzymes allows enhancement of novobiocin selectivity. *Chemical communications*, 47, 10569-71.
- PAUL, S. M., MYTELKA, D. S., DUNWIDDIE, C. T., PERSINGER, C. C., MUNOS, B. H., LINDBORG, S. R. & SCHACHT, A. L. 2010. How to improve R&D productivity: the pharmaceutical industry's grand challenge. *Nat Rev Drug Discov*, 9, 203-14.
- PAULSEN, H., KOSTER, H. & HEYNS, K. 1967. [Synthesis of 9-beta-L-sorbopyranosyl-adenine (9-beta-L-xylo-hexulopyranosyl-adenine)]. *Chem Ber*, 100, 2669-80.
- PEARCE, C. L., TEMPLEMAN, C., ROSSING, M. A., LEE, A., NEAR, A. M., WEBB, P. M., NAGLE, C. M., DOHERTY, J. A., CUSHING-HAUGEN, K. L., WICKLUND, K. G., CHANG-CLAUDE, J., HEIN, R., LURIE, G., WILKENS, L. R., CARNEY, M. E., GOODMAN, M. T., MOYSICH, K., KJAER, S. K., HOGDALL, E., JENSEN, A., GOODE, E. L., FRIDLEY, B. L., LARSON, M. C., SCHILDKRAUT, J. M., PALMIERI, R. T., CRAMER, D. W., TERRY, K. L., VITONIS, A. F., TITUS, L. J., ZIOGAS, A., BREWSTER, W., ANTON-CULVER, H., GENTRY-MAHARAJ, A., RAMUS, S. J., ANDERSON, A. R., BRUEGGMANN, D., FASCHING, P. A., GAYTHER, S. A., HUNTSMAN, D. G., MENON, U., NESS, R. B., PIKE, M. C., RISCH, H., WU, A. H. & BERCHUCK, A. 2012. Association between endometriosis and risk of histological subtypes of ovarian cancer: a pooled analysis of case-control studies. *The lancet oncology*, 13, 385-94.
- PEARL, L. H. & PRODROMOUC, C. 2000. Structure and in vivo function of Hsp90. *Curr Opin Struct Biol*, 10, 46-51.

- PECORELLI, S., BENEDET, J. L., CREASMAN, W. T. & SHEPHERD, J. H. 1999. FIGO staging of gynecologic cancer. 1994-1997 FIGO Committee on Gynecologic Oncology. International Federation of Gynecology and Obstetrics. *Int J Gynaecol Obstet*, 65, 243-9.
- PENG, Y., CHEN, L., LI, C., LU, W. & CHEN, J. 2001. Inhibition of MDM2 by hsp90 contributes to mutant p53 stabilization. *J Biol Chem*, 276, 40583-90.
- PEREGO, P., GIAROLA, M., RIGHETTI, S. C., SUPINO, R., CASERINI, C., DELIA, D., PIEROTTI, M. A., MIYASHITA, T., REED, J. C. & ZUNINO, F. 1996. Association between cisplatin resistance and mutation of p53 gene and reduced bax expression in ovarian carcinoma cell systems. *Cancer Res*, 56, 556-62.
- PEREGO, P., ROMANELLI, S., CARENINI, N., MAGNANI, I., LEONE, R., BONETTI, A., PAOLICCHI, A. & ZUNINO, F. 1998. Ovarian cancer cisplatin-resistant cell lines: multiple changes including collateral sensitivity to Taxol. *Ann Oncol*, 9, 423-30.
- PERKINS, D. N., PAPPIN, D. J., CREASY, D. M. & COTTRELL, J. S. 1999. Probability-based protein identification by searching sequence databases using mass spectrometry data. *Electrophoresis*, 20, 3551-67.
- PICCART, M. J., BERTELSEN, K., JAMES, K., CASSIDY, J., MANGIONI, C., SIMONSEN, E., STUART, G., KAYE, S., VERGOTE, I., BLOM, R., GRIMSHAW, R., ATKINSON, R. J., SWENERTON, K. D., TROPE, C., NARDI, M., KAERN, J., TUMOLO, S., TIMMERS, P., ROY, J. A., LHOAS, F., LINDVALL, B., BACON, M., BIRT, A., ANDERSEN, J. E., ZEE, B., PAUL, J., BARON, B. & PECORELLI, S. 2000. Randomized intergroup trial of cisplatin-paclitaxel versus cisplatin-cyclophosphamide in women with advanced epithelial ovarian cancer: three-year results. *J Natl Cancer Inst*, 92, 699-708.
- PLATT, F. M., NEISES, G. R., DWEK, R. A. & BUTTERS, T. D. 1994a. N-butyldeoxyojirimycin is a novel inhibitor of glycolipid biosynthesis. *J Biol Chem*, 269, 8362-5.
- PLATT, F. M., NEISES, G. R., KARLSSON, G. B., DWEK, R. A. & BUTTERS, T. D. 1994b. N-butyldeoxygalactonojirimycin inhibits glycolipid biosynthesis but does not affect N-linked oligosaccharide processing. *J Biol Chem*, 269, 27108-14.
- PLATT, F. M., REINKENSMEIER, G., DWEK, R. A. & BUTTERS, T. D. 1997. Extensive glycosphingolipid depletion in the liver and lymphoid organs of mice treated with N-butyldeoxyojirimycin. *J Biol Chem*, 272, 19365-72.
- PLUMB, J. A., STRATHDEE, G., SLUDDEN, J., KAYE, S. B. & BROWN, R. 2000. Reversal of drug resistance in human tumor xenografts by 2'-deoxy-5-azacytidine-induced demethylation of the hMLH1 gene promoter. *Cancer Res*, 60, 6039-44.
- PORTER, J. R., FRITZ, C. C. & DEPEW, K. M. 2010. Discovery and development of Hsp90 inhibitors: a promising pathway for cancer therapy. *Current opinion in chemical biology*, 14, 412-20.
- PORUCHYNSKY, M. S., GIANNAKAKOU, P., WARD, Y., BULINSKI, J. C., TELFORD, W. G., ROBEY, R. W. & FOJO, T. 2001. Accompanying protein alterations in malignant cells with a microtubule-polymerizing drug-resistance phenotype and a primary resistance mechanism. *Biochem Pharmacol*, 62, 1469-80.
- POSEY, S. C. & BIERER, B. E. 1999. Actin stabilization by jasplakinolide enhances apoptosis induced by cytokine deprivation. *J Biol Chem*, 274, 4259-65.
- POWERS, M. V. & WORKMAN, P. 2006. Targeting of multiple signalling pathways by heat shock protein 90 molecular chaperone inhibitors. *Endocr Relat Cancer*, 13 Suppl 1, S125-35.
- PRITCHARD, K. A., JR., ACKERMAN, A. W., GROSS, E. R., STEPP, D. W., SHI, Y., FONTANA, J. T., BAKER, J. E. & SESSA, W. C. 2001. Heat shock protein 90 mediates the balance of nitric oxide and superoxide anion from endothelial nitric-oxide synthase. *J Biol Chem*, 276, 17621-4.
- PRODROMOU, C., PANARETOU, B., CHOCHAN, S., SILIGARDI, G., O'BRIEN, R., LADBURY, J. E., ROE, S. M., PIPER, P. W. & PEARL, L. H. 2000. The ATPase cycle of Hsp90 drives a

- molecular 'clamp' via transient dimerization of the N-terminal domains. *EMBO J*, 19, 4383-92.
- PRODROMOU, C., ROE, S. M., O'BRIEN, R., LADBURY, J. E., PIPER, P. W. & PEARL, L. H. 1997. Identification and structural characterization of the ATP/ADP-binding site in the Hsp90 molecular chaperone. *Cell*, 90, 65-75.
- PURI, C., CHIBALINA, M. V., ARDEN, S. D., KRUPPA, A. J., KENDRICK-JONES, J. & BUSS, F. 2010. Overexpression of myosin VI in prostate cancer cells enhances PSA and VEGF secretion, but has no effect on endocytosis. *Oncogene*, 29, 188-200.
- RABILLOUD, T. (ed.) 2000. *Proteome Research: Two-Dimensional Gel Electrophoresis and Identification Methods*, New York: Springer.
- RABILLOUD, T. 2002. Two-dimensional gel electrophoresis in proteomics: old, old fashioned, but it still climbs up the mountains. *Proteomics*, 2, 3-10.
- RABILLOUD, T., CHEVALLET, M., LUCHE, S. & LELONG, C. 2010. Two-dimensional gel electrophoresis in proteomics: Past, present and future. *J Proteomics*, 73, 2064-77.
- RADANYI, C., LE BRAS, G., MARSAUD, V., PEYRAT, J. F., MESSAOUDI, S., CATELLI, M. G., BRION, J. D., ALAMI, M. & RENOIR, J. M. 2009. Antiproliferative and apoptotic activities of tosylcyclonovobiocic acids as potent heat shock protein 90 inhibitors in human cancer cells. *Cancer Lett*, 274, 88-94.
- RAMP, U., MAHOTKA, C., HEIKAUS, S., SHIBATA, T., GRIMM, M. O., WILLERS, R. & GABBERT, H. E. 2007. Expression of heat shock protein 70 in renal cell carcinoma and its relation to tumor progression and prognosis. *Histol Histopathol*, 22, 1099-107.
- RASK-ANDERSEN, M., ALMEN, M. S. & SCHIOTH, H. B. 2011. Trends in the exploitation of novel drug targets. *Nat Rev Drug Discov*, 10, 579-90.
- RAVAL, G. N., BHARADWAJ, S., LEVINE, E. A., WILLINGHAM, M. C., GEARY, R. L., KUTE, T. & PRASAD, G. L. 2003. Loss of expression of tropomyosin-1, a novel class II tumor suppressor that induces anoikis, in primary breast tumors. *Oncogene*, 22, 6194-203.
- REILLY, P. T., AFZAL, S., GORRINI, C., LUI, K., BUKHMAN, Y. V., WAKEHAM, A., HAIGHT, J., LING, T. W., CHEUNG, C. C., ELIA, A. J., TURNER, P. V. & MAK, T. W. 2011. Acidic nuclear phosphoprotein 32kDa (ANP32)B-deficient mouse reveals a hierarchy of ANP32 importance in mammalian development. *Proc Natl Acad Sci U S A*, 108, 10243-8.
- RENART, J., REISER, J. & STARK, G. R. 1979. Transfer of proteins from gels to diazobenzyloxymethyl-paper and detection with antisera: a method for studying antibody specificity and antigen structure. *Proc Natl Acad Sci U S A*, 76, 3116-20.
- RICANIADIS, N., KATAKI, A., AGNANTIS, N., ANDROULAKIS, G. & KARAKOUSIS, C. P. 2001. Long-term prognostic significance of HSP-70, c-myc and HLA-DR expression in patients with malignant melanoma. *Eur J Surg Oncol*, 27, 88-93.
- RICHTER, K., MOSER, S., HAGN, F., FRIEDRICH, R., HAINZL, O., HELLER, M., SCHLEE, S., KESSLER, H., REINSTEIN, J. & BUCHNER, J. 2006. Intrinsic inhibition of the Hsp90 ATPase activity. *The Journal of biological chemistry*, 281, 11301-11.
- RICHTER, K., MUSCHLER, P., HAINZL, O., REINSTEIN, J. & BUCHNER, J. 2003. Sti1 is a non-competitive inhibitor of the Hsp90 ATPase. Binding prevents the N-terminal dimerization reaction during the atpase cycle. *The Journal of biological chemistry*, 278, 10328-33.
- RIGHETTI, P. G. 1990. Recent developments in electrophoretic methods. *J Chromatogr*, 516, 3-22.
- RIGHETTI, P. G., CASTAGNA, A., ANTONUCCI, F., PIUBELLI, C., CECCONI, D., CAMPOSTRINI, N., RUSTICHELLI, C., ANTONIOLI, P., ZANUSSO, G., MONACO, S., LOMAS, L. & BOSCHETTI, E. 2005. Proteome analysis in the clinical chemistry laboratory: myth or reality? *Clin Chim Acta*, 357, 123-39.
- RISCH, H. A., MCLAUGHLIN, J. R., COLE, D. E., ROSEN, B., BRADLEY, L., FAN, I., TANG, J., LI, S., ZHANG, S., SHAW, P. A. & NAROD, S. A. 2006. Population BRCA1 and BRCA2

- mutation frequencies and cancer penetrances: a kin-cohort study in Ontario, Canada. *J Natl Cancer Inst*, 98, 1694-706.
- RITOSSA, F. 1962. A new puffing pattern induced by temperature shock and DNP in drosophila. *Experientia*, 18, 571-573.
- ROBERTS, D., SCHICK, J., CONWAY, S., BIADÉ, S., LAUB, P. B., STEVENSON, J. P., HAMILTON, T. C., O'DWYER, P. J. & JOHNSON, S. W. 2005. Identification of genes associated with platinum drug sensitivity and resistance in human ovarian cancer cells. *Br J Cancer*, 92, 1149-58.
- ROBERTS, D. V. 1977. *Enzyme kinetics*, Cambridge, Cambridge University Press.
- ROBINSON, D. N. 2010. 14-3-3, an integrator of cell mechanics and cytokinesis. *Small GTPases*, 1, 165-169.
- ROBYT, J. F. & WHITE, B. J. 1987. *Biochemical Techniques: Theory and Practice*, Monterey, CA, Brooks/Cole Publishing Company.
- ROE, S. M., PRODROMOU, C., O'BRIEN, R., LADBURY, J. E., PIPER, P. W. & PEARL, L. H. 1999. Structural basis for inhibition of the Hsp90 molecular chaperone by the antitumor antibiotics radicicol and geldanamycin. *J Med Chem*, 42, 260-6.
- ROSANO, L., DI CASTRO, V., SPINELLA, F., NICOTRA, M. R., NATALI, P. G. & BAGNATO, A. 2007. ZD4054, a specific antagonist of the endothelin A receptor, inhibits tumor growth and enhances paclitaxel activity in human ovarian carcinoma in vitro and in vivo. *Mol Cancer Ther*, 6, 2003-11.
- ROSENBERG, B., VANCAMP, L. & KRIGAS, T. 1965. Inhibition of Cell Division in Escherichia Coli by Electrolysis Products from a Platinum Electrode. *Nature*, 205, 698-9.
- ROSENBERG, B., VANCAMP, L., TROSKO, J. E. & MANSOUR, V. H. 1969. Platinum compounds: a new class of potent antitumour agents. *Nature*, 222, 385-6.
- RUDD, P. M., ELLIOTT, T., CRESSWELL, P., WILSON, I. A. & DWEK, R. A. 2001. Glycosylation and the immune system. *Science*, 291, 2370-6.
- RUTHERFORD, S. L. & LINDQUIST, S. 1998. Hsp90 as a capacitor for morphological evolution. *Nature*, 396, 336-42.
- SACHIDANANDAM, R., WEISSMAN, D., SCHMIDT, S. C., KAKOL, J. M., STEIN, L. D., MARTH, G., SHERRY, S., MULLIKIN, J. C., MORTIMORE, B. J., WILLEY, D. L., HUNT, S. E., COLE, C. G., COGGILL, P. C., RICE, C. M., NING, Z., ROGERS, J., BENTLEY, D. R., KWOK, P. Y., MARDIS, E. R., YEH, R. T., SCHULTZ, B., COOK, L., DAVENPORT, R., DANTE, M., FULTON, L., HILLIER, L., WATERSTON, R. H., MCPHERSON, J. D., GILMAN, B., SCHAFFNER, S., VAN ETTEN, W. J., REICH, D., HIGGINS, J., DALY, M. J., BLUMENSTIEL, B., BALDWIN, J., STANGE-THOMANN, N., ZODY, M. C., LINTON, L., LANDER, E. S., ALTSHULER, D. & INTERNATIONAL, S. N. P. M. W. G. 2001. A map of human genome sequence variation containing 1.42 million single nucleotide polymorphisms. *Nature*, 409, 928-33.
- SADDOUGHI, S. A., GENCER, S., PETERSON, Y. K., WARD, K. E., MUKHOPADHYAY, A., OAKS, J., BIELAWSKI, J., SZULC, Z. M., THOMAS, R. J., SELVAM, S. P., SENKAL, C. E., GARRETT-MAYER, E., DE PALMA, R. M., FEDAROVICH, D., LIU, A., HABIB, A. A., STAHELIN, R. V., PERROTTI, D. & OGRETMENTEN, B. 2013. Sphingosine analogue drug FTY720 targets I2PP2A/SET and mediates lung tumour suppression via activation of PP2A-RIPK1-dependent necroptosis. *EMBO Mol Med*, 5, 105-21.
- SAIN, N., KRISHNAN, B., ORMEROD, M. G., DE RIENZO, A., LIU, W. M., KAYE, S. B., WORKMAN, P. & JACKMAN, A. L. 2006. Potentiation of paclitaxel activity by the HSP90 inhibitor 17-allylamino-17-demethoxygeldanamycin in human ovarian carcinoma cell lines with high levels of activated AKT. *Mol Cancer Ther*, 5, 1197-208.
- SATURNO, G., VALENTI, M., DE HAVEN BRANDON, A., THOMAS, G. V., ECCLES, S., CLARKE, P. A. & WORKMAN, P. 2013. Combining trail with pi3 kinase or hsp90 inhibitors enhances apoptosis in colorectal cancer cells via suppression of survival signaling. *Oncotarget*.

- SAUNIER, B., KILKER, R. D., JR., TKACZ, J. S., QUARONI, A. & HERSCOVICS, A. 1982. Inhibition of N-linked complex oligosaccharide formation by 1-deoxynojirimycin, an inhibitor of processing glucosidases. *J Biol Chem*, 257, 14155-61.
- SAWAI, A., CHANDARLAPATY, S., GREULICH, H., GONEN, M., YE, Q., ARTEAGA, C. L., SELLERS, W., ROSEN, N. & SOLIT, D. B. 2008. Inhibition of Hsp90 down-regulates mutant epidermal growth factor receptor (EGFR) expression and sensitizes EGFR mutant tumors to paclitaxel. *Cancer Res*, 68, 589-96.
- SCAMBIA, G., FERRANDINA, G., MARONE, M., BENEDETTI PANICI, P., GIANNITELLI, C., PIANTELLI, M., LEONE, A. & MANCUSO, S. 1996. nm23 in ovarian cancer: correlation with clinical outcome and other clinicopathologic and biochemical prognostic parameters. *J Clin Oncol*, 14, 334-42.
- SCHEELE, G. A. 1975. Two-dimensional gel analysis of soluble proteins. Characterization of guinea pig exocrine pancreatic proteins. *J Biol Chem*, 250, 5375-85.
- SCHREIBER, S. L., CLAUS, R. E. & REAGAN, J. 1982. Ozonolytic cleavage of cycloalkenes to terminally differentiated products. *Tetrahedron Letters*, 23, 3867-3870.
- SCHULTE, T. W., AKINAGA, S., MURAKATA, T., AGATSUMA, T., SUGIMOTO, S., NAKANO, H., LEE, Y. S., SIMEN, B. B., ARGON, Y., FELTS, S., TOFT, D. O., NECKERS, L. M. & SHARMA, S. V. 1999. Interaction of radicicol with members of the heat shock protein 90 family of molecular chaperones. *Mol Endocrinol*, 13, 1435-48.
- SCHULTE, T. W., BLAGOSKLONNY, M. V., ROMANOVA, L., MUSHINSKI, J. F., MONIA, B. P., JOHNSTON, J. F., NGUYEN, P., TREPEL, J. & NECKERS, L. M. 1996. Destabilization of Raf-1 by geldanamycin leads to disruption of the Raf-1-MEK-mitogen-activated protein kinase signalling pathway. *Mol Cell Biol*, 16, 5839-45.
- SCHULTE, T. W. & NECKERS, L. M. 1998. The benzoquinone ansamycin 17-allylamino-17-demethoxygeldanamycin binds to HSP90 and shares important biologic activities with geldanamycin. *Cancer Chemother Pharmacol*, 42, 273-9.
- SCUDDER, P., NEVILLE, D. C., BUTTERS, T. D., FLEET, G. W., DWEK, R. A., RADEMACHER, T. W. & JACOB, G. S. 1990. The isolation by ligand affinity chromatography of a novel form of alpha-L-fucosidase from almond. *J Biol Chem*, 265, 16472-7.
- SCULLY, R., CHEN, J., PLUG, A., XIAO, Y., WEAVER, D., FEUNTEUN, J., ASHLEY, T. & LIVINGSTON, D. M. 1997. Association of BRCA1 with Rad51 in mitotic and meiotic cells. *Cell*, 88, 265-75.
- SCULLY, R. E. 1987. Classification of human ovarian tumors. *Environ Health Perspect*, 73, 15-25.
- SEMENZA, G. L. 2001. Regulation of hypoxia-induced angiogenesis: a chaperone escorts VEGF to the dance. *J Clin Invest*, 108, 39-40.
- SEROV, S. F., SCULLY, R. E. & SOBIN, L. H. 1973. Histological typing of ovarian tumours. Geneva, Switzerland: World Health Organization.
- SHARMA, S. V., AGATSUMA, T. & NAKANO, H. 1998. Targeting of the protein chaperone, HSP90, by the transformation suppressing agent, radicicol. *Oncogene*, 16, 2639-45.
- SHAW, P. E. 2007. Peptidyl-prolyl cis/trans isomerases and transcription: is there a twist in the tail? *EMBO Rep*, 8, 40-5.
- SHAYESTEH, L., LU, Y., KUO, W. L., BALDOCCHI, R., GODFREY, T., COLLINS, C., PINKEL, D., POWELL, B., MILLS, G. B. & GRAY, J. W. 1999. PIK3CA is implicated as an oncogene in ovarian cancer. *Nat Genet*, 21, 99-102.
- SHELTON, S. N., SHAWGO, M. E., MATTHEWS, S. B., LU, Y., DONNELLY, A. C., SZABLA, K., TANOL, M., VIELHAUER, G. A., RAJEWSKI, R. A., MATTS, R. L., BLAGG, B. S. & ROBERTSON, J. D. 2009. KU135, a novel novobiocin-derived C-terminal inhibitor of the 90-kDa heat shock protein, exerts potent antiproliferative effects in human leukemic cells. *Molecular pharmacology*, 76, 1314-22.

- SHINOHARA-GOTOH, Y., NISHIDA, E., HOSHI, M. & SAKAI, H. 1991. Activation of microtubule-associated protein kinase by microtubule disruption in quiescent rat 3Y1 cells. *Exp Cell Res*, 193, 161-6.
- SIDDIK, Z. H. 2003. Cisplatin: mode of cytotoxic action and molecular basis of resistance. *Oncogene*, 22, 7265-79.
- SIMPSON, R. J. 2003. *Proteins and proteomics: a laboratory manual*, Cold Spring Harbour, New York, Cold Spring Harbour Laboratory Press.
- SITTAMPALAM, G. S., GAL-EDD, N., ARKIN, M., AULD, D., AUSTIN, C., BEJCEK, B., GLICKSMAN, M., INGLESE, J., LEMMON, V., LI, Z., MCGEE, J., MCMANUS, O., MINOR, L., NAPPER, A., RISS, T., TRASK, O. J. & WEIDNER, J. (eds.) 2004. *Assay guidance manual*, Bethesda, MD, USA: Eli Lilly & Company and the National Center for Advancing Translational Sciences.
- SIUZDAK, G. 2003. *The expanding role of mass spectrometry in biotechnology*, San Diego, MCC Press.
- SKEEL, R. T. (ed.) 2007. *Handbook of cancer chemotherapy*, Philadelphia, PA, USA: Lippincott Williams & Wilkins.
- SMITH, L., LIND, M. J., WELHAM, K. J., CAWKWELL, L. & CANCER BIOLOGY PROTEOMICS, G. 2006. Cancer proteomics and its application to discovery of therapy response markers in human cancer. *Cancer*, 107, 232-41.
- SOGA, S., NECKERS, L. M., SCHULTE, T. W., SHIOTSU, Y., AKASAKA, K., NARUMI, H., AGATSUMA, T., IKUINA, Y., MURAKATA, C., TAMAOKI, T. & AKINAGA, S. 1999. KF25706, a novel oxime derivative of radicicol, exhibits in vivo antitumor activity via selective depletion of Hsp90 binding signaling molecules. *Cancer Res*, 59, 2931-8.
- SOLIT, D. B., ZHENG, F. F., DROBNJAK, M., MUNSTER, P. N., HIGGINS, B., VERBEL, D., HELLER, G., TONG, W., CORDON-CARDO, C., AGUS, D. B., SCHER, H. I. & ROSEN, N. 2002. 17-Allylamino-17-demethoxygeldanamycin induces the degradation of androgen receptor and HER-2/neu and inhibits the growth of prostate cancer xenografts. *Clin Cancer Res*, 8, 986-93.
- SOULE, H. D., VAZGUEZ, J., LONG, A., ALBERT, S. & BRENNAN, M. 1973. A human cell line from a pleural effusion derived from a breast carcinoma. *J Natl Cancer Inst*, 51, 1409-16.
- STEBBINS, C. E., RUSSO, A. A., SCHNEIDER, C., ROSEN, N., HARTL, F. U. & PAVLETICH, N. P. 1997. Crystal structure of an Hsp90-geldanamycin complex: targeting of a protein chaperone by an antitumor agent. *Cell*, 89, 239-50.
- STEEG, P. S., BEVILACQUA, G., POZZATTI, R., LIOTTA, L. A. & SOBEL, M. E. 1988. Altered expression of NM23, a gene associated with low tumor metastatic potential, during adenovirus 2 Ela inhibition of experimental metastasis. *Cancer Res*, 48, 6550-4.
- STEWART, D. J. 2007. Mechanisms of resistance to cisplatin and carboplatin. *Crit Rev Oncol Hematol*, 63, 12-31.
- STEWART, J. J., WHITE, J. T., YAN, X., COLLINS, S., DRESCHER, C. W., URBAN, N. D., HOOD, L. & LIN, B. 2006. Proteins associated with Cisplatin resistance in ovarian cancer cells identified by quantitative proteomic technology and integrated with mRNA expression levels. *Mol Cell Proteomics*, 5, 433-43.
- STRAVOPODIS, D. J., MARGARITIS, L. H. & VOUSINAS, G. E. 2007. Drug-mediated targeted disruption of multiple protein activities through functional inhibition of the Hsp90 chaperone complex. *Current medicinal chemistry*, 14, 3122-38.
- SUGANUMA, R., WALDEN, C. M., BUTTERS, T. D., PLATT, F. M., DWEK, R. A., YANAGIMACHI, R. & VAN DER SPOEL, A. C. 2005. Alkylated imino sugars, reversible male infertility-inducing agents, do not affect the genetic integrity of male mouse germ cells during short-term treatment despite induction of sperm deformities. *Biol Reprod*, 72, 805-13.

- SUN, J. & LIAO, J. K. 2004. Induction of angiogenesis by heat shock protein 90 mediated by protein kinase Akt and endothelial nitric oxide synthase. *Arterioscler Thromb Vasc Biol*, 24, 2238-44.
- SUPKO, J. G., HICKMAN, R. L., GREVER, M. R. & MALSPEIS, L. 1995. Preclinical pharmacologic evaluation of geldanamycin as an antitumor agent. *Cancer Chemother Pharmacol*, 36, 305-15.
- SZE, S. K., GE, Y., OH, H. & MCLAFFERTY, F. W. 2002. Top-down mass spectrometry of a 29-kDa protein for characterization of any posttranslational modification to within one residue. *Proc Natl Acad Sci U S A*, 99, 1774-9.
- TAVARIA, M., GABRIELE, T., KOLA, I. & ANDERSON, R. L. 1996. A hitchhiker's guide to the human Hsp70 family. *Cell Stress Chaperones*, 1, 23-8.
- TAYLOR, S., ACADEMIA, K., ALBURO, A., PAULUS, A., SMITH, K. & CORREA, T. (eds.) 2008. *A practical approach to proteomics*, Hercules, CA, USA: Bio-Rad Laboratories, Inc.
- TEODORI, E., DEI, S., MARTELLI, C., SCAPECCHI, S. & GUALTIERI, F. 2006. The functions and structure of ABC transporters: implications for the design of new inhibitors of Pgp and MRP1 to control multidrug resistance (MDR). *Curr Drug Targets*, 7, 893-909.
- THURSTON, D. E. 2007. *Chemistry and pharmacology of anticancer drugs*, Boca Raton, Florida, USA, CRC Press (Taylor & Francis).
- TIAN, Y., TAN, A. C., SUN, X., OLSON, M. T., XIE, Z., JINAWATH, N., CHAN, D. W., SHIH IE, M., ZHANG, Z. & ZHANG, H. 2009. Quantitative proteomic analysis of ovarian cancer cells identified mitochondrial proteins associated with Paclitaxel resistance. *Proteomics Clin Appl*, 3, 1288-95.
- TISSIERES, A., MITCHELL, H. K. & TRACY, U. M. 1974. Protein synthesis in salivary glands of *Drosophila melanogaster*: relation to chromosome puffs. *J Mol Biol*, 84, 389-98.
- TONGE, R., SHAW, J., MIDDLETON, B., ROWLINSON, R., RAYNER, S., YOUNG, J., POGNAN, F., HAWKINS, E., CURRIE, I. & DAVISON, M. 2001. Validation and development of fluorescence two-dimensional differential gel electrophoresis proteomics technology. *Proteomics*, 1, 377-96.
- TOWBIN, H., STAHELIN, T. & GORDON, J. 1979. Electrophoretic transfer of proteins from polyacrylamide gels to nitrocellulose sheets: procedure and some applications. *Proc Natl Acad Sci U S A*, 76, 4350-4.
- TREAT, J., SCHILLER, J., QUOIX, E., MAUER, A., EDELMAN, M., MODIANO, M., BONOMI, P., RAMLAU, R. & LEMARIE, E. 2002. ZD0473 treatment in lung cancer: an overview of the clinical trial results. *Eur J Cancer*, 38 Suppl 8, S13-8.
- TREPEL, J., MOLLAPOUR, M., GIACCONE, G. & NECKERS, L. 2010. Targeting the dynamic HSP90 complex in cancer. *Nat Rev Cancer*, 10, 537-49.
- UEHARA, Y., HORI, M., TAKEUCHI, T. & UMEZAWA, H. 1986. Phenotypic change from transformed to normal induced by benzoquinonoid ansamycins accompanies inactivation of p60src in rat kidney cells infected with Rous sarcoma virus. *Mol Cell Biol*, 6, 2198-206.
- UHLEN, M. 2008. Affinity as a tool in life science. *Biotechniques*, 44, 649-54.
- URH, M., SIMPSON, D. & ZHAO, K. 2009. Chapter 26 Affinity Chromatography: General Methods. In: RICHARD, R. B. & MURRAY, P. D. (eds.) *Methods in Enzymology*. Academic Press.
- VAN DER SPOEL, A. C., JEYAKUMAR, M., BUTTERS, T. D., CHARLTON, H. M., MOORE, H. D., DWEK, R. A. & PLATT, F. M. 2002. Reversible infertility in male mice after oral administration of alkylated imino sugars: a nonhormonal approach to male contraception. *Proc Natl Acad Sci U S A*, 99, 17173-8.
- VARELA, M. A. & AMOS, W. 2010. Heterogeneous distribution of SNPs in the human genome: microsatellites as predictors of nucleotide diversity and divergence. *Genomics*, 95, 151-9.

- VASEY, P. A., JAYSON, G. C., GORDON, A., GABRA, H., COLEMAN, R., ATKINSON, R., PARKIN, D., PAUL, J., HAY, A., KAYE, S. B. & SCOTTISH GYNAECOLOGICAL CANCER TRIALS, G. 2004. Phase III randomized trial of docetaxel-carboplatin versus paclitaxel-carboplatin as first-line chemotherapy for ovarian carcinoma. *J Natl Cancer Inst*, 96, 1682-91.
- VERMEULEN, K., VAN BOCKSTAELE, D. R. & BERNEMAN, Z. N. 2003. The cell cycle: a review of regulation, deregulation and therapeutic targets in cancer. *Cell Prolif*, 36, 131-49.
- VERRILLS, N. M., PO'UHA, S. T., LIU, M. L., LIAW, T. Y., LARSEN, M. R., IVERY, M. T., MARSHALL, G. M., GUNNING, P. W. & KAVALLARIS, M. 2006. Alterations in gamma-actin and tubulin-targeted drug resistance in childhood leukemia. *J Natl Cancer Inst*, 98, 1363-74.
- VOGEL, H. G. (ed.) 2002. *Drug discovery and evaluation - Pharmacological assays*, Germany: Springer.
- VOS, M. J., HAGEMAN, J., CARRA, S. & KAMPINGA, H. H. 2008. Structural and functional diversities between members of the human HSPB, HSPH, HSPA, and DNAJ chaperone families. *Biochemistry*, 47, 7001-11.
- VOSS, T. & HABERL, P. 2000. Observations on the reproducibility and matching efficiency of two-dimensional electrophoresis gels: consequences for comprehensive data analysis. *Electrophoresis*, 21, 3345-50.
- WALDEN, C. M., SANDHOFF, R., CHUANG, C. C., YILDIZ, Y., BUTTERS, T. D., DWEK, R. A., PLATT, F. M. & VAN DER SPOEL, A. C. 2007. Accumulation of glucosylceramide in murine testis, caused by inhibition of beta-glucosidase 2: implications for spermatogenesis. *J Biol Chem*, 282, 32655-64.
- WALSH, G. 2002. *Proteins: Biochemistry and Biotechnology*, USA, John Wiley & Sons Ltd.
- WANG, B., LIU, K., LIN, F. T. & LIN, W. C. 2004a. A role for 14-3-3 tau in E2F1 stabilization and DNA damage-induced apoptosis. *J Biol Chem*, 279, 54140-52.
- WANG, H. & HANASH, S. 2003. Multi-dimensional liquid phase based separations in proteomics. *J Chromatogr B Analyt Technol Biomed Life Sci*, 787, 11-8.
- WANG, H. X., SUN, W., LI, H. L. & ZHANG, W. Y. 2009. Quantitative differences in protein expression between cisplatin sensitive COC1 ovarian carcinoma cells and cisplatin resistant COC1/DDP cells. *Chin Med J (Engl)*, 122, 865-9.
- WANG, J. R., DE VILLENA, F. P., LAWSON, H. A., CHEVERUD, J. M., CHURCHILL, G. A. & MCMILLAN, L. 2012a. Imputation of single-nucleotide polymorphisms in inbred mice using local phylogeny. *Genetics*, 190, 449-58.
- WANG, L. N., TONG, S. W., HU, H. D., YE, F., LI, S. L., REN, H., ZHANG, D. Z., XIANG, R. & YANG, Y. X. 2012b. Quantitative proteome analysis of ovarian cancer tissues using a iTRAQ approach. *J Cell Biochem*, 113, 3762-72.
- WANG, W., KE, S., CHEN, G., GAO, Q., WU, S., WANG, S., ZHOU, J., YANG, X., LU, Y. & MA, D. 2004b. Effect of lung resistance-related protein on the resistance to cisplatin in human ovarian cancer cell lines. *Oncol Rep*, 12, 1365-70.
- WANG, X., LU, Y., YANG, J., SHI, Y., LAN, M., LIU, Z., ZHAI, H. & FAN, D. 2008. Identification of triosephosphate isomerase as an anti-drug resistance agent in human gastric cancer cells using functional proteomic analysis. *J Cancer Res Clin Oncol*, 134, 995-1003.
- WARBURG, O. 1956. On the origin of cancer cells. *Science*, 123, 309-14.
- WASHBURN, M. P., WOLTERS, D. & YATES, J. R. 2001. Large-scale analysis of the yeast proteome by multidimensional protein identification technology. *Nat Biotechnol*, 19, 242-7.
- WATSON, A. A., FLEET, G. W., ASANO, N., MOLYNEUX, R. J. & NASH, R. J. 2001. Polyhydroxylated alkaloids -- natural occurrence and therapeutic applications. *Phytochemistry*, 56, 265-95.

- WAYNE, N. & BOLON, D. N. 2007. Dimerization of Hsp90 is required for in vivo function. Design and analysis of monomers and dimers. *The Journal of biological chemistry*, 282, 35386-95.
- WELLS, L., VOSSELLER, K. & HART, G. W. 2001. Glycosylation of nucleocytoplasmic proteins: signal transduction and O-GlcNAc. *Science*, 291, 2376-8.
- WESSEL, D. & FLUGGE, U. I. 1984. A method for the quantitative recovery of protein in dilute solution in the presence of detergents and lipids. *Anal Biochem*, 138, 141-3.
- WESTERMEIER, R., NAVEN, T. & HOPKER, H. R. 2008. *Proteomics in practice: a guide to successful experimental design*, Weinheim, Wiley-VCH.
- WHITE, S. R., WILLIAMS, P., WOJCIK, K. R., SUN, S., HIEMSTRA, P. S., RABE, K. F. & DORSCHIED, D. R. 2001. Initiation of apoptosis by actin cytoskeletal derangement in human airway epithelial cells. *Am J Respir Cell Mol Biol*, 24, 282-94.
- WHITESSELL, L., MIMNAUGH, E. G., DE COSTA, B., MYERS, C. E. & NECKERS, L. M. 1994. Inhibition of heat shock protein HSP90-pp60v-src heteroprotein complex formation by benzoquinone ansamycins: essential role for stress proteins in oncogenic transformation. *Proc Natl Acad Sci U S A*, 91, 8324-8.
- WHITESSELL, L., SHIFRIN, S. D., SCHWAB, G. & NECKERS, L. M. 1992. Benzoquinonoid ansamycins possess selective tumoricidal activity unrelated to src kinase inhibition. *Cancer Res*, 52, 1721-8.
- WHO. 2013. *Cancer: fact sheet nr 297* [Online]. World Health Organization. Available: <http://www.who.int/mediacentre/factsheets/fs297/en/> [Accessed Nov 2013].
- WIERENGA, R. K., KAPETANIOU, E. G. & VENKATESAN, R. 2010. Triosephosphate isomerase: a highly evolved biocatalyst. *Cell Mol Life Sci*, 67, 3961-82.
- WIESE, M. & PAJEVA, I. K. 2001. Structure-activity relationships of multidrug resistance reversers. *Curr Med Chem*, 8, 685-713.
- WILKINS, M. R., SANCHEZ, J. C., GOOLEY, A. A., APPEL, R. D., HUMPHERY-SMITH, I., HOCHSTRASSER, D. F. & WILLIAMS, K. L. 1996. Progress with proteome projects: why all proteins expressed by a genome should be identified and how to do it. *Biotechnol Genet Eng Rev*, 13, 19-50.
- WITTMANN-LIEBOLD, B., GRAACK, H. R. & POHL, T. 2006. Two-dimensional gel electrophoresis as tool for proteomics studies in combination with protein identification by mass spectrometry. *Proteomics*, 6, 4688-703.
- WOLTERS, D. A., WASHBURN, M. P. & YATES, J. R. 2001. An automated multidimensional protein identification technology for shotgun proteomics. *Anal Chem*, 73, 5683-90.
- WORKMAN, P., BURROWS, F., NECKERS, L. & ROSEN, N. 2007. Drugging the cancer chaperone HSP90: combinatorial therapeutic exploitation of oncogene addiction and tumor stress. *Ann N Y Acad Sci*, 1113, 202-16.
- YAN, X. D., PAN, L. Y., YUAN, Y., LANG, J. H. & MAO, N. 2007. Identification of platinum-resistance associated proteins through proteomic analysis of human ovarian cancer cells and their platinum-resistant sublines. *J Proteome Res*, 6, 772-80.
- YANCIK, R. 1993. Ovarian cancer. Age contrasts in incidence, histology, disease stage at diagnosis, and mortality. *Cancer*, 71, 517-23.
- YANG, X., XING, H., GAO, Q., CHEN, G., LU, Y., WANG, S. & MA, D. 2005. Regulation of HtrA2/Omi by X-linked inhibitor of apoptosis protein in chemoresistance in human ovarian cancer cells. *Gynecol Oncol*, 97, 413-21.
- YILDIZ, Y., MATERN, H., THOMPSON, B., ALLEGOOD, J. C., WARREN, R. L., RAMIREZ, D. M., HAMMER, R. E., HAMRA, F. K., MATERN, S. & RUSSELL, D. W. 2006. Mutation of beta-glucosidase 2 causes glycolipid storage disease and impaired male fertility. *J Clin Invest*, 116, 2985-94.
- YOSHIDA, H., CHENG, W., HUNG, J., MONTELL, D., GEISBRECHT, E., ROSEN, D., LIU, J. & NAORA, H. 2004. Lessons from border cell migration in the Drosophila ovary: A role

- for myosin VI in dissemination of human ovarian cancer. *Proc Natl Acad Sci U S A*, 101, 8144-9.
- YOU, J. S., GELFANOVA, V., KNIERMAN, M. D., WITZMANN, F. A., WANG, M. & HALE, J. E. 2005. The impact of blood contamination on the proteome of cerebrospinal fluid. *Proteomics*, 5, 290-6.
- YUAN, Z. Q., SUN, M., FELDMAN, R. I., WANG, G., MA, X., JIANG, C., COPPOLA, D., NICOSIA, S. V. & CHENG, J. Q. 2000. Frequent activation of AKT2 and induction of apoptosis by inhibition of phosphoinositide-3-OH kinase/Akt pathway in human ovarian cancer. *Oncogene*, 19, 2324-30.
- ZAKERI, Z. F., WOLGEMUTH, D. J. & HUNT, C. R. 1988. Identification and sequence analysis of a new member of the mouse HSP70 gene family and characterization of its unique cellular and developmental pattern of expression in the male germ line. *Mol Cell Biol*, 8, 2925-32.
- ZDRAVESKI, Z. Z., MELLO, J. A., FARINELLI, C. K., ESSIGMANN, J. M. & MARINUS, M. G. 2002. MutS preferentially recognizes cisplatin- over oxaliplatin-modified DNA. *J Biol Chem*, 277, 1255-60.
- ZHA, J., HARADA, H., YANG, E., JOCKEL, J. & KORSMEYER, S. J. 1996. Serine phosphorylation of death agonist BAD in response to survival factor results in binding to 14-3-3 not BCL-X(L). *Cell*, 87, 619-28.
- ZHANG, D., TAI, L. K., WONG, L. L., CHIU, L. L., SETHI, S. K. & KOAY, E. S. 2005. Proteomic study reveals that proteins involved in metabolic and detoxification pathways are highly expressed in HER-2/neu-positive breast cancer. *Mol Cell Proteomics*, 4, 1686-96.
- ZHANG, L., CHEN, J. & FU, H. 1999. Suppression of apoptosis signal-regulating kinase 1-induced cell death by 14-3-3 proteins. *Proc Natl Acad Sci U S A*, 96, 8511-5.
- ZHANG, M., DAI, C., ZHU, H., CHEN, S., WU, Y., LI, Q., ZENG, X., WANG, W., ZUO, J., ZHOU, M., XIA, Z., JI, G., SAIYIN, H., QIN, L. & YU, L. 2011. Cyclophilin A promotes human hepatocellular carcinoma cell metastasis via regulation of MMP3 and MMP9. *Mol Cell Biochem*, 357, 387-95.
- ZHANG, S., SUN, Y., YUAN, Z., LI, Y., LI, X., GONG, Z. & PENG, Y. 2012. Heat shock protein 90beta inhibits apoptosis of intestinal epithelial cells induced by hypoxia through stabilizing phosphorylated Akt. *BMB Rep*, 46, 47-52.
- ZHANG, Z., BAST, R. C., JR., YU, Y., LI, J., SOKOLL, L. J., RAI, A. J., ROSENZWEIG, J. M., CAMERON, B., WANG, Y. Y., MENG, X. Y., BERCHUCK, A., VAN HAAFTEN-DAY, C., HACKER, N. F., DE BRUIJN, H. W., VAN DER ZEE, A. G., JACOBS, I. J., FUNG, E. T. & CHAN, D. W. 2004. Three biomarkers identified from serum proteomic analysis for the detection of early stage ovarian cancer. *Cancer Res*, 64, 5882-90.
- ZHAO, R., LEUNG, E., GRUNER, S., SCHAPIRA, M. & HOURY, W. A. 2010. Tamoxifen enhances the Hsp90 molecular chaperone ATPase activity. *PLoS one*, 5, e9934.
- ZHOU, M., ZHAO, Y., DING, Y., LIU, H., LIU, Z., FODSTAD, O., RIKER, A. I., KAMARAJUGADDA, S., LU, J., OWEN, L. B., LEDOUX, S. P. & TAN, M. 2010. Warburg effect in chemosensitivity: targeting lactate dehydrogenase-A re-sensitizes taxol-resistant cancer cells to taxol. *Mol Cancer*, 9, 33.
- ZHOU, Y., TOZZI, F., CHEN, J., FAN, F., XIA, L., WANG, J., GAO, G., ZHANG, A., XIA, X., BRASHER, H., WIDGER, W., ELLIS, L. M. & WEIHUA, Z. 2012. Intracellular ATP levels are a pivotal determinant of chemoresistance in colon cancer cells. *Cancer Res*, 72, 304-14.
- ZHU, Y., WU, R., SANGHA, N., YOO, C., CHO, K. R., SHEDDEN, K. A., KATABUCHI, H. & LUBMAN, D. M. 2006. Classifications of ovarian cancer tissues by proteomic patterns. *Proteomics*, 6, 5846-56.

Appendix: Accompanying DVD**Chapter 2:** Optimisation Strategies_Chapter 2**Chapter 3:** Cruz et al 2013_Chapter 3 – Cruz *et al.* (2013), Glycomimetic affinity-enrichment proteomics identifies partners for a clinically-utilized iminosugar, *Chemical Science***Chapter 4:** Protein Table with Spot Quantity Info_Tissues+Cells_Chapter 4**Chapter 5:** Enzyme Kinetics_Chapter 5

Cruz et al 2013_Chapter 5 – Cruz *et al.* (2013), Functional characterization of heat shock protein 90 targeted compounds, *Analytical Biochemistry*